Molecular investigation of the human neurovascular unit in depressed suicides with a history of childhood abuse

Marina Anna Wakid

Integrated Program in Neuroscience
Department of Neurology and Neurosurgery
McGill University, Montreal

June 2024

A thesis submitted to McGill University in partial fulfillment of the requirements of the degree of Doctor of Philosophy.

Acknowledgements

To my supervisor, Naguib Mechawar, I want to express my heartfelt thanks. As a budding undergraduate student back in 2013, you had entrusted me as a lab assistant; and what I learned from my experiences in your lab is what I could not learn from classes, textbooks, or finals—I learned that the life of a scientist is meant for me. As a PhD candidate, your trust in me has continued, granting me the intellectual freedom to explore research questions that fascinate me and teaching me to listen to the data when it tells a story. I am immensely grateful for your mentorship, as well as the stellar book recommendations.

To the members of my advisory committee, Kai-Florian Storch and Bruno Giros, thank you for your continued insight and belief in me.

I would also like to thank each and every member of the McGill Group for Suicide Studies (MGSS) over the years. It has been an honour to be amongst you and to learn from you. To my generation of PhD candidates, with whom I started this graduate journey, I will always cherish the silly times in the student office, the camaraderie at the bench, and the friendship outside of the lab. There were years when the MGSS felt like a Dream Team straight out of a collegiate movie, and those years are invaluable to me. I would especially like to thank my dear friends and colleagues: Daniel Almeida, my essential twin; Maria Antonietta Davoli, my lab mom; and Dominique Mirault, my partner in giggles. You are a part of my chosen family.

My chosen family extends beyond the world of science to my dear friends Zhanna Zhigalova, Laviva Mazhar, Sid Ahmed, and Alejandro Padilla. You have all been a source of laughter and cherished memories over the years, and I am so thankful.

To my parents, Jocelyne and Hany, you have been my trailhead on this journey. What's more, your endless love and support have carried me through. You fostered my curiosity for all things as a child, and from that, you have given me the greatest gift—lifelong curiosity. It is that curiosity that led me down the path to science.

And to my beloved boyfriend, Roeland Heerema, through it all, you have held my hand and my heart, and continue to do so. No words can truly convey how much it has meant to me every time you have rallied me, consoled me, inspired me, and laughed with me. We met because of science, and of all my experiences during this era of my life, knowing you has been the most magical.

Table of Contents

Abstract

Exposure to childhood abuse is a persisting global public health concern. In developed countries, 44% of children have been subjected to adverse experiences, while the percentage rises to 59% in developing countries. In both children and adults, a history of childhood abuse has consistently been associated with structural, functional, and molecular alterations to fronto-limbic areas of the brain, yet the effects of childhood abuse on neurosupportive systems, such as the neurovascular unit, remain poorly characterized in comparison. Compelling evidence supports abuse-induced vascular endothelial dysfunction that primes for the development of cardiovascular disease later in life. Yet, despite the importance of the neurovasculature in maintaining normal brain physiology, human neurovascular cells remain poorly characterized, particularly with regard to their contributory role in abuse-induced pathologies. In this thesis, I describe a novel standardized protocol to enrich and isolate microvessels from archived snap-frozen human cerebral cortex that preserves the structural integrity and multicellular composition of microvessel fragments. For the first time, using this protocol, microvessels were isolated from postmortem brain samples and comprehensively characterized as a structural unit using both RNA sequencing and Liquid Chromatography-Tandem Mass Spectrometry (LC-MS/MS). I then present a study achieving the first transcriptomic analysis of intact human microvessels isolated from postmortem ventromedial prefrontal cortex from controls and matched depressed suicides with a history of childhood abuse. Among brain regions implicated, the prefrontal cortex is particularly vulnerable as it mediates stress-evoked changes in cardiovascular activity. In this work, we combined differential gene expression analysis and network-based approaches to provide an integrative and unbiased characterization of male and female transcriptional profiles of the neurovascular unit in depressed suicides with histories of severe childhood abuse. Our findings point to significant differences between men and women, with the latter exhibiting widespread gene expression changes, including key vascular nodal regulators KLF2 and KLF4, alongside a broad downregulation of immune-related pathways. These results suggest that the neurovascular unit may play a larger role in mediating the neurobiological consequences of childhood abuse in women.

Résumé

L'exposition à la maltraitance infantile est un problème persistant de santé publique à l'échelle mondiale. Dans les pays développés, 44 % des enfants ont été soumis à des expériences défavorables, tandis que ce pourcentage atteint 59 % dans les pays en développement. Chez les enfants comme chez les adultes, les antécédents d'adversité au début de la vie ont toujours été associés à des altérations structurelles, fonctionnelles et moléculaires dans les zones fronto-limbiques du cerveau, mais les effets de l'adversité au début de la vie sur les systèmes cérébraux de soutien, tels que l'unité neurovasculaire, demeurent mal caractérisés. En effet, malgré l'importance de la neurovasculature dans le maintien d'une physiologie cérébrale normale, les cellules neurovasculaires humaines restent mal caractérisées, notamment en ce qui concerne leur rôle dans les pathologies associées à la maltraitance infantile. Dans le cadre de cette thèse, je décris un nouveau protocole standardisé pour l'enrichissement et l'isolation de microvaisseaux du cortex cérébral humain archivé et congelé. Cette méthode combine une homogénéisation mécanique et une centrifugation-séparation, ce qui permet de préserver l'intégrité structurelle et la composition multicellulaire des fragments de microvaisseaux ainsi isolés. À l'aide de cette méthode, des microvaisseaux ont été isolés pour la première fois à partir d'échantillons de cerveau postmortem avant d'être caractérisés de manière exhaustive en tant qu'unité structurelle à l'aide du séquençage de l'ARN et de la chromatographie liquide avec spectrométrie de masse en tandem (LC-MS/MS). Je présente ensuite une étude rapportant la première analyse transcriptomique de microvaisseaux intacts isolés à partir d'échantillons post-mortem du cortex préfrontal ventromédian provenant de sujets sains et de dépressifs suicidés appariés ayant un historique de maltraitance infantile sévère. Parmi les régions du cerveau impliquées dans les pathologies associées au stress chronique, le cortex préfrontal est particulièrement vulnérable car il est le médiateur des changements de l'activité cardiovasculaire provoqués par le stress. Dans ce travail, nous avons combiné l'analyse différentielle de l'expression génique et des approches basées sur les réseaux pour fournir une caractérisation intégrée et impartiale des profils transcriptionnels masculins et féminins de l'unité neurovasculaire chez au sein d'échantillons cérébraux de personnes avec un historique de maltraitance infantile.

Nos résultats mettent en évidence des différences majeures entre les hommes et les femmes, ces dernières présentant des changements généralisés dans l'expression des gènes, y compris les régulateurs clés des nœuds vasculaires KLF2 et KLF4, ainsi qu'une large régulation à la baisse des voies liées à l'immunité. Ces résultats suggèrent que l'unité neurovasculaire pourrait jouer un rôle plus important comme intermédiaire des conséquences neurobiologiques de la maltraitance infantile chez les femmes.

Contributions to Original Knowledge

This dissertation is presented in the manuscript-based format for Doctoral Theses, as described in the Thesis Preparation Guidelines by the Department of Graduate and Postdoctoral Studies at McGill University. The work described here was performed by Marina Wakid under the supervision of Dr. Naguib Mechawar. The thesis contains four chapters: chapter I is a comprehensive review of the current background literature relevant to this thesis; chapter II is a methodological manuscript that was published in *Brain, Behaviour, & Immunity—Health*; chapter III is an empirical manuscript that has been submitted for publication; chapter IV is a discussion of the findings from chapters II and III and also includes concluding remarks and future directions.

Chapter II: *Universal method for the isolation of microvessels from frozen brain tissue: A proof-of-concept multiomic investigation of the neurovasculature.*

In our first study, we developed a method to enrich and isolate microvessels from archived snap-frozen human brain using mechanical homogenization and centrifugation-separation that is gentle enough to dissociate brain tissue while preserving the structural integrity and multicellular composition of microvessel fragments. Our understanding of neurovascular development and function has been advanced largely by mouse models. While past mouse data have provided precious insight into defining core neurovascular gene expression and function, recent breakthroughs demonstrate that there are numerous species-specific differences between the mouse and human neurovasculature, revealing the partial utility of animal models for studying disease of the human CNS. Moreover, single-cell and single-nucleus sequencing appear to deplete populations of neurovascular cell types from human cortex samples, impeding analysis of human neurovascular transcriptomes. We amply demonstrate that microvessels isolated using our method are in high yield, possess all major neurovascular-associated cell types, and maintain their *in situ* cellular structure. To demonstrate the utility of microvessels isolated from postmortem ventromedial prefrontal cortex (vmPFC) tissue, we processed samples of extracted total RNA and total protein using RNA sequencing and LC-MS/MS, respectively. Bioinformatic processing and analysis of human transcriptomic and proteomic data

indicated that isolated samples showed major enrichment for brain microvascular endothelial cells (BMECs), pericytes, smooth muscle cells (SMCs), and astrocytic endfeet components at both the mRNA and protein level, generating the first multiomic datasets from human brain microvessels.

Chapter III: *Neurovascular dysfunction in the ventromedial prefrontal cortex of female depressed suicides with a history of childhood abuse.*

For our next study, we sought to examine the relationship between childhood abuse and neurovascular dysfunction in the vmPFC using unbiased data driven approaches. Given that disturbances in gene expression vary across cell type, the variability implicit to tissue homogenates can mask cell-type-specific transcriptomic changes associated with a history of childhood abuse. Strategies that either enrich for dissociated neurovascular cells or intact neurovascular structure are, therefore, crucial for tackling the downstream effects of tissue heterogeneity in molecular analyses. We, therefore, utilized the method developed in study I to isolate blood vessels, coupled with bulk RNA sequencing to investigate how a history of childhood abuse alters the transcriptomic landscape of the neurovascular unit. This approach allowed us to objectively identify candidate genes pertinent to human neurovascular dysfunction as opposed to relying on existing literature based on animal proxy-models or more limited human postmortem studies. In this study, we present the first comprehensive transcriptomic analysis of the neurovascular unit in depressed suicides with histories of childhood abuse, allowing us to speculate how childhood abuse induced alterations at the neurovascular unit lead to functional impacts on cortical function.

Contributions of Authors

Chapter I: The writing and literature review were conducted by Marina Wakid under the supervision of Naguib Mechawar.

Chapter II: Experimental Design: Marina Wakid, Daniel Almeida, Volodymyr Yerko, Elena Leonova-Erko, Maria Antonietta Davoli, Reza Rahimian
Characterization of Human Brain Samples: Gustavo Turecki, Naguib Mechawar
Data Collection: Marina Wakid, Vincent Richard
Data Analysis: Marina Wakid, Zahia Aouabed
Interpretation of results and manuscript preparation: Marina Wakid, Naguib Mechawar
Other Resources: René Zahedi, Christoph Borchers
All authors participated in the finalization of the manuscript.

Chapter III: Experimental Design: Marina Wakid, Daniel Almeida, Maria Antonietta Davoli
Characterization of Human Brain Samples: Gustavo Turecki, Naguib Mechawar
Data Collection: Marina Wakid
Data Analysis: Marina Wakid, Ryan Denniston, Anjali Chawla, Zahia Aouabed
Interpretation of results and manuscript preparation: Marina Wakid, Naguib Mechawar
Other Resources: Reza Rahimian, Volodymyr Yerko, Elena Leonova-Erko, Kristen Ellerbeck
All authors participated in the finalization of the manuscript.

Chapter IV: The writing of this section was conducted by Marina Wakid under the supervision of Naguib Mechawar.

List of figures used in Chapter I

List of Abbreviations

ACC: Anterior cingulate cortex
ACE: Adverse childhood experience
AQP4: Aquaporin 4
BBB: Blood-brain barrier
BMEC: Brain microvascular endothelial cells
CLDN5: Claudin 5
CPM: Counts per million
CRP: C-reactive protein
CTRL: Control
CVD: Cardiovascular disease
DEG: Differentially expressed gene
DGE Analysis: differential gene expression analysis
dlPFC: Dorsolateral prefrontal cortex
ELA: Early life adversity
ERG: ETS-related gene
FACS: Fluorescence-activated cell sorting
FANS: Fluorescence-activated nucleus sorting
FISH: Fluorescence in situ hybridization
GR: Glucocorticoid Receptor
HOMER2: Homer Scaffold Protein 2

HPA: hypothalamic-pituitary-adrenal axis
IFNγ: Interferon gamma
IL6: Interleukin 6
KLF2: Krüppel-like factor 2
KLF4: Krüppel-like factor 4
LAM: Laminin
MDD: Major depressive disorder
mPFC: medial prefrontal cortex
NR3C1: Nuclear Receptor Subfamily 3 Group C Member 1
NVU: Neurovascular unit
p2g: Peak-to-gene
PDGFRβ: Platelet-derived growth factor receptor beta
PECAM1: Platelet And Endothelial Cell Adhesion Molecule 1
PFC: Prefrontal cortex
PMI: Postmortem interval
RIN: RNA integrity number
RRHO: Rank-Rank Hypergeometric Overlap
TACC1: Transforming Acidic Coiled-Coil Containing Protein 1
TNFα: Tumor necrosis factor alpha
TPM: Transcripts per million
VCAM1: Vascular cell adhesion molecule 1
VIM: Vimentin
vmPFC: ventromedial prefrontal cortex
SMC: Smooth muscle cell
WGCNA: Weighted Gene Co-expression Network Analysis

I have a friend who's an artist and has sometimes taken a view which I don't agree with very well. He'll hold up a flower and say, 'Look how beautiful it is,' and I'll agree. Then he says, 'I as an artist can see how beautiful this is, but you as a scientist take this all apart and it becomes a dull thing,' and I think that he's kind of nutty. First of all, the beauty that he sees is available to other people and to me too, I believe. Although I may not be quite as refined aesthetically as he is, I can appreciate the beauty of a flower. At the same time, I see much more about the flower than he sees. I could imagine the cells in there, the complicated actions inside which also have a beauty. I mean it's not just beauty at this dimension of one centimetre; there is also beauty at a smaller dimension.

Richard Feynman
Nobel Prize Laureate in Physics, 1965
Discoverer of path integral formulation and Feynman diagrams

Chapter I: Comprehensive Review of the Literature

Early-life adversity and suicide

Physical, sexual, and/or emotional abuse or neglect experienced in early life can lead to profound disturbances in psychological and physical trajectories such that its pernicious effects linger as psychopathology and disease in adulthood. It is estimated that one in four children will experience childhood abuse at some point in their lifetime, and that one in seven children have experienced abuse in the past year (U.S. Department of Health and Human Services, Administration for Children and Families). Globally, an approximate 1 billion children and young adolescents (aged between 2–17 years) are exposed to violent behaviour (data in 2015; Hillis et al., 2016), where 44% of children in developed countries and 59% in developing countries have been victims of physical, emotional, or sexual violence or have been exposed to domestic or community violence in the year prior (Hillis et al., 2016). The statistics on these reports are a significant underestimate of just how prevalent childhood abuse remains, as most abuse remains unreported. Here, we define childhood abuse as negative early-life experiences associated with significantly increased lifetime risk for poorer health and social outcomes; and we will specifically explore the effects of psychosocial adversity surrounding relationships (with parents, caregivers, extended family, peers, community) and other social exposures that affect neurobiological processes (Martikainen et al., 2002). Examples of such adversities include, but are not limited to, exposure to and being the target of violence, caregiver psychopathology, unstable or deprived raising environments (e.g., inadequate foster or institutional care), hostile societal exposures such as crime and discrimination, as well as other causes of psychological stress. For brevity, we refer to these experiences as the aggregative “early life adversity” (ELA) to conceptualize the oftentimes complex combination of different types of abuse that individuals experience.

ELA constitutes a chronic form of stress, which is defined as a change in homeodynamic balance that requires a physiological and psychological response from the organism (Agorastos et al., 2019). Excessive and chronic stress exposure,

especially during developmentally sensitive stages of life (early childhood) may lead to an altered homeodynamic state and impact many physiological and psychological processes. Critically, ELA is associated with 44.6% of all psychiatric childhood-onset disorders and with 25.9–32.0% of adult-onset disorders (Green et al., 2010; Afifi et al., 2008; Bernet and Stein, 1999; Brown et al., 2009; Danese et al., 2009; Dube et al., 2003; Felitti et al., 1998; Gilbert et al., 2009; Mullen et al., 1996; Springer et al., 2007; Ahn et al., 2024), and further predicts a more severe clinical course of illness, including earlier age of onset, longer duration, increased comorbidity, and reduced responsiveness to treatment (Bernet and Stein, 1999; Du Rocher Schudlich et al., 2015; Gilbert et al., 2009; Klein et al., 2009; Lansford et al., 2002; Tunnard et al., 2014; Widom et al., 2007). Several lines of evidence also support a strong relationship between ELA and the onset and persistence of suicidality into adulthood (Bruffaerts et al., 2010; Enns et al., 2006; Gartland et al., 2022; Bahk et al., 2017; Angelakis et al., 2019; Dube et al., 2001; Afifi et al., 2008; Brezo et al., 2007; Brezo et al., 2008; Dube et al., 2001; Fergusson et al., 2000; Molnar et al., 2001). Indeed, it is estimated that ELA predicts up to 64% of suicidal behaviour in adulthood, and up to 80% in childhood and/or adolescence (Afifi et al., 2008; Dube et al., 2001; Molnar et al., 2001). Unsurprisingly, ELA confers a younger age of first suicide attempt (Lopez-Castroman et al., 2012).

What mediates the relationship between ELA and suicidality? It has been proposed that developmental dysregulations of cognitive, emotional, and behavioural traits are implicated (Turecki, 2014; Turecki and Brent, 2016). Changes in the early-life environment correlate with conserved behavioural phenotypes in both humans and other species; for instance, early social deprivation in non-human primates results in short- to long-term changes in affect, cognition, and social behaviour (French and Carp, 2016; Nelson et al., 2009; Pryce et al., 2004; Zhang et al., 2016), while individuals with a history of ELA typically exhibit consistent patterns of high impulsivity and aggression, high anxiousness trajectories, interpersonal difficulties, and impaired executive function (Brodsky et al., 2001; Hostinar et al., 2012; Johnson et al., 2002; Sinclair et al., 2007; Wanner et al., 2012; Yang and Clum, 2000), which have all been shown to contribute to

suicidality (Turecki, 2014; Turecki and Brent, 2016). There is, most certainly, a large body of existing literature establishing a strong association between ELA and suicidality. While the exact neurobiological processes underlying this heightened vulnerability remain unclear, there is compelling evidence pointing to aberrant brain-development trajectories.

In the following sections, several basic principles of neurodevelopment are reviewed in order to provide a context, and to understand patterns of atypical neurodevelopment among those with ELA.

Postnatal development of the brain parenchyma

The human postnatal brain follows a protracted course of development that extends into the third decade of life (Petanjek et al., 2011). Remarkable growth in gray and white matter occurs during the first two years, where 80–90% of the developing brain's adult volume is rapidly built and then followed by continued growth at an attenuated rate (Berens et al., 2017; Knickmeyer et al., 2008). These remarkable changes occur in an anatomical wave from "the bottom up", where the brain matures starting with brainstem structures and progresses upwards to the anterior-posterior and inferior-superior directions, finally ending with the prefrontal cortex (PFC; Gogtay et al., 2006). In a way that is complementary, functional development and maturation also display a "bottom up" trajectory, starting with basic sensory and motor functioning followed by language and executive functioning (e.g., working memory and cognitive control), and finally higher cognition (Fox et al., 2010).

Synaptogenesis and synaptic pruning are critical processes responsible for these developmental changes. The rapid expansion of the brain's volume during the early postnatal period is primarily driven by a surge in synaptogenesis, where an overproduction of synapses, dendrites, dendritic spines, and axons (Huttenlocher et al., 1982; LaMantia and Rakic, 1994; Petanjek et al., 2008) occurs under genetic control. The postnatal age at which there is a surge in synapse formation, and therefore high synaptic density, varies across brain regions (Huttenlocher, 1990; Huttenlocher and

Dabholkar, 1997; Michel and Garey, 1984; Travis et al., 2005); beginning with the visual cortex and other base structures, for which synaptogenesis peaks within the first 8 months of life, whereas more complex structures in the PFC reach their synaptogenic peak by the 15th postnatal month (Bourgeois et al., 1994; Huttenlocher and Dabholkar, 1997).

Once peak synaptogenesis is achieved, uncommitted synapses undergo pruning, which underpins the subsequent, attenuated growth phase. Pruning is influenced by experience, allowing neuronal networks to first generate and then fine-tune, becoming more organized, efficient, and optimized for maximal adaptation to the surrounding environment (Guido, 2008; Hong and Chen, 2011; Katz and Shatz, 1996). As with synaptogenesis, different regions similarly vary in their respective onset of synaptic pruning. Importantly, these timing differences dictate which regions remain sensitive to environmental input, as regions with delayed time periods of peak synaptogenesis also undergo experience-based pruning at a later point in development, with sensory and motor regions undergoing early dynamic reorganization, followed by association areas and the corpus callosum, and finally cortical structures involved in higher cognitive functions (Elston et al., 2009; Levitt, 2003; Tau and Peterson, 2010). During childhood, synaptic density within the PFC exceeds adult values by two to threefold (Huttenlocher, 1979; Petanjek et al., 2011). Interestingly, the PFC is characterized by a particularly high number of supernumerary synapses and undergoes experience-dependent pruning that extends up until the third decade of life (Huttenlocher, 1979; Petanjek et al., 2011). The final stage of brain development involves myelination, which also begins with sensory pathways myelinating first, followed by motor pathways and, finally, association areas (Barkovich et al., 1988; Girard et al., 1991; Kinney et al., 1988; Paus et al., 2001). The PFC, for instance, does not become fully myelinated until early adulthood (Arain et al., 2013; Miller et al., 2012). As is true for synaptic pruning, myelination programs seem to be, at least in part, experience-dependent (Fields, 2015; Hrvatin et al., 2018).

Postnatal development of the neurovasculature

One of the most salient features of human evolution is the significant increase in brain size from early hominins. This increase marks the basis of the higher cognitive function uniquely attributed to humans, facilitated by observed higher white matter volume, denser neuronal connectivity and, consequently, a greater ability to process information within the PFC (Schoenemann et al., 2005; Zhang et al., 2000). Neuronal metabolism is almost entirely aerobic and, therefore, relies on a constant supply of external glucose and oxygen for metabolic activity (Shulman et al., 2003). Like all cells and tissues of the body, the brain is supplied with blood by an intricate network of vasculature as its delivery system. Greater information processing capability, however, comes at a significant metabolic cost—the modern human brain consumes almost one quarter of the glucose and oxygen supply in the human body (Shulman et al., 2003; Bloom and Kupfer, 1995). Three compensatory mechanisms ensure that brain regulated appropriately: neurovascular coupling, in which increased neuronal activity (and therefore metabolic demand) is matched by increased blood flow (Iadecola et al., 1997; Erinjeri et al., 2002); cerebral vasoreactivity, in which there is high sensitivity to changes in arterial CO_2 and oxygen levels (Nordstrom et al., 1998; Johnston et al., 2003); and cerebral autoregulation, which counteracts the fluctuations in systemic arterial pressure that occur in everyday activities (Rapela et al., 1964).

There is still much to be learned about how the neurovasculature develops to become an efficient delivery system for blood supply. Regardless, research over the past decade has shown that the neurovascular and central nervous systems share common guidance cues for embryonic development and patterning (Eichmann and Thomas, 2013; Quaegebeur et al., 2011; Tam and Watts, 2010; Wälchli et al., 2015; Carmeliet and Tessier-Lavigne, 2005), affirming that neurovascular and neuronal structures develop, grow, and mature simultaneously. The brain's vasculature itself is dramatically different both morphologically and functionally at the prenatal versus postnatal period. Simultaneously to the neurogenic process, forebrain vascularization starts ventrally and progressively extends towards the dorsal forebrain (Lange et al., 2016; Karakatsani et al., 2019; Puelles et al., 2019), forming the embryonic vascular plexus. The embryonic

vascular plexus of the brain, a haphazard plexus of vessels with no true distinction between arteries, veins, and capillaries, is used as a scaffold for growth and refinement into the different vascular zones of the eventual adult brain (Herken et al., 1989; Wang et al., 1996; Fehér et al., 1996; Letourneur et al., 2014; Wang et al., 1992). Remarkably, arteries and veins only begin to take on their unique characteristics postnatally, while the deeper, intracortical microvascular network that lies beneath the surface of the brain parenchyma elaborates (Rowan and Maxwell, 1981).

At birth, the intracortical microvascular network begins as sparse and incomplete—a contrast to the marked density and stability of microvascular networks of the adult brain (Figure 1; Cudmore et al., 2017; Drew et al., 2010; Harb et al., 2013). The pattern of changes observed in this network echo that of neuronal synapse formation and elimination: for the first few months of human postnatal development and first postnatal month in mice, the capillary bed dramatically expands via angiogenesis (Figure 2; Harb et al., 2013, Keep and Jones, 1990; Norman and O'Kusky, 1986; Risser et al., 2009), and the process of neurovascular remodeling occurs through rounds of sprout formation followed by either maintenance or pruning of these sprouts (Harb et al., 2013; Rowan and Maxwell, 1981).

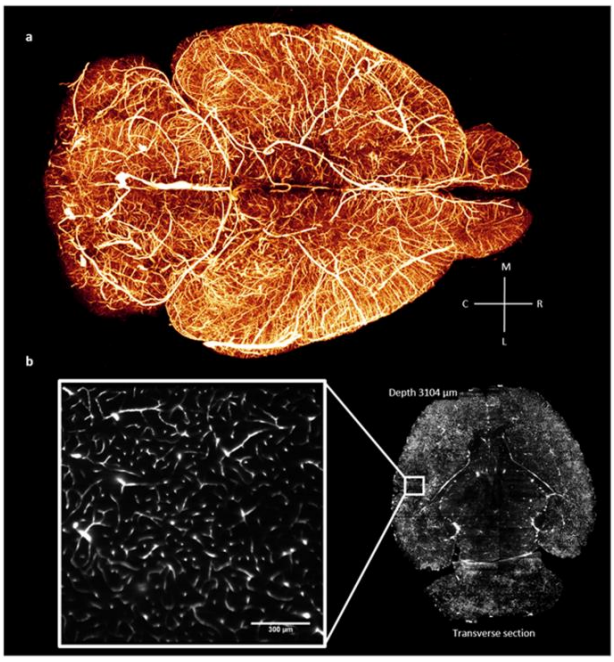

Figure 1: The adult brain exhibits marked density and stability of neurovascular networks. (**a**) 3D rendering of the whole mouse-brain vasculature acquired using light-sheet fluorescence microscopy and gel-BSA-FITC vascular staining. (**b**) Single frame showing details at the capillary level. (Figure sourced from Di Giovanna et al., 2018).

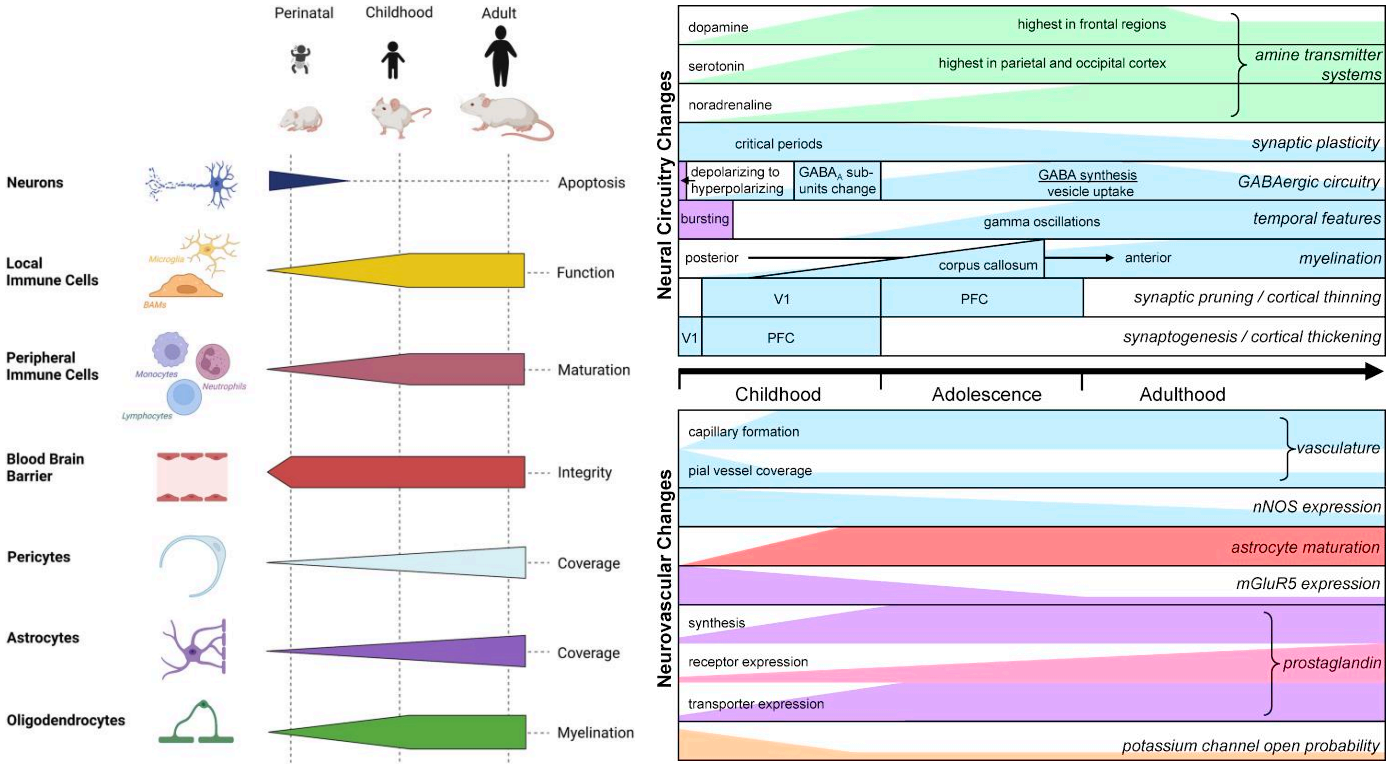

Figure 2: The neurovasculature experiences dramatic remodelling during the postnatal period. (Left) Schematic representation of the development of individual cell types and of the maturing neurovascular unit during embryonic and postnatal brain development in humans and rodents. Physiological neuronal apoptosis is high in the newborn brain and rapidly declines during perinatal period. The neurovascular network is established by birth but continues to change in the postnatal and juvenile brain. Astrocyte and pericyte coverage continue to increase in the postnatal and juvenile brain. (Right) Schematic summarizing the developmental time courses of changes in neuronal information processing mechanisms (top) and of components of the signalling pathways regulating blood flow and thus controlling the BOLD response (bottom). Changes shown in blue are from human data; green is from macaque; lilac from rat or mouse; red from cat; pink from pig; light orange from rabbit. (Left schematic adapted from Martino et al., 2023; Right schematic sourced from Harris et al., 2011).

Additionally, rodent studies have revealed that postnatal neurovascular remodelling occurs in an inside-to-outside fashion, in which the capillary beds of deeper cortical layers mature earlier (Norman and O'Kusky, 1986; Rowan and Maxwell, 1981), akin to the radial development of the neuronal architecture. By P15–P25 (a proxy for 5–15 years of age; Figure 3), capillary angiogenesis begins to subside, and capillary density stabilizes (Harb et al., 2013; Wälchli et al., 2015; Zeller et al., 1996) by virtue of pericyte and endothelial cell proliferation decline (Harb et al., 2013). This pattern is reflected in cortical cerebral blood flow, a metric that is highly correlated with vascular density, which is lowest during early postnatal ages, then gradually increases until the age of 7,

and subsequently declines to reach adult levels during the late teen years (Chiron et al., 1992, Takahashi et al., 1999). Grey and white matter tissues differ significantly in their metabolic demands, with white matter, rich in energy-efficient myelinated axons, consuming approximately 1/4 to 1/3 of the energy consumed by grey matter. Because of this, capillary networks within adult grey matter are significantly more elaborate, in fact, capillary density in grey matter doubles between birth to P20 (Figure 3), while the rise in capillary density in white matter is modest (Zeller et al., 1996).

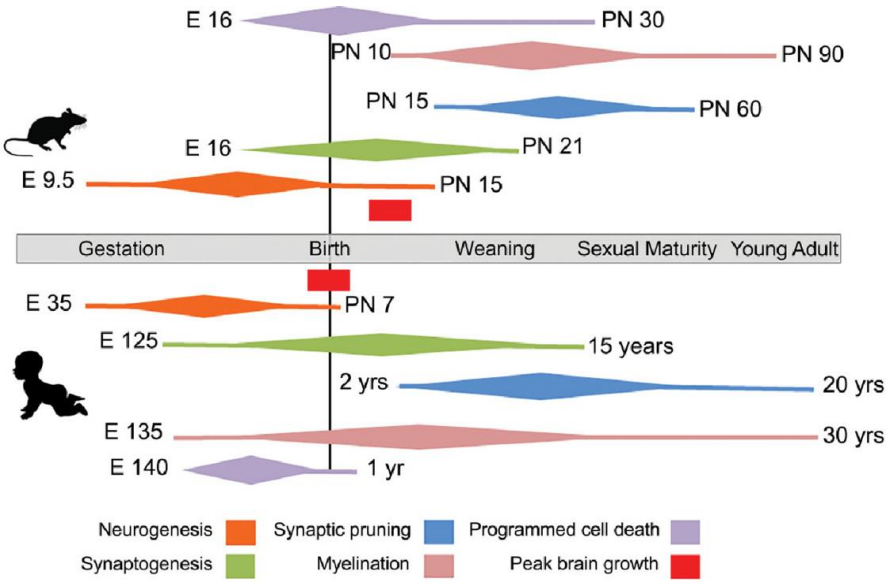

Figure 3: Comparative milestones in rodent and human postnatal brain development. Schematic summarizing approximate timelines of developmental processes in relation to the developmental milestones, birth, weaning, sexual maturity, and adulthood. Periods of growth spurts are shown in red. Individual processes are color-coded, with peak activity indicated by the widest portion of the diamond. (Schematic sourced from Zeiss, 2021).

Postnatal development of the neurovascular unit

BMECs play a central role in the neurovascular structure, yet blood vessels in the brain comprise several other neurovascular cell types, including pericytes, perivascular fibroblasts, vascular SMCs, and astrocytic endfeet (Wälchli et al., 2015a; Wälchli et al., 2015b; Ghajar et al., 2013). Together, these neurovascular cell types form the neurovascular unit (NVU; Figure 4), which is the functional correlate of the neurovasculature (Wälchli et al., 2015b; Muoio et al., 2014; Eichmann and Thomas, 2013). The recruitment and crosstalk between neurovascular cells are of absolute importance for the refinement and maturation of the blood-brain barrier (BBB), which consists of a set of highly regulated properties that will be thoroughly discussed later.

Intriguingly, barriergenesis extends into the postnatal period: Endothelial expression of efflux transporters (Daneman et al., 2010) and ABC-transporters (Ek et al., 2010) increases and major changes in the regional pattern of GLUT1 distribution occur (Harik et al., 1993; Zeller et al., 1996). Moreover, perivascular fibroblasts emerge on blood vessels between P5 and P14 (Jones et al., 2023), and endothelial tight junction structures increase in their density and complexity until adulthood (Daneman et al., 2010; Kniesel et al., 1996), resulting in the gradual sealing of the BBB until P33 or 15 years of age (Zeiss et al., 2021). This sealing is evidenced by *in situ* measurements of transendothelial electrical resistance (Butt et al., 1990) as well as vascular impermeability, which further benefits from the increasing coverage of the capillary wall by astrocytic endfeet at P14–P50. The establishment of a mature astrocytic–basement membrane interface (J. Xu & Ling, 1994; Seregi et al., 1987, Stichel et al., 1991) is marked by endfeet that carry out dynamic mRNA localization and local translation to sustain astrocytic regulatory functions at the neurovascular interface (Avila-Gutierrez et al., 2024).

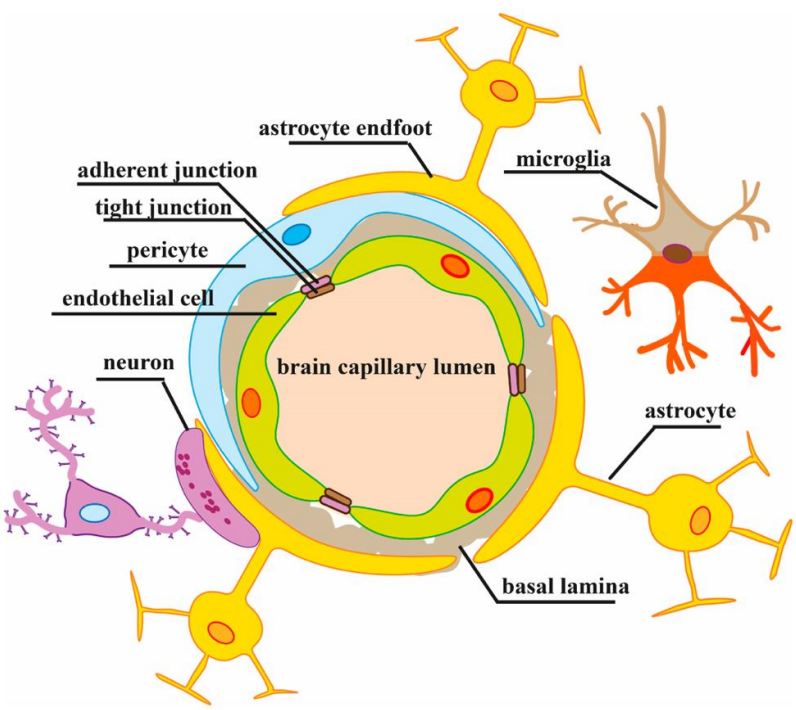

Figure 4: The organization of the neurovascular unit. The NVU is composed of BMECs, astrocytes and pericytes or smooth muscle cells. The BMECs form the BBB providing low paracellular permeability via a set of tight and adherence junctions which seal adjacent BMECs together. Pericytes partially surround the endothelium and, along with BMECs, are enclosed in the basement membrane. Astrocytic endfeet are in close contact with endothelial cells and pericytes, covering 99% of the vessel surface. The perivascular network of astrocytes connects the blood vessel with neurons. (Schematic sourced from Fock & Parnova, 2023)

The anatomy and physiological function of the vmPFC

Investigations into the mechanisms underlying stress-induced pathologies have identified dysfunction in a number of cortical and subcortical brain areas, among which, significant changes in the vmPFC are widely reported (Drevets et al., 2008; Price et al., 2010; Fredericks et al., 2006). An inclusive definition of the human vmPFC zone refers to the whole area of PFC that is both ventral and medial (i.e., superior and inferior medial gyri, anterior cingulate gyrus, gyrus rectus, medial orbital gyrus, and the adjacent sulci), corresponding to areas 24, 25, 32, 11, and 10 of the Brodmann map (Figure 5; Delgado et al., 2016). Within the vmPFC, cell distribution exhibits distinct spatial patterns; the anterior area shows a higher density of layer IV granule cells compared to posterior regions, while the medial areas of the vmPFC display higher densities of layer Va pyramidal cells compared to the more lateral areas along the orbital surface (Delgado et al., 2016; Mackey et al., 2010; Bhanji et al., 2019).

The structural connectivity of the vmPFC shows distinct patterning from other areas of PFC. Notably, unlike the lateral parts of the orbitofrontal cortex, the vmPFC has few direct inputs from sensory regions. Similarly, unlike the lateral prefrontal regions, it has few direct inputs from the motor cortex (Ongur et al., 2003; Ongur et al., 2000). There are prominent outputs from vmPFC to the hypothalamus, periaqueductal gray, amygdala, hippocampus, nucleus accumbens, and superior temporal cortex (Wallis et al., 2011; Price and Drevets, 2010), as well as long-range connections to the posterior cingulate cortex (Greicius et al., 2009). Patterns of connectivity differ between sub-areas within the vmPFC: there are more prominent projections from the amygdala to posterior areas of vmPFC (areas 24 and 25; Price and Drevets, 2010), but more prominent connections between the ventral areas of vmPFC and the ventral and medial areas of the striatum (i.e., nucleus accumbens), whereas more dorsal areas of vmPFC connect with anterior and dorsal areas of striatum (Haber and Knutson, 2010; Lehericy et al., 2004). Finally, vmPFC projections to hypothalamus are mostly from posterior areas of vmPFC (i.e., area 25; Price and Drevets, 2010).

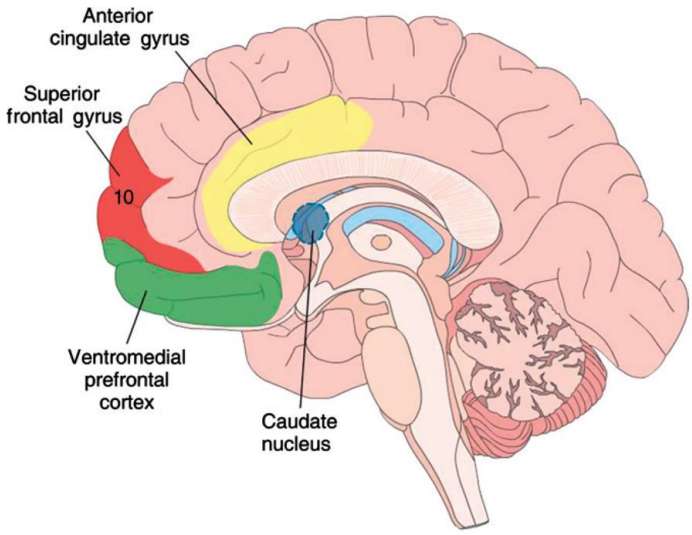

Figure 5: Anatomical location of the vmPFC in the human brain. (Schematic sourced from Baars and Gage, 2013).

Together, generated rodent, monkey, and human data converge to characterize the vmPFC as a key node in the neuronal circuitry underlying reward processing, value-based decision making, and regulation of negative emotion. Numerous human functional imaging studies have linked vmPFC activity with value and reward processing in an array of decision-making contexts (Liu et al., 2011; Levy and Glimcher, 2012; Hiser and Koenigs, 2018), while electrophysiological recordings in primates and rats have demonstrated that the vmPFC encodes the reward properties of stimuli (Tremblay and Schultz, 1999; Lopatina et al., 2016; Hiser and Koenigs, 2018), and targeted vmPFC lesions in monkeys disrupt reward-guided decision making (Izquierdo et al., 2004; Noonan et al., 2010). A second domain of function in which the vmPFC is understood to play a major role is the regulation of negative emotion. Indeed, damage to the vmPFC impairs the recall of extinction learning (Morgan et al., 1993; Quirk et al., 2000; Hiser and Koenigs, 2018). This is supported by evidence showing that vmPFC neurons fire during extinction recall, and that stimulation of these neurons reduces conditioned fear responses during the extinction phase (Milad and Quirk, 2002). These findings, coupled with studies demonstrating that vmPFC stimulation suppresses amygdala activity (Quirk et al., 2003; Rosenkranz et al., 2003, Likhtik et al., 2005), suggest a mechanism by which vmPFC regulates the expression of fear responses through inhibition of the amygdala. Notably, sex differences in the anatomy and function

of the vmPFC, at baseline and following chronic stress, remain understudied. To date, one study has observed heightened behavioural inhibition sensitivity and increased functional connectivity between the vmPFC and posterior parietal areas in females compared to males (Jung et al., 2002).

The relationship between the vmPFC and the broader vascular system

The vmPFC is also involved in mediating autonomic responses to emotional stimuli. On the cardiovascular system, this modulation is characterized by an influence on arterial blood pressure, regional blood flow, cardiac sympathetic and parasympathetic responses, as well as heart rate and peripheral vascular resistance (Shah et al., 2019; Verberne and Owens, 1998; Critchley et al., 2000; Damasio et al., 2000; Phillips et al., 2003). Seminal anatomical studies (van der Kooy et al., 1982; Neafsey et al., 1986; Hurley et al., 1991; Takagishi and Chiba, 1991) have described widespread vmPFC efferences to brain nuclei involved in cardiovascular control, including the amygdala, the lateral hypothalamus, the periaqueductal gray, the nucleus of the solitary tract, and the caudal and the rostral ventrolateral medulla. When the vmPFC is stimulated, mean arterial pressure decreases, sympathetic tone is inhibited, and glutamatergic synapses in the vmPFC modulate the parasympathetic component of the baroreflex (Owens and Verberne, 2001). Inactivation of the vmPFC, however, withdraws parasympathetic input to the baroreflex while sympathetic input is maintained (Resstel et al., 2004), suggesting that the vmPFC modulates the vagal efferent outflow to the heart (Wong et al., 2007). Relevant to this discussion, the vmPFC is essential for sympathetic cardiovascular activation to stressful stimuli (Frysztak RJ, Neafsey, 1994; Schaeuble et al., 2019).

The distinction between the blood vessel, the neurovascular unit, and the blood-brain barrier

Insofar as this body of writing has discussed the neurovasculature and the neurovascular unit as separate entities, on the contrary, the two are intertwined. The

neurovasculature, or blood vessels, specifically refers to the anatomical structures that transport blood throughout the brain and can be divided into the anatomical zones of the arteriovenous axis: arteries, veins, and capillaries. In contrast, the NVU encompasses a more complex concept that includes not only endothelial cells of the blood vessels themselves but also integrates cross-talking perivascular cell types, such as astrocytic endfeet, mural cells (pericytes and SMCs), and can extend to the perivascular subtype of T cells, fibroblasts, and microglia (Figure 4; McConnell et al., 2017). In essence, the NVU is the functional correlate of the blood vessel, with its various cell types working in concert to i) establish the BBB properties and ii) interact with neuronal processes to modulate the overall function of the NVU and coordinate neurovascular responses to both central and peripheral signals.

In this section, how the blood vessel, the NVU, and the BBB are intertwined is described. Biological barriers provide a functional boundary between circulating blood and interstitial fluid to establish two distinct physiological compartments essential for mammalian life. Of the numerous biological barriers present within the body, the BBB situated along the neurovasculature, is the most tightly regulated. The neurovasculature originates with a dense network of large extracranial and intracranial cerebral arteries that spread across the entire pial surface, from which penetrating arteries extend deep into the cortex, giving rise to the capillaries where the BBB property emerge. Along this pathway, blood vessels undergo numerous structural changes, adapting from large arteries to smaller arterioles and capillaries (which are also considered the microvasculature), which facilitate the selective permeability and protective functions of the BBB. Arteries descending into the brain from the subarachnoid space are structured with SMCs positioned between endothelial cells and a basement membrane, surrounded by the perivascular (Virchow-Robin) space, and then by astrocytic endfeet (Figure 6; McConnell et al., 2017). As vessels penetrate deeper into the brain and reach the level of the capillaries, the ultrastructure comprises continuous non-fenestrated BMECs. At this level, microvessels lose their SMC coverage in replacement of another mural cell type, pericytes, which are positioned between the BMECs and astrocytic endfeet (Figure 7).

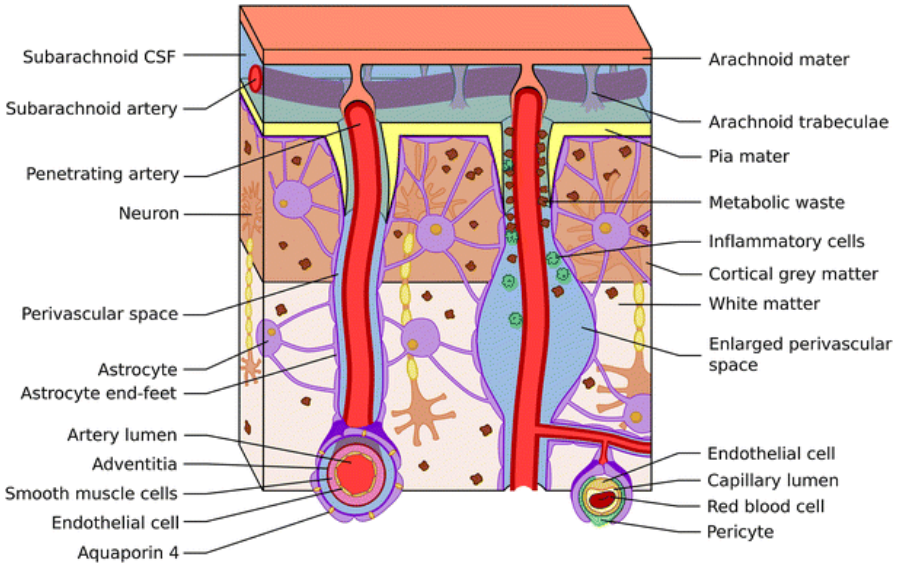

Figure 6: Arteries descending into the brain from the subarachnoid space. The perivascular space is bounded by the adventitia of the vessel and the astrocyte endfeet. (schematic sourced from Ramirez et al., 2016).

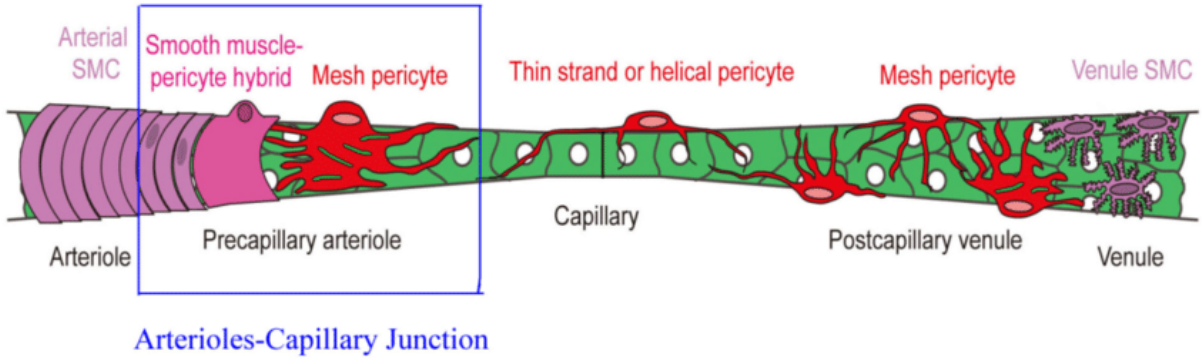

Figure 7: Continuum of mural cell types along the cerebral microvessels. Arterioles are wrapped by a continuous of SMCs. As the vessel diameter decreases to that of the capillary (the vessel size of the microvasculature), SMCs are replaced by pericytes. (Schematic sourced from Yang et al., 2017).

The long list of functions critical to brain health that are performed by NVU relies heavily on three key biological processes: (i) establishment of a barrier preventing paracellular diffusion of blood-borne polar substances (Tsukita et al., 2001), (ii) establishment of a barrier preventing lateral diffusion of integral membrane proteins and lipids between the apical and basolateral compartments of BMECs (van Meer and Simons, 1986) in order to maintain cell polarization (Schneeberger and Lynch, 1992; Cereijido et al., 1998), and (iii) an intracellular signalling platform. These three processes are made possible by the unique morphology presented by BMECs (Figure 8). Tight junctions, which are enriched in BMECs, are composed of integral membrane proteins known as occludins, claudins

and junctional adhesion molecules; and establish intercellular contacts between adjacent BMECs via recruitment of membrane-associated cytoplasmic scaffolding proteins such as zonula occludens proteins which, in turn, tether to the actin cytoskeleton via small GTPases and heterotrimeric G-proteins (Figure 8; Vorbrodt and Dobrogowska, 2003; Luissint et al., 2012). The resulting effect is anastomosing networks of tight junction strands that form “kissing points” to eliminate the paracellular space between adjacent endothelial cells (Tsukita et al., 2001). Because tight junctions impede the flow of polar solutes and ions (save for the smallest) from the blood to the brain and vice-versa, tight junction proteins confer a high transepithelial electrical resistance (TEER) *in vivo* of approximately ~1800 $\Omega.cm^2$ (Butt et al., 1990; Lo et al., 1999), which is considered a measure of barrier integrity. These BMECs precisely regulate the movement of substances between the blood and brain parenchyma through the expression of membrane-bound efflux transporters and highly specific nutrient transporters (Betz et al., 1980; Cordon-Cardo et al., 1989; Mittapalli et al., 2010; Thiebaut et al., 1989). When barrier dysfunction occurs, it leads to hyperpermeable microvessels and contributes to disease progression by allowing entry of immune cells and other foreign molecules into the brain parenchyma.

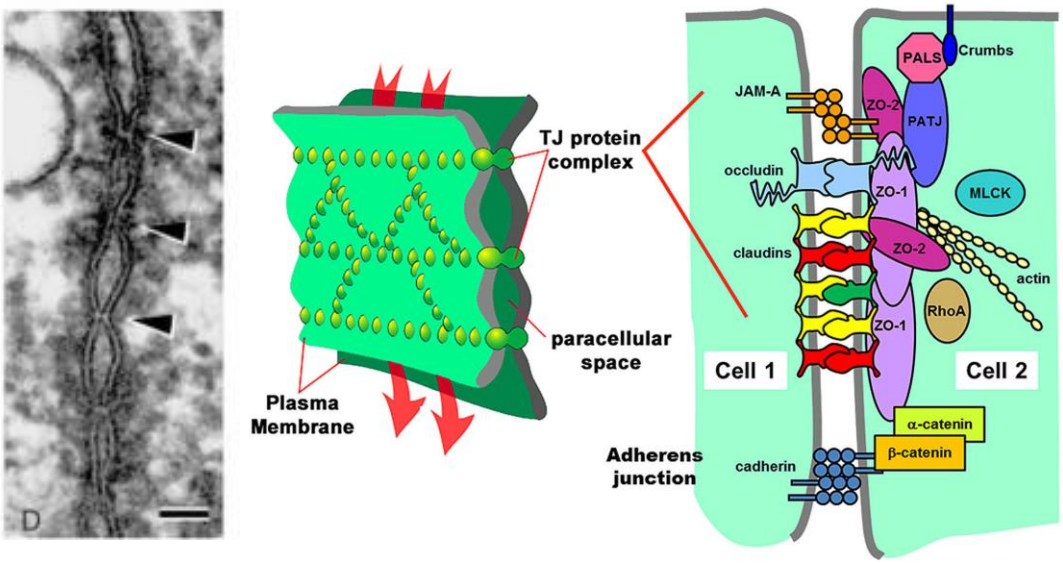

Figure 8: Structure of tight junctions at the NVU, needed for the blood-brain barrier property. (Left) Electron micrograph of the junctional complex in mouse. (Right) Schematic showing protein components of several tight junctions between two BMECs. Tight junctions are composed of several proteins, including transmembrane proteins that are connected to the actin cytoskeleton by scaffold proteins. Among these transmembrane proteins, claudins are

the main structural determinants of paracellular permeability. (EM image sourced from Tsukita, 2004; schematic sourced and modified from Mitchell & Koval, 2010).

With an estimated length of approximately 640 kilometers (Begley and Brightman, 2003), the combined surface area of microvessels in the brain is 150–200 cm^2/g of tissue, equating to ~15–20 m^2 per adult human brain. This elaborate meshwork of microvessels provides blood flow to all brain regions, where every neuron is ~8–20 μm from a blood vessel (Schlageter et al., 1999), and delivers continuous supplies of oxygen, glucose and amino acids to neurons.

Postnatal brain development and subsequent function is shaped by experience

What is the purpose of protracted brain development? Namely that it provides the opportunity for development to be organized by early-life experiences and to fine-tune brain circuitry accordingly (Johnson, 2001). Genetic mechanisms predominate the prenatal period yet, by contrast, the postnatal period relies heavily on environmental input. The timing of environmental input heavily shapes the brain's potential for normative development. The brain is 'experience-expectant'—it assumes that certain signals from the environment will be available at certain points in development, and experiences that take place during highly plastic time windows, also known as sensitive periods, are particularly critical. These sensitive periods are regarded as evolutionarily advantageous because they allow the brain to capitalize on environmental signals (Bick and Nelson, 2016), to shape to the demands of the surrounding environment and propagate survival (Magill et al., 2013), and to facilitate progressively complex cognition, rather than exclusively relying on genetic signalling. However, it also leaves the brain susceptible to negative exposures, such as ELA.

Biological embedding of ELA during sensitive periods

Stress signals a perceived threat, prompting immediate changes in behaviour as well as possible modification of future behaviours. More precisely, exposure to stress activates a physiological response aimed at restoring homeostasis (Lupien et al., 2009), involving

multiple levels of the central nervous system that regulate decision-making, learning and memory, as well as hormonal, autonomic, and emotional responses. Specific types of stressors elicit distinct neuronal populations to perceive threat and mount an adaptive response. For example, physical stressors such as bodily trauma, extreme temperatures, and blood loss activate hypothalamic regions and the brainstem (Fenoglio et al., 2006), whereas psychological stressors engage brain regions that are involved in emotional regulation (the amygdala and the PFC; Salzman and Fusi, 2010), learning and memory (the hippocampus; Battaglia et al., 2011), and decision-making (the PFC; Fellows and Farah, 2007). These systems, however, are interconnected, as physical stress typically elicits a psychological response, and psychological stress can have physical effects. The duration (or chronicity) of stress greatly impacts the physiological response: acute stress prompts a rapid surge in neurotransmission and stimulation of the hypothalamic-pituitary-adrenal (HPA) axis, resulting in glucocorticoid production, which is then followed by a rapid return to baseline levels (Charmandari et al., 2005; Herman et al., 2016). While these transient responses are evolutionarily adaptive, chronic stress complicates this dynamic. Prolonged exposure to stress can lead to a dual outcome where the physiological mechanisms that initially protect the body begin to cause harm, affecting normal functioning in response to daily events. In the face of chronic stress, protection and self-damage emerge as two opposing faces of the body's physiological response against everyday events.

Experience-dependent programming, also known as "biological embedding" (Danese et al., 2011; Miller et al., 2011), is the process by which experiences during the postnatal period instigate a biological response that induce persistent, stable changes in the function of a biological system, with latent consequences for development, behaviour, and health—even into adulthood (Shenhar-Tsarfaty et al., 2015; Chen et al., 2011; Hertzman and Boyce, 2010). The "allostatic overload" paradigm (McEwen, 1998) proposes that adverse exposures during sensitive periods alter emergent neuronal systems (Fox et al., 2010; Nelson and Gabard-Durnam, 2020), giving way to "trajectory effects" where subsequent developmental trajectories are changed; and "cumulative effects", whereby repeated exposure to many adversities in early life elevates the risk of

negative outcome in late life (Felitti et al., 1998; Danese et al., 2009; Flaherty et al., 2013) in a dose-response relationship (McEwen and Gianaros, 2011). Because the brain is not privileged from allostatic load, chronic stress triggers sustained and progressive changes in gene expression, cytoarchitecture, and neuronal firing patterns throughout the brain (Lupien et al., 2009, McEwen et al., 2007) that can be regarded as chronic “wear and tear” to brain health, gradually impairing its function and resilience (Figure 9). There is robust evidence supporting allostatic load conceptualization of the impact that ELA has on health and behavioural outcomes (Rogosch et al., 2011; Piotrowski et al., 2020; Danese and McEwen, 2012; Barboza Solís et al., 2015; Tomasdottir et al., 2015; Widom et al., 2015; Berg et al., 2017; Thayer et al., 2016; Danese et al., 2009; Flaherty et al., 2013; Liu et al., 2013; De Bellis et al., 2014; Nelson et al., 2020; Bellis et al., 2019; Nelles-McGee et al. 2021). As mentioned earlier, children are rarely exposed to a single event or simply one type of adverse experience, which lends to the concept of “cumulative risk”. Importantly, it is the nature *and* number of adverse life events one is exposed to (Felitti et al., 1998, Gershon et al., 2013), the precise timing of exposure (Kaplow and Widom, 2007), severity of ELA, sex of the individual, and presence of predisposing genetic polymorphisms associated with a stress-induced pathology (for e.g., major depressive disorder; MDD; Buchmann et al., 2013; Caspi et al., 2003) that can profoundly disturb biological systems.

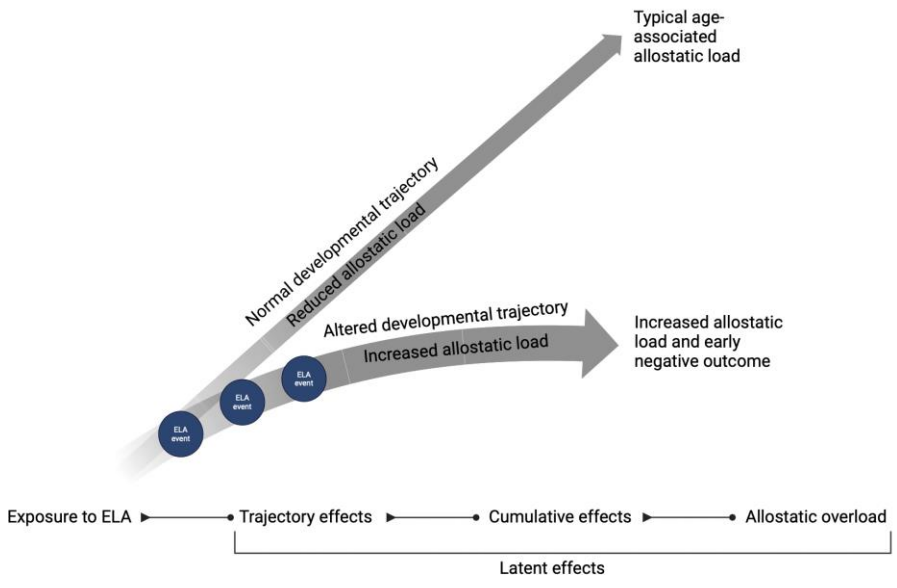

Figure 9: Schematic showing allostatic load conceptualization of the impact that ELA has on health and behavioural outcomes. Chronic stress, such as that induced by ELA experienced during sensitive periods, can hinder recovery to original homeostatic levels and, as a result, a newly defined set point is established over time, leading to deviations away from normative development. Thus, the difference between the new and old set points can be understood as the 'cumulative burden of adaptation to ELA'—i.e., allostatic load.

When trying to understand the etiopathological mechanisms that underlie ELA, neurotoxicity remains at the forefront of possibilities. The “neurotoxicity hypothesis” posits that early and repeated elevation of stress mediators, such as glucocorticoids, hinders growth in stress-sensitive brain regions via mechanisms like oxidative damage (Uno et al., 1994). Stress mediators that may be at work in this context include cortisol, pro-inflammatory cytokines, steroids, excitatory amino acids (e.g., glutamate), neuropeptides and various other molecules (for e.g., brain-derived neurotrophic factor (BDNF)) and endogenous opioids (Joels and Baram, 2009). Each stress operates within its specific spatial and temporal domains and, when triggered by stress, these mediators contribute to allostasis through a complex, interconnected regulatory network. For example, stress-induced glucocorticoids can suppress (Sapolsky et al., 2000) the production of pro-inflammatory cytokines, while catecholamines may enhance it. Similarly, pro- and anti-inflammatory cytokines, produced by various cell types, mutually regulate each other. Furthermore, the sympathetic nervous system plays a critical role in this nonlinear network by influencing all associated systems (Borovikova et al., 2000), while the parasympathetic nervous system generally acts to counterbalance the sympathetic system's effects. Critically, each one of these mediators is understood to impact the function of the neurovasculature (Brezzo et al., 2020; Longden et al., 2014; Krause et al., 2006; Jackson et al., 2022).

The structural and functional consequences of early life adversity on the brain

The consequences of ELA on the structural properties of brain development, as well as regional functionality, have been investigated in a number of studies. It has been consistently found that abused children exhibit reduced brain volumes, with alterations observed in temporal, frontal, parietal, and occipital regions, and in overall cortical gray and white matter volume (De Bellis et al., 1999; De Bellis et al., 2002; Carrion et al., 2001; Hanson et al., 2010; De Brito et al., 2013). Notably, smaller amygdala volumes have been observed in abused children (Hanson et al., 2015), along with an inverse relationship between abuse and amygdala volumes (Edmiston et al., 2011). Similarly,

hippocampal volume shows an inverse relationship with abuse (Edmiston et al., 2011), with decreased hippocampal volumes also observed (Tupler and De Bellis, 2006; Carrion et al., 2007; Rao et al., 2010; Edmiston et al., 2011; Hanson et al., 2015).

Additionally, studies have reported smaller total volumes and lower white matter in the PFC of abused children (De Bellis et al., 2002), although larger volumes have been observed in specific regions such as the middle inferior and ventral regions (Richert et al., 2006; Carrion et al., 2009) and superior/dorsal regions (Carrion et al., 2009). Recent studies have observed changes in PFC regions implicated in cognitive and emotional control, where higher levels of abuse were associated with greater decreases in volume (Edmiston et al., 2011). Notably, reductions were found in the orbitofrontal cortex, a region known for its role in reinforcement-based decision making and emotional regulation (Schoenbaum et al., 2007; Hanson et al., 2010; De Brito et al., 2013; Kelly et al., 2013), and in the dorsolateral prefrontal cortex, which is involved in working memory, cognitive regulation of emotion, and planning (Hanson et al., 2010; Levy and Goldman-Rakic, 2000; Miller and Cohen, 2001; Ochsner et al., 2002).

With regard to structural connectivity of the brain, one group used multimodal neuroimaging to model neurodevelopmental trajectories over childhood with structure–function coupling (SC–FC) and found that a typically general linear decrease in SC-FC with age was replaced by a unique, curvilinear trajectory in the high-adversity group, indicative of accelerated neurodevelopment starting at 4.5 years (Chan et al., 2024). Reductions in total corpus callosum volumes and its anterior and posterior mid-body and splenium subregions have been observed (De Bellis et al., 2002; Teicher et al., 2004; Carrion et al., 2009). An even greater number of studies have described functional alterations in circuitries that support higher-level emotional and cognitive functioning, as demonstrated by cognitive task completion (Pechtel and Pizzagalli, 2011; De Bellis and Hooper, 2012; Carrion et al., 2008; Bruce et al., 2013; Van Veen and Carter, 2002; Roger et al., 2010; Hughes and Yeung, 2011), as well as response to social and emotional input (da Silva Ferreira et al., 2014, Graham et al., 2013, McCrory et al., 2011; Bogdan et al., 2012; White et al., 2012, Cicchetti and Curtis,

2005; Curtis and Cicchetti, 2011; Pollak et al., 1997; Pollak et al., 2001; Shackman and Pollak, 2014).

The macroscopic effects of early life adversity are accompanied by alterations in circuits integral to stress responses (Rodrigues et al., 2009; Bolton et al., 2018; Oomen et al., 2010; Peña et al., 2014), with ever-increasing evidence that these alterations extend to the cellular and molecular levels. For example, ELA is associated with numbers of mature myelinating oligodendrocytes, accompanied by decreased numbers of more immature oligodendrocyte-lineage cells (Tanti et al., 2018) and significant reduction in the thickness of myelin sheaths around small-diameter axons (Lutz et al., 2017). Moreover, a 3-fold increase in the proportion of unmyelinated parvalbumin+ interneurons with a perineuronal net is observed in those with ELA (Théberge et al., 2024), as well as increased densities and morphological complexity of perineuronal net (Tanti et al., 2022). As suggested by these observations, ELA-induced changes are not explained by a single gene, but by hundreds of genes dysregulated over multiple cell types (Kos et al., 2023). Exposure to ELA results in pervasive transcriptional changes in GABAergic and glutamatergic neurons, along with altered neurophysiological responses to subsequent stressors (Kos et al., 2023). Other changes observed are increased expression of OXTR in the anterior cingulate cortex (ACC; Almeida et al., 2022), altered microglial phagocytic capacity (Reemst et al., 2022), increased expression of genes involved in cytokine activity (Schwaiger et al., 2016), altered voltage gated sodium (Na_V) channels properties in NG2+ glia (Treccani et al., 2021), as well as enriched plasticity signatures in females but decreased plasticity enrichment in males (Peña et al., 2019). These widespread molecular consequences of ELA may manifest as temporally-specific transcriptional changes across the life-span (Suri et al., 2014).

The neurovasculature matches pathological brain alterations

Supplied by the neurovasculature, the brain is entirely dependent upon the delivery of oxygen and nutrients provided by circulation (Attwell and Laughlin, 2001; Peters et al., 2004). Because of this dependency, neurons and neurovascular cells form a

functionally integrated network, whereby neuronal activity and cerebral blood flow are tightly coupled, and the metabolic demands of neurons are proportionally matched by blood supply. In the adult brain, the functional coupling between neuronal activity and cerebral blood flow, referred to as “neurovascular coupling”, has been recorded for over a century (Roy and Sherrington, 1890), and has broad implications in health and disease (Cauli and Hamel, 2010; Drake and Iadecola, 2007; Zlokovic, 2010). At birth, remarkably, neurovascular coupling is not functional, with many studies in both humans and rodent models reporting differences in hemodynamic responses in the early postnatal brain compared to adults (Anderson et al., 2001; Born et al., 1996; Kozberg et al., 2013; Meek et al., 1998). At approximately P15, small, localized hemodynamic responses are initially detected within the capillary bed. These responses gradually expand, leading to the dilation of larger arteries that supply the active region. This process continues until it reaches adult-like levels of evoked hyperemia by P23 (corresponding to pre-teen years in humans). These findings clearly demonstrate that the mechanisms required to fully actuate hemodynamic responses still develops and matures postnatally, a conclusion that is highly consistent with the extensive neuronal and neurovascular development in the postnatal brain summarized earlier. After birth, sensory-related neuronal activity refines neurovascular networks into their mature form (Argandona and Lafuente, 2000; Black et al., 1987; Sirevaag et al., 1988), as it does for neuronal circuits (Katz and Shatz, 1996; Zhang and Poo, 2001). Indeed, diminished sensory input—whether through complete deafferentation, genetic impairment at thalamocortical synapses, or reduced sensory-related neuronal activity—leads to decreased endothelial cell proliferation and vascular density in layer IV of the primary somatosensory cortex (Lacoste et al., 2014). Conversely, increased sensory inputs enhance vascular density and branching, demonstrating that neuronal activity can shape the developing vasculature. This suggests that postnatal vascular maturation is driven not only by angiogenic transcriptional programs but also by environmental stimuli (Lacoste et al., 2014).

In light of such observations, one speculates that the neurovasculature may be differentially regulated under pathological conditions in which neuronal activity is

affected, particularly when these conditions occur during sensitive periods. Neurovascular changes in the vmPFC or other brain regions have not yet been explored in adults with histories of ELA or in children with recent adverse experiences. However, based on animal studies, it is plausible that excessive neuronal activation as a result of ELA may similarly trigger long-term deficits in microvascular networks. With regard to neurovascular coupling, mice subjected to chronic stress presented reduced neuronal and hemodynamic responses to forelimb stimuli due to reduced dilation of parenchymal arterioles and decreased smooth muscle$_{KIR}$ current density (Han et al., 2019; Longden et al., 2014). Additionally, mice displayed an inability to increase arterial contractility, which could be attributed to a lower hyperpolarizing contribution from Kv7.4 channels (Staehr et al., 2022). These observations suggest a potential parallel in humans where ELA might similarly impact neurovascular dynamics and resultant brain health. Mice susceptible to chronic stress also show a significant reduction in claudin5 (CLDN5) expression in the nucleus accumbens of males (Menard et al., 2017a) and in the PFC of females (Dion-Albert et al., 2022), regions critical for mood regulation. Other studies have additionally observed malformations of tight junctions in the PFC, hippocampus, and amygdala of rats (Xu et al., 2019**;** Santha et al., 2015). Other iterations of chronic stress have led to vascular leakage, termed microbleeds, scattered stochastically in the brains of stress-susceptible, but not resilient or non-stressed control mice (Lehmann et al., 2018; Lehmann et al., 2020, Lehmann et al., 2022). At the sites of these microbleeds, fibrinogen deposition and angiogenic markers were detected (Lehmann et al., 2020; Lehmann et al., 2022). Transcriptomic profiling of isolated BMECs showed enrichment for pathways involved in neurovascular response to injury that suggest a temporal sequence of inflammation, oxidative stress, growth factor signalling, and wound healing (i.e., platelet aggregation, hemostasis, fibrinogen deposition, and angiogenesis); however, insufficient numbers of microbleeds repair following cessation of stress (Lehmann et al., 2022).

Cerebral microbleeds in humans strongly correlate with peripheral inflammation (Shoamanesh et al. 2015). In fact, where there is vascular and endothelial dysfunction, there is inflammation. Studies consistently report a pro-inflammatory state following

chronic stress, suggesting a closely intertwined pathophysiology between neurovascular function and inflammatory immune pathways. Stress-susceptible mice show cytokine-dependent recruitment of peripheral monocytes into the perivascular space (Menard et al., 2017b; Wohleb et al., 2013; Lehmann et al., 2022) and leakage of the pro-inflammatory cytokine interleukin 6 (IL6) into the brain parenchyma through increased vascular transcytosis (facilitated by downregulated CLDN5; Menard et al., 2017b). Several other rodent studies report complementary iterations of BBB compromise with increased extravasation in several areas of the brain after stress (Sharma and Dey, 1986**;** Skultetyova et al., 1998**;** Gomez-Gonzalez and Escobar, 2009**;** Xu et al., 2019; Solarz et al., 2021). Based on these observations, one might speculate that recruited leukocytes act on BMECs, contributing to the disruption of BBB integrity. However, strictly following the cessation of chronic stress, one study reported the recruitment of anti-inflammatory CCR2+ monocytes to microbleed sites, where they engaged in phagocytosis of fibrinogen, aiding in neurovascular repair (Lehmann et al., 2022). This suggests that the temporal sequelae of immune responses may vary over time, with distinct functions observed during the active phase of chronic stress and after its cessation. Recruitment of these pro-inflammatory mediators from the periphery to the brain are accompanied by a similar activation of the resident immune cells of the brain, microglia, which undergo morphological and functional changes to become active participants in the inflammatory response to chronic stress. Microglia proximal to microbleeds possess transcriptomes enriched for pathways associated with inflammation, phagocytosis, oxidative stress, and extracellular matrix remodeling (Lehmann et al., 2018). Taken together, these findings support a key role for the NVU in etiopathological mechanisms prompted by chronic stress.

Observations made in clinical populations with histories of ELA

Assessing NVU dysfunction in living individuals with histories of ELA is particularly difficult due to the constraints of non-invasive techniques. More invasive techniques that allow for direct characterization of the NVU are not feasible in living subjects; thus, proxy markers suggestive of NVU dysfunction, such as the presence of certain serum

proteins, are used to infer the state of the NVU. Histories of ELA are associated with significantly increased levels of soluble fibrinogen (Zeugmann et al., 2013), an inflammatory marker indicative of cardiovascular and neurovascular disorders, as well as elevated levels of astrocytic S100β (Falcone et al., 2015), a marker of BBB dysfunction. Numerous studies have reported an association between ELA and elevated levels of circulating pro-inflammatory markers, namely acute phase protein C-reactive protein (CRP), and cytokines IL6 and tumor necrosis factor alpha (TNFα; Danese et al., 2009; Baumeister et al., 2016; Matthews et al., 2014; Coelho et al., 2014; Renna et al., 2021). Highly reproducible *in vitro* and *in vivo* evidence has shown that administration of pro-inflammatory cytokines, such as TNFα, IL1β and interferon gamma (IFNγ), results in a dose-dependent increase in BBB permeability via increased expression of ICAM1 and VCAM1 on the luminal surface of BMECs (Zameer and Hoffman, 2003; Henninger et al., 1997; Haraldsen et al., 1996; Becker et al., 1991). However, the robustness of this association is undermined by other studies reporting non-significant results, substantial heterogeneity in experimental design, differences in the definitions and assessment of ELA, the populations studied, and the statistical methods employed (Slopen et al., 2013, Coelho et al., 2014; Carpenter et al., 2012; Kuhlman et al., 2023; Counotte et al., 2019; de Mendonca Filho et al., 2023). A definitive meta-analysis by Baumeister et al. (2016) established a significant association between ELA and certain inflammatory markers, with the largest effect sizes observed for TNFα, followed by IL6, and then CRP, the latter of which has been linked to changes in cortical thickness and subcortical volumes (Orellana et al., 2024). This finding supports the groundbreaking life-course study by Danese et al. (2007), which linked traumatic exposures in the first decade of life to significantly elevated circulating pro-inflammatory markers in adulthood, with the same group later validating this association in ELA-exposed participants of the Dunedin Multidisciplinary Health and Development Study (Danese et al., 2009, Danese et al., 2009). Indeed, elevated TNFα, IL6 and CRP seem to be repeat offenders in their ability to linger into adulthood (Miller and Cole, 2012; Archer et al., 2012; Bertone-Johnson et al., 2012; Carpenter et al., 2010; Carroll et al., 2013; Danese et al., 2009; Danese et al., 2009; Baumeister et al., 2016; Matthews et al., 2014, Coelho et al., 2014; Dennison et al., 2012; Di Nicola et al., 2013;

Frodl et al., 2012; Gouin et al., 2012; Hartwell et al., 2013; Hepgul et al., 2012; Kiecolt-Glaser et al., 2011; Lacey et al., 2013; Lu et al., 2013; Rooks et al., 2012; Slopen et al., 2010; Pedrotti Moreira et al., 2018; Bertone-Johnson et al., 2012; Hartwell et a., 2013). Other elevated pro-inflammatory markers emerge in ELA-exposed populations, including IL1β (Hartwell et al., 2013; Lu et al., 2013), TGFB1 (Tietjen et al., 2012), b-FGF, IL1, TGFβ3, VEGF (Lu et al., 2013), fibrinogen (Coelho et al., 2014).

Another clinical observation that is telling of vascular and endothelial dysfunction in those with ELA is the dose-dependent association between exposure to adverse childhood experiences (ACEs) and the incidence of cardiovascular disease (CVD; Zou et al., 2024), such as ischemic heart disease and stroke (Chen et al., 2023; Fuller-Thomson et al., 2010; Loucks et al., 2014; Thurston et al., 2017; Thurston et al., 2014; Riley et al., 2010; Su et al., 2015; Dong et al., 2004). This association was first highlighted in the landmark CDC-Kaiser Permanente ACE study (Felitti et al., 1998), and has been consistently supported by subsequent research, including a 2017 systematic review where 92% of studies confirmed the association between ACEs and CVD (Basu et al., 2017). This is, perhaps, unsurprising for the reason that corticotropin-releasing hormone, released during HPA activation, leads to increases in heart rate, cardiac output, and mean arterial pressure by norepinephrine and epinephrine secretion (Nijsen et al., 2000), as well as direct regulatory actions on nitric oxide-dependent vasodilation and vascular permeability (Hillhouse et al., 2006). With pathophysiological mechanisms by which ELA promotes CVD largely identified from pre-clinical mouse models of chronic stress (Ho et al., 2016), these mechanisms are now being translated to human adults (Jenkins et al., 2021). Specifically, young adults moderate-to-severe ELA demonstrate multiple indicators of vascular dysfunction in the medial prefrontal cortex (mPFC): endothelial dysfunction (as measured by flow-mediated dilation; Jenkins et al., 2021; Rodriguez-Miguelez et al., 2022), arterial stiffening (Kellum et al., 2023; Rafiq et al., 2020), increased vascular resistance across small, conduit, and large blood vessels, as well as reduced blood flow of the mPFC region (Rodriguez-Miguelez et al., 2022). Higher systolic and diastolic blood pressure may underlie these changes in the mPFC vasculature. As described in previous

sections, decreased vmPFC activity is observed in individuals with ELA, and decreased vmPFC activity contributes to elevated blood pressure. Critically, the described relationship between ELA and vascular dysfunction remains robust, even in the absence of group differences for circulating lipids, glucose, or physical activity (Jenkins et al., 2021); and persists even after adjusting for smoking, and illicit drug use (Su et al., 2015).

Factors moderating the impacts of early-life adversity

A key insight from both human and animal studies is that the effects of ELA on epigenomic, transcriptomic, and behavioural outcomes are influenced by individual differences. These differences include factors such as sex, age, and the specific characteristics of the abuse, including its type, duration, and severity (Barnett Burns et al., 2018). One possible explanation is that various factors may influence where an individual's tolerance threshold to stress lies. Indeed, theoretical frameworks such as the two-hit and three-hit models of stress vulnerability suggest that the adverse effects of stress exposure are contingent upon a threshold that differs from one person to another. These models postulate that multiple "hits" or adverse events across different stages of life or simultaneously can cumulatively affect an individual's resilience to stress, ultimately impacting their vulnerability to physiological or psychological disorders (Calabrese et al., 2007; Daskalakis et al., 2013; De Kloet et al., 1998; Danielsdottir et al., 2014; Ahn et al., 2024; Alon et al., 2024).

Significant sex differences exist in the incidence, manifestation, and treatment outcome and side effects of many neurological, psychiatric, and stress-induced disorders (Altemus et al., 2014; Bale and Epperson, 2017; Parekh et al., 2011). Furthermore, the majority of research into the neurobiological bases of disorders, development of new treatments, and identification of risk factors has predominantly focused on male subjects or has not adequately considered sex differences. Across various species, there are notable sex differences in the amount of biological and behavioural investment in reproduction, as well as differences in gestation and/or postnatal care, with females

making considerably greater investment in rearing offspring. These differences likely influence the evolution of sex-specific traits in the brain and body, supporting roles in resource acquisition, bonding, protection, and mate selection through signals like visual, chemical, auditory, motor, and tactile cues. For instance, in certain bird species, brain regions are specifically adapted for song learning, production, and reception (Gontard-Danek and Møller). These adaptations are driven by different pressures on males and females; males use song to attract mates, while females assess song quality to select suitable partners (Gontard-Danek and Møller). In environments marked by adversity, such as resource scarcity or predation, these signalling systems might adapt differently. For example, males in resource-poor settings might decrease their song vigor, while females could alter their standards for song quality. Consequently, ELA could differently influence brain development in males and females, leading to region-specific brain changes geared towards survival and reproductive behaviours. Thus far, chromosomal and epigenetic drivers of neurodevelopment in the male and female brain have been identified. These drivers differentially affect parental genetic imprinting, epigenetic programming of gene expression, hormonal effects, and sex differences in immune function and activation (Bordt et al., 2020; VanRyzin et al., 2020) and, in turn, affect neurogenesis, circuit assembly, pruning, plasticity, timing of neurodevelopmental events, and downstream gene expression (McCarthy et al., 2012) in a constellation of cells within the brain (neuronal, glial, vascular, and immune) as well as their sensitivity to both internal signals (hormonal, neuronal, and immune) and external ones (pre- and postnatal environment). Sex-specific differences in the adult pro-inflammatory state have only recently been underscored by systematic comparisons between males and females, indicating more severe implications for females who experience ELA. One study established that the correlation between ELA and CRP levels is primarily driven by adult females, regardless of the type or multiplicity of abuse encountered (Baldwin et al., 2018). These factors make it challenging to address sex differences in response to ELA; despite this, some rodent studies have shown that males appear to be more prone to anxiety-like and cognitive outcomes following ELA (Llorente et al., 2009; Loi et al., 2014; Sutanto et al., 1996), whereas other studies have found that female rodents are more sensitive to ELA in other behavioural domains (Fuentes et al., 2014; Gracia-Rubio

et al., 2016; Sasagawa et al., 2017). Neurobiological sex differences have also been described, such that ELA hinders neurogenesis in pre-pubertal females, but promotes neurogenesis in pre-pubertal males (Loi et al., 2014; Oomen et al., 2009). It is reasonable to suggest that baseline differences in epigenetic and transcriptional programs may underlie sex-specific vulnerabilities (Jessen and Auger, 2011; Labonte et al., 2017), yet studies must simultaneously examine the impact of ELA on brain development in both sexes, analyzing changes across implicated brain regions to fully understand these differences.

The timing and duration of early life adversity (ELA) significantly influence the nature and extent of its effects. Specifically, the developmental period during which ELA occurs can critically affect the type, direction, and magnitude of behavioral, epigenetic, and transcriptomic changes (Bai et al., 2012; Molet et al., 2014; Peña et al., 2013). This is partly because different brain regions have distinct neurodevelopmental timelines and periods of plasticity, which can affect how and when they are impacted by ELA. Additionally, the cumulative effects of ELA can manifest over an individual's lifespan. For example, evidence suggests that while males exposed to ELA may exhibit resilience during adolescence, they typically display deficits later in adulthood (Blaze et al., 2013; Loi et al., 2014; Suri et al., 2014; Suri et al., 2013). These findings highlight the complexity of the impacts of ELA and underscore the importance of considering the timing of adversity in developmental studies.

Although ELA is strongly associated with an increased risk of adult psychopathology, research into how specific adversities impact epigenomic and transcriptomic patterns has yielded inconsistent results (Barnett Burns et al., 2018). While some studies suggest that particular types of ELA are linked to specific outcomes (Houtepen et al., 2016; Kang et al., 2013; Melas et al., 2013; Perroud et al., 2011), larger international studies indicate that the cumulative effect of multiple adversities may better explain the connection between ELA and psychopathological outcomes than any single type of stressor (Green et al., 2010; Kessler et al., 2010; MacMillan et al., 2001). For example, Teicher and colleagues demonstrated that exposure to multiple forms of ELA leads to

significantly more deleterious effects than merely the sum of its parts (Teicher et al., 2006) and, as reported by Perroud and colleagues, the severity of childhood sexual abuse *and* the number of different types of abuse positively correlated with glucocorticoid receptor (NR3C1) methylation (Perroud et al., 2011). These findings echo the allostatic load conceptualization of ELA, as previously discussed.

From tissue homogenates to cell-type specific approaches

Gene expression is fundamental to understanding disease manifestation and progression. Differential gene expression, which is ubiquitously regarded as a quantifiable proxy for variances in gene activity, reveals how genes are expressed differently between pathologic and healthy states, allowing inferences to be made as to which molecular mechanisms underlie disease. These genes often regulate essential neurobiological functions such as cell signalling or immune responses. Bulk-tissue RNA sequencing yields an average gene expression profile from a mixed group of heterogeneous cell types, but it does not distinguish the specific expression patterns of individual cell populations. Because not all cell types contribute equally to disease progression (Skene et al., 2018), bulk tissue analyses may mask the roles of specific cells crucial to the development of disease. Consequently, it is essential to analyze gene expression specifically in implicated cell types to gain more precise biological insights—a notion that also applies to the neurobiological consequences of ELA. For instance, findings in Alzheimer's disease (Mathys et al., 2023), autism spectrum disorders (Velmeshev et al., 2019), and schizophrenia (Skene et al., 2018; Torshizi et al., 2020a; Torshizi et al., 2020b) have all demonstrated how specific cell types are most relevant to respective pathologies. It is conceivable that ELA may disproportionately impact specific cell populations (Habib et al., 2016; Lake et al., 2016, 2018; Nagy et al., 2020). However, many studies on the molecular changes associated with ELA have relied on analyses of bulk-tissue homogenates, obscuring finer distinctions, and making it difficult to determine whether observed differences are due to the disease state, variations in cellular composition, or technical artifacts. As a result,

employing targeted enrichment strategies is essential to effectively parse tissue heterogeneity in transcriptomic analyses.

An integrative model of the long-term consequences of early-life adversity

Thus far, this introduction has laid down a theoretical framework for how ELA might alter trajectories of neurodevelopment, postulating potential effects at the NVU. Given that neurovascular function is highly responsive to environmental signals, and its regulatory properties are ubiquitous throughout brain health and functionality, the NVU poses as an interesting avenue for exploring the long-term impacts of ELA. But other significant advances have already been made in understanding the pervasive effects of ELA, particularly the molecular mechanisms that are involved within the brain. Seminal findings of molecular pathways that are altered by ELA have been investigated on a system-by-system basis, and, altogether, ELA is associated with dysregulation of the HPA-axis, neurotrophins and plasticity, myelination, as well as GABAergic, glutamatergic, serotonergic and neuropeptidergic signalling (Schar et al., 2022; Maniam et al., 2014; Birnie et al., 2020; Lutz et al., 2017; Tanti et al., 2018; Karst et al., 2023; Haikonen et al., 2023; Ramkumar et al., 2024; Ellis et al., 2021). Disturbances in these molecular pathways have been shown to explain, at least in part, ELA-associated structural and functional differences in circuits involved in threat detection, emotional regulation, stress-reactivity, reward anticipation and social cognition (Bick and Nelson, 2016; Kim et al., 2013; Teicher et al., 2016; Tottenham et al., 2010). Consequently, they impact the observed macroscopic cytoarchitectural aspects such as cortical thinning and other structural alterations in regions that regulate mood and emotions (Bick and Nelson, 2016; Edmiston et al., 2011; Teicher and Samson, 2016; Teicher et al., 2016). Functionally, these structural changes are likely to translate into stable behavioural phenotypes, where humans with a history of ELA typically show high levels of impulsivity and aggressive behaviours, high anxiousness trajectories, interpersonal difficulties, and impaired executive function (Brodsky et al., 2001; Hostinar et al., 2012; Johnson et al., 2002; Sinclair et al., 2007; Wanner et al., 2012; Yang and Clum, 2000). Critically, these behavioural phenotypes have all been shown to associate with suicidal

behaviour (Turecki, 2014; Turecki and Brent, 2016). Future research, however, is needed to better understand how ELA-induced neurovascular dysfunction contributes to behavioural changes associated with psychopathology.

From a mechanistic standpoint, it remains unclear how ELA may elicit neurovascular dysfunction in humans, or how neurovascular dysfunction integrates with other system disturbances. Although the BBB is functionally distinct from the peripheral vasculature and possesses a highly specialized NVU to precisely regulate the influx and efflux between the blood and brain parenchyma (Daneman and Prat, 2015; Kadry et al., 2020; Luissint et al., 2012), the entire blood supply of the brain relies on the dorsal aorta (Purves et al., 2001). This reliance therefore raises the question of whether the NVU might also be susceptible to the systemic vascular effects of ELA, if the vasculature of the body is vulnerable to the effects of ELA, then why not vasculature of the brain as well?

Hypotheses and aims

As reviewed in previous sections, ELA leads to long-lasting adaptations in transcriptomic programs within the brain, pointing to potentially profound implications for neurovascular function and BBB integrity. While these studies have been crucial to our understanding of ELA, those conducted using human postmortem brain samples have primarily focused on non-vascular components, such as neurons and myelin. Although a rich body of animal studies underscores the perturbations induced by ELA on the NVU, the translation of these findings to human pathology is entirely absent due to the scarcity of studies leveraging direct and invasive techniques in postmortem brain samples. The complexity of the NVU, and its critical role in mediating responses between the brain parenchyma and peripheral circulation, establishes it as a pivotal but underexplored target in understanding the pathogenic sequelae of ELA. The overarching goal of this dissertation is to, therefore, expand our understanding of the NVU-specific molecular changes associated with a history of childhood abuse in the human brain***. Our general hypothesis was that a history of ELA would be associated with transcriptomic changes indicating NVU-specific dysfunction in the vmPFC of depressed suicides with a history of ELA. A secondary hypothesis was that a signature of a pro-inflammatory state, as evidenced by specific gene expression profiles, would be observed alongside NVU dysfunction.***

Aim 1: Develop a method for the effective enrichment and isolation of microvessels from frozen brain tissue that is compatible with high throughput techniques.

Given our overarching goal, the necessity to develop a method that enabled the compressive characterization of postmortem brain vessels *ex situ* became evident. Here, we share our methodology that seeks to bridge this gap by introducing a standardized protocol for the isolation of microvessels from postmortem human brain tissues. The development of this simple method was not only critical and foundational to our subsequent work investigating NVU changes in ELA, but also serves as a valuable tool for anyone studying the NVU in any disease context who wishes to perform translational work using postmortem brain tissue. This aim is explored in Chapter II.

Aim 2: Isolate microvessels from the postmortem vmPFC of healthy controls and depressed suicides with a history of ELA, and process samples for bulk RNA sequencing.

Prior to Aim 2, direct evidence implicating NVU dysfunction in the pathophysiology of ELA has relied primarily on rodent models of chronic stress. Leveraging the isolation method outlined in our previous study (Aim 1), we set out to generate the first transcriptomic dataset derived from intact microvessels isolated from human vmPFC samples from healthy controls and matched depressed suicides with a history of ELA. This aim is explored in Chapter III.

Aim 3: Perform differential gene expression and network-based analyses to identify gene candidates implicated in ELA, after which differential expression of gene candidates are validated *in situ* using fluorescence in situ hybridization (FISH) on vmPFC tissue sections.

In Aim 3, we combined differential gene expression analysis and network-based approaches to provide an integrative and unbiased characterization of NVU specific transcriptional profiles in humans with histories of ELA. After identifying key differentially expressed genes in ELA, differential expression of two gene candidates was validated using FISH on vmPFC tissue sections from healthy controls and depressed suicides with a history of ELA.

We anticipate that these experiments will add to our understanding of the neurovascular dysfunction through which ELA contributes to stress-induced pathologies in the adult brain by identifying key differentially expressed genes that belong to impacted neurovascular pathways.

Simplicity is the ultimate sophistication.

Attributed to Leonardo da Vinci
Renaissance man in art, science, and engineering

Chapter II

Universal method for the isolation of microvessels from frozen brain tissue: A proof-of-concept multiomic investigation of the neurovasculature

Marina Wakid,[a,b] Daniel Almeida,[a,b] Zahia Aouabed,[a] Reza Rahimian,[a] Maria Antonietta Davoli,[a] Volodymyr Yerko,[a]Elena Leonova-Erko,[a] Vincent Richard,[d] René Zahedi,[d] Christoph Borchers,[d] Gustavo Turecki,[a,b,c] and Naguib Mechawar[a,b,c,*]

[a]McGill Group for Suicide Studies, Douglas Research Centre, Montréal, Quebec, Canada
[b]Integrated Program in Neuroscience, McGill University, Montréal, Quebec, Canada
[c]Department of Psychiatry, McGill University, Montréal, Quebec, Canada
[d]Segal Cancer Proteomics Centre, Lady Davis Institute for Medical Research, Jewish General Hospital, McGill University, Montréal, Quebec, Canada

Published in Brain, Behaviour, & Immunity – Health. 2023 Dec; 34: 100684.
Published online 2023 Sep 21. doi: 10.1016/j.bbih.2023.100684

Abstract

The neurovascular unit, comprised of vascular cell types that collectively regulate cerebral blood flow to meet the needs of coupled neurons, is paramount for the proper function of the central nervous system. The neurovascular unit gatekeeps blood-brain barrier properties, which experiences impairment in several central nervous system diseases associated with neuroinflammation and contributes to pathogenesis. To better understand function and dysfunction at the neurovascular unit and how it may confer inflammatory processes within the brain, isolation and characterization of the neurovascular unit is needed. Here, we describe a singular, standardized protocol to enrich and isolate microvessels from archived snap-frozen human and frozen mouse cerebral cortex using mechanical homogenization and centrifugation-separation that preserves the structural integrity and multicellular composition of microvessel fragments. For the first time, microvessels are isolated from postmortem ventromedial prefrontal cortex tissue and are comprehensively investigated as a structural unit using both RNA sequencing and Liquid Chromatography with tandem mass spectrometry (LC-MS/MS). Both the transcriptome and proteome are obtained and compared, demonstrating that the isolated brain microvessel is a robust model for the NVU and can be used to generate highly informative datasets in both physiological and disease contexts.

Keywords: Neurovascular unit, Blood-Brain Barrier, Microvessels, Postmortem, RNA sequencing, LC-MS/MS

Highlights

- Method presents singular protocol to isolate microvessels from postmortem and frozen mouse cortex.
- High yield of microvessels with preserved integrity were isolated, and compatible with high-throughput techniques.
- The transcriptome and proteome of isolated microvessels from human vmPFC tissue were characterized.
- Limitations of past isolation methods are overcome, and standardized cross-species comparisons are made possible.

1. Introduction

To meet the metabolic needs of the 86 billion neurons in the human brain, an elaborate 400 mile-long microvascular network (Iadecola, 2017; Kisler et al., 2017) supplies blood flow to the deep structures of the cerebral hemispheres and gatekeeps blood-brain barrier (BBB) properties. Extensive research efforts have underscored the BBB as a highly selective cellular system. Ultrastructurally, the BBB consists of continuous non-fenestrated brain microvascular endothelial cells (BMECs) that precisely regulate movement between the blood and brain interface through the expression of specialized solute carriers and efflux transporters (Daneman, 2012; Betz and Goldstein, 1978; Betz et al., 1980; Cordon-Cardo et al., 1989; Thiebaut et al., 1989; Loscher and Potschka, 2005a; Mittapalli et al., 2010; Zlokovic, 2008). BMECs, along with astrocytic endfeet and mural cells (pericytes or smooth muscle cells), positioned at the vascular basement membrane, are the cell types that comprise the neurovascular unit (NVU) (McConnell et al., 2017) and work in concert to implement coordinated vascular responses to central and peripheral signals. Such responses include the continuous delivery of oxygen and glucose to neurons (Mintun et al., 2001; Hoge et al., 1999; Fox et al., 1988; De Vivo et al., 1991; Farrell and Pardridge, 1991; Gerhart et al., 1989), homeostatic maintenance of the brain (Jeong et al., 2006; Gendelman et al., 2009; Wilhelm et al., 2007; Mokgokong et al., 2014; Smith and Rapoport, 1986), the regulation of cerebral blood flow (Mathiesen et al., 1998; Caesar et al., 2003; Iadecola, 1993; Roy and

Sherrington, 1890; Fergus and Lee, 1997) and clearance of interstitial fluid (Verheggen et al., 2018; Deane et al., 2009; Iliff et al., 2012; Iliff et al.). An underappreciated lens through which to investigate disease, NVU dysfunction contributes to cognitive decline in Aβ and tau pathology (Iturria-Medina et al., 2016; Montagne et al., 2015; Sweeney et al., 2015; Arvanitakis et al., 2016; Toledo et al., 2013; Rosenberg, 2014), traumatic brain injury (Stein et al., 2002; Schwarzmaier et al., 2010; Dietrich et al., 1994; del Zoppo and Mabuchi, 2003; Schroder et al., 1998; von Oettingen et al., 2002; Shapira et al., 1993; Baldwin et al., 1996; Hicks et al., 1997; Baskaya et al., 1997), perivenous myelin lesions presented in multiple sclerosis (Gaitan et al., 2013; Buch et al., 2021; Geraldes et al., 2020; Al-Louzi et al., 2022; Khan et al., 2010; Doepp et al., 2011), as well as multiphasic changes in BBB permeability after stroke (Liu et al., 2018; Lin et al., 2008; Strbian et al., 2008; Durukan and Tatlisumak, 2009; Pillai et al., 2009). Disease states may arise when BBB function can no longer match the needs of the central nervous system (CNS), which confers dire consequences for the ability of the BBB to communicate both with cells within the brain parenchyma and with cells in the periphery. Indeed, the BBB acts as the interface between the brain and peripheral systems through which neuroimmune interactions occur (Quan and Banks, 2007)and is highly responsive to immune activity encroaching the brain. Such interactions include, but are not limited to: regulation of major efflux transporter P-glycoprotein 1 (ABCB1), endothelial Toll-like receptor and NOD-like receptor activation by TNFα signalling (Erickson and Banks, 2018; Nagyoszi et al., 2010, 2015), as well as modulation of Na–K–Cl cotransporter, which is critical for cerebral ionic homeostasis, by IL6 secretion from astrocytes (Sun et al., 1997). The BBB itself secretes substances that interact with the neuroimmune system, including cytokines, prostaglandins, and nitric oxide (Fabry et al., 1993; Mandi et al., 1998; McGuire et al., 2003; Reyes et al., 1999). These substances may be constitutively expressed or pathologically induced, as shown by IL8 in HIV infection (Hofman et al., 1999), invasion of autoreactive $CD4^+$ T cells in multiple sclerosis (Traugott et al., 1983), microglial release of TNFα with cocaine exposure (Lewitus et al., 2016), and nitric oxide release in Alzheimer's disease (Dorheim et al., 1994). Because of its bipolar nature, dysfunction of the BBB can arise from, and be further aggravated by, either the CNS or peripheral compartments. Evidence of

neurovascular dysfunction has similarly been observed in bipolar disorder (Kamintsky et al., 2020), schizophrenia (Kirkpatrick and Miller, 2013; Axelsson et al., 1982; Campana et al., 2023; Goldwaser et al., 2022), major depressive disorder (Torres-Platas et al., 2014; Gal et al., 2023; Najjar et al., 2013), and Parkinson's disease (Al-Bachari et al., 2020; Fowler et al., 2021).

Our understanding of neurovascular development and function has been advanced largely by mouse models. Functional characteristics of the BBB are regulated at the transcriptomic level and, in recent years, different methodologies have been employed to investigate the neurovascular transcriptome. Single-cell sequencing studies have leveraged transgenic-reporter claudin-5-GFP (Vanlandewijck et al., 2018; He et al., 2018), Tie2–eGFP (Zhang et al., 2014), and Pdgfrb-eGFP (He et al., 2016a) mouse lines in conjunction with fluorescence-activated cell sorting (FACS) to generate highly informative transcriptomic datasets of mouse BMECs and other vascular cell types, whereas other studies have carried out RNA sequencing of BMECs isolated from Rosa-tdTomato; VE-Cadherin-CreERT2 mouse models of stroke, multiple sclerosis, traumatic brain injury and seizure (Munji et al., 2019). While past mouse data have provided precious insight into defining core NVU gene expression and underscores the relevance of transcriptomic profiling for better understanding neurovascular function (and dysfunction), recent breakthroughs demonstrate that there are numerous species-specific differences between mouse and human neurovasculature, including solute carrier and efflux transporter expression (Munji et al., 2019; Garcia et al., 2022; Yang et al., 2022). Such findings reveal the partial utility of animal models for studying disease of the human CNS. Due to the scarcity of well-preserved human brain tissue available for research, transcriptomic profiling in human brain samples has been considerably more limited, leaving the investigation of vascular cells neglected in favour of non-vascular cell types, such as neurons and oligodendrocytes. In addition, single-cell or single-nucleus sequencing used to profile expression in *all* cell populations yield very low populations of endothelial cells and pericytes from human adult and embryonic cortex samples despite vessel density ranging between 361 and 811 vessels/mm^2 (Klein et al., 1986; Wu et al., 2004; Weber et al., 2008) at an overall

endothelial cell density of 4504 ± 2666 cells/mm^2 (Ventura-Antunes et al., 2022). Such techniques seem to deplete vascular cells/nuclei for reasons that are not understood and have impeded analysis of human neurovascular transcriptomes (Nagy et al., 2020; Velmeshev et al., 2019; Mathys et al., 2019; Grubman et al., 2019; Jakel et al., 2019). Recently, detailed transcriptome-wide atlases of human and mouse brain vascular nuclei were generated by two independent groups (Garcia et al., 2022; Yang et al., 2022), both addressing the underrepresentation of vascular cell types and elaborating on species-specific differences in NVU gene expression. Such progress and tools deepen our understanding of human NVU function, yet certain limitations that persist challenge further progress in the field: single-cell and single-nucleus sequencing remains inaccessible to many due to high costs and lack of bioinformatic expertise. Moreover, there is heavy reliance on brain banks for well-characterized frozen human brain tissue, which also requires considerable adaptation of techniques initially optimized for fresh tissue and creates even further disparity in how mouse and human brain tissue are utilized, even with the same experimental question in mind. The biological and bioinformatic biases these experimental decisions create and their extent are unknown. Understanding the molecular mechanisms of NVU dysfunction can be achieved by examining gene expression changes in brain microvessels in different disease contexts; and the limited number of existing human neurovascular datasets motivates transcriptomic characterization of more human samples. While it is understood that BMECs perform the BBB function and that other vascular-associated cell types critically regulate that function, the study of microvessels as a preserved unit provides greater insight into the neurovasculature in a manner that dissociated cell types cannot. To this aim, we use a singular, standardized protocol to enrich and isolate microvessels from archived snap-frozen human and frozen mouse cerebral cortex using mechanical homogenization and centrifugation-separation that is gentle enough to dissociate brain tissue while preserving the structural integrity and multicellular composition of microvessel fragments.

The common issue of multiple or contaminating cell types in samples used for tissue-derived RNA sequencing has been largely eliminated by single-cell workflows.

However, single-cell and single-nucleus workflows introduce other significant challenges: measurements typically suffer from large fractions of observed zeros, possibly due to technical limitations or randomness (Hicks et al., 2018; Bacher and Kendziorski, 2016). Moreover, tissue dissociation and storage biases can induce unwanted transcriptomic alterations and cell type composition differences (Denisenko et al., 2020). Because of this, bulk and single-cell sequencing are complementary strategies in which the former approach warrants a versatile and effective method for isolating the NVU from human brain. Several approaches attempting to investigate the isolated NVU have been developed in the past, albeit with major drawbacks: FACS-sorting with antibodies against PECAM1/CD31 and CD13 (targeting the endothelial cell membrane and pericyte cell membrane, respectively) require fresh brain tissue (Yang et al., 2022), as do other iterations of microvessel isolation for cell culture expansion (Navone et al., 2013; van Beijnum et al., 2008). Opting instead for selective capture of endothelial and other vascular-associated cells from frozen human brain by laser capture microdissection (LCM) (Kinnecom and Pachter, 2005; Mojsilovic-Petrovic et al., 2004; Harris et al., 2008; Song et al., 2020a) demands considerable optimization if microvessels are to be used for high-throughput applications downstream (Almeida and Turecki, 2022). Finally, past attempts at microvessel isolation from frozen brain homogenates have only yielded samples suitable for qPCR and Western blot (Bourassa et al., 2019), and more comprehensive knowledge obtained from high-throughput techniques is currently lacking from such studies. Critically, microvessels isolated using the described method are in high yield, possess all major vascular-associated cell types, and maintain their *in situ* cellular structure, making them suitable for characterization using high-throughput techniques. The advantages of this simple protocol are manifold: it does not require the experimental setup needed by single-nucleus sorting, nor does it require transgenic mice (Lee et al., 2019), enzymatic dissociation (Crouch and Doetsch, 2018; Lee et al., 2019; Spitzer et al., 2023), or fresh brain tissue (Crouch and Doetsch, 2018; Lee et al., 2019; Spitzer et al., 2023). Importantly, this is the first standardized microvessel isolation method demonstrated to work with snap-frozen brain tissue and that is compatible across high-throughput

downstream applications, removing unknown biases introduced by the use of varied isolation methods.

We have successfully applied the described protocol to postmortem ventromedial prefrontal cortex (vmPFC) tissue from individuals having died suddenly with no neurological or psychiatric disorder as well as mouse forebrain tissue, as proof of concept that the same procedure can be used in both species. To demonstrate the utility of microvessels isolated from postmortem vmPFC tissue, we processed 5 samples of extracted total RNA and 3 samples of extracted total protein using RNA sequencing and liquid chromatography with tandem mass spectrometry (LC-MS/MS), respectively. Moreover, we sorted endothelial nuclei from isolated microvessels using fluorescence-activated nuclei sorting (FANS) as proof of concept that specific neurovascular cell types may be further purified if needed. Bioinformatic processing and analysis of human transcriptomic and proteomic data indicated that isolated samples showed major enrichment for BMEC, pericyte, SMC, and astrocytic endfeet components at both the mRNA and protein level, generating the first multiomic datasets from human brain microvessels.

2. Materials

2.1. Biological materials

2.1.1. Human cortex This study was approved by the Douglas Hospital Research Ethics Board and written informed consent from next of kin was obtained for each individual included in this study. For each individual, the cause of death was determined by the Quebec Coroner's Office and medical records were obtained. Samples were obtained from Caucasian individuals having died suddenly with no neurological or psychiatric disorder (Table 1). Postmortem brain tissues were provided by the Douglas–Bell Canada Brain Bank (www.douglasbrainbank.ca). Frozen grey matter samples were dissected from the vmPFC (Brodmann area 11) by expert brain bank staff stored at −80 °C. The postmortem interval (PMI) is a metric for the delay between an individual's death, the collection and processing of the brain. To assess RNA quality, RNA integrity number (RIN) was measured for brain samples using tissue homogenates, with an

average value of 5.34. A total of 5 subjects were subjected to RNA sequencing and 3 subjects were subjected to Liquid Chromatography with tandem mass spectrometry (LC-MS/MS).

Note: *All experiments involving the use of human brain samples must be performed in accordance with the relevant institutional and national regulations. Use of postmortem tissues was approved by the Institutional Review Board of the Douglas Hospital.*

2.1.2. Mouse cortex Male C57BL/6J mice (n = 2) aged between 120 and 126 days of age were bred, housed, and cared for in accordance with the Canadian Council on Animal Care guidelines (CCAC; http://ccac.ca/en_/standards/guidelines), and all methods were approved by the Animal Care Committee from the Douglas Institute Research Center under protocol number 5570. Mice were housed in standard conditions at 22 ± 1 °C with 60% relative humidity, and a 12-h light-dark cycle with food and water available *ad libitum* (Isingrini et al., 2017). Following pertinent guidelines and regulations, the mice were anesthetized via intraperitoneal injection of ketamine (10 mg/ml)/xylazine (1 mg/ml) and transcardially perfused with cold PBS 1X. The frontal cortices were removed and immediately frozen in liquid nitrogen and then stored at −80 °C.

2.2. Reagents

- Sucrose (Fisher Scientific, cat. no. S5-500)
- Bovine serum albumin (Sigma-Aldrich, cat. no. A3912)
- DEPC-treated water (Invitrogen™, cat. no. 46–2224)
- SIGMA*FAST*™ BCIP®/NBT tablets (Sigma-Aldrich, cat. no. B5655-25TAB)
- Ethanol 70% (vol/vol) and 100% (Sigma-Aldrich)
- Methanol 100% (Sigma-Aldrich)
- 1X Phosphate buffered saline (*Wisent Bioproducts, D-PBS,* cat. no. 311-425-CL)
- Single Cell RNA Purification Kit (Norgen Biotek Corp., cat. no. 51800)
- TapeStation RNA ScreenTape (Agilent, cat. no. 5067–5576) or TapeStation High Sensitivity RNA ScreenTape (Agilent, cat. no. 5067–5579)
- TapeStation RNA ScreenTape sample buffer (Agilent, cat. no. 5067–5577) or TapeStation High Sensitivity RNA ScreenTape sample buffer (Agilent, cat. no. 5067–5580)

- SMARTer Stranded Total RNA-Seq Kit v3 - Pico Input Mammalian (Takara Bio Inc., cat. no. 634485)
- NucleoMag NGS Clean-up and Size Select beads (Takara Bio Inc., cat. no. 744970.50)
- 0.5% Triton X dissolved in PBS (Triton X-100 from Thermo Fisher Scientific, cat. no. AAA16046AE)
- Normal donkey serum (Jackson ImmunoResearch Laboratories Inc., cat. no. 017-000-121)
- Recombinant Alexa Fluor® 647 Anti-ERG antibody [EPR3864] (Abcam, cat. no. ab196149)
- Anti-Aquaporin 4 antibody [4/18] (Abcam, cat. no. ab9512)
- Anti-Claudin 5 antibody (Abcam, cat. no. ab15106)
- Anti-Laminin antibody (Sigma-Aldrich, cat. no. L9393)
- Anti-Myelin Basic Protein antibody (BioLegend, cat. no. *SMI-99P)*
- Anti-NeuN antibody, clone A60 (Sigma-Aldrich, cat. no. MAB377)
- Anti-PDGFRB monoclonal antibody (G.290.3) (Thermo Fisher Scientific, cat. no. PIMA515143)
- Anti- PECAM-1 antibody (JC70) (Santa Cruz Biotechnology Inc., cat. no. sc-53411)
- Anti-Vimentin antibody [RV202] (Abcam, cat. no. ab8978)
- VECTASHIELD® Antifade Mounting Medium with DAPI (Vector Laboratories, cat. no. H-1200-10)
- VECTASHIELD® Vibrance Antifade Mounting Media (Vector Laboratories, cat. no. H-1700-10)
- Single Cell RNA Purification Kit (Norgen Biotek Corp., cat. no. 51800)
- Hoechst 33342 (Invitrogen™, cat. no. H3570)
- cOmplete™ EDTA-free Protease Inhibitor Cocktail *(Roche,* cat. no. 04693132001)
- Phosphatase Inhibitor Cocktail 2 (Sigma-Aldrich, cat. no. P5726)
- Pierce™ BCA Protein Assay Kit (Pierce Biotechnology Inc., cat. no. 23225)
- Sodium dodecyl sulfate (SDS; Sigma-Aldrich)
- 100 mM TRIS (pH 7.8; Sigma-Aldrich)

2.3. Equipment

- Vortex mixer
- Lite High Speed Centrifuge Tubes, 15 mL (FroggaBio, cat. no. TL15-500B)
- Lite High Speed Centrifuge Tubes, 50 mL (FroggaBio, cat. no. TL50-500B)
- Costar® Stripette® serological pipettes (10 ml capacity, Corning Inc., cat. no. CLS4488)
- GentleMACS™ C Tubes (Miltenyi Biotec, cat. no. 130-093-237)

- GentleMACS™ Dissociator (Miltenyi Biotec, cat. no. 130-093-235)
- Point-tip forceps
- Razor blades
- Flat-ended spatula
- Weighing boats
- Analytical Weighing scale
- Low Protein Binding Microcentrifuge Tubes, 1.5 ml (Thermo Fisher Scientific, cat. no. 90410)
- Fisherbrand™ Sure One™ Low Retention Non-Filtered Pipette Tips, 1000 µL (Fisher Scientific, cat. no. 02-707-026)
- Dry ice
- Wet ice
- Refrigerated benchtop centrifuge for 15 mL tubes (Beckman Coulter, model Allegra X–14R)
- Refrigerated benchtop centrifuge for 1.5 mL tubes (Eppendorf, model 5430)
- Vacuum-aspiration system
- FlowTubes™ with strainer cap (Canada Peptide, cat. no. FCT-9005)
- Oven (37 °C) (Fisher Scientific, model Fisherbrand™ Isotemp™)
- Multipurpose Digital Shaker (Mandel Scientific Inc., model Labnet Orbit 1000)
- Nunc™ Lab-Tek™ II Chamber Slide™ System (Thermo Fisher Scientific, cat. no. 154453)
- Fisherbrand™ Premium Cover Glasses (Fisher Scientific, cat. no. 12-548-5P)
- Agilent TapeStation (Agilent Technologies, model 2200 TapeStation)
- Flow Cytometer (BD Biosciences, model BD FACSAria™ Fusion)
- Thermocycler (Applied Biosystems Corporation, model ProFlex PCR)
- Probe-based sonicator (Fisher Scientific, model Thermo Sonic Dismembrator)
- Heat block with tube rack

2.4. Reagent setup

2.4.1. Homogenization Buffer preparation Prepare **fresh** Homogenization Buffer (1M sucrose + 1% BSA dissolved in DEPC-treated water) and keep at 4 °C until thoroughly chilled. If transcriptomic techniques are to be used downstream to microvessel isolation, it is recommended to use DEPC-treated water as opposed to Millipore water, as early work done by our group has demonstrated that DEPC treatment preserves an approximate 10% of transcripts that are otherwise lost when processing samples for RNA sequencing (Supplementary Table 1). DEPC treatment functions as a cost-effective RNAse inhibitor when homogenizing brain tissue in large volumes of buffer.

2.4.2. BCIP/NBT substrate preparation If microvessel detection parallel to isolation is desired, BCIP/NBT (5-bromo-4-chloro-3'-indolyphosphate and nitro-blue tetrazolium) can be used as a chromogenic substrate for endothelial enzyme alkaline phosphatase. SIGMAFAST™ BCIP®/NBT tablet (Sigma-Aldrich, Missouri, United States) should be crushed and then dissolved in the fresh Homogenization Buffer according to the manufacturer's instructions (1 tablet per 10 ml of solution). Crushing the tablet first encourages faster dissolution in the highly viscous buffer. Within the brain, alkaline phosphatase is localized to cerebral blood vessels (Shimizu, 1950; Leduc and Wislocki, 1952; Bourne, 1958; Becker et al., 1960; Bannister and Romanul, 1963; Romanul and Bannister, 1962; Ball et al., 2002). BCIP is hydrolyzed by the alkaline phosphatase expressed exclusively in endothelial cells to form a blue intermediate that is then oxidized by NBT to produce a dimer, leaving an intense insoluble purple dye.

2.4.3. Protein extraction buffer Prepare 100 mM TRIS at pH 7.8 with 5% final volume of sodium dodecyl sulfate (SDS).

3. Method

By virtue of a preserved basement membrane, the structures isolated using the described method contain all neurovascular-associated cell types and, therefore, are referred to as “microvessels”. The following protocol describes the specific steps used to isolate and enrich microvessels with retained *in situ* morphology, which is achieved by using semi-automated dissociation of microdissected brain tissue into a homogenate followed by low-speed centrifugation (schematic overview in Fig. 1). These steps have been optimized to isolate microvessels from 100 mg of frozen brain tissue, processing a maximum of 4 samples at a time.

3.1. Tissue microdissection

Timing ~5 mins per sample

1. Set up dissection station adjacent to an analytical balance needed to weigh microdissected brain tissue. Wash all dissection tools (point-tip forceps, razor

blades, flat-ended spatula), bench, and any surface used in 70% (vol/vol) ethanol prior to microdissection. Sufficiently chill a fresh weigh boat, 1.5 ml Eppendorf tubes, and point-tip forceps on dry ice while leaving razor blades at room temperature.

2. Cut tissue using a razor blade and weigh 100 mg of frozen tissue per sample using an analytical scale. Keep tissue on dry ice while microdissecting to minimize degradation and transfer to a chilled 1.5 ml Eppendorf tube. Clean razor, forceps, and spatula with 70% ethanol (vol/vol) and use a fresh weigh boat between samples.

Note: *Postmortem human tissue can contain transmissible pathogens. Take appropriate precautions, including wearing PPE, and seek medical attention if the scalpel breaks skin.*

3.2. Tissue homogenization and cellular fractionation

Timing 45 mins–1h

3. Set up homogenization station adjacent to benchtop gentleMACS™ Dissociator. Place gentleMACS™ C Tubes, 15 ml falcon tubes, and Homogenization Buffer on ice while keeping microdissected brain tissue samples on dry ice.

Note*: Experimental objective must be decided at this step. If either transcriptomic, proteomic investigation, or immunofluorescent visualization is desired, then prepare Homogenization Buffer without BCIP/NBT tablet. If detection of microvessels is to be performed using BCIP/NBT substrate, BCIP/NBT must be prepared in the Homogenization Buffer, as described above.*

4. Using a serological pipette, transfer 2 ml of cold Homogenization Buffer to a gentleMACS™ C Tube and then transfer 100 mg brain tissue from 1.5 ml Eppendorf tube to gentleMACS™ C Tube. Ensure that tissue is fully submerged in Homogenization Buffer while gently agitating the tube for 30 seconds to encourage thawing and osmotic equilibrium (Fig. 2a). See Troubleshooting Step 1 in Supplementary Table 3.

5. Snap gentleMACS™ C Tube into the Dissociator and run the rotating paddle on program Lung 02.01 (Fig. 1). For the first half of the Lung 02.01 program, the speed of the rotating paddle is gradually increased to its maximum in a clockwise direction, and then in an anti-clockwise direction for the second half of the program. The duration of the program is 37 seconds.
6. After tissue homogenization is complete, return gentleMACS™ C Tube to ice and pipette an additional 8 ml of cold Homogenization Buffer into the tube, topping up the homogenate to 10 ml. Gently invert to mix and collect homogenate (Fig. 2b–c).
7. Using a serological pipette, transfer the 10 ml of homogenate to a chilled 15 ml falcon tube, including any foam produced during paddle rotation (Fig. 2d).
8. Gently invert to mix homogenate one more time before centrifugation in order to prevent the formation of a foamy seal atop the homogenate when left sitting. Centrifuge homogenates at 3200 g for 30 mins at 4 °C. Once centrifugation is complete, a microvessel-enriched pellet will form at the bottom of the falcon tube (Fig. 2e). See Troubleshooting Step 2 in Supplementary Table 3.
9. Carefully vacuum-aspirate the supernatant (which may include an upper layer of clumped dissociated myelin, similar to milk skin on top of boiled milk) without disturbing the microvessel-enriched pellet (Fig. 2e–f).
10. Gently resuspend the pellet in 400µl of cold PBS and pipette 50 ul of resuspended pellet into each well of an 8-well chamber slide (Nunc™ Lab-Tek™ II Chamber Slide™ System, Thermo Scientific™, Massachusetts, United States) (Fig. 2g). Leave the chamber slide open-faced in a 37 °C oven overnight. Once the PBS has evaporated, microvessels will dry flush to the surface of the slide.

3.3. Detection of microvessels from the enriched pellet using BCIP/NBT substrate

Timing 35–40 mins

Yield and stability of microvessel isolation can be assessed using chromogenic substrate BCIP/NBT to visualize endothelial enzyme alkaline phosphatase. When detecting microvessels with BCIP/NBT, the process of staining microvessels occurs throughout homogenization and centrifugation steps (steps 5–11) (Fig. 2h).

11. After resuspension of the pellet (section 3.2, step 10), fix microvessels by covering them to a depth of 2–3 cm with ice-cold 100% methanol. Cover chamber slide with lid and allow cells to fix for 15 min on ice or at 4 °C.
12. Aspirate 100% methanol and wash wells in 1X PBS three times for 5 min.
13. Remove the media chamber carefully with the provided chamber removal tool, according to the manufacturer's instructions.
14. Mount the microvessels using VECTASHIELD Vibrance Antifade Mounting Media (California, United States) and place coverslip.

3.4. Detection of microvessels from the enriched pellet using immunohistochemistry

Timing 4–4.5 hours, spread across 3 days (2 overnight incubations)

Greater immunophenotypic characterization of isolated microvessels can be carried out following the resuspension of additional microvessel-enriched pellets. Primary antibodies raised against canonical expression markers for BMECs (Laminin and PECAM1), tight junctions (CLDN5), pericytes (PDGFRβ), smooth muscle cells (Vimentin), and astrocytic endfeet (AQP4) are utilized, along with appropriate fluorophore-conjugated secondary antibodies to characterize collected microvessels thoroughly.

15. After resuspension of the pellet (section 3.2, step 10), fix microvessels by covering them to a depth of 2–3 cm with ice-cold 100% methanol. Cover chamber slide with lid and allow cells to fix for 15 min on ice or at 4 °C.

***Note**: Immunofluorescent visualization must omit any steps in which the microvessel-enriched pellet is filtered through a cellular strainer because microvessels cannot be released from the strainer and, therefore, cannot be mounted onto a microscope slide.*

16. Aspirate 100% methanol and wash wells in 1X PBS three times for 5 min.
17. Incubate microvessels in blocking buffer (1% BSA + 0.5% Triton X dissolved in PBS) under agitation for 60 min at 4 °C.

18. Aspirate blocking solution and pipette into each well 500 µl of primary antibody dilution (1:500 in 1% BSA + 2% normal donkey serum + 0.5% Triton X dissolved in PBS) and incubate under agitation overnight at 4 °C.
19. Aspirate primary antibody dilution and wash wells in 1X PBS three times for 5 min.
20. Incubate microvessels in fluorophore-conjugated secondary antibody dilution (1:500–1:1000 in 1% BSA + 2% normal donkey serum + 0.5% Triton X dissolved in PBS) and incubate under agitation for 2 hours at room temperature, protected from all light.
21. Aspirate secondary antibody dilution and wash wells in 1X PBS three times for 5 min.
22. Remove the media chamber carefully with the provided chamber removal tool, according to the manufacturer's instructions.
23. Mount the microvessels using VECTASHIELD Antifade Mounting Medium with DAPI (California, United States) and place coverslip.

To expand upon experimental applications possible with isolated human brain microvessels, we adapted several downstream techniques including: total RNA extraction, RNA library construction for downstream RNA sequencing, fluorescence-activated nuclei sorting (FANS) of endothelial nuclei, and total protein extraction for downstream Liquid Chromatography with tandem mass spectrometry (LC-MS/MS).

3.5. RNA extraction from isolated microvessels

Timing 30–40 mins

Total RNA extraction from isolated microvessels begins with resuspension of the microvessel-enriched pellet (section 3.2, step 10), followed by filtration through a 35 µm cellular strainer in which microvessels become trapped. From these entrapped microvessels, total RNA is immediately extracted using the Single Cell RNA Purification Kit (Norgen Biotek Corp., Ontario, Canada). After total RNA is successfully extracted, a stopping point is possible during which extracted RNA is frozen and stored at −80 °C.

24. Gently resuspend the pellet (section 3.2, step 10) in 500 µl of cold PBS and gradually pipette through a 35 µm Strainer Cap for *FlowTubes*™ (Canada Peptide, Quebec, Canada) using vacuum-aspiration underneath to encourage filtration. The result is intact microvessels trapped within the strainer mesh, where smaller cellular debris and free-floating nuclei have passed through. See Troubleshooting Step 3 in Supplementary Table 3.
25. Using a flat-ended spatula and point-tip forceps, swiftly push and pull out the strainer mesh, removing it from its plastic frame (Fig. 2i).
26. Immediately submerge the mesh into 100 µl of RL buffer in a 1.5 ml Eppendorf tube, according to step 1A of the manufacturer's protocol.
27. Transfer 100 µl of fresh 70% ETOH, pipette 10 times to wash through the mesh (you may briefly vortex for good measure).
28. Discard the mesh and follow steps according to the manufacturer's instructions, including on-column DNase digestion.
29. Quantify RNA using the Agilent TapeStation 2200 or other quantification system of choice (for total RNA concentration and RIN, see Supplementary Table 2). Freeze and store RNA sample at −80 °C.

STOPPING POINT: *tubes of total RNA should be frozen and stored at −80 °C.*

3.6. Protein extraction from microvessel-enriched pellet or strained microvessels

Timing 1 hour 10 mins–1 hour 15 mins

Total protein has been successfully extracted from either the microvessel-enriched pellet or microvessels stained through a cellular sieve, with one modification to Homogenization Buffer preparation required in which cOmplete™ EDTA-free Protease Inhibitor Cocktail (Roche, Basel, Switzerland) and Phosphatase Inhibitor Cocktail 2 (Sigma-Aldrich, Missouri, United States) are added according to the manufacturer's instructions and based on final volume prepared. With the procedure identical to when using strained microvessels (kept on a strainer), we elaborate protein extraction from frozen microvessel-enriched pellets (pellets stored at −80 °C after section 3.2, step 10). After total protein is successfully extracted, a stopping point is possible during which extracted protein is frozen and stored at −80 °C.

30. Resuspend frozen pellet in 5% sodium dodecyl sulfate (SDS), 100 mM TRIS (pH 7.8), transfer to a 1.5 ml Eppendorf tube and extract protein by heating to 99 °C for 10 minutes on a heat block with tube rack.
31. Subject resuspended pellets to probe-based sonication using a Thermo Sonic Dismembrator at 25% amplitude for 3 cycles for 5 seconds.
32. Clarify lysates by centrifugation at 20,000 g for 5 minutes.
33. For estimation of protein concentration, aliquot approximately 10% of the sample and dilute to <1% SDS and use for estimation of protein concentration by Pierce™ bicinchoninic acid assay (BCA) Protein Assay Kit (Pierce Biotechnology Inc., Massachusetts, United States).

STOPPING POINT: *tubes of total protein should be frozen and stored at −80 °C*

Note: *Total protein and total RNA extraction from the same microvessel-enriched pellet has not been validated. Two microvessel-enriched pellets per sample should be prepared, one for RNA and one for protein extraction.*

3.7. FANS-sorting of endothelial nuclei from microvessel-enriched pellet

Timing 2 hours 5 mins preparation, ∼1–2 hours sorting

If further isolation of BMECs from the microvessel-enriched pellet is desired, FANS-sorting of ETS-related gene $(ERG)^+$ BMECs from the obtained microvessel-enriched pellet can be performed. ERG is a transcription factor whose expression in normal physiological conditions is found exclusively in endothelial nuclei, making it a highly specific pan-endothelial nuclear marker (Nikolova-Krstevski et al., 2009; Miettinen et al., 2011; He et al., 2018; Garcia et al., 2022; Yang et al., 2022). FANS of BMECs can be carried out following the resuspension of the microvessel-enriched pellet (section 3.2, step 10).

34. Resuspend the microvessel-enriched pellet in 500 µl of cold PBS and centrifuge a second time at 500 g for 3 min at 4 °C. Aspirate supernatant, removing any remaining sucrose.

35. For a second time, resuspend the washed pellet in 250 µl of the following antibody solution: recombinant Alexa Fluor® 647 anti-ERG (1:100 dilution; ab196149, Abcam, Massachusetts, United States) in 0.5% BSA + 0.1% Triton in PBS. Transfer to a 1.5 ml Eppendorf tube and incubate under gentle agitation for 2 hours at 4 °C.
36. In the last 10 minutes of the 2 h incubation, add 1 µl of Hoechst 33342 dye (Invitrogen, Massachusetts, United States) to stain nuclear DNA.
37. Filter the suspension through a 35 µm FlowTubes™ with strainer cap and transfer flow-through into a FACS tube.
38. The BD FACSAria™ Fusion Flow Cytometer (BD Biosciences, California, United States) was used to sort our ERG$^+$ population. The gating strategy used for sorting was as follows: doublet discrimination was achieved by gating Hoechst 33342 stained singlets in a FSC-A versus Hoechst-A plot using a 350 nm UV laser and a 450/50 filter. The subsequent ERG$^+$ population was gated in an Alexa Fluor 647-A vs. FSC-A plot using a 640 nm laser in combination with a 730/45 filter. Gating was applied to filter singlets using physical parameters and violet fluorescence (405-nm laser, 525/50 filter). Nonoverlapping gates were adjusted to collect endothelial nuclei based on Alexa Fluor® 647 anti-ERG immunoreactivity (640-nm laser, 730/45 filter). This approach was chosen due to the well-known observation that forward scatter is proportional to size.

4. High-throughput applications of isolated microvessels

4.1. Library construction and RNA sequencing

Microvessel-enriched pellets yielded an average of 8.54 µg/µl of total RNA per sample (Supplementary Table 2). Libraries were then constructed using the SMARTer Stranded Total RNA-Seq Kit v3 - Pico Input Mammalian (Takara Bio Inc., Shiga, Japan), which features integration of unique molecular identifiers (UMIs). Libraries were constructed using 10 ng of RNA as input, 2 minutes of fragmentation at 94 °C (Applied Biosystems Corporation, model ProFlex PCR), 5 cycles of amplification at PCR1 (addition of Illumina adapters and indexes), 12 cycles of amplification at PCR2 (final RNA-seq library amplification) and clean-up of final library using NucleoMag NGS Clean-up and Size Select beads (Takara Bio Inc., Shiga, Japan). Libraries were then quantified at the

Genome Quebec Innovation Centre (Montreal, Quebec) using a KAPA Library Quantification kit (Kapa Biosystems, USA), and average fragment size was determined using a LabChip GX (PerkinElmer, USA) instrument. Libraries were sequenced on the NovaSeq 6000 system (*Illumina*, Inc., California, United States) using S4 flow cells with 100bp PE sequencing kits.

4.2. Bioinformatic pipeline and analyses of RNA sequencing data

4.2.1. UMI extraction, alignment, de-duplication, metrics and gene counting RNA sequencing of microvessel libraries yielded an average of ~72 million reads per library, which were then processed following our in-house bioinformatic pipeline. Briefly, UMI extraction based on fastq files was performed using the module extract of umi_tools (v.1.1.2) (Smith et al., 2017). Reads were then aligned to the Human Reference Genome (GRCh38) using the STAR software v2.5.4b (Dobin et al., 2013) with Ensembl v90 as the annotation file and using the parameters: **-twopassMode Basic --outSAMprimaryFlag AllBestScore --outFilterIntronMotifs RemoveNoncanonical --outSAMtype BAM SortedByCoordinate --quantMode TranscriptomeSAM GeneCounts**. Resultant bam files were then sorted and indexed using SAMtools (v.1.3.1) (Li et al., 2009), and duplicate reads with the same UMI were removed using the dedup module of umi_tools (v.1.1.2) (Smith et al., 2017). Different metrics, including the fraction of the exonic, intronic, and intergenic reads were calculated using the CollectRnaSeqMetrics module of Picard (version 1.129; Picard2019toolkit, Broad Institute, GitHub repository). The expected counts and the transcripts per million (TPMs) were generated using RSEM (v1.3.3; reverse strand mode) (Li and Dewey, 2011). The number of reads, alignment percentages, genomic contamination, and duplication rate for each sample are shown in the Supplementary data.

4.2.2. Computational deconvolution of RNA sequencing data Two approaches were used for computational deconvolution of RNA sequencing data. The first approach was performed using the web tool BrainDeconvShiny (https://voineagulab.shinyapps.io/BrainDeconvShiny/), which implements the best-performing algorithms and all cell type signatures for brain, as well as goodness-of-fit

calculations based on benchmark work conducted by Sutton et al. (2022). UMI counts for each gene were converted to transcripts per million (TPMs) to account for the varying length of gene and sequencing depth of each sample, facilitating comparisons across samples. Genes with zero TPMs were removed; 34370 genes from the original 58303 passed this QC criteria and were then used as input into the BrainDeconvShiny tool. Deconvolution was performed twice: the first approach used average expression in control samples from the Velmeshev et al. (2019) single nuclei dataset (raw data available through the Sequence Read Archive, accession number PRJNA434002; analyzed data available at https://autism.cells.ucsc.edu) as the reference signature for annotated cell types and CIBERSORT v1.04 algorithm to deconvolute sample profiles and estimate cell type composition. The second approach used the MultiBrain (MB) composite signature (Sutton et al., 2022) generated by averaging the expression signatures of five datasets for five cell types (neurons, astrocytes, oligodendrocytes, microglia, and endothelia). MB was used as cell type signatures for deconvolution of our dataset using CIBERSORT v1.04.

The second approach to deconvolution was performed in-house. Postmortem NVU single-nucleus data generated on the 10X Genomics Chromium system was accessed from Yang et al. (2022; raw sequencing data are accessible on GEO using the accession code GSE163577) and used as the reference signature. Seurat (Stuart et al., 2019) was used to pre-process raw count expression data, removing genes with less than 3 cells or cells with less than 200 expressed genes. 23054 genes from a total of 23537 and 141468 nuclei from a total of 143793 passed these QC criteria. Counts per million (CPM) values were averaged across nuclei of each cell type to generate the Yang signature input for the CIBERSORTX tool (Newman et al., 2019).

4.3. Gas Chromatography−Mass spectrometry (LC-MS) with tandem mass tag fractionation

4.3.1. Protein digestion and TMT labelling Extracted proteins were reduced with 20 mM tris(2-carboxyethyl)phosphine (TCEP) at 60 °C prior to alkylation with 25 mM iodoacetamide at room temperature for 30 minutes in the dark. An equivalent of 10

µ*g* of total protein was used for proteolytic digestion using suspension trapping (S-TRAP). Briefly, samples were acidified with phosphoric (1.3% final concentration) and then diluted 6-fold in STRAP loading buffer (9:1 methanol:water in 100 mM TEAB, pH 8.5). Samples were loaded onto S-TRAP Micro cartridges (Protifi LLC, Huntington, NY) prior to centrifugation at 2000*g* for 2 minutes and washed three times with 50 µl of STRAP loading buffer. Proteins were digested with trypsin (Sigma Corporation, Kanagawa, Japan) at a 1:10 enzyme to substrate enzyme-to-substrate ratio for 2 hours at 47 °C. Peptides were sequentially eluted in 100 mM TEAB, 0.1% formic acid in water, and 50% acetonitrile and lyophilized to dryness prior to labelling with TMT 10plex reagents according to the vendor's specifications (Thermo Fisher Scientific, Massachusetts, United States).

4.3.2. Offline high-pH reversed-phase fractionation Labelled peptides were pooled and again lyophilized to dryness, and then reconstituted in 5 mM ammonium formate and fractionated offline by high pH reversed-phase separation using a Waters Xbridge Peptide BEH C18 column (2.1 × 150mm, 2.5 µm) (Waters Corp., Massachusetts, United States) and an Agilent 1290 LC system (Agilent Technologies, California, United States). Binary gradient elution was performed at a flow rate of 400 µL/minute using mobile phase A) 5 mM ammonium formate adjusted with ammonium hydroxide to pH 10, and B) 100% acetonitrile using the following program: 0 min, 0% B; 2min, 0% B; 2.1min, 5% B; 25min, 30% B; 30min, 80% B; 32min, 80% B; 2 min post-run, 0% B. Fractions were collected every 30 seconds and the first and last 7 fractions were concatenated such that even and odd samples were pooled separately, resulting in 20 fractions in total.

4.3.3. LC-MS/MS Samples were analyzed by data- dependent acquisition (DDA) using an Easy-nLC 1200 online coupled to a Q Exactive Plus (both Thermo Fisher Scientific, Massachusetts, United States). Samples were first loaded onto a pre-column (Acclaim PepMap 100 C18, 3 µm particle size, 75 µm inner diameter x 2 cm length) in 0.1% formic acid (buffer A). Peptides were then separated using a 60-min binary gradient ranging from 3 to 40% B (84% acetonitrile, 0.1% formic acid) on the analytical column

(Acclaim PepMap 100 C18, 2 µm particle size, 75 µm inner diameter x 25 cm length) at 300 nL/min. MS spectra were acquired from m/z 350-1500 at a resolution of 70,000, with an automatic gain control (AGC) target of 1×10^6 ions and a maximum injection time of 50 ms. The 15 most intense ions (charge states +2 to +4) were isolated with a window of m/z 1.2, an AGC target of 2 × 104, and a maximum injection time of 64 ms and fragmented using a normalized higher-energy collisional dissociation (HCD) energy of 28. MS/MS spectra were acquired at a resolution of 17,500 and the dynamic exclusion was set to 30 s.

4.3.4. Bioinformatic pipeline and analyses of MS data DDA MS raw data was processed with Proteome Discoverer 2.5 (Thermo Scientific, Massachusetts, United States) and searched using Sequest HT against a FASTA file containing all reviewed protein sequences of the canonical human proteome without isoforms downloaded from Uniprot (https://www.uniprot.org). The enzyme specificity was set to trypsin with a maximum of 2 missed cleavages. Carbamidomethylation of cysteine was set as static modification and methionine oxidation as variable modification. The precursor ion mass tolerance was set to 10 ppm, and the product ion mass tolerance was set to 0.02 Da. The percolator node was used, and the data was filtered using a false discovery rate (FDR) cut-off of 1% at both the peptide and protein level. The Minora feature detector node of Proteome Discoverer was used for precursor-based label-free quantitation.

5. Results

5.1. Immunophenotypic characterization reveals isolated brain microvessels have preserved morphology and expression integrity

Human brain microvessels were isolated from 5 frozen vmPFC grey matter samples microdissected from healthy individuals who died from peripheral diseases or natural events (Table 1). Because the same basement membrane that maintains the integrity of the endothelium also ensheaths astrocytic endfeet as well as pericytes or smooth muscle cells, it is impossible to isolate solely BMECs and, therefore, isolated microvessels also contain microvessel-associated cell types. Notably, the described method allows for isolation of microvessels from other brain regions (data not shown)

and has additionally been performed using the dorsolateral prefrontal cortex (dlPFC, Brodmann area 8/9), the primary visual cortex (Brodmann area 17), as well as the hippocampus (Brodmann area 28).

Following isolation of human brain microvessels, chromogenic staining of resuspended pellets using BCIP/NBT (5-bromo-4-chloro-3'-indolyphosphate and nitro-blue tetrazolium), a substrate for endothelial enzyme alkaline phosphatase, demonstrated isolation and enrichment of predominantly microvessels from vmPFC tissue samples (Fig. 3a–b), with similar success when isolating microvessels from mouse cortex (Fig. 3c). The cytoarchitecture of brain microvessels is both complex and comprised of several cell types; thus, following the isolation of brain microvessels, we aimed to characterize the structure and morphological integrity of isolated microvessels. Immunophenotypic characterization of several NVU markers revealed expression of vimentin (VIM; anti-Vimentin antibody RV202, Abcam), laminins (LAM; anti-Laminin antibody L9393, Sigma-Aldrich), claudin 5 (CLDN5, anti-Claudin 5 antibody ab15106, Abcam), platelet-derived growth factor receptor beta (PDGFRβ, anti-PDGFRβ monoclonal antibody G.290.3, Thermo Fisher Scientific) and aquaporin 4 (AQP4, anti-Aquaporin 4 antibody [4/18], Abcam). More precisely, vimentin (Fig. 4a–b), a regulator of actin cytoskeleton primarily in smooth muscle (Chang and Goldman, 2004) and to a lesser extent endothelial cells (Boraas and Ahsan, 2016) and pericytes (Bandopadhyay et al., 2001), as well as laminins (Fig. 4c), the major basement membrane component responsible for signal transduction via interaction with cell surface receptors (Aumailley and Smyth, 1998), are expressed continuously and homogeneously across the entire length of the endothelial surface. CLDN5, a major functional constituent of tight junctions (Greene et al., 2019), was also stained with no apparent discontinuity, suggesting that endothelial tight junctions were preserved (Fig. 4d). Pericyte coverage of BMECs, immunolabeled by regulator of angiogenesis and vascular stability PDGFRβ (Winkler et al., 2010), was detected adhering to the surface of microvessels (Fig. 4e). These results suggest that the overall *in situ* brain microvessel structure is conserved after isolation.

Astrocytes serve multiple essential functions in supporting normal brain physiology (Kimelberg and Nedergaard, 2010). This is, in part, due to the extension of astrocytic endfeet that surround approximately 99% of the cerebrovascular surface (Mathiisen et al., 2010) which, in conjunction with pericytes (Winkler et al., 2011), regulate expression of molecules that form the BBB including: tight junction, enzymatic, and transporter proteins (Abbott et al., 2006, 2010; Wolburg et al., 2009). Although astrocytes were not co-isolated with microvessels, their perivascular endfeet are ensheathed within the same vascular basement membrane as endothelial cells and pericytes, making it possible that astrocytic endfeet remained attached after tissue homogenization. Because of this, we further observed astrocyte vascular coverage of isolated microvessels. AQP4, a water channel protein essential for the maintenance of osmotic composition and volume within the interstitial, glial, and neuronal compartments (Nagelhus and Ottersen, 2013; Papadopoulos and Verkman, 2013), is expressed at the vessel-facing astrocytic membrane and superimposes the walls of isolated microvessels (Fig. 4f).

Finally, we examined possible contamination of our microvessel preparations by other cell types found within the brain. Immunolabelling for myelin basic protein (MBP; anti-Myelin Basic Protein antibody, BioLegend) was not detected (Fig. 4g), nor did immunolabelling for neuronal nuclear protein (NeuN; anti-NeuN antibody clone A60, Sigma-Aldrich) reveal the presence of neuronal elements (Fig. 4h). Thus, neurons and oligodendrocytes were consistently not observed to be co-isolated with microvessels. Together, these results indicate that the described protocol allows for the isolation and enrichment of structurally preserved brain microvessel fragments that are comprised of BMECs, astrocytic endfeet, pericytes, and tight junction proteins.

5.2. Computational deconvolution and characterization of transcriptomic data indicates high microvessel yield after isolation

To estimate the enrichment of our microvessel preparations, we performed computational deconvolution using the BrainDeconvShiny tool (https://voineagulab.shinyapps.io/BrainDeconvShiny/) and calculated TPMs as input

(Fig. 5a–b). To demonstrate stability of outcome regardless of resources used, different iterations of deconvolution were performed using the CIBERSORT v1.04 algorithm to estimate cell type composition and either the single-nucleus dataset from Velmeshev et al. (2019; VL) (Velmeshev et al., 2019) or the MultiBrain (MB) dataset from Sutton et al. (2022) (Sutton et al., 2022) as the reference signature. Regardless of the approach used, majority endothelial gene expression was estimated, with an average of 94.92% using the VL dataset (Fig. 5a) and an impressive 86.91% using the MB dataset (Fig. 5b), which is a composite signature generated by quantile-normalising and averaging five previously published datasets. Some contamination from neurons (1.29% and 4.66%, respectively), as well as negligible contamination from oligodendrocytes, was observed. When using either dataset as the reference signature, a limited presence of astrocytic genes was observed (1.16% and 6.11%, respectively), which may represent the contribution of astrocytic endfeet that cover the length of the neurovasculature. To estimate the multicellular composition of our microvessels at a finer resolution, computational deconvolution was performed a third time using the reference single-nucleus data generated by Yang et al. (2022), in which the different neurovascular cell type signatures were determined (Fig. 5c). Averaged CPMs across nuclei of each cell type were used as input for the CIBERSORTX tool (Newman et al., 2019), which estimated an average composition of 44.02% capillary and 37.62% SMC, along with much lower estimations for pericyte, arterial, venous, astrocyte and perivascular fibroblast genes (Fig. 5c). Although differentially distributed along the arteriovenous axis, both SMCs and pericytes are embedded within the vascular basement membrane (McConnell et al., 2017) and, therefore, it is unlikely that our isolated method preferentially selects one cell type over the other. Because of this, and the known similarity in molecular signature between SMCs and pericytes (Chasseigneaux et al., 2018; Muhl et al., 2020), as well as the high percentage of captured capillary segments (in which pericytes are predominantly observed) (Sweeney et al., 2016; Gonzales et al., 2020; Hartmann et al., 2021; Alarcon-Martinez et al., 2018), the surprisingly low estimation of pericyte genes may represent a limitation in comparing single-nucleus and bulk tissue datasets to one another. Critically, an average of 90.4% of the total TPMs across samples were assigned to NVU-constituent cell types.

To explore our transcriptomic data, TPMs were averaged across the 5 subjects, and the top 10% of most highly expressed genes were designated (a total of 3437 genes) and used as input for over-representation analysis (ORA) using the enrichR package in R, selecting the “Descartes Cell Types and Tissue 2021” database to identify gene sets that are statistically over-represented (Fig. 6a–b and Supplementary Table 4). The threshold value of enrichment was selected by a p-value <0.05 and, as shown, over-represented genes were dramatically enriched for vascular-related terms, such as “Vascular endothelial cells in Cerebellum” and “Vascular endothelial cells in Cerebrum”. Genes behind enriched terms were extracted and the expression of a subset of known brain endothelial, pericyte, astrocytic, and smooth muscle genes in isolated microvessels were examined (Fig. 6c–i). As expected, microvessels had increased expression of canonical endothelial genes such as CLDN5, CDH5, SLC2A1, ABCB1, VWF, and MFSD2A, with the highest expression in endothelial genes ACTG1, B2M, BSG, EEF1A1, HLA-B, HLA-E, SPARCL1, TMSB10, and VIM (Fig. 6a).

Additionally, there was enrichment for other neurovascular cell types, as suggested by canonical pericyte genes PDGFRβ, MCAM, RGS5, AGRN, and NOTCH3 (Fig. 6b), as well as canonical smooth muscle genes ACTA2, MYL6, MYL9, TAGLN, and LGALS1 (Fig. 6c). Highest expression was detected in pericyte genes CALD1, FN1, IFGBP7, RGS5, SPARC, and SPARCL1 (Fig. 6b); as well as smooth muscle genes ACTG1, ACTN4, CALD1, MYL6, and PTMA (Fig. 6c). Complimentary to immunophenotypic characterization of isolated microvessels, several genes whose products are involved in junctional complex maintenance and organization (tight junctions, Fig. 6f; adherens junctions, Fig. 6g) are found in the top 10% of most highly expressed genes, for e.g., CLDN5, CTNNB1, CTNND1, ITGB1, JAM1, OCLN, TJP1, and TJP2; with additional vascular makers expressed at lower transcripts per million present throughout the entire dataset. Expression of astrocytic genes was observed to a lesser extent, several which have been previously validated as markers of astrocytic processes or endfeet (Boulay et al., 2017; Derouiche and Geiger, 2019; Sakers et al., 2017), namely EZR, GJA1, RDX, SLC1A2, and SLC1A3 (Fig. 6h). To better visualize the proportion of expression

contributed by these genes, TPMs were summarized by cell type over the total number of TPMs (Fig. 6i), demonstrating an overrepresentation of endothelial, smooth muscle cell, and pericyte genes in samples.

Intriguingly, results from ORA reveal genes that are of interest in numerous disease contexts. Enriched in the described dataset is gene CLDN5, an indispensable junctional protein for the correct organization of tight junctions and maintenance of BMEC integrity (Greene et al., 2019), which was previously reported to be downregulated in the nucleus accumbens of depressed suicides (Menard et al., 2017) by altered epigenetic regulation via histone deacetylase 1 (HDAC1) (Dudek et al., 2020). Enriched pericyte genes TXNIP, RUNX1T1, ITGA1 and, DOCK9 are also reported to be differentially expressed in Schizophrenia (Puvogel et al., 2022). Similarly enriched in this dataset are angiogenic growth factors EGFL7, FLT1, VWF, and antigen-presentation machinery B2M and HLA-E, all of which are upregulated in a subpopulation of angiogenic BMECs from subjects with Alzheimer's disease (Lau et al., 2020), suggesting a compensatory angiogenic and immune response in AD pathogenesis. Likewise, endothelial genes PICALM, INPP5D, ADAMTS1, and PLCG2 that are found in the top 10% of the microvessel dataset are differentially expressed in Alzheimer's disease (Yang et al., 2022). Recent breakthroughs in deciphering the underlying etiology of Huntington's disease reveal aberrant downregulation of endothelial ABCB1, ABCG2, SLC2A1, and MFSD2A as well as mural PDGFRB, SLC20A2 and FTH1 (Garcia et al., 2022) – mutations in which are known to cause HD-like syndromes with primary pathology localized in the basal ganglia (Chinnery et al., 2007; Tadic et al., 2015). Indeed, human brain microvessel datasets integrated with others, like those from experimental models, will expedite our understanding of neurovascular contributions to mood disorders and neurodegenerative disease, and even further propagate hypothesis generation for established vascular diseases, such as white matter vascular dementia in which each cell type of the NVU exhibits a specific disease-associated expression signature (Mitroi et al., 2022).

During neuroinflammation, the BBB endothelium reconfigures its landscape of adhesion molecules, cytokines, chemokines, and reactive oxygen species, combined with reduced expression of junctional molecules. These changes prime for bidirectional interaction between the neuroimmune and peripheral immune compartments and enable increased recruitment of circulating leukocytes across the BBB. The top 10% of most highly expressed genes were also assessed for overlap with a curated immune-related gene list (Immunome Database accessed at https://www.innatedb.com/redirect.do?go=resourcesGeneLists, data originally provided by http://structure.bmc.lu.se/idbase/immunome/) (Breuer et al., 2013; Ortutay et al., 2007), sharing 145 out of 824 validated genes involved in immunological processes (Fig. 6j), including notable immune factors CX3CL1, IFNGR1, CD74, IL4R, CXCL2, CXCL12, CD81, IRF1, MIF, as well as HLAs (HLA-A, HLA-B, HLA-C, HLA-E, HLA-F, HLA-DRA, HLA-DPA1, HLA-DPB1). Moreover, adhesion molecules known to mediate cell-cell adhesion at the BBB are also present, including: CD44, previously implicated in monocyte transmigration (He et al., 2016b) and T-cell-endothelial cell interaction (Flynn et al., 2013), MCAM, which mediates recruitment of pathogenic $CD4^+$ T lymphocytes (Charabati et al., 2023) as well as T helper (T_H) 1 cells (Breuer et al., 2018), and ICAM2, which is also critical for T helper (T_H) 1 cell diapedesis (Laschinger et al., 2002). Other well-characterized immune, adhesion, and trafficking molecules in our data are listed in the Supplementary data.

5.3. High correspondence between generated transcriptomic data and published neurovascular dataset

As a means to assess our isolation method, our top 10% of most highly expressed genes were juxtaposed to validated neurovascular cell type-defining markers, as designated by Garcia et al. (2022) based on sequencing of 4992 and 11,689 vascular nuclei from *ex vivo* and postmortem brain tissue, respectively. Results indicated substantial overlap between the three datasets for all NVU-constituent cell types (Fig. 7), including arteriole-defining genes (Fig. 7a), capillary-defining genes (Fig. 7b), venule-defining genes (Fig. 7c), arteriolar SMC-defining genes (Fig. 7d), pericyte-defining genes (Fig. 7e), venular SMC-defining genes (Fig. 7f), and perivascular

fibroblast-defining genes (Fig. 7g). Interestingly, overlap was consistently greater between the two postmortem datasets.

5.4. Proteomic characterization of isolated brain microvessels

While transcript level may show positive correlations with protein level, protein abundance should not necessarily be inferred from RNA sequencing counts (Nie et al., 2006; Vogel and Marcotte, 2012); hence, interrogation of the highly dynamic proteome is needed to speculate the functional consequences of changes in protein expression. We sought to interrogate NVU-specific proteomic signatures using total protein extracted from isolated microvessels. Microvessel-enriched pellets were prepared from 3 frozen vmPFC grey matter samples microdissected from healthy individuals who died of peripheral diseases or natural events (Table 1). Although resuspended and strained pellets yield sufficient protein needed to perform LC-MS/MS (validated, data not shown), straining was omitted in favour of protein extraction directly from pellets to maximize microvessel material input for proteomic interrogation. Using Tandem Mass Tag (TMT) isobaric labeling and sample fractionation of peptides, global, relative quantitation of a total of 1638 individual proteins were detected from microvessel-enriched pellets (quality parametres shown in Supplementary Fig. 2). Importantly, there was significant overlap between transcriptomic and proteomic output, with 1635/1638 (99.8%) of detected proteins likewise identified in the transcriptomics data (albeit no corresponding transcripts were detected for proteins F9, DCD, and SERPINB12); and with 961/1638 (58.7%) proteins found in the top 10% of most highly expressed transcripts, resulting in an overall 23% overlap between high expressors in both datasets (Fig. 8a).

Proteins known to be expressed by vascular-associated cell types and perivascular extracellular matrix were positively identified in all 3 samples. Several canonical endothelial markers were detected with high peptide abundance, including vimentin, several protein subunits of laminin (LAMA3, LAMA5, LAMB2, LAMC1, LAMC3), OCLN, TJP1, TJP2, VWF, VWA1, BSG, PECAM1, Monocarboxylate transporter 1 (SLC16A1), broad substrate specificity ATP-binding cassette transporter (ABCG2), ESAM, CLDN5, CDH5, ATP-binding cassette sub-family B member 1 (ABCB1), ATP-binding cassette

sub-family D member 3 (ABCD3), and Protocadherin-1 (PCDH1) (normalized average abundance for these proteins are listed in Fig. 8b). As expected, enrichment terms returned by ORA (using corresponding gene names as input) were predominantly vascular-associated (Fig. 8c and Supplementary Table 5), and normalized abundance of known brain endothelial, pericyte, astrocytic and smooth muscle cell proteins were high (Fig. 8d–i).

The BBB poses a major pharmacological barrier as BMECs express a vast array of enzymes and transport systems that facilitate brain uptake processes of essential nutrients and neuroactive agents across the BBB (Hediger et al., 2004), controlling the rate and extent to which drugs are able to reach the brain parenchyma via the transcellular pathway (Ballabh et al., 2004). There is a pressing need for improved knowledge surrounding the expression and functionality of these systems at the human BBB as the majority of data comes from either *in vitro* cell culture or animal studies, making *in vitro* to *in vivo* or interspecies scaling less reliable. Analyses revealed high abundance of SLC2A1/GLUT1, a transmembrane protein responsible for the facilitated diffusion of glucose (Mueckler and Thorens, 2013), and the two glutamate transporters SLC1A2/EAAT2 and SLC1A3/EAAT1 in brain microvessels. Transporters SLC7A5/LAT1 and SLC3A2/4F2hc, which supply the brain with large neutral amino acids (Yanagida et al., 2001; Nakamura et al., 1999; Nicklin et al., 2009), and SLC16A1/MCT1 and SLC16A2/MCT8, which are involved in the transport of monocarboxylates (Vijay and Morris, 2014) and T3 thyroid hormone (Trajkovic et al., 2007) at the BBB, respectively, are also found in the described proteomic dataset. Also found are ABCB1/P-glycoprotein and breast cancer-related protein ABCG2/BCRP, the principal ABC efflux transporters (Begley, 2004; Loscher and Potschka, 2005b; Sun et al., 2003) that limit entry of drug candidates, toxic compounds, as well as xenobiotics from the central nervous system (Agarwal et al., 2010, 2011a, 2011b; Chen et al., 2009; de Vries et al., 2007a; Polli et al., 2009). Due to major species-specific differences in transporter expression profiles, there is utility in obtaining absolute protein amounts as they may elucidate the contribution of each transporter in facilitating the entry of endogenous substances and nutrients like glucose, glutamate, and amino and

fatty acids into the brain, in addition to drugs and other xenobiotics that exploit these mechanisms (Hindle et al., 2017).

5.5. Further deconstruction of isolated brain microvessels using FANS

The use of frozen brain tissue demands sorting of target nuclei as opposed to intact cells and, therefore, requires the use of nuclear fluorescent tags to facilitate the isolation of endothelial nuclei. Expression of transcription factor ETS-related gene (ERG) has been previously validated as an endothelial-specific nuclear marker (Miettinen et al., 2011; Haber et al., 2015; Kim et al., 2013; Birdsey et al., 2015) and is found in the top 10% most highly expressed genes from isolated microvessels (TPM shown in Fig. 9a). As an additional testament to the versatility in downstream use of the described method, resuspended microvessels subjected to a 2-h incubation with anti-ERG antibody under rotation is sufficient for vascular disassembly and to expose the ERG epitope for endothelial nuclei immunolabelling (Fig. 9b) without the need for enzymatic digestion as previously described (Crouch and Doetsch, 2018; Pastrana et al., 2009; Codega et al., 2014). Critically, a 2-h incubation in combination with the appropriate gating strategy adjusted to collect endothelial nuclei, is sufficient for the purification of endothelial nuclei from frozen postmortem brain tissue (data not shown). The potential to isolate ERG^+ endothelial nuclei from postmortem microvessels under different physiological conditions (Plane et al., 2010; Ohab et al., 2006; Yamashita et al., 2006; Kojima et al., 2010; Bardehle et al., 2013; Greenberg, 2014; Paul et al., 2012) is an advantage of our approach and addresses a growing interest in the use of primary BMECs, circumventing phenotypical or gene expression changes induced in primary BMEC cultures by prolonged adherence steps used in other isolation protocols (Durafourt et al., 2013; De Groot et al., 2000; Goldeman et al., 2020; Lyck et al., 2009).

6. Discussion

We describe a singular, standardized protocol to enrich and isolate microvessels from archived snap-frozen human brain tissue with the ability to apply the same protocol to frozen mouse cerebral cortex. Integral to this method are three factors that confer gentility and simplicity: 1) the correct molarity of the sucrose-based buffer separates

and cushions microvessels during centrifugation-separation, 2) centrifugation-separation of microvessels from the rest of the tissue homogenate occurs in a 10 ml volume, which facilitates the formation of a microvessel-enriched pellet as heavier structures reach the bottom of the 15 ml falcon tube, and 3) the limited number of wash steps minimizes eventual damage done to the integrity of microvessel fragments. Microvessel enrichment and stability were assessed by chromogenic staining of microvessels using BCIP/NBT substrate and, through immunophenotypic characterization, we show that isolated microvessel fragments are comprised of NVU cellular components including BMECs, astrocytic endfeet, pericytes, as well as tight junction protein complexes. The demonstrated genteness and simplicity of the approach, in turn, confer versatility in the high-throughput techniques that can be utilized downstream to microvessel isolation, as demonstrated here with RNA sequencing and LC-MS/MS.

This protocol should have excellent reproducibility in isolating intact microvessels from any region of the adult human brain. It should be noted, however, that the current version of the protocol may need adjustments if myelin content of brain samples used is high, as dissociated myelin (which travels to the top of the homogenate; section 2.2, step 10) may interfere with the formation of a microvessel-enriched pellet (which travels to the bottom of the homogenate; section 2.2, step 10). As reported, microvessels isolated using the described method are in high yield without other contaminating cell types. However, the protocol enriches for but does not purify microvessels, so a limited proportion of contamination from non-vascular cell types might be found in collected pellets. Limited expression of neuronal markers is observed during computational deconvolution of RNA sequencing data; however, whether a minority of neurons are indeed co-enriched with microvessels remains unclear, as co-enrichment of neurons was not observed during immunophenotypic characterization of isolated microvessels. While some co-enrichment is consistent with the technically unavoidable capture of some parenchymal cells when utilizing a method suitable for frozen postmortem brain tissue (which necessitates as few and as gentle steps as possible), the human BBB atlases generated by Yang et al. (2022) and Garcia et al. (2022) reveal that “canonically neuronal” genes are also expressed in vascular-associated cell types. Therefore, it is

possible that counts for such genes indeed originate from vascular-associated cells and not neurons. Additionally, representation of all vascular-associated cell types might not be uniform, as different cell types may vary across brain regions and even brain subregions, and different cell types may be differentially susceptible to steps taken during RNA or protein extraction. Nonetheless, in the absence of harsh experimental steps, it is reasonable to assume that the proportions of vascular-associated cell types found within isolated microvessels represent the natural multicellular composition of vasculature within the brain. During the development of this protocol, several brain tissue samples were used possessing a range of values for PMI, RIN, pH, and other metrics, including age at death, manner of death, freezer storage time, and prior medication exposure. Although not systematically assessed, success in isolating and enriching microvessels from different tissue samples was consistent and robust across variations in such quality metrics (as demonstrated here by the wide range of age and PMI across subjects shown in Table 1). We attribute such reproducibility to the protective nature of the vascular basement membrane that may protect the vessel structure and its contents against changes experienced by the brain parenchyma during the postmortem interval. Despite this, it is recommended to utilize postmortem samples with quality metrics PMI, RIN, and pH that indicate moderate to good quality, which is a fundamental prerequisite to investigating complex brain disorders using molecular profiling techniques. Inevitably, studies that make use of isolated human microvessels will encounter high inter-subject variation in both RNA and protein yield as well as experimental read-out. Large cohorts with matched subjects (if studying disease and/or sex differences) would be required to power a study investigating how brain vascular gene or proteomic expression varies with factors such as brain region, age, or disease. Although sensitivity of mass spectrometers has been greatly improved over the years (Hahne et al., 2013; Hebert et al., 2018; Shishkova et al., 2016, 2018; Timp and Timp, 2020), as well as peptide separation for untargeted proteome analysis (Shishkova et al., 2016, 2018; Toth et al., 2019), the literature consistently shows that high output from mass spectrometry relies on a balance between sample quantity as well as sample complexity. Because protein extracted from microvessels, as opposed to bulk tissue, could be considered a sample lacking complexity, it is reasonable to assume that this

relays to lower output, which may be further impacted by several low signal-to-noise events that result in unidentified peptides (Griss et al., 2016) and a more limited dynamic range of peptide detection (Timp and Timp, 2020).

Our successfully generated datasets promise a more complete approach to investigating BBB function and disease, where one arm of a study may leverage experimental animal or cell culture models to identify pertinent biological mechanisms, and the other arm may utilize microvessels isolated from human brain to provide insight into species-specific differences and other limitations of experimental models. Species differences in disease-affected neuronal and myeloid gene expression have been characterized by single-cell or single-nucleus sequencing (Cosacak et al., 2022; Friedman et al., 2018; Kamath et al., 2022), but such differences in neurovascular gene expression have only just begun to be comprehensively analyzed, and solely in Huntington's disease and Alzheimer's disease (Garcia et al., 2022; Yang et al., 2022). Despite limited data, it has become evident there are striking differences, with one study reporting 142 mouse-enriched genes, including Vtn, Slco1c1, Slc6a20a, Atp13a5, Slc22a8, and 211 human-enriched genes, including SLCO2A1, GIMAP7, and A2M (Song et al., 2020b). Yang et al. (2022) further reported hundreds of species-enriched genes in BMECs and pericytes, finding that BMECs and pericytes exhibit the greatest transcriptional divergence in several vascular solute transporters (for e.g., GABA transporter *SLC6A12*) and genes of disease and pharmacological importance. This observation was corroborated by Garcia et al. (2022), who further detailed that species-specific differentially expressed genes (DEGs) were strongly enriched for marker genes of vascular-associated cell types, indicating that cell type identity markers were among those that vary the most between species. Breakthroughs can similarly be made using the described method, with the added benefit that microvessels kept as a structurally intact unit provide insight into the neurovasculature in a manner that nuclei or dissociated cells cannot: not only is unwanted technical-related depletion of vascular-associated cells avoided, but cytoplasm, which carries much higher amounts of mRNA and protein, as well as interstitium are also preserved. This is not trivial, as work done by others comparing microglia single cells versus single nuclei from postmortem tissue

reveals that certain populations of genes are depleted in nuclei compared to whole cells. Those depleted were previously implicated in microglial activation, such as APOE, SPP1, CST3, and CD74, totalling 18% of previously identified microglial-disease-associated genes (Thrupp et al., 2020). While there is undeniable benefit in characterizing disease-related changes at the cell type level, the neurovasculature is so interconnected that dysfunction is typically observed in all vascular-associated cells, conferring whole-unit dysfunction that becomes difficult to parse when looking at its individual nuclei. We put forward the ATP-binding cassette (ABC) transporter family as an interesting candidate that can be further explored using microvessels isolated from postmortem brain. The human genome carries 48 different ABC transporters (Gil-Martins et al., 2020; Morris et al., 2017; Robey et al., 2018), several of which are expressed in the CNS, primarily at the BBB (Gil-Martins et al., 2020). Dysfunction of ABC transporters, at expression and/or activity level, has been repeatedly associated with neurological disease (Gil-Martins et al., 2020); and of note are the functionally important yet redundant ABCB1 and ABCG2, both of which have been observed in our transcriptomic and proteomic datasets. For example, ABCB1 is culpable in the neuroinflammatory mechanisms of multiple sclerosis, where ABCB1 expression and activity are significantly decreased by mechanisms involving $CD4^+$ T cells (Kooij et al., 2010), which is just one aspect of the broad barrier impairment that permits lymphocytes activated in the periphery to infiltrate the CNS (Cashion et al., 2023; Ortiz et al., 2014). Moreover, numerous drug candidates show potential anticancer effects against different brain cancer cell lines *in vitro* and yet, their efficacy *in vivo* and in clinical trials has been considerably more modest, in large part due to ABCB1/ABCG2-mediated efflux at the BBB. Both ABCB1 and ABCG2, which are expressed on the luminal membrane of BMECs (Biegel et al., 1995; Cooray et al., 2002; Eisenblatter and Galla, 2002; Zhang et al., 2003), present a double-edged sword at the blood-brain barrier: on the one hand, ABCB1/ABCG2-mediated efflux is vital for protecting the brain; on the other hand, several anticancer drugs have been identified as substrates of ABCB1 and/or ABCG2 (de Vries et al., 2007b; Agarwal and Elmquist, 2012; Traxl et al., 2019), and their function restricts brain uptake of anticancer drugs, significantly limiting their efficacy in the treatment of primary and metastatic brain tumors (de Vries et al.,

2007b; Agarwal and Elmquist, 2012; Juliano and Ling, 1976; Doyle et al., 1998; Marchetti et al., 2008; Agarwal et al., 2011c; de Gooijer et al., 2018; Sorf et al., 2018; Schinkel et al., 1994). Efforts to better understand ABCB1/ABCG2 expression and circumvent the restriction of drug uptake have been considerable. Previous studies point to a lower ABCB1/ABCG2 ratio (Dehouck et al., 2022; Uchida et al., 2011), whereas our findings exhibit a higher ABCB1/ABCG2 ratio. This discrepancy may be an insight into the interindividual differences that give rise to variable drug responses, a common clinical challenge. Several synonymous single nucleotide polymorphisms (SNPs) that affect function and substrate binding have been identified in both transporters (Kimchi-Sarfaty et al., 2007; Fung and Gottesman, 2009; Dickens et al., 2013; Furukawa et al., 2009; Delord et al., 2013; El Biali et al., 2021). The individuals studied here were all of French-Canadian origin, a group with a distinct genotype, and so certain SNPs that affect mRNA stability or transporter activity may, in turn, modulate translational output of ABCB1 relative to ABCG2, as has been observed with ABCB1 SNPs (Wang et al., 2005). It should be noted, however, that these studies (including ours) comprised of small cohorts and warrant further investigations with larger sample sizes.

In sum, the isolated brain microvessel is a robust model for the NVU and can be used to generate a variety of highly dimensional datasets. The availability of characterized human neurovascular transcriptomes and proteomes can aid in identifying potential roles for BMECs and pericytes in the pathogenesis of neurological and psychiatric disorders and additionally aid in assessing the expression of molecules with potential relevance to drug delivery and novel therapies (e.g., SLCs, ABCs, and large molecule receptors) across the human brain vasculature.

Declaration of competing interest

None.

Acknowledgements

The authors have no competing interests to declare. This study was funded by an ERA NET Neuron grant and a CIHR Project grant to N.M. M.W. and R.R. respectively received scholarship and fellowship support from the FRQ-S. The Douglas-Bell Canada Brain Bank is supported in part by platform support grants from the Réseau Québécois sur le Suicide, les Troubles de l'Humeur et les Troubles Associés (FRQ-S), Healthy Brains for Healthy Lives (CFREF), and Brain Canada. The present study used the services of the Molecular and Cellular Microscopy Platform (MCMP) at the Douglas Research Centre. The authors would like to thank the expert help of Douglas-Bell Canada Brain Bank staff members (J. Prud'homme, M. Bouchouka, D. Mirault, V. Lariviere, A. Baccichet), the technology development team at the McGill University and Genome Quebec Innovation Centre, and the Segal Cancer Proteomics Centre at the Lady Davis Institute. The authors would also like to thank Dr. Ghazal Fakhfouri for rearing and providing the mice used in this study.

7. References

Abbott N.J., Ronnback L., Hansson E. Astrocyte-endothelial interactions at the blood-brain barrier. Nat. Rev. Neurosci. 2006;7(1):41–53. doi: 10.1038/nrn1824.

Abbott N.J., Patabendige A.A., Dolman D.E., Yusof S.R., Begley D.J. Structure and function of the blood-brain barrier. Neurobiol. Dis. 2010;37(1):13–25. doi: 10.1016/j.nbd.2009.07.030.

Agarwal S., Elmquist W.F. Insight into the cooperation of P-glycoprotein (ABCB1) and breast cancer resistance protein (ABCG2) at the blood-brain barrier: a case study examining sorafenib efflux clearance. Mol. Pharm. 2012;9(3):678–684.

Agarwal S., Sane R., Gallardo J.L., Ohlfest J.R., Elmquist W.F. Distribution of gefitinib to the brain is limited by P-glycoprotein (ABCB1) and breast cancer resistance protein (ABCG2)-mediated active efflux. J. Pharmacol. Exp. Therapeut. 2010;334:147–155. doi: 10.1124/jpet.110.167601.

Agarwal S., Hartz A.M., Elmquist W.F., Bauer B. Breast cancer resistance protein and P-glycoprotein in brain cancer: two gatekeepers team up. Curr. Pharmaceut. Des. 2011;17:2793–2802. doi: 10.2174/138161211797440186.

Agarwal S., Sane R., Ohlfest J.R., Elmquist W.F. The role of the breast cancer resistance protein (ABCG2) in the distribution of sorafenib to the brain. J. Pharmacol. Exp. Therapeut. 2011;336:223–233. doi: 10.1124/jpet.110.175034.

Agarwal S., Sane R., Ohlfest J.R., Elmquist W.F. The role of the breast cancer resistance protein (ABCG2) in the distribution of sorafenib to the brain. J. Pharmacol. Exp. Therapeut. 2011;336(1):223–233.

Al-Bachari S., Naish J.H., Parker G.J.M., Emsley H.C.A., Parkes L.M. Blood-brain barrier leakage is increased in Parkinson's disease. Front. Physiol. 2020;11.

Al-Louzi O., Govindarajan S.T., Tauhid S., et al. Central vein sign profile of newly developing lesions in multiple sclerosis: a 3-year longitudinal study. Neurol Neuroimmunol. Neuroinflamm. 2022;9(1) doi: 10.1212/NXI.0000000000001120.

Alarcon-Martinez L., et al. Capillary pericytes express alpha-smooth muscle actin, which requires prevention of filamentous-actin depolymerization for detection. Elife. 2018;7 doi: 10.7554/eLife.34861.
Almeida D., Turecki G. Profiling cell-type specific gene expression in post-mortem human brain samples through laser capture microdissection. Methods. 2022;207:3–10. doi: 10.1016/j.ymeth.2022.08.013.

Arvanitakis Z., Capuano A.W., Leurgans S.E., Bennett D.A., Schneider J.A. Relation of cerebral vessel disease to Alzheimer's disease dementia and cognitive function in elderly people: a cross-sectional study. Lancet Neurol. 2016;15(9):934–943. doi: 10.1016/S1474-4422(16)30029-1.

Aumailley M., Smyth N. The role of laminins in basement membrane function. J. Anat. 1998;193(Pt 1):1–21. doi: 10.1046/j.1469-7580.1998.19310001.x.

Axelsson R., Martensson E., Alling C. Impairment of the blood-brain barrier as an aetiological factor in paranoid psychosis. Br. J. Psychiatry. 1982;141:273–281.

Bacher R., Kendziorski C. Design and computational analysis of single-cell RNA-sequencing experiments. Genome Biol. 2016;17:63. doi: 10.1186/s13059-016-0927-y.

Baldwin S.A., Fugaccia I., Brown D.R., Brown L.V., Scheff S.W. Blood-brain barrier breach following cortical contusion in the rat. J. Neurosurg. 1996;85(3):476–481. doi: 10.3171/jns.1996.85.3.0476.

Ball H.J., McParland B., Driussi C., Hunt N.H. Isolating vessels from the mouse brain for gene expression analysis using laser capture microdissection. Brain Res. Brain Res. Protoc. 2002;9(4):206–213. doi: 10.1016/s1385-299x(02)00147-2.

Ballabh P., Braun A., Nedergaard M. The blood-brain barrier: an overview: structure, regulation, and clinical implications. Neurobiol. Dis. 2004;16:1–13. doi: 10.1016/j.nbd.2003.12.016.

Bandopadhyay R., Orte C., Lawrenson J.G., Reid A.R., De Silva S., Allt G. Contractile proteins in pericytes at the blood-brain and blood-retinal barriers. J. Neurocytol. 2001;30(1):35–44.

Bannister R.G., Romanul F.C. The localization of alkaline phosphatase activity in cerebral blood vessels. J. Neurol. Neurosurg. Psychiatry. 1963;26(4):333–340. doi: 10.1136/jnnp.26.4.333.

Bardehle S., et al. Live imaging of astrocyte responses to acute injury reveals selective juxtavascular proliferation. Nat. Neurosci. 2013;16:580–586. doi: 10.1038/nn.3371.

Baskaya M.K., Rao A.M., Dogan A., Donaldson D., Dempsey R.J. The biphasic opening of the blood-brain barrier in the cortex and hippocampus after traumatic brain injury in rats. Neurosci. Lett. 1997;226(1):33–36. doi: 10.1016/s0304-3940(97)00239-5.

Becker N.H., Goldfischer S., Shin W.Y., Novikoff A.B. The localization of enzyme activities in the rat brain. J. Biophys. Biochem. Cytol. 1960;8(3):649–663. doi: 10.1083/jcb.8.3.649.

Begley D.J. ABC transporters and the blood-brain barrier. Curr. Pharmaceut. Des. 2004;10:1295–1312. doi: 10.2174/1381612043384844.

Betz A.L., Goldstein G.W. Polarity of the blood-brain barrier: neutral amino acid transport into isolated brain capillaries. Science. 1978;202:225–227. doi: 10.1126/science.211586.

Betz A.L., Firth J.A., Goldstein G.W. Polarity of the blood-brain barrier: distribution of enzymes between the luminal and antiluminal membranes of brain capillary endothelial cells. Brain Res. 1980;192:17–28. doi: 10.1016/0006-8993(80)91004-5.

Biegel D., Spencer D.D., Pachter J.S. Isolation and culture of human brain microvessel endothelial cells for the study of blood-brain barrier properties in vitro. Brain Res. 1995;692(1–2):183–189.

Birdsey G.M., et al. The endothelial transcription factor ERG promotes vascular stability and growth through Wnt/beta-catenin signaling. Dev. Cell. 2015;32:82–96. doi: 10.1016/j.devcel.2014.11.016.

Boraas L.C., Ahsan T. Lack of vimentin impairs endothelial differentiation of embryonic stem cells. Sci. Rep. 2016;6.

Boulay A.C., et al. Translation in astrocyte distal processes sets molecular heterogeneity at the gliovascular interface. Cell Discov. 2017;3 doi: 10.1038/celldisc.2017.5.

Bourassa P., Tremblay C., Schneider J.A., Bennett D.A., Calon F. Beta-amyloid pathology in human brain microvessel extracts from the parietal cortex: relation with cerebral amyloid angiopathy and Alzheimer's disease. Acta Neuropathol. 2019;137(5):801–823. doi: 10.1007/s00401-019-01967-4.

Bourne G.H. Histochemical demonstration of phosphatases in the central nervous system of the rat. Exp. Cell Res. 1958;14(1):101–117.

Breuer K., Foroushani A.K., Laird M.R., Chen C., Sribnaia A., Lo R., et al. InnateDB: systems biology of innate immunity and beyond--recent updates and continuing curation. Nucleic Acids Res. 2013;41(Database issue):D1228–D1233.

Breuer J., Korpos E., Hannocks M.J., Schneider-Hohendorf T., Song J., Zondler L., et al. Blockade of MCAM/CD146 impedes CNS infiltration of T cells over the choroid plexus. J. Neuroinflammation. 2018;15(1):236.

Buch S., Saville J.W., Schifitto G., et al. Revealing vascular abnormalities and measuring small vessel density in multiple sclerosis lesions using USPIO. Neuroimag Clin. 2021;29 doi: 10.1016/j.nicl.2020.102525.

Caesar K., Thomsen K., Lauritzen M. Dissociation of spikes, synaptic activity, and activity-dependent increments in rat cerebellar blood flow by tonic synaptic inhibition. Proc. Natl. Acad. Sci. U. S. A. 2003;100(26):16000–16005. doi: 10.1073/pnas.2635195100.

Campana M., Lohrs L., Strauss J., Munz S., Oviedo-Salcedo T., Fernando P., et al. Blood-brain barrier dysfunction and folate and vitamin B12 levels in first-episode schizophrenia-spectrum psychosis: a retrospective chart review. Eur. Arch. Psychiatr. Clin. Neurosci. 2023

Cashion J.M., Young K.M., Sutherland B.A. How does neurovascular unit dysfunction contribute to multiple sclerosis? Neurobiol. Dis. 2023;178

Chang L., Goldman R.D. Intermediate filaments mediate cytoskeletal crosstalk. Nat. Rev. Mol. Cell Biol. 2004;5(8):601–613. doi: 10.1038/nrm1438.

Charabati M., Zandee S., Fournier A.P., Tastet O., Thai K., Zaminpeyma R., et al. MCAM+ brain endothelial cells contribute to neuroinflammation by recruiting pathogenic CD4+ T lymphocytes. Brain. 2023;146(4):1483–1495.

Chasseigneaux S., et al. Isolation and differential transcriptome of vascular smooth muscle cells and mid-capillary pericytes from the rat brain. Sci. Rep. 2018;8 doi: 10.1038/s41598-018-30739-5.

Chen Y., et al. P-glycoprotein and breast cancer resistance protein influence brain distribution of dasatinib. J. Pharmacol. Exp. Therapeut. 2009;330:956–963. doi: 10.1124/jpet.109.154781.

Chinnery P.F., et al. Clinical features and natural history of neuroferritinopathy caused by the FTL1 460InsA mutation. Brain. 2007;130(Pt 1):110–119. doi: 10.1093/brain/awl319.

Codega P., et al. Prospective identification and purification of quiescent adult neural stem cells from their in vivo niche. Neuron. 2014;82:545–559. doi: 10.1016/j.neuron.2014.02.039.

Cooray H.C., Blackmore C.G., Maskell L., Barrand M.A. Localisation of breast cancer resistance protein in microvessel endothelium of human brain. Neuroreport. 2002;13(16):2059–2063.

Cordon-Cardo C., O'Brien J.P., Boccia J., Casals D., Bertino J.R., Melamed M.R. Multidrug-resistance gene (P-glycoprotein) is expressed by endothelial cells at blood-brain barrier sites. Proc. Natl. Acad. Sci. U.S.A. 1989;86:695–698. doi: 10.1073/pnas.86.2.695.

Cosacak M.I., et al. Single cell/nucleus transcriptomics comparison in zebrafish and humans reveals common and distinct molecular responses to Alzheimer's disease. Cells. 2022;11 doi: 10.3390/cells11111807.

Crouch E.E., Doetsch F. FACS isolation of endothelial cells and pericytes from mouse brain microregions. Nat. Protoc. 2018;13(4):738–751. doi: 10.1038/nprot.2017.158.

Daneman R. The blood-brain barrier in health and disease. Ann. Neurol. 2012;72:648–672. doi: 10.1002/ana.23648.

de Gooijer M.C., Buil L.C.M., Citirikkaya C.H., Hermans J., Beijnen J.H., van Tellingen O. ABCB1 attenuates the brain penetration of the PARP inhibitor AZD2461. Mol. Pharm. 2018;15(11):5236–5243.

De Groot C.J., et al. Isolation and characterization of adult microglial cells and oligodendrocytes derived from postmortem human brain tissue. Brain Res. Brain Res. Protoc. 2000;5:85–94. doi: 10.1016/s1385-299x(99)00059-8.

De Vivo D.C., Trifiletti R.R., Jacobson R.I., Ronen G.M., Behmand R.A., Harik S.I. Defective glucose transport across the blood-brain barrier as a cause of persistent

hypoglycorrhachia, seizures, and developmental delay. N. Engl. J. Med. 1991;325(11):703–709. doi: 10.1056/NEJM199109053251006.

de Vries N.A., et al. P-glycoprotein and breast cancer resistance protein: two dominant transporters working together in limiting the brain penetration of topotecan. Clin. Cancer Res. 2007;13:6440–6449. doi: 10.1158/1078-0432.CCR-07-1335.

de Vries N.A., Zhao J., Kroon E., Buckle T., Beijnen J.H., van Tellingen O. P-glycoprotein and breast cancer resistance protein: two dominant transporters working together in limiting the brain penetration of topotecan. Clin. Cancer Res. 2007;13(21):6440–6449.

Deane R., Bell R.D., Sagare A., Zlokovic B.V. Clearance of amyloid-beta peptide across the blood-brain barrier: implication for therapies in Alzheimer's disease. CNS Neurol. Disord.: Drug Targets. 2009;8(1):16–30. doi: 10.2174/187152709787601867.

Dehouck M.P., Tachikawa M., Hoshi Y., Omori K., Maurage C.A., Strecker G., et al. Quantitative targeted absolute proteomics for better characterization of an in vitro human blood-brain barrier model derived from hematopoietic stem cells. Cells. 2022;11(24).

del Zoppo G.J., Mabuchi T. Cerebral microvessel responses to focal ischemia. J. Cerebr. Blood Flow Metabol. 2003;23(8):879–894. doi: 10.1097/01.WCB.0000078322.96027.78.

Delord M., Rousselot P., Cayuela J.M., Sigaux F., Guilhot J., Preudhomme C., et al. High imatinib dose overcomes insufficient response associated with ABCG2 haplotype in chronic myelogenous leukemia patients. Oncotarget. 2013;4(10):1582–1591.

Denisenko E., Guo B.B., Jones M., et al. Systematic assessment of tissue dissociation and storage biases in single-cell and single-nucleus RNA-seq workflows. Genome Biol. 2020;21(1):130. doi: 10.1186/s13059-020-02048-6.

Derouiche A., Geiger K.D. Perspectives for ezrin and radixin in astrocytes: kinases, functions and pathology. Int. J. Mol. Sci. 2019;20 doi: 10.3390/ijms20153776.

Dickens D., Owen A., Alfirevic A., Pirmohamed M. ABCB1 single nucleotide polymorphisms (1236C>T, 2677G>T, and 3435C>T) do not affect transport activity of human P-glycoprotein. Pharmacogenetics Genom. 2013;23(6):314–323.

Dietrich W.D., Alonso O., Halley M. Early microvascular and neuronal consequences of traumatic brain injury: a light and electron microscopic study in rats. J Neurotrauma. 1994;11(3):289–301. doi: 10.1089/neu.1994.11.289.

Dobin A., Davis C.A., Schlesinger F., et al. STAR: ultrafast universal RNA-seq aligner. Bioinformatics. 2013;29(1):15–21. doi: 10.1093/bioinformatics/bts635.

Doepp F., Paul F., Valdueza J.M., Schmierer K., Schreiber S.J. Venous drainage in multiple sclerosis: a combined MRI and ultrasound study. Neurology. 2011;77(18):1745–1751. doi: 10.1212/WNL.0b013e318236f0ea.

Dorheim M.A., Tracey W.R., Pollock J.S., Grammas P. Nitric oxide synthase activity is elevated in brain microvessels in Alzheimer's disease. Biochem. Biophys. Res. Commun. 1994;205(1):659–665.

Doyle L.A., Yang W., Abruzzo L.V., Krogmann T., Gao Y., Rishi A.K., et al. A multidrug resistance transporter from human MCF-7 breast cancer cells. Proc. Natl. Acad. Sci. U. S. A. 1998;95(26):15665–15670.

Dudek K.A., et al. Molecular adaptations of the blood-brain barrier promote stress resilience vs. depression. Proc. Natl. Acad. Sci. U. S. A. 2020;117(6):3326–3336. doi: 10.1073/pnas.1914655117.

Durafourt B.A., Moore C.S., Blain M., Antel J.P. Isolating, culturing, and polarizing primary human adult and fetal microglia. Methods Mol. Biol. 2013;1041:199–211. doi: 10.1007/978-1-62703-520-0_19.

Durukan A., Tatlisumak T. Post-ischemic blood-brain barrier leakage in rats: one-week follow-up by MRI. Brain Res. 2009;1280:158–165. doi: 10.1016/j.brainres.2009.05.025.

Eisenblatter T., Galla H.J. A new multidrug resistance protein at the blood-brain barrier. Biochem. Biophys. Res. Commun. 2002;293(4):1273–1278.

El Biali M., Karch R., Philippe C., Haslacher H., Tournier N., Hacker M., et al. ABCB1 and ABCG2 together limit the distribution of ABCB1/ABCG2 substrates to the human retina and the ABCG2 single nucleotide polymorphism Q141K (c.421C> A) may lead to increased drug exposure. Front. Pharmacol. 2021;12.

Erickson M.A., Banks W.A. Neuroimmune axes of the blood-brain barriers and blood-brain interfaces: bases for physiological regulation, disease states, and pharmacological interventions. Pharmacol. Rev. 2018;70(2):278–314.

Fabry Z., Fitzsimmons K.M., Herlein J.A., Moninger T.O., Dobbs M.B., Hart M.N. Production of the cytokines interleukin 1 and 6 by murine brain microvessel endothelium and smooth muscle pericytes. J. Neuroimmunol. 1993;47(1):23–34.

Farrell C.L., Pardridge W.M. Blood-brain barrier glucose transporter is asymmetrically distributed on brain capillary endothelial lumenal and ablumenal membranes: an electron microscopic immunogold study. Proc. Natl. Acad. Sci. U. S. A. 1991;88(13):5779–5783. doi: 10.1073/pnas.88.13.5779.

Fergus A., Lee K.S. GABAergic regulation of cerebral microvascular tone in the rat. J. Cerebr. Blood Flow Metabol. 1997;17(9):992–1003. doi: 10.1097/00004647-199709000-00009.

Flynn K.M., Michaud M., Madri J.A. CD44 deficiency contributes to enhanced experimental autoimmune encephalomyelitis: a role in immune cells and vascular cells of the blood-brain barrier. Am. J. Pathol. 2013;182(4):1322–1336.

Fowler A.J., Ahn J., Hebron M., Chiu T., Ayoub R., Mulki S., et al. CSF MicroRNAs reveal impairment of angiogenesis and autophagy in Parkinson disease. Neurol.Genet. 2021;7(6):e633.

Fox P.T., Raichle M.E., Mintun M.A., Dence C. Nonoxidative glucose consumption during focal physiologic neural activity. Science. 1988;241(4864):462–464. doi: 10.1126/science.3260686.

Friedman B.A., et al. Diverse brain myeloid expression profiles reveal distinct microglial activation states and aspects of Alzheimer's disease not evident in mouse models. Cell Rep. 2018;22:832–847. doi: 10.1016/j.celrep.2017.12.066.

Fung K.L., Gottesman M.M. A synonymous polymorphism in a common MDR1 (ABCB1) haplotype shapes protein function. Biochim. Biophys. Acta. 2009;1794(5):860–871.

Furukawa T., Wakabayashi K., Tamura A., Nakagawa H., Morishima Y., Osawa Y., et al. Major SNP (Q141K) variant of human ABC transporter ABCG2 undergoes lysosomal and proteasomal degradations. Pharm. Res. (N. Y.) 2009;26(2):469–479.

Gaitan M.I., de Alwis M.P., Sati P., Nair G., Reich D.S. Multiple sclerosis shrinks intralesional, and enlarges extralesional, brain parenchymal veins. Neurology. 2013;80(2):145–151. doi: 10.1212/WNL.0b013e31827b916f.

Gal Z., Torok D., Gonda X., Eszlari N., Anderson I.M., Deakin B., et al. Inflammation and blood-brain barrier in depression: interaction of CLDN5 and IL6 gene variants in stress-induced depression. Int. J. Neuropsychopharmacol. 2023;26(3):189–197.

Garcia F.J., Patel K., Costa A.S.H., et al. Single-cell dissection of the human brain vasculature. Nature. 2022;603(7897):893–899. doi: 10.1038/s41586-022-04521-7.

Gendelman H.E., Ding S., Gong N., et al. Monocyte chemotactic protein-1 regulates voltage-gated K+ channels and macrophage transmigration. J. Neuroimmune Pharmacol. 2009;4(1):47–59. doi: 10.1007/s11481-008-9135-1.

Geraldes R., Esiri M.M., DeLuca G.C., Palace J. Vascular disease and multiple sclerosis: a post-mortem study exploring their relationships. Brain. 2020;143(10):2998–3012. doi: 10.1093/brain/awaa255.

Gerhart D.Z., LeVasseur R.J., Broderius M.A., Drewes L.R. Glucose transporter localization in brain using light and electron immunocytochemistry. J. Neurosci. Res. 1989;22(4):464–472. doi: 10.1002/jnr.490220413.

Gil-Martins E., Barbosa D.J., Silva V., Remiao F., Silva R. Dysfunction of ABC transporters at the blood-brain barrier: role in neurological disorders. Pharmacol. Ther. 2020;213.

Goldeman C., Ozgur B., Brodin B. Culture-induced changes in mRNA expression levels of efflux and SLC-transporters in brain endothelial cells. Fluids Barriers CNS. 2020;17:32. doi: 10.1186/s12987-020-00193-5.

Goldwaser E.L., Swanson R.L., 2nd, Arroyo E.J., Venkataraman V., Kosciuk M.C., Nagele R.G., et al. A preliminary report: the Hippocampus and surrounding temporal cortex of patients with schizophrenia have impaired blood-brain barrier. Front. Hum. Neurosci. 2022;16.

Gonzales A.L., et al. Contractile pericytes determine the direction of blood flow at capillary junctions. Proc. Natl. Acad. Sci. U. S. A. 2020;117(45):27022–27033. doi: 10.1073/pnas.1922755117.

Greenberg D.A. Cerebral angiogenesis: a realistic therapy for ischemic disease? Methods Mol. Biol. 2014;1135:21–24. doi: 10.1007/978-1-4939-0320-7_2.

Greene C., Hanley N., Campbell M. Claudin-5: gatekeeper of neurological function. Fluids Barriers CNS. 2019;16(1):3. doi: 10.1186/s12987-019-0123-z.

Griss J., et al. Recognizing millions of consistently unidentified spectra across hundreds of shotgun proteomics datasets. Nat. Methods. 2016;13:651–656. doi: 10.1038/nmeth.3902.

Grubman A., Chew G., Ouyang J.F., et al. A single-cell atlas of entorhinal cortex from individuals with Alzheimer's disease reveals cell-type-specific gene expression regulation. Nat. Neurosci. 2019;22(12):2087–2097. doi: 10.1038/s41593-019-0539-4.

Haber M.A., et al. ERG is a novel and reliable marker for endothelial cells in central nervous system tumors. Clin. Neuropathol. 2015;34:117–127. doi: 10.5414/NP300817.

Hahne H., et al. DMSO enhances electrospray response, boosting sensitivity of proteomic experiments. Nat. Methods. 2013;10:989–991. doi: 10.1038/nmeth.2610.

Harris L.W., Wayland M., Lan M., et al. The cerebral microvasculature in schizophrenia: a laser capture microdissection study. PLoS One. 2008;3(12) doi: 10.1371/journal.pone.0003964.

Hartmann D.A., et al. Brain capillary pericytes exert a substantial but slow influence on blood flow. Nat. Neurosci. 2021;24(4):633–645. doi: 10.1038/s41593-020-00793-2.

He L., Vanlandewijck M., Raschperger E., et al. Analysis of the brain mural cell transcriptome. Sci. Rep. 2016;6doi: 10.1038/srep35108.

He X., Shi X., Puthiyakunnon S., Zhang L., Zeng Q., Li Y., et al. CD44-mediated monocyte transmigration across Cryptococcus neoformans-infected brain microvascular endothelial cells is enhanced by HIV-1 gp41-I90 ectodomain. J. Biomed. Sci. 2016;23:28.

He L., Vanlandewijck M., Raschperger E., et al. Single-cell RNA sequencing of mouse brain and lung vascular and vessel-associated cell types. Sci. Data. 2018;5 doi: 10.1038/sdata.2018.160.

Hebert A.S., et al. Improved precursor characterization for data-dependent mass spectrometry. Anal. Chem. 2018;90:2333–2340. doi: 10.1021/acs.analchem.7b04808.

Hediger M.A., et al. The ABCs of solute carriers: physiological, pathological and therapeutic implications of human membrane transport proteins. Pflugers. Arch. 2004;447(5):465–468. doi: 10.1007/s00424-003-1192-y.

Hicks R.R., Baldwin S.A., Scheff S.W. Serum extravasation and cytoskeletal alterations following traumatic brain injury in rats. Comparison of lateral fluid percussion and cortical impact models. Mol. Chem. Neuropathol. 1997;32(1):1–16. doi: 10.1007/BF02815164.

Hicks S.C., Townes F.W., Teng M., Irizarry R.A. Missing data and technical variability in single-cell RNA-sequencing experiments. Biostatistics. 2018;19(4):562–578. doi: 10.1093/biostatistics/kxx053.

Hindle S.J., et al. Evolutionarily conserved roles for blood-brain barrier xenobiotic transporters in endogenous steroid partitioning and behavior. Cell Rep. 2017;21:1304–1316. doi: 10.1016/j.celrep.2017.10.026.

Hofman F.M., Chen P., Incardona F., Zidovetzki R., Hinton D.R. HIV-1 tat protein induces the production of interleukin-8 by human brain-derived endothelial cells. J. Neuroimmunol. 1999;94(1–2):28–39.

Hoge R.D., Atkinson J., Gill B., Crelier G.R., Marrett S., Pike G.B. Linear coupling between cerebral blood flow and oxygen consumption in activated human cortex. Proc. Natl. Acad. Sci. U. S. A. 1999;96(16):9403–9408. doi: 10.1073/pnas.96.16.9403.

Iadecola C. Regulation of the cerebral microcirculation during neural activity: is nitric oxide the missing link? Trends Neurosci. 1993;16(6):206–214. doi: 10.1016/0166-2236(93)90156-g.

Iadecola C. The neurovascular unit coming of age: a journey through neurovascular coupling in health and disease. Neuron. 2017;96:17–42. doi: 10.1016/j.neuron.2017.07.030

Iliff JJ, Wang M, Zeppenfeld DM, et al. Cerebral arterial pulsation drives paravascular CSF-interstitial fluid exchange in the murine brain. J. Neurosci.

Iliff J.J., Wang M., Liao Y., et al. A paravascular pathway facilitates CSF flow through the brain parenchyma and the clearance of interstitial solutes, including amyloid β Sci. Transl. Med. 2012;4(147):147ra111. doi: 10.1126/scitranslmed.3003748.

Isingrini E., Perret L., Rainer Q., et al. Genetic elimination of dopamine vesicular stocks in the nigrostriatal pathway replicates Parkinson's disease motor symptoms without neuronal degeneration in adult mice. Sci. Rep. 2017;7(1) doi: 10.1038/s41598-017-12810-9.

Iturria-Medina Y., Sotero R.C., Toussaint P.J., et al. Early role of vascular dysregulation on late-onset Alzheimer's disease based on multifactorial data-driven analysis. Nat. Commun. 2016;7 doi: 10.1038/ncomms11934.

Jakel S., Agirre E., Mendanha Falcão A., et al. Altered human oligodendrocyte heterogeneity in multiple sclerosis. Nature. 2019;566(7745):543–547. doi: 10.1038/s41586-019-0903-2.

Jeong S.M., Park S.W., Kim H.J., Kim N.H., Park J.W. Changes in magnesium concentration in the serum and cerebrospinal fluid of neuropathic rats. Acta Anaesthesiol. Scand. 2006;50(2):211–216. doi: 10.1111/j.1399-6576.2006.00925.x.

Juliano R.L., Ling V. A surface glycoprotein modulating drug permeability in Chinese hamster ovary cell mutants. Biochim. Biophys. Acta. 1976;455(1):152–162.

Kamath T., et al. Single-cell genomic profiling of human dopamine neurons identifies a population that selectively degenerates in Parkinson's disease. Nat. Neurosci. 2022;25:588–595. doi: 10.1038/s41593-022-01061-1.

Kamintsky L., Cairns K.A., Veksler R., Bowen C., Beyea S.D., Friedman A., et al. Blood-brain barrier imaging as a potential biomarker for bipolar disorder progression. Neuroimag.Clin. 2020;26.

Khan O., Filippi M., Freedman M.S., et al. Chronic cerebrospinal venous insufficiency and multiple sclerosis. Ann. Neurol. 2010;67(3):286–290. doi: 10.1002/ana.22001.

Kim S., et al. ERG immunohistochemistry as an endothelial marker for assessing lymphovascular invasion. Kor. J. Pathol. 2013;47:355–364. doi: 10.4132/KoreanJPathol.2013.47.4.355.

Kimchi-Sarfaty C., Oh J.M., Kim I.W., Sauna Z.E., Calcagno A.M., Ambudkar S.V., et al. A "silent" polymorphism in the MDR1 gene changes substrate specificity. Science. 2007;315(5811):525–528.

Kimelberg H.K., Nedergaard M. Functions of astrocytes and their potential as therapeutic targets. Neurotherapeutics. 2010;7(4):338–353. doi: 10.1016/j.nurt.2010.07.006.

Kinnecom K., Pachter J.S. Selective capture of endothelial and perivascular cells from brain microvessels using laser capture microdissection. Brain Res. Brain Res. Protoc. 2005;16(1–3):1–9. doi: 10.1016/j.brainresprot.2005.08.002.

Kirkpatrick B., Miller B.J. Inflammation and schizophrenia. Schizophr. Bull. 2013;39(6):1174–1179.

Kisler K., Nelson A.R., Montagne A., Zlokovic B.V. Cerebral blood flow regulation and neurovascular dysfunction in Alzheimer disease. Nat. Rev. Neurosci. 2017;18:419–434. doi: 10.1038/nrn.2017.48.

Klein B., Kuschinsky W., Schrock H., Vetterlein F. Interdependency of local capillary density, blood flow, and metabolism in rat brains. Am. J. Physiol. 1986;251(6 Pt 2):H1333–H1340. doi: 10.1152/ajpheart.1986.251.6.H1333.

Kojima T., et al. Subventricular zone-derived neural progenitor cells migrate along a blood vessel scaffold toward the post-stroke striatum. Stem Cell. 2010;28:545–554. doi: 10.1002/stem.306.

Kooij G., van Horssen J., de Lange E.C., Reijerkerk A., van der Pol S.M., van Het Hof B., et al. T lymphocytes impair P-glycoprotein function during neuroinflammation. J. Autoimmun. 2010;34(4):416–425.

Laschinger M., Vajkoczy P., Engelhardt B. Encephalitogenic T cells use LFA-1 for transendothelial migration but not during capture and initial adhesion strengthening in healthy spinal cord microvessels in vivo. Eur. J. Immunol. 2002;32(12):3598–3606.

Lau S.F., Cao H., Fu A.K.Y., Ip N.Y. Single-nucleus transcriptome analysis reveals dysregulation of angiogenic endothelial cells and neuroprotective glia in Alzheimer's disease. Proc. Natl. Acad. Sci. U. S. A. 2020;117(47):25800–25809. doi: 10.1073/pnas.2008762117.

Leduc E.H., Wislocki G.B. The histochemical localization of acid and alkaline phosphatases, non-specific esterase and succinic dehydrogenase in the structures comprising the hemato-encephalic barrier of the rat. J. Comp. Neurol. 1952;97(2):241–279. doi: 10.1002/cne.900970203.

Lee Y.K., Uchida H., Smith H., Ito A., Sanchez T. The isolation and molecular characterization of cerebral microvessels. Nat. Protoc. 2019;14(10):3059–3081. doi: 10.1038/s41596-019-0212-0.

Lewitus G.M., Konefal S.C., Greenhalgh A.D., Pribiag H., Augereau K., Stellwagen D. Microglial TNF-alpha suppresses cocaine-induced plasticity and behavioral sensitization. Neuron. 2016;90(3):483–491.

Li B., Dewey C.N. RSEM: accurate transcript quantification from RNA-Seq data with or without a reference genome. BMC Bioinf. 2011;12:323. doi: 10.1186/1471-2105-12-323.

Li H., et al. The sequence alignment/map format and SAMtools. Bioinformatics. 2009;25(16):2078–2079. doi: 10.1093/bioinformatics/btp352.

Lin C.Y., Chang C., Cheah J.H., et al. Dynamic changes in vascular permeability, cerebral blood volume, vascular density, and size after transient focal cerebral ischemia in rats: evaluation with contrast-enhanced magnetic resonance imaging. J. Cerebr. Blood Flow Metabol. 2008;28(7):1491–1501. doi: 10.1038/jcbfm.2008.42.

Liu P., Wu H., Yang H., et al. Time-course investigation of blood-brain barrier permeability and tight junction protein changes in a rat model of permanent focal ischemia. J. Physiol. Sci. 2018;68(2):121–127. doi: 10.1007/s12576-016-0516-6.

Loscher W., Potschka H. Blood-brain barrier active efflux transporters: ATP-binding cassette gene family. NeuroRx. 2005;2:86–98. doi: 10.1602/neurorx.2.1.86.

Loscher W., Potschka H. Blood-brain barrier active efflux transporters: ATP-binding cassette gene family. NeuroRx. 2005;2:86–98. doi: 10.1602/neurorx.2.1.86.

Lyck R., et al. Culture-induced changes in blood-brain barrier transcriptome: implications for amino-acid transporters in vivo. J. Cerebr. Blood Flow Metabol. 2009;29:1491–1502. doi: 10.1038/jcbfm.2009.72.

Mandi Y., Ocsovszki I., Szabo D., Nagy Z., Nelson J., Molnar J. Nitric oxide production and MDR expression by human brain endothelial cells. Anticancer Res. 1998;18(4C):3049–3052.

Marchetti S., de Vries N.A., Buckle T., Bolijn M.J., van Eijndhoven M.A., Beijnen J.H., et al. Effect of the ATP-binding cassette drug transporters ABCB1, ABCG2, and ABCC2 on erlotinib hydrochloride (Tarceva) disposition in in vitro and in vivo pharmacokinetic studies employing Bcrp1-/-/Mdr1a/1b-/- (triple-knockout) and wild-type mice. Mol. Cancer Therapeut. 2008;7(8):2280–2287.

Mathiesen C., Caesar K., Akgören N., Lauritzen M. Modification of activity-dependent increases of cerebral blood flow by excitatory synaptic activity and spikes in rat

cerebellar cortex. J. Physiol. 1998;512(Pt 2):555–566. doi: 10.1111/j.1469-7793.1998.555be.x.

Mathiisen T.M., Lehre K.P., Danbolt N.C., Ottersen O.P. The perivascular astroglial sheath provides a complete covering of the brain microvessels: an electron microscopic 3D reconstruction. Glia. 2010;58(9):1094–1103. doi: 10.1002/glia.20990.

Mathys H., Davila-Velderrain J., Peng Z., et al. Single-cell transcriptomic analysis of Alzheimer's disease. Nature. 2019;570(7761):332–337. doi: 10.1038/s41586-019-1195-2.

McConnell H.L., Kersch C.N., Woltjer R.L., Neuwelt E.A. The translational significance of the neurovascular unit. J. Biol. Chem. 2017;292(3):762–770. doi: 10.1074/jbc.R116.760215.

McGuire T.R., Trickler W.J., Hock L., Vrana A., Hoie E.B., Miller D.W. Release of prostaglandin E-2 in bovine brain endothelial cells after exposure to three unique forms of the antifungal drug amphotericin-B: role of COX-2 in amphotericin-B induced fever. Life Sci. 2003;72(23):2581–2590.

Menard C., et al. Social stress induces neurovascular pathology promoting depression. Nat. Neurosci. 2017;20(12):1752–1760. doi: 10.1038/s41593-017-0010-3.

Miettinen M., Wang Z.F., Paetau A., et al. ERG transcription factor as an immunohistochemical marker for vascular endothelial tumors and prostatic carcinoma. Am. J. Surg. Pathol. 2011;35(3):432–441. doi: 10.1097/PAS.0b013e318206b67b.

Mintun M.A., Raichle M.E., Kilbourn M.R., Wooten G.F., Welch M.J. Blood flow and oxygen delivery to human brain during functional activity: theoretical modeling and experimental data. Proc. Natl. Acad. Sci. U. S. A. 2001;98(12):6859–6864. doi: 10.1073/pnas.111164398.

Mitroi D.N., Tian M., Kawaguchi R., Lowry W.E., Carmichael S.T. Single-nucleus transcriptome analysis reveals disease- and regeneration-associated endothelial cells in white matter vascular dementia. J. Cell Mol. Med. 2022;26(6):3183–3195. doi: 10.1111/jcmm.17315.

Mittapalli R.K., Manda V.K., Adkins C.E., Geldenhuys W.J., Lockman P.R. Exploiting nutrient transporters at the blood-brain barrier to improve brain distribution of small molecules. Ther. Deliv. 2010;1:775–784. doi: 10.4155/tde.10.76.

Mojsilovic-Petrovic J., Nesic M., Pen A., Zhang W., Stanimirovic D. Development of rapid staining protocols for laser-capture microdissection of brain vessels from human and rat coupled to gene expression analyses. J. Neurosci. Methods. 2004;133(1–2):39–48. doi: 10.1016/j.jneumeth.2003.09.026.

Mokgokong R., Wang S., Taylor C.J., Barrand M.A., Hladky S.B. Ion transporters in brain endothelial cells that contribute to formation of brain interstitial fluid. Pflugers. Arch. 2014;466(5):887–901. doi: 10.1007/s00424-013-1342-9.

Montagne A., Barnes S.R., Sweeney M.D., et al. Blood-brain barrier breakdown in the aging human hippocampus. Neuron. 2015;85(2):296–302. doi: 10.1016/j.neuron.2014.12.032.

Morris M.E., Rodriguez-Cruz V., Felmlee M.A. SLC and ABC transporters: expression, localization, and species differences at the blood-brain and the blood-cerebrospinal fluid barriers. AAPS J. 2017;19(5):1317–1331.

Mueckler M., Thorens B. The SLC2 (GLUT) family of membrane transporters. Mol. Aspect. Med. 2013;34:121–138. doi: 10.1016/j.mam.2012.07.001.

Muhl L., et al. Single-cell analysis uncovers fibroblast heterogeneity and criteria for fibroblast and mural cell identification and discrimination. Nat. Commun. 2020;11:3953. doi: 10.1038/s41467-020-17740-1.

Munji R.N., Soung A.L., Weiner G.A., Sohet F., Semple B.D., Trivedi A., et al. Profiling the mouse brain endothelial transcriptome in health and disease models reveals a core blood-brain barrier dysfunction module. Nat. Neurosci. 2019;22(11):1892–1902. doi: 10.1038/s41593-019-0497-x.

Nagelhus E.A., Ottersen O.P. Physiological roles of aquaporin-4 in brain. Physiol. Rev. 2013;93(4):1543–1562. doi: 10.1152/physrev.00011.2013.

Nagy C., Torres-Platas S.G., Mechawar N., Turecki G. Single-nucleus transcriptomics of the prefrontal cortex in major depressive disorder implicates oligodendrocyte precursor cells and excitatory neurons. Nat. Neurosci. 2020;23(6):771–781. doi: 10.1038/s41593-020-0621-y.

Nagyoszi P., Wilhelm I., Farkas A.E., Fazakas C., Dung N.T., Hasko J., et al. Expression and regulation of toll-like receptors in cerebral endothelial cells. Neurochem. Int. 2010;57(5):556–564.

Nagyoszi P., Nyul-Toth A., Fazakas C., Wilhelm I., Kozma M., Molnar J., et al. Regulation of NOD-like receptors and inflammasome activation in cerebral endothelial cells. J. Neurochem. 2015;135(3):551–564.

Najjar S., Pearlman D.M., Devinsky O., Najjar A., Zagzag D. Neurovascular unit dysfunction with blood-brain barrier hyperpermeability contributes to major depressive disorder: a review of clinical and experimental evidence. J. Neuroinflammation. 2013;10:142.

Nakamura E., et al. 4F2 (CD98) heavy chain is associated covalently with an amino acid transporter and controls intracellular trafficking and membrane topology of 4F2 heterodimer. J. Biol. Chem. 1999;274:3009–3016. doi: 10.1074/jbc.274.5.3009.

Navone S.E., Marfia G., Invernici G., et al. Isolation and expansion of human and mouse brain microvascular endothelial cells. Nat. Protoc. 2013;8(9):1680–1693. doi: 10.1038/nprot.2013.107.

Newman A.M., et al. Determining cell type abundance and expression from bulk tissues with digital cytometry. Nat. Biotechnol. 2019;37(7):773–782. doi: 10.1038/s41587-019-0114-2.

Nicklin P., et al. Bidirectional transport of amino acids regulates mTOR and autophagy. Cell. 2009;136:521–534. doi: 10.1016/j.cell.2008.11.044.
Nie L., Wu G., Zhang W. Correlation of mRNA expression and protein abundance affected by multiple sequence features related to translational efficiency in Desulfovibrio vulgaris: a quantitative analysis. Genetics. 2006;174(4):2229–2243. doi: 10.1534/genetics.106.065862.

Nikolova-Krstevski V., Wang X., Yu J., et al. ERG is required for the differentiation of embryonic stem cells along the endothelial lineage. BMC Dev. Biol. 2009;9:72. doi: 10.1186/1471-213X-9-72.

Ohab J.J., Fleming S., Blesch A., Carmichael S.T. A neurovascular niche for neurogenesis after stroke. J. Neurosci. 2006;26:13007–13016. doi: 10.1523/JNEUROSCI.4323-06.2006.

Ortiz G.G., Pacheco-Moises F.P., Macias-Islas M.A., Flores-Alvarado L.J., Mireles-Ramirez M.A., Gonzalez-Renovato E.D., et al. Role of the blood-brain barrier in multiple sclerosis. Arch. Med. Res. 2014;45(8):687–697.

Ortutay C., Siermala M., Vihinen M. Molecular characterization of the immune system: emergence of proteins, processes, and domains. Immunogenetics. 2007;59(5):333–348.

Papadopoulos M.C., Verkman A.S. Aquaporin water channels in the nervous system. Nat. Rev. Neurosci. 2013;14(4):265–277. doi: 10.1038/nrn3468.

Pastrana E., Cheng L.C., Doetsch F. Simultaneous prospective purification of adult subventricular zone neural stem cells and their progeny. Proc. Natl. Acad. Sci. U. S. A. 2009;106:6387–6392. doi: 10.1073/pnas.0810407106.

Paul G., et al. The adult human brain harbors multipotent perivascular mesenchymal stem cells. PLoS One. 2012;7doi: 10.1371/journal.pone.0035577.

Pillai D.R., Dittmar M.S., Baldaranov D., et al. Cerebral ischemia-reperfusion injury in rats--a 3 T MRI study on biphasic blood-brain barrier opening and the dynamics of edema formation. J. Cerebr. Blood Flow Metabol. 2009;29(10):1846–1855. doi: 10.1038/jcbfm.2009.106.

Plane J.M., Andjelkovic A.V., Keep R.F., Parent J.M. Intact and injured endothelial cells differentially modulate postnatal murine forebrain neural stem cells. Neurobiol. Dis. 2010;37:218–227. doi: 10.1016/j.nbd.2009.10.008.

Polli J.W., et al. An unexpected synergist role of P-glycoprotein and breast cancer resistance protein on the central nervous system penetration of the tyrosine kinase inhibitor lapatinib (N-3-chloro-4-[(3-fluorobenzyl)oxy]phenyl-6-[5-([2-(methylsulfonyl)ethyl]aminomethyl)-2-furyl]-4-quinazolinamine; GW572016) Drug Metab. Dispos. 2009;37:439–442. doi: 10.1124/dmd.108.024646.

Puvogel S., et al. Single-nucleus RNA sequencing of midbrain blood-brain barrier cells in schizophrenia reveals subtle transcriptional changes with overall preservation of cellular proportions and phenotypes. Mol. Psychiatr. 2022;27(9):4731–4740. doi: 10.1038/s41380-022-01796-0.

Quan N., Banks W.A. Brain-immune communication pathways. Brain Behav. Immun. 2007;21(6):727–735.

Reyes T.M., Fabry Z., Coe C.L. Brain endothelial cell production of a neuroprotective cytokine, interleukin-6, in response to noxious stimuli. Brain Res. 1999;851(1–2):215–220.

Robey R.W., Pluchino K.M., Hall M.D., Fojo A.T., Bates S.E., Gottesman M.M. Revisiting the role of ABC transporters in multidrug-resistant cancer. Nat. Rev. Cancer. 2018;18(7):452–464.

Romanul F.C., Bannister R.G. Localized areas of high alkaline phosphatase activity in the terminal arterial tree. J. Cell Biol. 1962;15(1):73–84. doi: 10.1083/jcb.15.1.73.

Rosenberg G.A. Blood-brain barrier permeability in aging and Alzheimer's disease. J. Prev. Alzheimers Dis. 2014;1(3):138–139. doi: 10.14283/jpad.2014.25.

Roy C.S., Sherrington C.S. On the regulation of the blood-supply of the brain. J. Physiol. 1890;11(1–2):85–158. doi: 10.1113/jphysiol.1890.sp000321.
Sakers K., et al. Astrocytes locally translate transcripts in their peripheral processes. Proc. Natl. Acad. Sci. U. S. A. 2017;114(17):E3830–E3838. doi: 10.1073/pnas.1617782114.

Schinkel A.H., Smit J.J., van Tellingen O., Beijnen J.H., Wagenaar E., van Deemter L., et al. Disruption of the mouse mdr1a P-glycoprotein gene leads to a deficiency in the blood-brain barrier and to increased sensitivity to drugs. Cell. 1994;77(4):491–502.

Schroder M.L., Muizelaar J.P., Fatouros P.P., Kuta A.J., Choi S.C. Regional cerebral blood volume after severe head injury in patients with regional cerebral ischemia. Neurosurgery. 1998;42(6):1276–1280. doi: 10.1097/00006123-199806000-00042. ; discussion 1280-1271.

Schwarzmaier S.M., Kim S.W., Trabold R., Plesnila N. Temporal profile of thrombogenesis in the cerebral microcirculation after traumatic brain injury in mice. J. Neurotrauma. 2010;27(1):121–130. doi: 10.1089/neu.2009.1114.

Shapira Y., Setton D., Artru A.A., Shohami E. Blood-brain barrier permeability, cerebral edema, and neurologic function after closed head injury in rats. Anesth. Analg. 1993;77(1):141–148. doi: 10.1213/00000539-199307000-00028.

Shimizu N. Histochemical studies on the phosphatase of the nervous system. J. Comp. Neurol. 1950;93(2):201–217. doi: 10.1002/cne.900930203.

Shishkova E., Hebert A.S., Coon J.J. Now, more than ever, proteomics needs better chromatography. Cell Syst. 2016;3:321–324. doi: 10.1016/j.cels.2016.10.007.

Shishkova E., et al. Ultra-high pressure (>30,000 psi) packing of capillary columns enhancing depth of shotgun proteomic analyses. Anal. Chem. 2018;90:11503–11508. doi: 10.1021/acs.analchem.8b02766.

Smith Q.R., Rapoport S.I. Cerebrovascular permeability coefficients to sodium, potassium, and chloride. J. Neurochem. 1986;46(6):1732–1742. doi: 10.1111/j.1471-4159.1986.tb08491.x.
Smith T., Heger A., Sudbery I. UMI-tools: modeling sequencing errors in Unique Molecular Identifiers to improve quantification accuracy. Genome Res. 2017;27(3):491–499. doi: 10.1101/gr.209601.116.

Song H.W., Castrillon-Rodriguez E., Armstrong E.A., et al. Transcriptomic comparison of human and mouse brain microvessels. Sci. Rep. 2020;10(1) doi: 10.1038/s41598-020-69096-7.

Song H.W., et al. Transcriptomic comparison of human and mouse brain microvessels. Sci. Rep. 2020;10doi: 10.1038/s41598-020-69096-7.

Sorf A., Hofman J., Kucera R., Staud F., Ceckova M. Ribociclib shows potential for pharmacokinetic drug-drug interactions being a substrate of ABCB1 and potent inhibitor of ABCB1, ABCG2 and CYP450 isoforms in vitro. Biochem. Pharmacol. 2018;154:10–17.

Spitzer D., Combes F., Colonna M. A flow cytometry-based protocol for syngenic isolation of neurovascular unit cells from mouse and human tissues. Nat. Protoc. 2023 doi: 10.1038/s41596-023-00805-y.

Stein S.C., Chen X.H., Sinson G.P., Smith D.H. Intravascular coagulation: a major secondary insult in nonfatal traumatic brain injury. J. Neurosurg. 2002;97(6):1373–1377. doi: 10.3171/jns.2002.97.6.1373.

Strbian D., Durukan A., Pitkonen M., et al. The blood-brain barrier is continuously open for several weeks following transient focal cerebral ischemia. Neuroscience. 2008;153(1):175–181. doi: 10.1016/j.neuroscience.2008.02.012.

Stuart T., et al. Comprehensive integration of single-cell data. Cell. 2019;177(7) doi: 10.1016/j.cell.2019.05.031. 1888-1902 e1821.

Sun D., Lytle C., O'Donnell M.E. IL-6 secreted by astroglial cells regulates Na-K-Cl cotransport in brain microvessel endothelial cells. Am. J. Physiol. 1997;272(6 Pt 1):C1829–C1835.

Sun H., Dai H., Shaik N., Elmquist W.F. Drug efflux transporters in the CNS. Adv. Drug Deliv. Rev. 2003;55:83–105. doi: 10.1016/s0169-409x(02)00172-2.

Sutton G.J., et al. Comprehensive evaluation of deconvolution methods for human brain gene expression. Nat. Commun. 2022;13(1):1358. doi: 10.1038/s41467-022-28655-4.

Sweeney M.D., Sagare A.P., Zlokovic B.V. Cerebrospinal fluid biomarkers of neurovascular dysfunction in mild dementia and Alzheimer's disease. J. Cerebr. Blood Flow Metabol. 2015;35(6):1055–1068. doi: 10.1038/jcbfm.2015.76.

Sweeney M.D., Ayyadurai S., Zlokovic B.V. Pericytes of the neurovascular unit: key functions and signaling pathways. Nat. Neurosci. 2016;19(6):771–783. doi: 10.1038/nn.4288.

Tadic V., et al. Primary familial brain calcification with known gene mutations: a systematic review and challenges of phenotypic characterization. JAMA Neurol. 2015;72(4):460–467. doi: 10.1001/jamaneurol.2014.3889.

Thiebaut F., Tsuruo T., Hamada H., Gottesman M.M. Immunohistochemical localization in normal tissues of different epitopes in the multidrug transport protein P170: evidence for localization in brain capillaries and crossreactivity of one antibody with a muscle protein. J. Histochem. Cytochem. 1989;37:159–164. doi: 10.1177/37.2.2463300.

Thrupp N., Sala Frigerio C., Wolfs L., Skene N.G., Fattorelli N., Poovathingal S., et al. Single-nucleus RNA-seq is not suitable for detection of microglial activation genes in humans. Cell Rep. 2020;32(13).

Timp W., Timp G. Beyond mass spectrometry, the next step in proteomics. Sci. Adv. 2020;6doi: 10.1126/sciadv.aax8978.

Toledo J.B., Arnold S.E., Raible K., et al. Contribution of cerebrovascular disease in autopsy confirmed neurodegenerative disease cases in the National Alzheimer's Coordinating Centre. Brain. 2013;136(9):2697–2706. doi: 10.1093/brain/awt188.

Torres-Platas S.G., Cruceanu C., Chen G.G., Turecki G., Mechawar N. Evidence for increased microglial priming and macrophage recruitment in the dorsal anterior cingulate white matter of depressed suicides. Brain Behav. Immun. 2014;42:50–59.

Toth G., Panic-Jankovic T., Mitulovic G. Pillar array columns for peptide separations in nanoscale reversed-phase chromatography. J. Chromatogr. A. 2019;1603:426–432. doi: 10.1016/j.chroma.2019.06.067.

Trajkovic M., et al. Abnormal thyroid hormone metabolism in mice lacking the monocarboxylate transporter 8. J. Clin. Invest. 2007;117:627–635. doi: 10.1172/JCI28253.

Traugott U., Reinherz E.L., Raine C.S. Multiple sclerosis. Distribution of T cells, T cell subsets and Ia-positive macrophages in lesions of different ages. J. Neuroimmunol. 1983;4(3):201–221.

Traxl A., Mairinger S., Filip T., Sauberer M., Stanek J., Poschner S., et al. Inhibition of ABCB1 and ABCG2 at the mouse blood-brain barrier with marketed drugs to improve brain delivery of the model ABCB1/ABCG2 substrate [(11)C]erlotinib. Mol. Pharm. 2019;16(3):1282–1293.

Uchida Y., Ohtsuki S., Katsukura Y., Ikeda C., Suzuki T., Kamiie J., et al. Quantitative targeted absolute proteomics of human blood-brain barrier transporters and receptors. J. Neurochem. 2011;117(2):333–345.

van Beijnum J.R., Rousch M., Castermans K., van der Linden E., Griffioen A.W. Isolation of endothelial cells from fresh tissues. Nat. Protoc. 2008;3(7):1085–1091. doi: 10.1038/nprot.2008.71.

Vanlandewijck M., He L., Mäe M.A., et al. A molecular atlas of cell types and zonation in the brain vasculature. Nature. 2018;554(7693):475–480. doi: 10.1038/s41586-018-0232-x.

Velmeshev D., Schirmer L., Jung D., et al. Single-cell genomics identifies cell type-specific molecular changes in autism. Science. 2019;364(6441):685–689. doi: 10.1126/science.aav8130.

Ventura-Antunes L., Dasgupta O.M., Herculano-Houzel S. Resting rates of blood flow and glucose use per neuron are proportional to number of endothelial cells available per neuron across sites in the rat brain. Front. Integr. Neurosci. 2022;16 doi: 10.3389/fnint.2022.821850.

Verheggen I.C.M., Van Boxtel M.P.J., Verhey F.R.J., Jansen J.F.A., Backes W.H. Interaction between blood-brain barrier and glymphatic system in solute clearance. Neurosci. Biobehav. Rev. 2018;90:26–33. doi: 10.1016/j.neubiorev.2018.03.028.

Vijay N., Morris M.E. Role of monocarboxylate transporters in drug delivery to the brain. Curr. Pharmaceut. Des. 2014;20:1487–1498. doi: 10.2174/13816128113199990462.

Vogel C., Marcotte E.M. Insights into the regulation of protein abundance from proteomic and transcriptomic analyses. Nat. Rev. Genet. 2012;13(4):227–232. doi: 10.1038/nrg3185.

von Oettingen G., Bergholt B., Gyldensted C., Astrup J. Blood flow and ischemia within traumatic cerebral contusions. Neurosurgery. 2002;50(4):781–788. doi: 10.1097/00006123-200204000-00019. discussion 788-790.

Wang D., Johnson A.D., Papp A.C., Kroetz D.L., Sadee W. Multidrug resistance polypeptide 1 (MDR1, ABCB1) variant 3435C>T affects mRNA stability. Pharmacogenetics Genom. 2005;15(10):693–704.

Weber B., Keller A.L., Reichold J., Logothetis N.K. The microvascular system of the striate and extrastriate visual cortex of the macaque. Cerebr. Cortex. 2008;18(10):2318–2330. doi: 10.1093/cercor/bhm259.

Wilhelm I., Fazakas C., Molnár J., et al. Regulation of cerebral endothelial cell morphology by extracellular calcium. Phys. Med. Biol. 2007;52(20):6261–6274. doi: 10.1088/0031-9155/52/20/012.

Winkler E.A., Bell R.D., Zlokovic B.V. Pericyte-specific expression of PDGF beta receptor in mouse models with normal and deficient PDGF beta receptor signaling. Mol. Neurodegener. 2010;5:32. doi: 10.1186/1750-1326-5-32.

Winkler E.A., Bell R.D., Zlokovic B.V. Central nervous system pericytes in health and disease. Nat. Neurosci. 2011;14(11):1398–1405. doi: 10.1038/nn.2946.

Wolburg H., Noell S., Mack A., Wolburg-Buchholz K., Fallier-Becker P. Brain endothelial cells and the glio-vascular complex. Cell Tissue Res. 2009;335(1):75–96. doi: 10.1007/s00441-008-0658-9.

Wu E.X., Tang H., Jensen J.H. High-resolution MR imaging of mouse brain microvasculature using the relaxation rate shift index Q. NMR Biomed. 2004;17(8):507–512. doi: 10.1002/nbm.921.

Yamashita T., et al. Subventricular zone-derived neuroblasts migrate and differentiate into mature neurons in the post-stroke adult striatum. J. Neurosci. 2006;26:6627–6636. doi: 10.1523/JNEUROSCI.0149-06.2006.

Yanagida O., et al. Human L-type amino acid transporter 1 (LAT1): characterization of function and expression in tumor cell lines. Biochim. Biophys. Acta. 2001;1514:291–302. doi: 10.1016/s0005-2736(01)00384-4.

Yang A.C., Stevens M.Y., Chen M.B., et al. A human brain vascular atlas reveals diverse mediators of Alzheimer's risk. Nature. 2022;603(7897):885–892. doi: 10.1038/s41586-021-04369-3.

Zhang W., Mojsilovic-Petrovic J., Andrade M.F., Zhang H., Ball M., Stanimirovic D.B. The expression and functional characterization of ABCG2 in brain endothelial cells and vessels. Faseb. J. 2003;17(14):2085–2087.

Zhang Y., Chen K., Sloan S.A., et al. An RNA-sequencing transcriptome and splicing database of glia, neurons, and vascular cells of the cerebral cortex. J. Neurosci. 2014;34(36):11929–11947. doi: 10.1523/JNEUROSCI.1860-14.2014.

Zlokovic B.V. The blood-brain barrier in health and chronic neurodegenerative disorders. Neuron. 2008;57:178–201. doi: 10.1016/j.neuron.2008.01.003.

8. Tables and Figures

Experiment type	Brain ID	Sex	Age (years)	Cause of death	PMI (hours)	Tissue pH
RNA seq	1	Female	76	Polytrauma (accident)	26.5	6.5
RNA seq	2	Female	51	Pulmonary embolism	111.3	6.5
RNA seq	3	Male	26	Polytrauma (car accident)	12.0	6.8
RNA seq	4	Female	28	Undetermined	80.0	6.5
RNA seq	5	Female	45	Pulmonary embolism	39.5	5.7
Mass spec	6	Male	45	Gun wound	20.5	6.6
Mass spec	7	Male	54	Cardiac arrest	25.3	6.6
Mass spec	8	Male	63	Fall from several metres	13.0	6.8

Table 1: Background information on human subjects whose vmPFC tissue was studied. Information includes sex, age, cause of death, postmortem interval (PMI), and tissue pH.

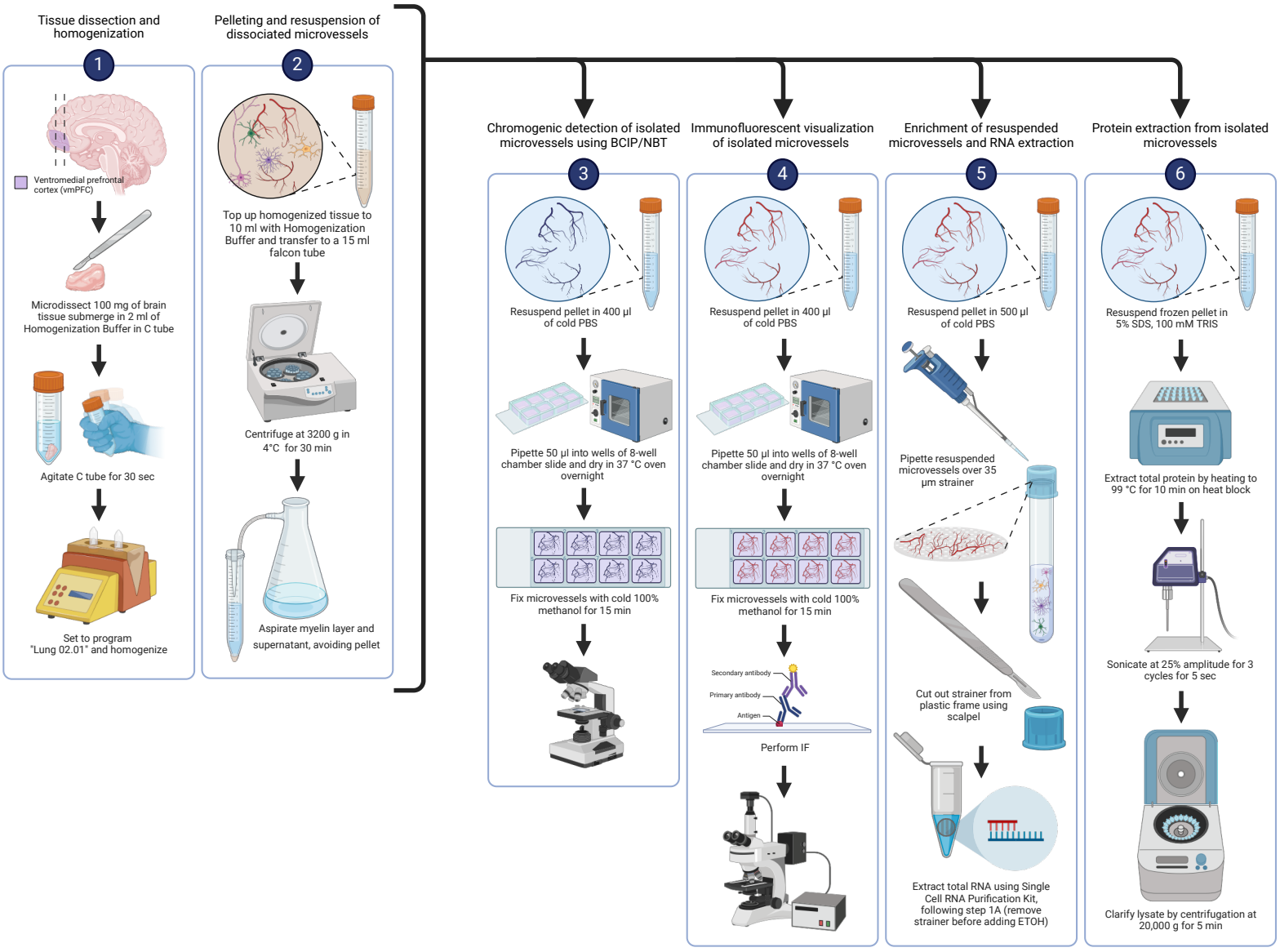
Tissue dissection and homogenization
1
Ventromedial prefrontal cortex (vmPFC)
Microdissect 100 mg of brain tissue submerge in 2 ml of Homogenization Buffer in C tube
Agitate C tube for 30 sec
Set to program "Lung 02.01" and homogenize
Pelleting and resuspension of dissociated microvessels
2
Top up homogenized tissue to 10 ml with Homogenization Buffer and transfer to a 15 ml falcon tube
Centrifuge at 3200 g in 4°C for 30 min
Aspirate myelin layer and supernatant, avoiding pellet
Chromogenic detection of isolated microvessels using BCIP/NBT
3
Resuspend pellet in 400 µl of cold PBS
Pipette 50 µl into wells of 8-well chamber slide and dry in 37 °C oven overnight
Fix microvessels with cold 100% methanol for 15 min
Immunofluorescent visualization of isolated microvessels
4
Resuspend pellet in 400 µl of cold PBS
Pipette 50 µl into wells of 8-well chamber slide and dry in 37 °C oven overnight
Fix microvessels with cold 100% methanol for 15 min
Secondary antibody
Primary antibody
Antigen
Perform IF
Enrichment of resuspended microvessels and RNA extraction
5
Resuspend pellet in 500 µl of cold PBS
Pipette resuspended microvessels over 35 µm strainer
Cut out strainer from plastic frame using scalpel
Extract total RNA using Single Cell RNA Purification Kit, following step 1A (remove strainer before adding ETOH)
Protein extraction from isolated microvessels
6
Resuspend frozen pellet in 5% SDS, 100 mM TRIS
Extract total protein by heating to 99 °C for 10 min on heat block
Sonicate at 25% amplitude for 3 cycles for 5 sec
Clarify lysate by centrifugation at 20,000 g for 5 min

Figure 1: Stage 1: After the vmPFC is dissected from a coronal slice containing the frontal lobe, 100 mg of vmPFC tissue is more precisely microdissected using a sterile blade or scalpel. Afterwards, the vmPFC tissue sample is dissociated in Homogenization Buffer using the GentleMACS™ Dissociator. Stage 2: Following dissociation, the sample is centrifuged at 3200 g for 30 mins in order to pellet dissociated microvessels. Additional downstream applications can be applied using microvessel-enriched pellets as shown in stages 3–6 by BCIP/NBT detection, immunofluorescent visualization, total RNA extraction, and total protein extraction, respectively. Image generated using BioRender.

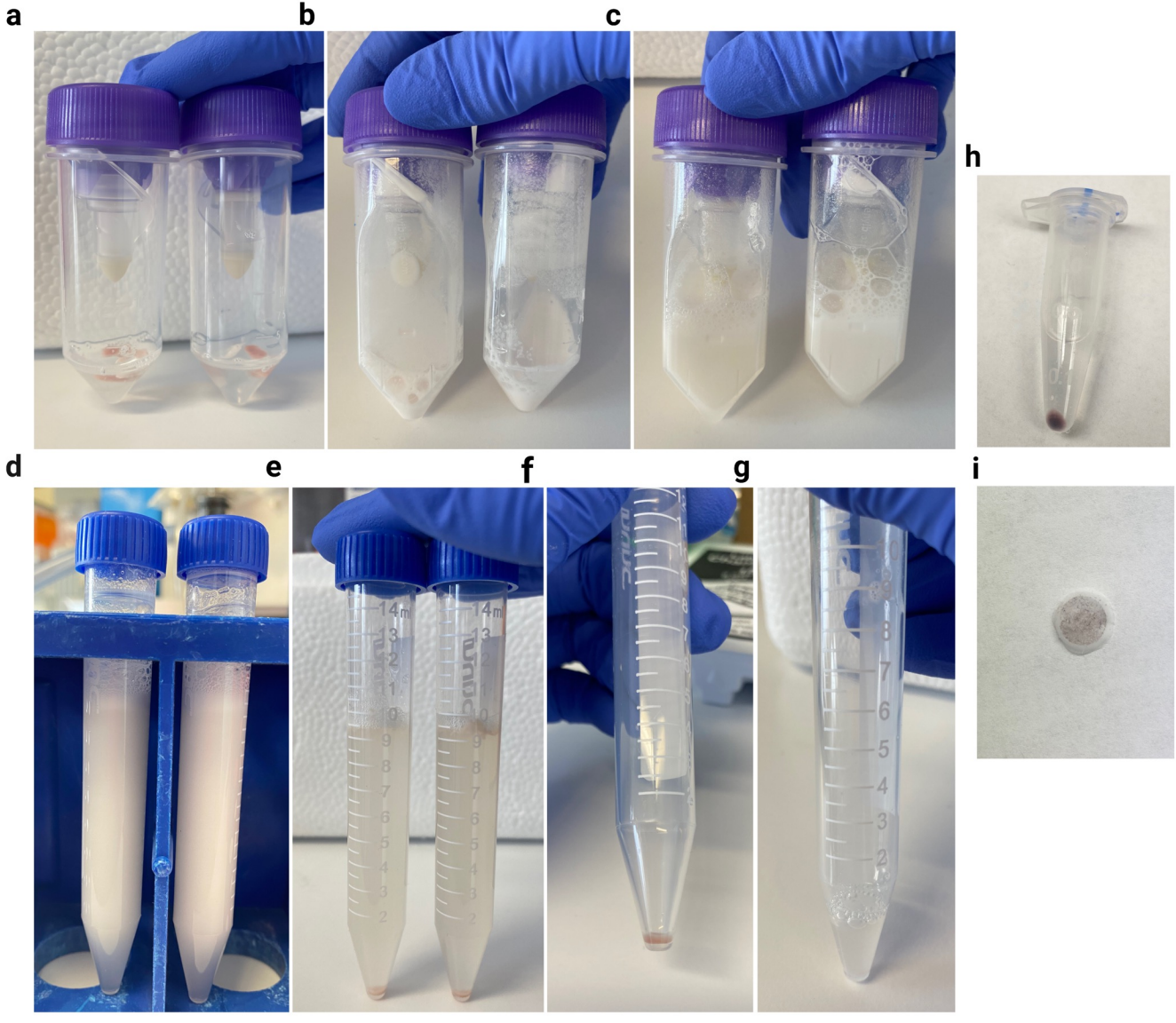
a
b
c
h
d
e
f
g
i

Figure 2: a-g) Overview of experimental steps taken to collect and resuspend pelleted microvessels (BCIP/NBT staining is omitted). a) 100 mg of vmPFC tissue submerged in 2 ml of Homogenization Buffer. b) 100 mg of vmPFC tissue after homogenization. c) Lysate topped-up to 10 ml with Homogenization Buffer. d) Lysate transferred to 15 ml falcon tube. e-f) After centrifugation at 3200*g* for 30 min, a microvessel-enriched pellet forms at the bottom of the tube. g) microvessel-enriched pellet is resuspended in 500 µl of PBS. h-i) Output of experimental steps when BCIP/NBT staining is used. h) Example of BCIP/NBT-stained microvessel pellet, which lends a purple colour to the pellet. i) BCIP/NBT-stained microvessels trapped within the meshwork of a cellular strainer.

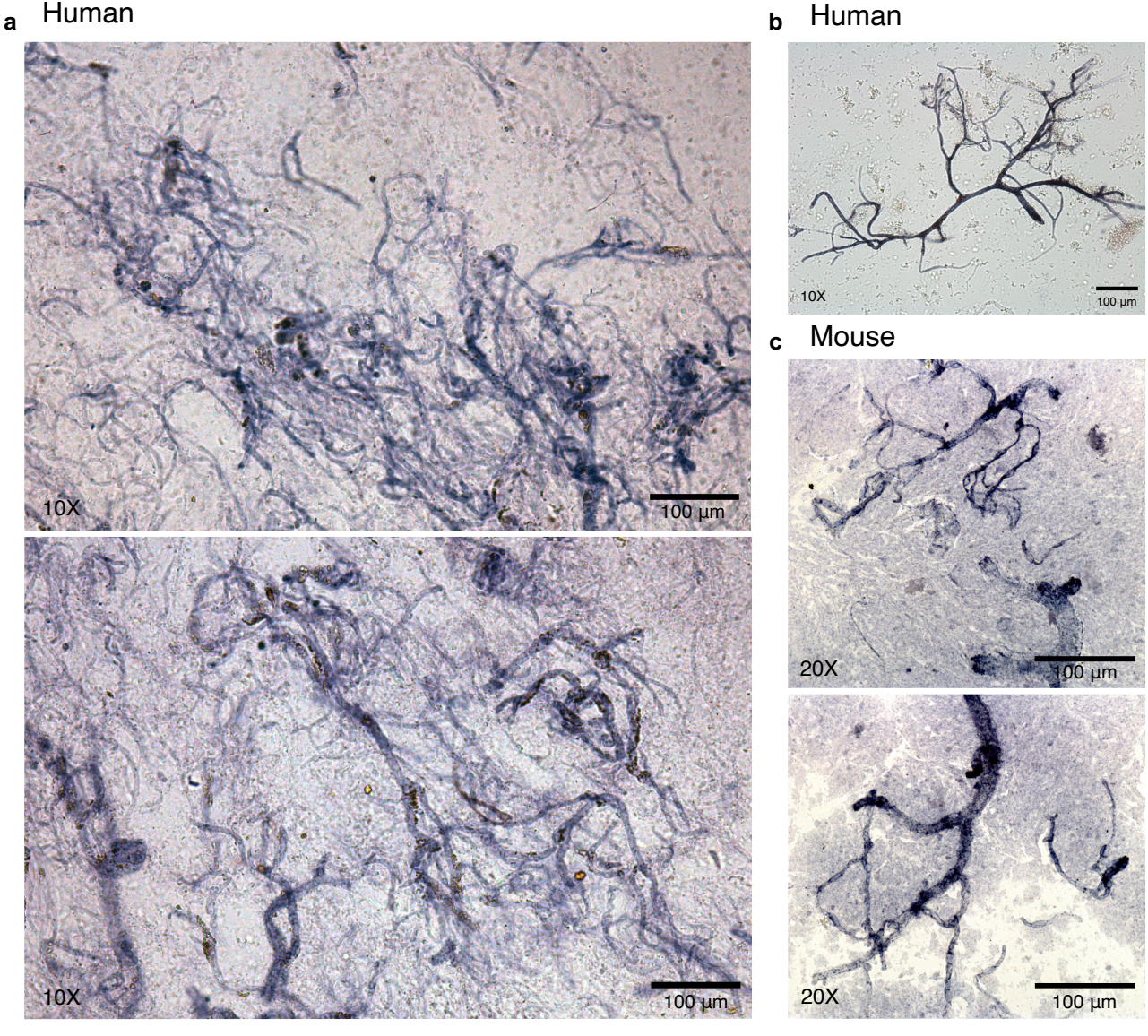
a
Human
10X
100 µm
10X
100 µm
b
Human
10X
100 µm
c
Mouse
20X
100 µm
20X
100 µm

Figure 3: a-c) Isolated microvessels are enriched from brain tissue following the described protocol. a-c) Brightfield images of chromogenically stained microvessels using BCIP/NBT substrate demonstrated isolation and enrichment of predominantly microvessels from postmortem vmPFC tissue samples. b) example of preserved microvessel morphology and integrity isolated from postmortem vmPFC tissue. c) Similar microvessel enrichment was observed when the same protocol was carried out using mouse cortex.

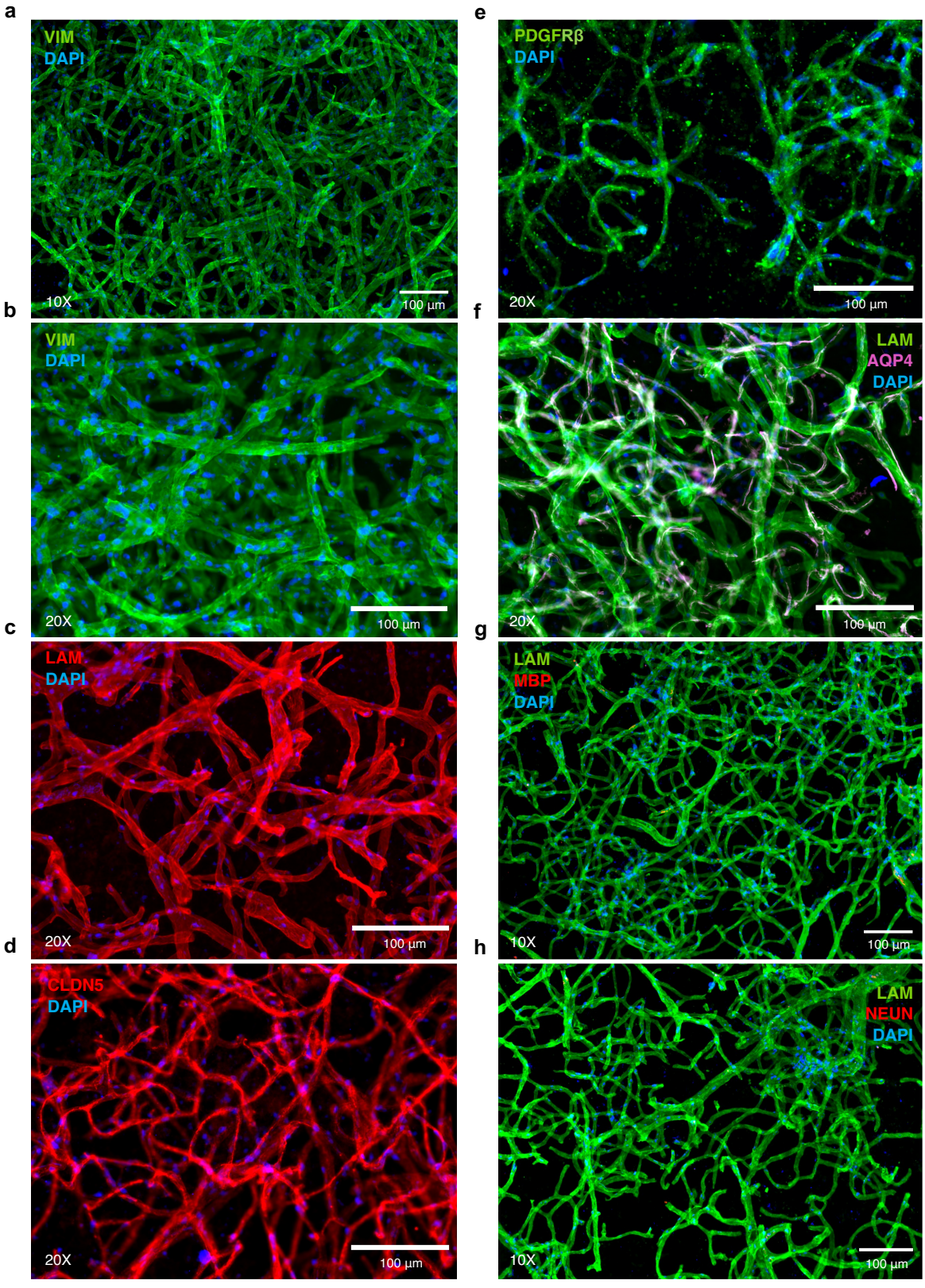
a
VIM
DAPI
10X
100 µm
b
VIM
DAPI
20X
100 µm
c
LAM
DAPI
20X
100 µm
d
CLDN5
DAPI
20X
100 µm
e
PDGFRβ
DAPI
20X
100 µm
f
LAM
AQP4
DAPI
20X
100 µm
g
LAM
MBP
DAPI
10X
100 µm
h
LAM
NEUN
DAPI
10X
100 µm

Figure 4: a-b) Endothelial and smooth muscle cells immunolabelled for vimentin (green). c) Extracellular matrix laminins expressed by vascular-related cell types are immunolabelled (red). d) Endothelial cell tight junctions immunolabelled for CLDN5 (red). e) Pericytes immunolabelled for PDGFRβ (green). f) AQP4 expressed by the vessel-facing astrocyte membrane is immunolabelled (magenta) and laminins (green). g) Oligodendrocyte marker MBP (red) shows an absence of immunoreactivity in microvessel preparations; similarly, h) neuronal marker NeuN (red) shows an absence of immunoreactivity in microvessel preparations. Nuclei were stained with DAPI (blue) in all micrographs.

a

Deconvolution against VL dataset using CIBERSORT v1.04

	Cell Type				
Subject	Neurons	Astrocytes	Oligodendrocytes	Microglia	Endothelia
1	4.00	4.92	2.15	0.00	88.93
2	0.00	0.62	1.51	0.00	97.86
3	0.00	0.51	2.37	0.78	96.34
4	5.81	0.25	0.97	0.00	92.96
5	0.00	0.99	0.50	0.00	98.52
Average	1.29	1.16	1.85	0.16	94.92

Dataset provided by Velmeshev et al. 36 and performed using BrainDeconvShiny tool

b

Deconvolution against MB dataset using CIBERSORT v1.04

	Cell Type				
Subject	Neurons	Astrocytes	Oligodendrocytes	Microglia	Endothelia
1	12.35	11.82	0	0.00	75.83
2	0.00	5.78	0	0.00	94.22
3	0.00	3.30	0	3.97	92.73
4	16.52	5.53	0	0.00	77.95
5	0.00	6.19	0	0.00	93.81
Average	4.66	6.11	0	1.06	86.91

Multibrain composite signature generated by Sutton et al. 202213 and performed using BrainDeconvShiny

c

Deconvolution against Yang dataset using CIBERSORTX

	Cell Type														
Subject	Neuron	Oligo	OPC	Ependymal	M. Fibro	Microglia	T cell	P. Fibro	Astrocyte	Venous	Arterial	Capillary	SMC	Pericyte	Total Vascular
1	6.40	0.00	0	0	3.63	0.00	5.31	2.84	1.87	0	0.00	33.17	46.77	0.00	84.66
2	0.00	0.00	0	0	1.36	0.00	1.49	0.00	1.76	0	0.00	66.82	28.58	0.00	97.15
3	0.60	0.00	0	0	0.81	0.69	5.79	3.18	0.00	0	8.44	36.11	44.39	0.00	92.11
4	8.41	0.00	0	0	2.58	0.00	6.49	4.35	0.00	0	6.74	26.55	44.87	0.00	82.52
5	0.00	0.00	0	0	1.11	0.00	3.25	1.03	0.37	0	0.00	65.74	25.73	2.77	95.64
Average	4.01	0.14	0	0	2.01	0.24	5.64	2.33	0.98	0	2.53	44.02	37.62	0.46	90.42

Figure 5: a-b) Using the BrainDeconvShiny tool, different iterations of computational deconvolution were performed to demonstrate stability of outcome when using our microvessel isolation preparations. a) The average expression from every control sample from the VL dataset was calculated and used as cell type signatures for deconvolution of our dataset using CIBERSORT v1.04. b) The MB (MultiBrain) is a composite signature generated by Sutton et al. (2022) by averaging the expression signatures of five datasets for five cell types (neurons, astrocytes, oligodendrocytes, microglia, and endothelia). MB was used as cell type signatures for deconvolution of our dataset using CIBERSORT v1.04. c) In-house analysis where the average expression from every control sample from the Yang dataset was calculated and used as cell type signatures for deconvolution of our dataset using CIBERSORTX. Heattables were generated using the gt package in R.

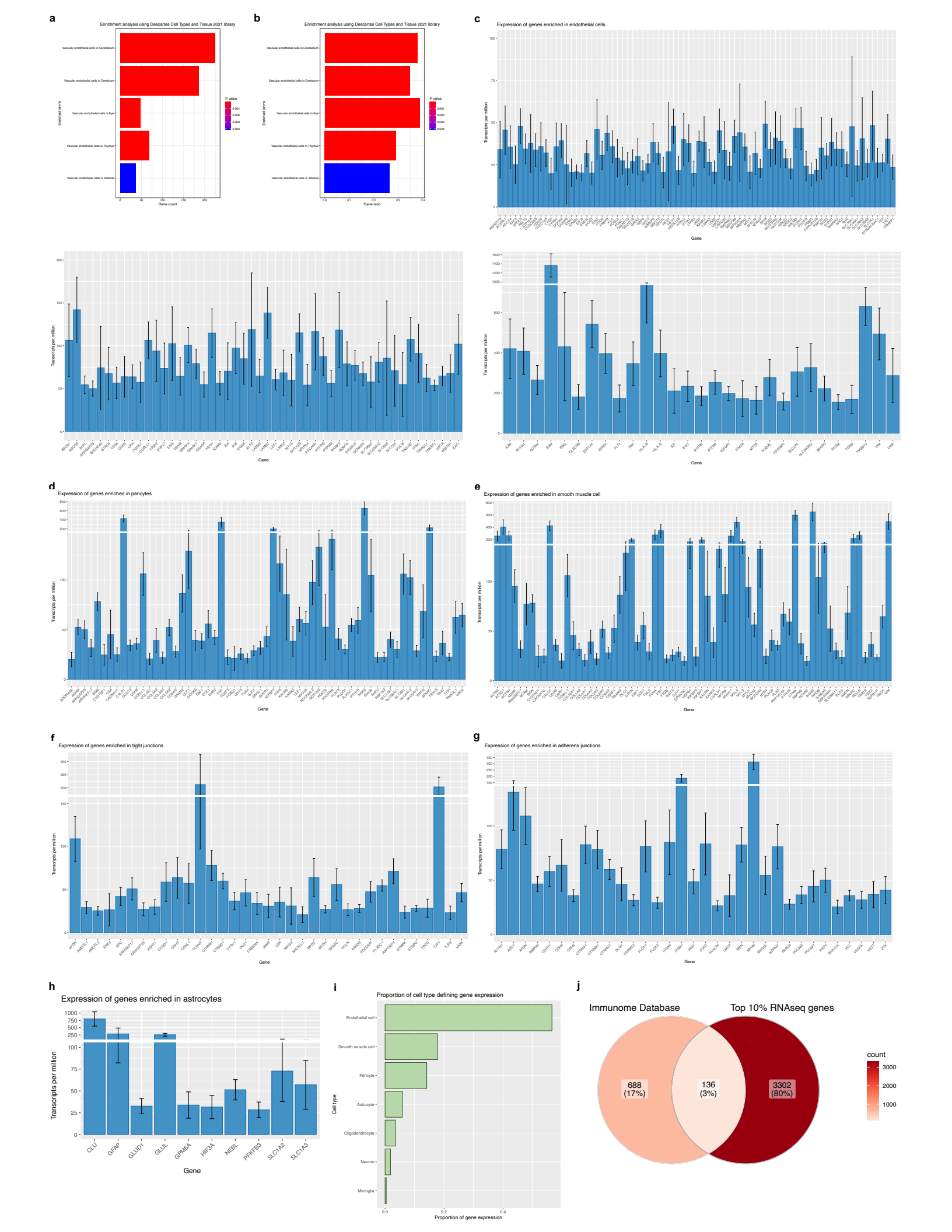
a
Enrichment analysis using Descartes Cell Types and Tissue 2021 library
Vascular endothelial cells in Cerebellum
Vascular endothelial cells in Cerebrum
Vascular endothelial cells in Eye
Vascular endothelial cells in Thymus
Vascular endothelial cells in Adrenal
Enrichet terms
Gene count
P value
b
Enrichment analysis using Descartes Cell Types and Tissue 2021 library
Gene ratio
c
Expression of genes enriched in endothelial cells
Transcripts per million
Gene
d
Expression of genes enriched in pericytes
e
Expression of genes enriched in smooth muscle cell
f
Expression of genes enriched in tight junctions
g
Expression of genes enriched in adherens junctions
h
Expression of genes enriched in astrocytes
CLU
GFAP
GLUD1
GLUL
GPM6A
HIF3A
NEBL
PFKFB3
SLC1A2
SLC1A3
i
Proportion of cell type defining gene expression
Endothelial cell
Smooth muscle cell
Pericyte
Astrocyte
Oligodendrocyte
Neuron
Microglia
Cell type
Proportion of gene expression
j
Immunome Database
Top 10% RNAseq genes
688
(17%)
136
(3%)
3302
(80%)
count
3000
2000
1000

Figure 6: a-b) Enrichment analysis of averaged 10% of most highly expressed genes (3437 genes) returns predominantly vascular-related terms. Over-representation analysis (ORA) using the enrichR package in R and the “Descartes Cell Types and Tissue 2021” database was used to identify gene sets that are statistically over-represented. The threshold value of enrichment was selected by a p-value <0.05, indicating that over-represented genes were significantly enriched for vascular-related terms. a) Count for genes in our dataset that are present in returned gene sets. b) Ratio for genes in our dataset that are present in returned gene sets, determined by the total number of genes in each set. c-i) Isolated microvessels have increased expression of canonical neurovascular-related genes. c) Bar plots showing TPMs for endothelial-defining genes, displayed according to general expression range. Highest expression found in endothelial genes B2M, BSG, FLT1, IFITM3, MT2A, SLC2A1, VIM, and VWF. d) Bar plot showing TPMs for pericyte-defining genes. Highest expression was detected in pericyte genes CALD1, FN1, IGFBP7, RGS5, and SPARCL1. e) Bar plot showing TPMs for smooth muscle cell-defining genes. Highest expression was detected in smooth muscle genes ACTG1, ACTN4, MYL6, PTMA, and TAGLN. f) Bar plot showing TPMs for tight junction-defining genes and g) Bar plot showing TPMs for adherens junction-defining genes. Several genes encoding for junctional proteins are found in the top 10% of most highly expressed genes, including CLDN5, CTNNB1, CTNND1, OCLN, JAM1, TJP1, and TJP2. h) Bar plot showing TPMs for astrocyte-defining genes. Astrocytic gene expression was predominantly limited to markers of astrocytic processes or endfeet, namely CLU, GFAP, and GLUL. i) TPMs from neurovascular-related genes were summarized according to cell type expression, demonstrating an overrepresentation of endothelial, smooth muscle cell, and pericyte genes. j) Overlap between top 10% of most highly expressed genes from our RNA sequencing data and immune genes found within the Immunome Database. Bar plots were generated using the ggplot package and Venn diagram was generated using the ggVennDiagram package in R.

a

Overlap between Garcia et al. arteriole markers and top 10% of RNAseq highly expressed genes

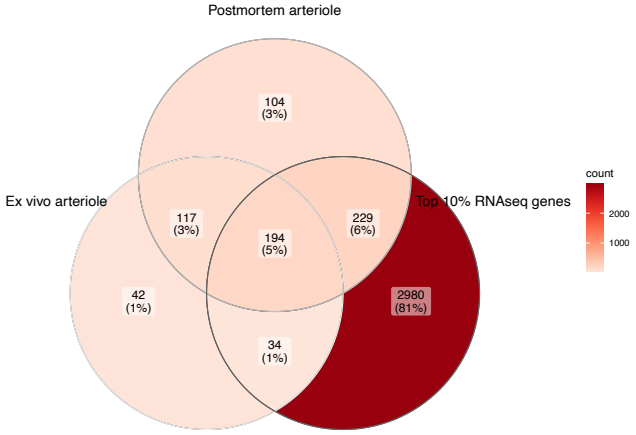

b

Overlap between Garcia et al. capillary markers and top 10% of RNAseq highly expressed genes

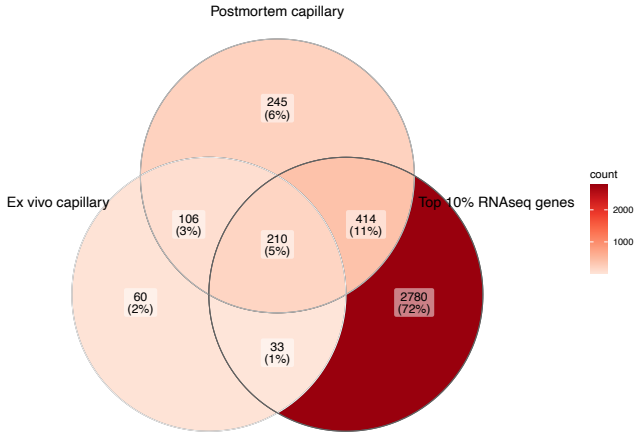

c

Overlap between Garcia et al. venule markers and top 10% of RNAseq highly expressed genes

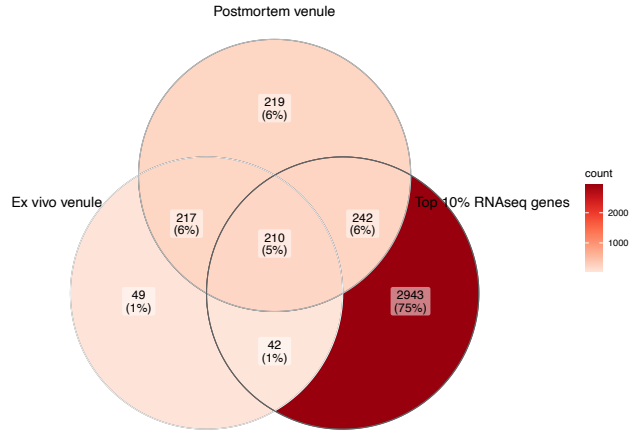

d

Overlap between Garcia et al. arteriolar SMC markers and top 10% of RNAseq highly expressed genes

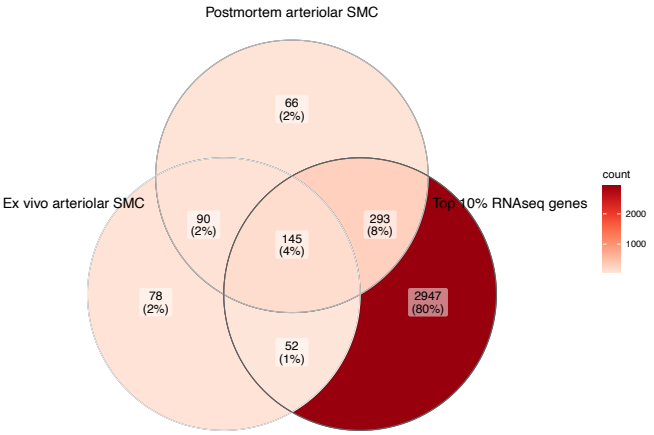

e

Overlap between Garcia et al. pericyte markers and top 10% of RNAseq highly expressed genes

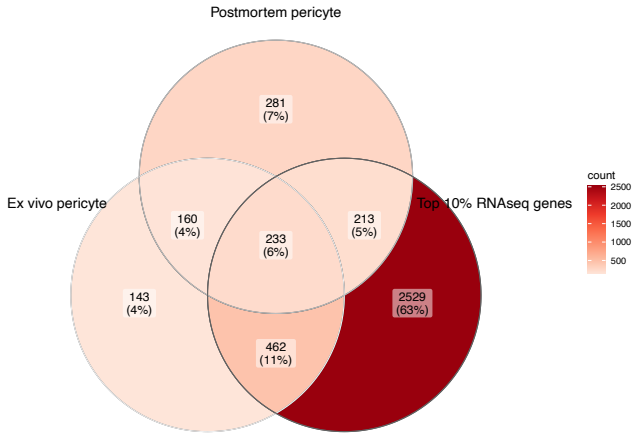

f

Overlap between Garcia et al. venular SMC markers and top 10% of RNAseq highly expressed genes

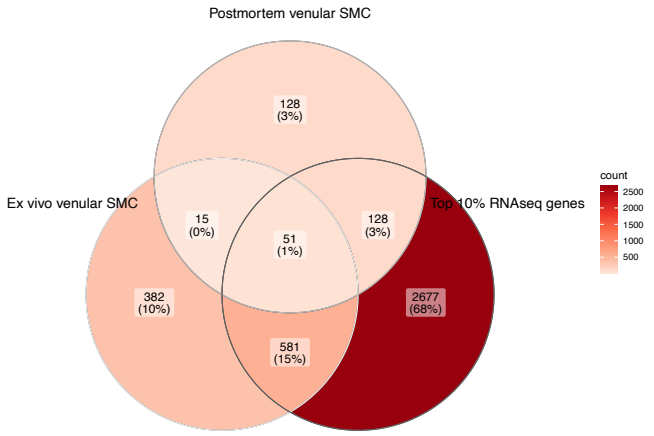

g

Overlap between Garcia et al. fibroblast markers and top 10% of RNAseq highly expressed genes

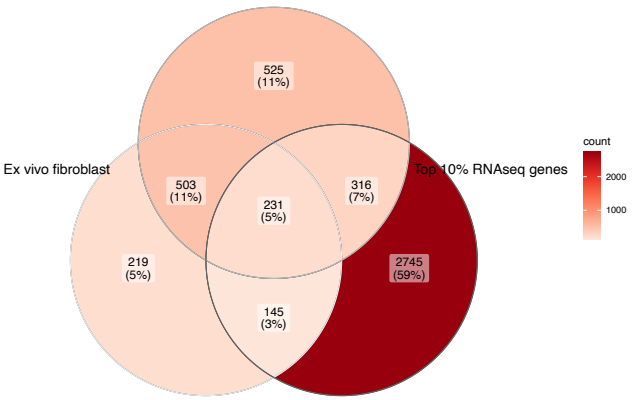

Figure 7: a-g) Overlap between the top 10% of most highly expressed genes from our RNA sequencing data and published NVU dataset. Validated neurovascular cell type markers were obtained from Garcia et al. (2022) postmortem and human ex vivo single-nucleus sequencing datasets (found under Supplementary Table 2) and compared for potential overlap with the top 10% of most highly expressed genes from our data. Results indicate a significant overlap between the three datasets for all NVU-related cell types. a) Arteriole-defining genes. b) Capillary-defining genes. c) Venule-defining genes. d) Arteriolar SMC-defining genes. e) Pericyte-defining genes. f) Venular SMC-defining genes. g) Fibroblast-defining genes. Venn diagrams were generated using the ggVennDiagram package in R.

a

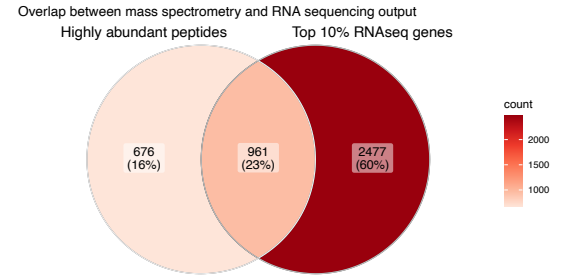

b

Gene	Protein product	Normalized abundance
ABCB1	ATP-binding cassette sub-family B member 1	24289.33
ABCD3	ATP-binding cassette sub-family D member 3	2658.70
ABCG2	Broad substrate specificity ATP-binding cassette transporter ABCG2	5820.07
BSG	Basigin	10243.33
CDH5	Cadherin-5	3523.03
CLDN5	Claudin-5	3749.77
ESAM	Endothelial cell-selective adhesion molecule	5216.87
LAMA3	Laminin subunit alpha-3	1370.67
LAMA5	Laminin subunit alpha-5	45940.30
LAMB2	Laminin subunit beta-2	75206.77
LAMC1	Laminin subunit gamma-1	78217.13
LAMC3	Laminin subunit gamma-3	8674.87
OCLN	Occludin	5962.83
PCDH1	Protocadherin-1	1323.90
PECAM1	Platelet endothelial cell adhesion molecule	9541.33
SLC16A1	Monocarboxylate transporter 1	6584.73
TJP1	Tight junction protein ZO-1	33614.17
TJP2	Tight junction protein ZO-2	2383.70
VIM	Vimentin	210675.97
VWA1	von Willebrand factor A domain-containing protein 1	14203.10
VWF	von Willebrand factor	31440.13

c

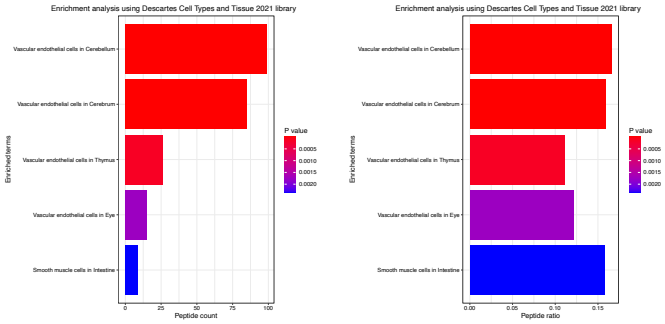

d

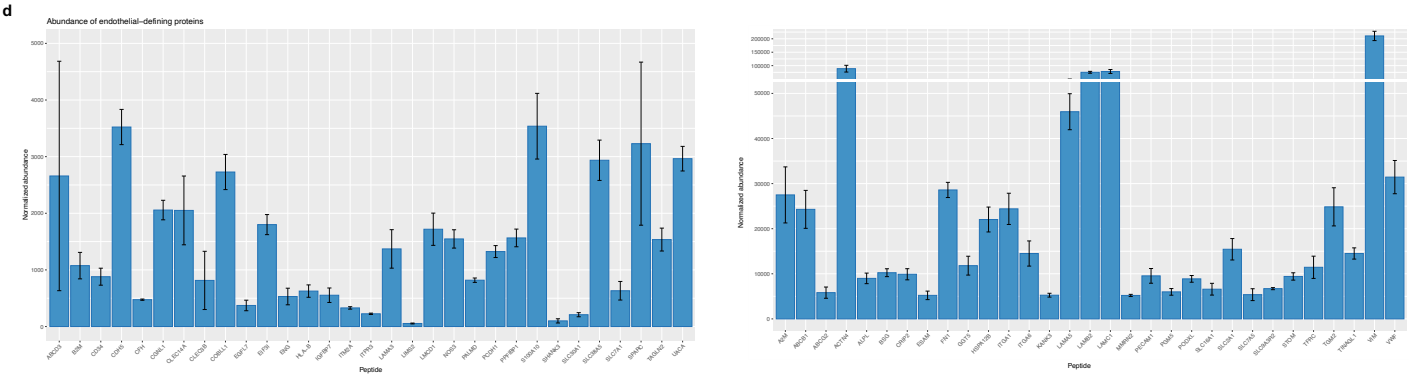

e

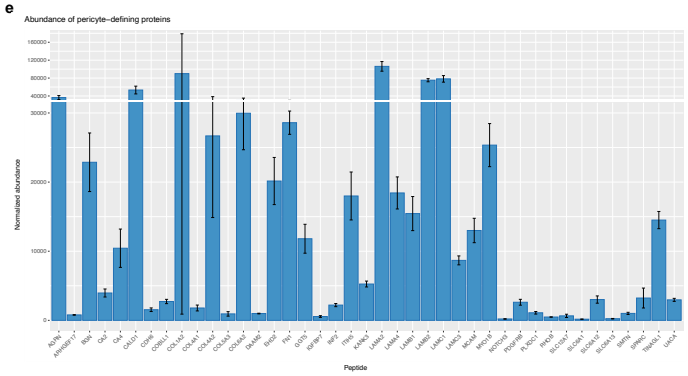

f

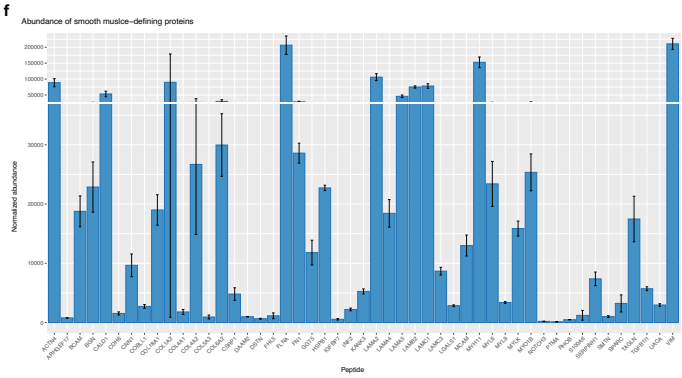

g

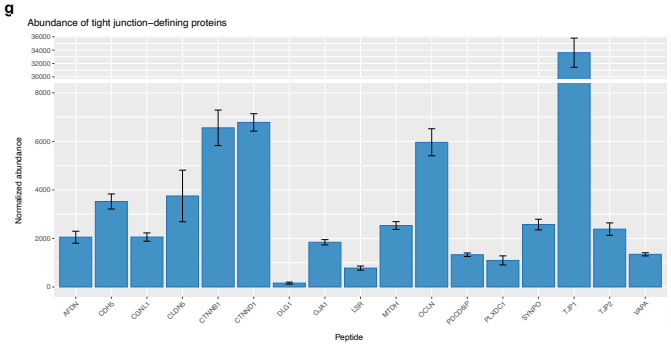

h

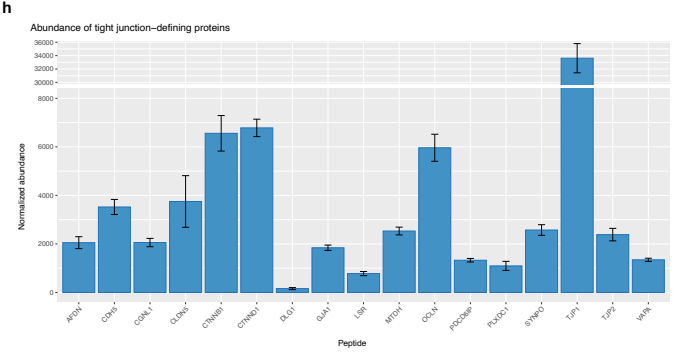

i

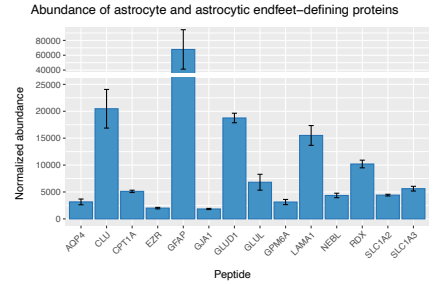

Figure 8: a-i) There is substantial overlap between transcriptomic and proteomic data output. a) 1635/1637 (99.9%) of proteins likewise identified in the transcriptomics data, and with 1024/1637 (62.6%) proteins found in the top 10% of most highly expressed genes. b) Several canonical BMEC markers were detected with high normalized average abundance. c) Over-representation analysis using the enrichR package in R and the "Descartes Cell Types and Tissue 2021" database was used to identify statistically over-represented sets. Genes corresponding to proteins detected during LC-MS/MS were used as input and the threshold value of enrichment was selected by a p-value <0.05. Output indicated that over-represented proteins were significantly enriched for vascular-related terms. a) Count for peptides in our dataset that are present in returned sets. b) Ratio for peptides in our dataset that are present in returned sets, determined by the total number in each set. d) Bar plot showing normalized abundance for endothelial cell-defining proteins. e) Bar plot showing normalized abundance for pericyte-defining proteins. f) Bar plot showing normalized abundance for smooth muscle cell defining-proteins. g) Bar plot showing normalized abundance for tight junction defining-proteins. h) Bar plot showing normalized abundance for adherens junction-defining proteins. i) Bar plot showing normalized abundance for astrocyte and astrocytic endfeet-defining proteins. Bar plots generated using the ggplot package and Venn diagram generated using the ggVennDiagram package in R.

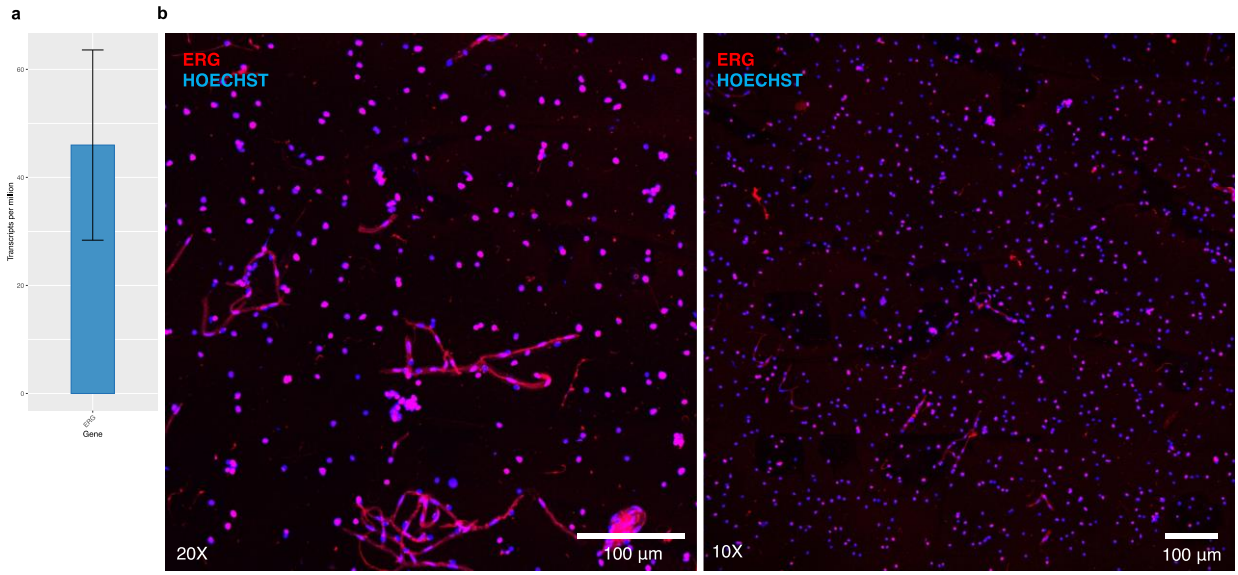

Figure 9: Isolated microvessels can be used to further sort endothelial nuclei. a) ERG is a top 10% most highly expressed gene in isolated microvessels. b) Dissociated endothelial nuclei immunolabelled with ERG conjugated to Alexa-647 antibody prior to FANS protocol. Resuspended microvessels subjected to a 2-h incubation with anti-ERG antibody under rotation is sufficient for immunolabelling of endothelial nuclei prior to FANS sorting.

Transition from Study 1 to Study 2

In our first study, we developed an effective method for the enrichment and isolation of microvessels from human postmortem brain tissue that is compatible with downstream high throughput techniques. For our next study, we aimed to utilize the microvessel enrichment and isolation method to obtain microvessel samples from postmortem brain tissue belonging to those with histories of ELA. By ensuring that isolated microvessels are of sufficient yield and integrity for downstream high-throughput techniques, our next goal was to conduct an unbiased, data-driven analysis that would allow us to characterize long-term impacts at the NVU associated with ELA. The rationale behind this was manifold: first and foremost, the impact of ELA on cellular and molecular components and BBB permeability still is largely unexplored in the literature, including limited knowledge of region- and sex-dependent differences in NVU integrity and function, and their potential modulation by ELA. Before this body of work, the literature consisted entirely of reports focused on the impact of stress on CLDN5 expression and the formation of stochastic stress-induced microbleeds in rodents. Because of this, there were very few single gene candidates relevant to the human neurovasculature to investigate by a hypothesis-driven approach for study 2. Secondly, we had the unique opportunity to generate the first NVU-specific whole transcriptome dataset from ELA-affected individuals. Generating a whole transcriptome dataset would enable us to conduct comprehensive analyses that were not previously feasible, including identifying all differentially expressed genes, as well as pathways and networks affected by ELA— a rich resource for the research community trying to validate findings from animal models, and for comparisons with neuropsychiatric or neurodegenerative disorders. Other critical the nature of the data generated. Namely, we opted to obtain whole transcriptome data to, therefore, understand changes in gene regulation that persist after ELA, instead of generating proteomic data from isolated microvessels. Although proteins are the functional units of the cell, longstanding issues with dynamic range and limitations in sensitivity associated with current LC-MS/MS technologies would hinder the depth with which we could detect and quantify the proteome, especially with lower input samples (isolated microvessels) versus bulk tissue. Regardless of this choice, our microvessel

isolation method remains compatible with, and ready to use for when these technologies improve. Secondly, we chose to sequence samples of *intact* isolated microvessels, rather than further sorting them into their constituent cell type nuclei using FANS for sequencing. This decision was made to preserve cytosolic transcripts, which would be lost during the nuclei sorting process. By maintaining the integrity of the microvessels, we aimed to capture a more complete and accurate representation of the transcriptomic profile, reflecting the native cellular condition within the NVU. To the best of our knowledge, this study represents the first comprehensive characterization of the long-term impacts on NVU associated with ELA in either animal or postmortem human brain samples.

The brain stands on the top of the organs, and is the work of a refined artist.

Paul Ehrlich
Nobel Prize Laureate in Physiology or Medicine, 1908
Intentional discoverer of the first treatment for syphilis
Accidental discoverer of the blood-brain barrier

Chapter III

Neurovascular dysfunction in the ventromedial prefrontal cortex of female depressed suicides with a history of childhood abuse

Marina Wakid [a b], Daniel Almeida [a b], Ryan Denniston [a], Anjali Chawla [a b], Zahia Aouabed [a], Maria Antonietta Davoli [a], Reza Rahimian [a], Kristin Ellerbeck [a], Volodymyr Yerko [a], Elena Leonova-Erko [a], Gustavo Turecki [a b c], Naguib Mechawar [a b c]

[a] McGill Group for Suicide Studies, Douglas Research Centre, Montréal, Quebec, Canada

[b] Integrated Program in Neuroscience, McGill University, Montréal, Quebec, Canada

[d] Department of Psychiatry, McGill University, Montréal, Quebec, Canada

Manuscript submitted for publication

Abstract

Exposure to early life adversity (ELA) poses a significant global public health concern, with profound pathophysiological implications for affected individuals. Studies suggest that ELA contributes to endothelial dysfunction, bringing into question the functional integrity of the neurovascular unit in brain regions vulnerable to chronic stress. Despite the importance of the neurovasculature in maintaining normal brain physiology, human neurovascular cells remain poorly characterized, particularly with regard to their contributory role in ELA-associated pathophysiologies. In this study, we present the first comprehensive transcriptomic analysis of intact microvessels isolated from postmortem ventromedial prefrontal cortex samples from adult healthy controls and matched depressed suicides with histories of ELA. Our findings point to substantive differences between men and women, with the latter exhibiting widespread gene expression changes at the neurovascular unit, including the key vascular nodal regulators KLF2 and KLF4, alongside a broad downregulation of immune-related pathways. These results suggest that the neurovascular unit plays a larger role in the neurobiological consequences of ELA in human females.

1. Introduction

Exposure to adverse childhood experiences (ACEs), defined as physical, sexual, and/or emotional abuse or neglect, is a persisting global public health concern. In developed countries, 44% of children have been subjected to ACEs, while the percentage rises to 59% in developing countries (Hillis et al., 2016). ELA can lead to profound disturbances in psychological and physical trajectories that, in turn, strongly correlate with increased lifetime risk of negative health outcomes. Notably, compelling evidence supports ACE-induced vascular endothelial dysfunction, characterized by increased arterial stiffness, higher peripheral vascular resistance, and reduced endothelial function (Su et al., 2014; Jenkins et al., 2021). Such dysfunction primes for the development of cardiovascular disease later in life (Chen et al., 2023; Fuller-Thomson et al., 2010; Loucks et al., 2014; Thurston et al., 2017; Thurston et al., 2014; Riley et al., 2010; Su et al., 2015; Dong et al., 2004; Felitti et al., 1998). The observed correlation between ELA and cardiovascular disease is physiologically sound. Indeed, the prefrontal cortex, an emotion-modulating (Pessoa, 2008) core component of a broader network of forebrain systems, mediates stress-evoked changes in cardiovascular activity (Ginty et al., 2017; Thayer et al., 2012); and there is ample evidence demonstrating sustained and pervasive molecular (Blaze et al., 2013; Lutz, Tanti et al., 2017; Usui et al., 2021; Oldham Green et al., 2021; Pena et al., 2019), cellular (Monroy et al., 2010; Tanti et al., 2018; Tanti et al., 2022; Gildawie et al., 2020) and functional abnormalities (van Harmelen et al., 2010; van Harmelen et al., 2014a; van Harmelen et al., 2014b; Hostinar et al., 2012; Kim et al., 2013; Ansell et al., 2012) of the prefrontal cortex following ELA. Although the blood-brain barrier (BBB) is functionally distinct from the peripheral vasculature and possesses a highly specialized neurovascular unit (NVU) to precisely regulate the influx and efflux between the blood and brain parenchyma (Luissint et al., 2012), the entire blood supply of the brain relies on the dorsal aorta (Purves et al., 2001). This reliance therefore maintains a structural connection to the peripheral vasculature, raising the question as to whether the NVU is similarly affected by ELA. Critically, ELA is associated with 44.6% of all psychiatric childhood-onset disorders and with 25.9% to 32.0% of adult-onset disorders (Green et al., 2010), such as major depressive disorder (MDD) (LeMoult et al., 2020; Nomura et al., 2002; Raposo et al., 2014; Cabrera et al.,

2007; Hayashi et al., 2015; Alon et al., 2024). Despite this, direct evidence implicating NVU dysfunction in the pathophysiology of ELA relies primarily on rodent models of chronic stress, which have focused on downregulated tight junction protein Claudin5 (CLDN5) (Dion-Albert et al., 2022; Dudek et al., 2020; Menard et al., 2017) or on the formation of cerebral microbleeds (Lehmann et al., 2018; Lehmann et al., 2020; Samuels et al., 2023; Lehmann et al., 2022). In contrast, studies investigating NVU dysfunction in adult humans with histories of ELA are limited to non-invasive techniques that characterize markers of plasma inflammation (Danese et al., 2007; Baumeister et al., 2016; Coelho et al., 2014; Takizawa et al., 2015; Danese et al., 2011; Slopen et al., 2013), using these markers to infer the state of the NVU. Critically, the use of animal proxy models cannot completely recapitulate human experience and its effects on human neurobiology (van der Worp et al., 2010), and recent breakthroughs have demonstrated that there are numerous species-specific differences between mouse and human neurovasculature (Munji et al., 2019; Garcia et al., 2022; Yang et al., 2022). For this reason, we set out to generate the first transcriptomic dataset derived from intact microvessels isolated from postmortem ventromedial prefrontal cortex (vmPFC) samples from controls and matched depressed suicides with a history of ELA. Isolated microvessels effectively capture the NVU, comprising brain microvascular endothelial cells (BMECs) sealed by tight junction proteins, astrocytic endfeet, and mural cells (McConnell et al., 2017). Here, we combined differential gene expression analysis and network-based approaches to provide an integrative and unbiased characterization of male and female transcriptional profiles of the NVU in humans with histories of ELA.

2. Methods

2.1. Human postmortem brain samples

This study was approved by the Douglas Hospital Research Ethics Board. Brains were donated to the Douglas-Bell Canada Brain Bank (www.douglasbrainbank.ca; Montreal, Canada) following written informed consent from next of kin, in the context of collaboration with the Quebec Coroner's Office. Phenotypic information was retrieved through standardized psychological autopsies (Dumais et al., 2005). In brief, proxy-based interviews with one or more informants best acquainted with the deceased were

supplemented with information from archival material obtained from hospitals, Coroner's office, and social services. Clinical vignettes were then produced and assessed by a panel of clinicians to generate a diagnosis based on the DSM-IV. Toxicological assessments and medication prescription are also obtained. As described previously (Lutz, Tanti et al., 2017), characterization of early-life histories was based on adapted Childhood Experience of Care and Abuse interviews assessing experiences of sexual and physical abuse, as well as neglect (Bifulco et al., 1994), and for which scores from siblings are highly concordant (Bifulco et al., 1997). The severity of ELA was assessed based on reports of non-random major physical and/or sexual abuse during childhood (up to 15 years). Only cases with the maximum severity ratings of 1 and 2 were included in this study. Because of this narrow selection criterion, it was not possible to stratify different types of abuse within the sample. Presence of any or suspected neurological/neurodegenerative disorder reported in clinical files constituted an exclusion criterion. Individuals were all Caucasians of French-Canadian descent. Samples from 21 healthy controls (CTRLs; 13 males, 8 females) and 24 depressed suicides with a history of severe childhood abuse (ELA; 17 males, 7 females) were analyzed in this study. Group characteristics are described in Table 1.

2.2. Tissue dissections

Grey matter samples were dissected from the vmPFC by expert brain bank staff on fresh-frozen 0.5 cm-thick coronal sections with the guidance of a human brain atlas (Majtanik and Paxinos, 2016). vmPFC samples were dissected in sections equivalent to plate 3 (approximately −48 mm from the center of the anterior commissure) of this atlas, corresponding to Brodmann areas 11 and 12. Samples in every form, whether extracted total RNA, RNA sequencing library, or mounted tissue sections, were stored frozen at -80° C until further use.

2.3. Microvessel isolation from tissue microdissection

To capture the complete, multicellular composition of the NVU, microvessels were enriched and isolated using our recently developed protocol (Wakid et al., 2023), which is a method that is gentle enough to dissociate brain tissue while preserving the

structural integrity and multicellular composition of microvessels. In brief, 100 mg of microdissected vmPFC grey matter was homogenized in 2 ml of cold homogenization buffer (1M sucrose + 1% BSA dissolved in DEPC-treated water) using the benchtop gentleMACS™ Dissociator (Miltenyi Biotec, Germany) with the rotating paddle set to the Lung 02.01 program. After tissue homogenization, an additional 8 ml of cold homogenization buffer was pipetted into the tube, topping up the homogenate to 10 ml. The homogenate was gently inverted to mix, and then centrifuged at 3200 g for 30 min at 4° C. Following centrifugation, a microvessel-enriched pellet formed at the bottom of the falcon tube, after which the supernatant was carefully vacuum-aspirated (which may include an upper layer of clumped dissociated myelin) without disturbing the microvessel-enriched pellet. To assess RNA quality, RNA integrity number (RIN) was measured for microvessel isolation samples, with an average value of 4.

2.4. Visualization of microvessels from the enriched pellet using immunofluorescence

Immunophenotypic characterization of isolated microvessels was carried out following the resuspension of microvessel-enriched pellets, as per Wakid et al., 2023. Pellets were gently resuspended in 400 µl of cold PBS and 50 µl of the resuspension was pipetted into each well of an 8-well chamber slide (Nunc™ Lab-Tek™ II Chamber Slide™ System; Thermo Scientific™, United States). The chamber slide was left open-faced to incubate in a 37°C oven overnight, allowing microvessels to dry flush to the surface of the slide after the PBS evaporated. After drying, microvessels were fixed by covering them to a depth of 2–3 cm with ice-cold 100% methanol for 15 min on ice or at 4°C. Subsequently, the methanol was aspirated, and the wells were washed with 1X PBS three times for 5 min each. Microvessels were then incubated in blocking buffer (1% BSA + 0.5% Triton X dissolved in PBS) under gentle agitation for 60 min at 4°C. Afterwards, blocking solution was replaced with 500 µl of primary antibody dilution (1:500 in 1% BSA + 2% normal donkey serum + 0.5% Triton X dissolved in PBS) and incubated under gentle agitation overnight at 4°C. Primary antibody dilution was then aspirated and wells were washed in 1X PBS three times for 5 min each. Microvessels were finally incubated in fluorophore-conjugated secondary antibody dilution (1:500 in

1% BSA + 2% normal donkey serum + 0.5% Triton X dissolved in PBS) under gentle agitation for 2 hours at room temperature, protected from all light. Following washes, the media chamber was removed, and the microscope slide carrying microvessels was coverslipped using VECTASHIELD Antifade Mounting Medium with DAPI (Vector Laboratories, Inc., United States). To visualize the expression of canonical NVU markers, primary antibodies targeting key expression markers were used: for BMECs, Laminin (anti-Laminin antibody L9393; Sigma-Aldrich, United States) and PECAM1 (Anti-PECAM-1 antibody (JC70); Santa Cruz Biotechnology Inc., United States); for tight junctions, CLDN5 (anti-Claudin 5 antibody ab15106; Abcam, United Kingdom); for pericytes, PDGFRβ (anti-PDGFRβ monoclonal antibody G.290.3; Thermo Fisher Scientific, United States); for smooth muscle cells, Vimentin (anti-Vimentin antibody RV202; Abcam, United Kingdom); and for astrocytic endfeet, AQP4 (anti-Aquaporin 4 antibody [4/18]; Abcam, United Kingdom). We also employed appropriate fluorophore-conjugated secondary antibodies to thoroughly characterize the collected microvessels.

2.5. Extraction of total RNA from isolated microvessels

For RNA extraction experiments, the microvessel-enriched pellet was gently resuspended in 500 µl of cold PBS and gradually pipetted through a 35 µm Strainer Cap for *FlowTubes*™ (Canada Peptide, Canada) using vacuum-aspiration underneath to encourage filtration. The result is intact microvessels trapped within the strainer mesh, where smaller cellular debris and free-floating nuclei have passed through. Using a flat-ended spatula and point-tip forceps, the strainer mesh was removed from its plastic frame and immediately submerged into 100 µl of RL buffer from the Single Cell RNA Purification Kit (Norgen Biotek Corp., Canada), according to step 1A of the manufacturer's protocol. The mesh was discarded after transferring 100 µl of fresh 70% ETOH and pipetting 10 times. Total RNA extraction, including on-column DNase digestion, were followed through according to the manufacturer's instructions. RNA concentration and RIN were quantified using the Agilent TapeStation 2200. RNA samples were then frozen and stored at -80° C until further use.

2.6. Library construction and bulk RNA sequencing

Microvessel-enriched pellets yielded an average of 10.7 ng/µl of total RNA per sample. Libraries were constructed using the SMARTer Stranded Total RNA-Seq Kit v3 - Pico Input Mammalian (Takara Bio Inc., Japan), which features integration of unique molecular identifiers (UMIs) to allow for the distinction between true biological duplicates and PCR duplicates. Libraries were constructed using 10 ng of RNA as input, 2 minutes of fragmentation at 94°C (ProFlex PCR; Applied Biosystems Corporation, United States), 5 cycles of amplification at PCR1 (the addition of Illumina adapters and indexes), 12 cycles of amplification at PCR2 (the final RNA-seq library amplification) and clean-up of final library using NucleoMag NGS Clean-up and Size Select beads (Takara Bio Inc., Japan). Libraries were then quantified at the Genome Quebec Innovation Centre (Montreal, Quebec) using a KAPA Library Quantification kit (Kapa Biosystems, United States), and average fragment size was determined using a LabChip GX (PerkinElmer, United States) instrument. Libraries were sequenced on the NovaSeq 6000 system (*Illumina*, Inc., United States) using S4 flow cells with 100bp PE sequencing kits.

2.7. Bioinformatic pipeline and analyses of RNA sequencing data

2.7.1. UMI extraction, alignment, de-duplication, metrics and generation of count matrix

Bulk RNA sequencing of microvessel libraries yielded an average of ~64 million reads per library, which were then processed following our in-house bioinformatic pipeline to generate a count matrix with contributions of phenotype (53.3% ELA) and sex (33.3% female). UMI extraction based on fastq files was performed using the module extract from umi_tools (v.1.1.2; Smith et al., 2017). Reads were then aligned to the Human Reference Genome (GRCh38) using STAR software (v2.5.4b; Dobin et al., 2013), with Ensembl v90 as the annotation file and using the parameters: **--twopassMode Basic --outSAMprimaryFlag AllBestScore --outFilterIntronMotifs RemoveNoncanonical --outSAMtype BAM SortedByCoordinate --quantMode TranscriptomeSAM GeneCounts**. Resulting bam files were sorted and indexed using SAMtools (v.1.3.1; Li et al., 2009). Duplicate reads with the same UMI were removed using the dedup module

of umi_tools (v.1.1.2; Smith et al., 2017). Different metrics, including the fraction of exonic, intronic and intergenic reads were calculated using the CollectRnaSeqMetrics module of Picard (v.1.129; Broad Institute), and the expected counts were generated using RSEM (v1.3.3; reverse strand mode; Li and Dewey, 2011). RNA sequencing metrics are shown in Supplementary Table 1.

2.7.2. RNA sequencing deconvolution

10X Chromium for single-nucleus data from human brain vasculature were accessed from Yang et. al (2022) and used as a reference to perform bioinformatic deconvolution of our bulk RNA sequencing data. Seurat (Stuart et al., 2019) was used to pre-process raw count expression data, removing genes with less than 3 cells or cells with less than 200 expressed genes. 23054 genes from a total of 23537 and 141468 nuclei from a total of 143793 passed these QC criteria. To generate the Yang signature input for the CIBERSORTx deconvolution tool (Newman et al., 2019), CPM values were averaged across nuclei of each cell type.

2.7.3. Differential gene expression analysis and normalization

All subsequent analyses were performed in R (v 2023.06.0+421). Differential gene expression (DGE) was performed using DESeq2 (1.42.0; Love et al., 2014), an R package for differential analysis of sequencing data to estimate fold-change and significance testing using a negative binomial distribution. Male and female count data were separated, but the same pre-filtering step was applied to both, removing genes with raw counts <25 in 85% of subjects. Data for both males and females were each processed and analysed as follows: **Preprocessing:** key metadata variables Age, pH, PMI, and RIN scaled using the scale function, and Group was converted to a categorical variable using the factor function. **Normalization and PCA Implementation:** Using DESeq2, the count data was normalized via the median of ratios method and stabilized via the vst function, followed by Principal Component Analysis (PCA) to assess potential outliers and the influence of potential covariates on gene expression profiles (Supplementary Fig. 1). **Correlation and Regression Analysis:** Linear regression was employed by the lm function to establish correlations between principal components and

covariates, quantifying the relationships between transcriptional variations and covariates. Covariates with correlations p.adj < 0.05 were deemed significant and were added to the design formula required by DEseq2. For males, age (PC3: p.adj = 0.007; r^2 = 0.23) and pH (PC2: p.adj = 0.00043; r^2 = 0.36) were identified as covariates and, for females, age (PC2: p.adj = 0.036; r^2 = 0.30) was identified as a covariate. **Differential Expression Model Setup:** An initial DE model is constructed using DESeq2, with relevant covariates included in the design formula. **Normalization and Surrogate Variable Analysis (SVA):** counts are normalized using the median of ratios method. The SVA package is then incorporated to identify and include surrogate variables (SVs) in the model to account for potential unobserved confounders or unmodeled artifacts. A revised DE model is created, integrating the computed SVs alongside the original covariates (Supplementary Fig. 1). **Differential gene expression (DGE):** DGE analysis is conducted using the revised model, and *p*-values were adjusted for multiple testing using the procedure of Benjamini and Hochberg (Benjamini and Hochberg, 1995). An adjusted p-value (p.adj) < 0.05 and fold change ≥10% (|log2(fold change)|≥log2(1.1)) were used to designate significant differentially expressed genes (DEGs).

2.7.4. PsyGeNET analysis

The list of ELA-associated DEGs from males and females was separately queried in the PsyGeNET database (Gutierrez-Sacristan et al., 2017) using the psygenet2r R package. The psygenetGene function was used with database = “ALL” and other parameters set to default to retrieve information about associations between our specific genes and psychiatric diseases. To concisely visualize the output, we generated an evidence index barplot showing, for each psychiatric disorder, the number of gene-disease associations.

2.7.5. Functional enrichment analysis

Metascape (Zhou et al., 2019) was used to perform an in-depth enrichment analysis of identified DEGs, with the aim of elucidating the functional pathways and cell-type signature significantly associated with identified DEGs. Metascape utilizes Fisher’s exact test to compute p-values and enrichment factors for each ontology category. The

input species was set to Homo Sapiens, and a tailored selection of databases was used for annotation, membership, and enrichment analysis (FDR < 0.05) was used. The background gene set used for the enrichment analysis comprised genes that passed the filtering threshold during DGE analysis (i.e. those input into DGE analysis). Only pathway terms with a p.adj < 0.05, a minimum count of three, and an enrichment factor > 1.5 were considered significant.

2.7.6. Gene set enrichment analysis (GSEA)

For differential expression results, GSEA (Subramanian et al., 2005) was performed using the fgsea package (Korotkevich et al., 2019). A log2 fold change-ranked list of genes was generated, a combined list of gene sets from Reactome pathways, Gene Ontology Molecular Functions (GOMF), KEGG pathways, and WikiPathways was compiled from MSigDB (Subramanian et al., 2005), and the following parameters were used for the fgsea function: minSize = 15, maxSize = 500; and any pathways with Benjamini-Hochberg p.adj < 0.05 were considered to be significantly enriched. Finally, we ran collapsedPathways with pval.threshold = 0.05 to get the main pathways for each cluster. An additional GSEA was performed for the female data using Brain.GMT (Hagenauer et al., 2024), which consists of curated brain-related gene sets.

2.7.7. Rank-rank hypergeometric overlap

A threshold free, rank-rank hypergeometric overlap (RRHO) analysis was performed using the RRHO2 R package (Cahill et al., 2018). Genes were scored using the product of the logFC and the negative log base 10 uncorrected *p*-value taken from DGE analysis in the male and female datasets separately. The scored gene lists were input to RRHO2_initialize function (with method “hyper” and log10.ind “TRUE”) and the results were plotted using the RRHO2_heatmap function.

2.7.8. Weighted Correlation Network Analysis

Weighted correlation network analysis (WGCNA) (Langfelder and Horvath, 2008) was performed to explore the relationship between co-expressed gene modules and exposure to ELA using data specifically from females. This focus on females was

chosen based on the results from DGE analysis, which indicated that the female NVU is more greatly affected by ELA compared to males. A pre-filtering step was first applied, removing genes with raw counts <20, followed by normalization via DESeq2's normalizeCounts function and variance stabilizing transformation. Transformed counts were corrected for the effect of age using limma (Ritchie et al., 2015), because it was previously identified as a covariate for females CTRL vs ELA groups. A network was constructed using the following parametres: soft power threshold = 14, networkType="signed", minimum module size = 100, mergeCutHeight = 0.2, maxBlockSize = 30000, and deepSplit = 3. For each identified module, the eigengene was calculated alongside its correlation with ELA status. Finally, gene significance and module membership were calculated. For modules turquoise and black, the topmost hub gene was identified using the chooseTopHubInEachModule function. Other hub genes within these modules were identified based on their soft connectivity scores, which were calculated using the function softConnectivity. Although the main network was a signed type to preserve the directional information of gene correlations within our dataset, soft connectivity scores were computed using the default unsigned method, allowing us to identify highly central and connected genes regardless of whether they are up- or down-regulated or whether they positively or negatively influence other module genes. Genes with soft connectivity scores exceeding hub-defining threshold were deemed hub genes. For the turquoise and black modules, a hub-defining threshold was set using the histogram distribution of soft connectivity scores across all module genes. An observed 'elbow' point, indicative of a significant change in the distribution pattern, was identified and used as a natural cutoff to distinguish hub genes.

2.7.9. Identification of genes with KLF2 or KLF4 binding motifs

Identification of genes that are potentially regulated by KLF2/4 was performed using a snATAC-seq dataset previously generated by our group (Chawla et al., 2023). This dataset includes comprehensive profiling of open chromatin across all cell types of the brain, including a vascular cluster. The Cisbp position weight matrix (PWM) was used to find motif occurrences of KLF2/4 in any open chromatin peaks identified in the snATAC-seq dataset. To find target genes of KLF2/4 transcription factor binding sites, we used

Peak-to-gene (p2g) linkages, which were computed using Pearson correlation between snATAC-seq open chromatin peak accessibility and paired snRNA-seq gene expression within 500Kbp windows. Moreover, KLF2/4 transcription factor motif containing p2g links were further restricted to those with the highest enrichment for these binding sites. In order to do this, we ran Homer **findMotifsGenome.pl with -find <motif file> option for our motifs of interest.** As a result, Motif Score (log odds score of the motif matrix, higher scores are better matches) were obtained, and KLF2/4 p2g links with motif scores >= median motif score across all peaks were retained (Median value = 8.28). Finally, among filtered p2g links with highest evidence for KLF2/4 transcription factor motifs, only peaks which also showed differentially high accessibility (FDR < 0.05 & LOGFC > 0.5) in the vascular cell type cluster compared to other brain cell types were kept.

2.8. *In situ* quantification of DEGs

2.8.1. Validation of DEGs with fluorescence *in situ* hybridization

DEG candidates were validated using fluorescence *in situ* hybridization (FISH). Frozen vmPFC blocks of (primarily) grey matter were prepared from the same CTRL and ELA female subjects that were sequenced, cut into serial 10 µm-thick sections with a cryostat, and mounted on Superfrost charged slides. FISH was performed using Advanced Cell Diagnostics RNAscope® probes and reagents following the manufacturer's instructions. Sections were first fixed in cold 10% neutral buffered formalin for 15 min, dehydrated by increasing gradient of ethanol baths, and then air dried for 5 min. Hybridization with Hs-KLF2 (408711-C-1; Advanced Cell Diagnostics, United States) and Hs-KLF4 (457461-C-2; Advanced Cell Diagnostics, United States) probes was conducted for 2 hours at 40°C in a humidity-controlled oven. Amplifiers were added using the proprietary AMP reagents and the signal was visualized through probe-specific HRP-based detection by tyramide signal amplification (TSA) with Opal dyes Opal 520 and Opal 570 (FP1487001KT and FP1488001KT; Akoya Biosciences, United States) diluted to 1:700. Immunofluorescent blood vessels were observed in the same sections, post-hybridization. Sections were washed in PBS and then incubated overnight at 4 °C under constant agitation with anti-laminin antibody (anti-Laminin

antibody L9393; Sigma-Aldrich, United States) diluted in blocking solution (1:500 in 2% normal donkey serum + 0.2% Triton X dissolved in PBS). After washing in 1X PBS three times for 5 min each, sections were incubated for 2 h at room temperature in fluorophore-conjugated secondary antibody (1:500; Alexa Fluor® 647 AffiniPure™ Donkey Anti-Rabbit IgG (H+L), 711-605-152; Jackson ImmunoResearch Laboratories, United States). TrueBlack was used to remove endogenous autofluorescence from lipofuscin and cellular debris. Slides were finally coverslipped in Vectashield mounting medium with DAPI to enable nuclear staining (Vector Laboratories, Inc., United States).

2.8.2. Imaging and analysis of *in situ* mRNA expression of DEG candidates

Images were acquired with an Olympus VS120 slide scanner and, for each experiment and subject, the whole section was scanned and imaged using a ×20 objective. Exposure parameters were kept consistent between subjects for each set of experiment, where the TRITC channel was designated for a DEG candidate (either KLF2 or KLF4) and the Cy5 channel was designated for laminin. As TSA amplification with Opal dyes yields a high signal-to-noise ratio, parameters were optimized so that autofluorescence from lipofuscin and cellular debris was filtered out. Microvessels were defined by tubular structures with laminin signal (a validated marker that is exclusively expressed by endothelial cells. Image analysis was performed in QuPath (v 0.5.1). Each subject had one section stained with KLF2 or KLF4, as well as DAPI and laminin. To recapitulate the non-discriminatory approach that was used during microvessel isolation, where microvessels of all diameters from every spatial point within the tissue sample is isolated, grey matter microvessels in stained tissue sections were randomly sampled for analysis. This was conducted by carrying out the following steps: grey matter area was outlined using the polygon annotation tool and computing intensity features (namely mean and standard deviation) with a preferred pixel size of 1 μm for the TRITC channel across the entire grey matter area. A grid with spacing of 1000x1000 μm was overlaid onto the section, and each tile covering grey matter was numbered. Using a random number generator, 5 grey matter tiles were selected and annotated using the square annotation tool. Nuclei that did not display laminin staining but were in direct contact with the vessel surface were classified as constituent cells of the NVU.

Consequently, these nuclei were included in the analysis as integral components of the NVU. To automate microvessel detection and include those with contacting nuclei, a pixel thresholder for laminin was set, turning these areas into detections within the 5 selected tiles. Similarly, DAPI-stained nuclei were detected. Custom Groovy scripts were used to merge detections of nuclei in contact with microvessels into singular detections and convert these detection objects into annotations. A pixel thresholder was established in the TRITC channel to identify puncta, using a calculated threshold value of the mean + (5 x standard deviation). Using the pixel thresholder, the area of annotated microvessels covered by target puncta in the TRITC channel was measured, from which the percent area covered by target puncta within these annotated microvessels was calculated. Percent area covered by target puncta was the preferred measure to reflect RNA expression, as punctate labeling generated by FISH often aggregates into clusters that cannot readily be dissociated into single dots or molecules.

2.8.3. Statistical analyses for FISH experiments

For each subject, mean percent area for KLF2/4 expression were calculated, and the following statistical analyses were conducted in R using the stats and car packages: the Shapiro-Wilk test was utilized to assess the normality of the data and Levene's Test was conducted to compare the variances between groups. For KLF2, a student's t-test was applied to test the hypothesis that KLF2 expression was higher in the CTRL group than in the ELA group. For KLF4, a Welch's Two Sample t-test was utilized to assess the same hypothesis under the assumption of unequal variances.

3. Results

3.1. Immunophenotypic characterization of isolated brain microvessels: preserved morphology and expression integrity

The angioarchitecture of brain microvessels is composed of several neurovascular cell types. To characterize the composition and morphological integrity of microvessels isolated by our method, we utilized immunostaining to visualize and assess a range of NVU markers. We examined vimentin (VIM), primarily found in smooth muscle cells (Chang and Goldman, 2004); laminin (LAM), a marker of endothelial cells (Yousif et al.,

2013); claudin5 (CLDN5), the primary constituent of endothelial tight junctions (Greene et al., 2019); Platelet-derived growth factor receptor beta (PDGFRβ), a marker of pericytes (Winkler et al., 2010); and Aquaporin4 (AQP4), which is localized to astrocytic endfeet (De Bellis et al., 2017).

We observed that LAM, the major basement membrane component responsible for signal transduction (Aumailley and Smyth, 1998), and VIM, a regulator of the actin cytoskeleton (Chang and Goldman, 2004), were continuously and homogeneously expressed along the entire length of the vascular surface (Fig. 1b). Additionally, CLDN5 displayed consistent expression throughout microvessels, indicative of well-preserved endothelial tight junctions (Greene et al., 2019) (Fig. 1c). PDGFRβ, a regulator of angiogenesis and vascular stability (Winkler et al., 2010), was also expressed on the microvessel surface (Fig. 1d). Furthermore, AQP4, a water channel protein crucial for maintaining osmotic balance in the interstitial, glial, and neuronal compartments (Nagelhus and Ottersen, 2013), was superimposed along the microvessel walls (Fig. 1e), suggesting that astrocytic endfeet coverage on the microvessel surfaces is preserved. Overall, our microvessel isolation methodology, as outlined in Wakid et al., 2023, effectively enriches microvessels in high yield and maintains their structural integrity *ex vivo*.

3.2. Profiling isolated microvessels of the human vmPFC by bulk sequencing

3.2.1. Computational estimation of cell type proportion from sequenced microvessels shows enrichment for neurovascular cell types

To confirm the enrichment of microvessels and estimate the proportions of neurovascular cell types that have been enriched, we used the CIBERSORTX algorithm (Newman et al., 2019) to deconvolute our microvessel RNA sequencing data. To do so, 10X Chromium for single-nucleus data from human brain vasculature was accessed from Yang et. al (2022) and used as the average reference signatures to deconvolute our data against. The Yang dataset is particularly useful in this regard, as it contains single nucleus information for all neurovascular cell types as well as non-vascular cell types, and stratified information according to neurovascular tree zonation, distinguishing

the differences between capillary, arterial and venous endothelial cell gene expression. Deconvolution of our data revealed a significant enrichment for neurovascular cell types across subjects (Fig. 2b), accounting for an average of 81.7% of the sequenced genes (plots for representative NVU markers in Supplementary Fig. 2). This percentage was calculated by summing together the percentages of each neurovascular cell type to obtain a cumulative value representing the total percentage for each subject. The T cell category was included as a neurovascular cell type, so that venous + capillary + arterial + mural cell + perivascular fibroblast + astrocyte + T cell estimates was taken as the sum percentage. T cells were included because there is substantial evidence describing resident memory T cells, a distinct memory T cell population disconnected from the circulating memory T cell pool (Smolders et al., 2018, Wakim et al., 2012), that reside in the perivascular Virchow-Robin space underneath astrocytic endfeet (2010; van Horssen et al., 2005; Smolders et al., 2018; Smolders et al., 2013). The decision to include cell types found within the perivascular space was bolstered by the presence of validated perivascular T cell markers CD163 (Kim et al., 2006), LYVE1 (Siret et al., 2022), and CD206/MRC1 (Koizumi et al., 2019), as well as astrocytic endfeet markers AQP4, GJA1, and SLC1A2 (Boulay et al., 2017) within our dataset, indicating successful isolation of the entire NVU, up to the glial limitans. A more detailed list of T cell, perivascular macrophage, and astrocytic endfeet markers found within our data is shown in Supplementary Table 2.

Importantly, a high representation of capillary (33.3%) and mural cell (32.6%) assigned genes were estimated (Fig. 2c), as is typically observed in the microvessel zone (Hirschi and D'Amore, 1996). In contrast, there was more limited representation of genes assigned to arterial (1.3%) but no venous endothelial cells, which corroborates with the intended objective of isolating the smallest of vessels from brain tissue, as well as lower estimations for astrocyte, perivascular fibroblast, and T cell genes (Fig. 2c). The average percentage estimate of summed neurovascular genes did not differ between groups (W = 295, p-value = 0.337; Supplementary Fig. 2), nor did the average percentage estimate for capillary genes (W = 253, p-value = 0.991; Supplementary Fig. 2) or mural cell genes ($t(43) = 0.91953$, $p = 0.3629$; Supplementary Fig. 2). As

previously reported (Wakid et al., 2023), microvessels isolated using the described method are obtained in high yield. Although the protocol enriches for microvessels, it does not purify them; consequently, a limited proportion of non-vascular cell types are co-enriched in the collected pellets, as estimated by computational deconvolution (Fig. 2b-c). This outcome is to be expected when using postmortem tissue, as reported by others, a subset of "vasculature-coupled" neuronal and glial cells with distinct expression signatures (from the corresponding canonical cell types) are physically adhered to microvessels (Garcia et a., 2022). Taking this into consideration, we compared deconvolution estimates per subject against two exclusion criteria: 1) neuronal contamination exceeding two standard deviations from the mean, and/or 2) oligodendrocyte contamination exceeding two standard deviations from the mean, as both scenarios were shown to skew subsequent analyses. Adhering to these criteria, 4 subjects (2 CTRL and 2 ELA); the matching between the groups remained unaffected. Transcript Per Million (TPM) values for cell type-defining genes in CTRLs and ELA subjects illustrate that our data predominantly reflect transcripts from neurovascular cells (Fig. 2d). This is evidenced by the high expression of endothelial markers such as VWF, EPAS1, SLC2A1, and A2M. In contrast, there is more limited expression of the astrocytic endfeet marker AQP4, and minimal expression of the astrocytic nuclear marker SOX9, neuronal markers TH and CALB2, oligodendrocytic markers OLIG2 and SOX10, and microglial markers CX3CR1 and P2RY12. This pattern highlights the successful capture of the NVU in our dataset.

3.2.2. Neurovascular changes in the vmPFC of cases

Our understanding of neurovascular-related changes in psychopathologies and ELA remains limited in humans, and particularly with respect to NVU-specific sex differences. To date, no studies have specifically investigated how these differences may manifest. In this study, both male and female subjects were included in CTRL and ELA groups but with no prior evidence of major sex differences nor *a priori* hypothesis that sex differences manifest after ELA, we initially conducted DGE analysis with the sexes pooled together. We identified a total of 463 DEGs, comprising 281 upregulated and 182 downregulated genes ($p.adj < 0.05$, $|\log2(\text{fold change})| \geq \log2(1.1)$), associated

with a history of ELA irrespective of sex (select DEGs previously implicated in the literature are highlighted in Supplementary Fig. 2; a comprehensive list of DEGs is presented in Supplementary Table 3). Further examination, however, highlighted a proportion of DEGs showing marked sex-driven expression differences, most notably among females (representative plots provided in Supplementary Fig. 3).

The potential influence of sex on gene expression was thoroughly investigated through several rigorous analytical avenues. A correlation analysis between principal components and sex revealed significant, moderate associations for specific components—namely PC1 ($p = 0.0082$, $r^2 = 0.152$), PC3 ($p = 0.03$, $r^2 = 0.104$), and PC5 ($p = 0.0067$, $r^2 = 0.159$) – suggesting sex contributes to variance in our data. Additionally, Welch Two Sample t-test was conducted to determine whether the mean values of PC1 (which attributes to 35.4% of variation) are significantly different between males (mean = 3.776618) and females (mean = -7.553237), yielding t(27.245) = 2.7398, p-value = 0.01072, with 95% confidence interval [2.848402 19.811307], suggesting that there are differences in the expression patterns captured by PC1 between the two sexes. Similarly, the mean values of PC5 are significantly different between males (mean = 1.293569) and females (mean = -2.587138), yielding t(22.219) = 2.5907, p-value = 0.01661, with 95% confidence interval [0.7759907 6.9854226]. Further, Welch Two Sample t-tests comparing the mean values of principal components between sexes – particularly for PC1 and PC5 – indicated significant differences in expression patterns between males and females. Specifically, PC1 (which accounts for 35.4% of variation) showed a mean difference (mean in males = 3.776618; mean in females = -7.553237) with a t-value of 2.7398 ($p = 0.01072$, 95% confidence interval [2.848402, 19.811307]), and PC5 also demonstrated a significant mean difference (mean in males = 1.293569; mean in females = -2.587138; $t = 2.5907$, $p = 0.01661$, 95% confidence interval [0.7759907, 6.9854226]).

Finally, the DESeq function was used to explore the Sex:Group interaction, looking specifically at the interaction between the factors "Sex" and "Group" as a means to assess whether the effect of ELA is different between males and females. Intriguingly,

many DEGs identified by the Sex:Group interaction exhibit sexual divergence in their differential expression (representative DEGs are presented in Supplementary Fig. 3), where 66.4% of DEGs demonstrate that the effect of ELA is more pronounced in females compared to males (summary of Cook's distances for female subjects in Supplementary Fig. 3). The observation of sexual dimorphism, coupled with the presence of approximately double the number of males compared to females in both groups, prompted our decision to analyze male and female counts separately and, as a result, characterize the sex-specific effects of ELA on gene expression, providing a more nuanced understanding of the underlying biology.

3.2.3. Sex-driven differences in the vmPFC neurovascular transcriptome of cases

To identify sex-specific differences in gene expression patterns between CTRL and ELA groups, we performed DGE analysis separately in males and females. In males, we identified a total of 34 DEGs, with 19 upregulated and 15 downregulated genes in cases vs controls ($p.adj < 0.05$, $|\log2(\text{fold change})| \geq \log2(1.1)$; Fig. 3a-c, Supplementary Table 4). This contrasted with females which displayed 774 DEGs, with 343 upregulated and 431 downregulated genes in cases vs controls ($p.adj < 0.05$, $|\log2(\text{fold change})| \geq \log2(1.1)$; Fig. 3e-g, Supplementary Table 5). The magnitude to which the female NVU was affected was greater, with an average log2 fold change of 0.645 for females (equivalent to a fold change of approximately 1.564, or a 56% change in expression), compared to an average log2 fold change of 0.350 for males (equivalent to a fold change of approximately 1.275, or a 28% expression change). This indicates that the female NVU experiences substantially greater transcriptomic disturbances in depressed suicides with a history of ELA compared to males. The robustness of these sex differences was supported by a sub-sampling analysis: to ensure that the results output for male subjects was not skewed by certain subjects that had not been previously detected as outliers, 8 male CTRL subjects and 8 male ELA subjects were randomly selected (these numbers are equal to the total number of females in the CTRL and ELA groups), and DGE analysis was repeated as described above. DGE analysis of subset male subjects was repeated 4 times and the output results demonstrated remarkable consistency across each iteration, as well as with the main DGE analysis of the full male cohort,

underscoring the reliability and stability of the observed sex differences in response to ELA.

To assess whether critical genes at the NVU were impacted in cases, we cross-referenced DEGs identified in males and females with neurovascular cell type defining markers from recent studies by Yang et al. (2022) and Garcia et al. (2022) (Supplementary Fig. 3). Male DEGs included PTGS2, a marker of BMECs, along with TACC1, TIMP3, CDC42EP4, and DIO3OS, all of which exhibit high expression levels in pericytes. Conversely, the female NVU revealed a distinct signature, showcasing DEGs that included several neurovascular cell type defining markers. Noteworthy among these are CSF1 (log2 fold change = -0.77, p.adj = 0.0003, Fig. 3h), essential for monocyte maintenance (35508166**,** 24890514) and proliferation (Pierce et al., 1990; Zhou et al., 2022; Mossadegh-Keller et al., 2013); FGF1 (log2 fold change = -0.89, p.adj = 0.00023, Fig. 3h), a potent mitogen and angiogenic factor (Stokes et al., 1990); and its receptor FGFR3 (log2 fold change = -0.70, p.adj = 0.038, Fig. 3h).

Binding partners KLF2 (log2 fold change = -1.44, p.adj = 0.00083, Fig. 3h-i) and KFL4 (log2 fold change = -1.50, p.adj = 0.0003, Fig. 3h-i) were both downregulated in female cases (but not males with ELA, KLF2: p.adj = 0.92; KLF4: p.adj = 0.84). The Krüppel-like family of transcription factors (KLFs) plays a pivotal role in regulating endothelial biology, of which KLF2/4 are enriched in the endothelium and affect virtually all key endothelial functions. More precisely, KLF2/4 confer endothelial barrier integrity by inducing expression of multiple anti-inflammatory and anti-thrombotic factors, such as eNOS (Hamik et al., 2007; Chiplunkar et al., 2013) and thrombomodulin (Hamik et al., 2007), VEGFR2 (Chiplunkar et al., 2013), and by regulating endothelial expression of CAMs, NF-kB, and tight junction proteins CLDN5 and occludin (Zhang et al., 2020; Shi et al., 2013; Chiplunkar et al., 2013; Lin et al., 2010). Moreover, KLF2 orchestrates vascular homeostasis and serves as a central transcriptional switch point between a pro-inflammatory, atheroprone versus quiescent, atheroresistant endothelial phenotype, in which KLF2 determines endothelial transcription programs (> 1000 genes, Dekker et al., 2006) that control key functional pathways such as cell migration, vasomotor

function, inflammation, and hemostasis (Dekker et al., 2006; Lin, Z et al., 2005; Lee et al., 2006). Similarly downregulated in females is CLDN5 (log2 fold change = -0.65, p.adj = 0.012, Fig. 3h), a major determinant of BBB integrity that is downregulated by chronic stress (Menard et al., 2017; Dudek et al., 2020; Dion-Albert et al., 2022). Other female DEGs with well characterized functions at the NVU include VLDLR, HSPB1, HYAL1, HYAL2, ST6GALNAC3, ADGRA2, BST2, VCAM1, IL32, SOX18, MT2A, CTSB, RGL3, PAG1, and GJA4. Additionally, several ATP-binding cassette transporters (ABCs) and solute carriers (SLCs) are also differentially expressed, namely ABCD3, ABCA5, SLC24A4, SLC36A4, SLC4A7, SLC25A36, SLC9A3R2, SLC35A4, SLC6A6, SLC39A14, SLC8B1, SLC22A3, SLC7A10.

A hypergeometric test revealed a statistically significant overlap between female DEGs and neurovascular cell type defining markers (hypergeometric p-value = 2.48×10^{-7}). Focusing solely on DEGs that overlap with neurovascular cell type defining markers, KLF2 emerged as the 6th most significant, and the foremost with a well-characterized function. Both KLF2 and KLF4, known for their redundant and overlapping functions in regulating endothelial cell properties and vascular integrity, exhibited a high mean average expression and a large log2 fold change (KLF2: top 0.14% for log2 fold change, KLF4: top 0.10% for log2 fold change). Thus, we chose to experimentally validate the expression changes of KLF2/4 using FISH in the same female CTRL and ELA subjects that were previously sequenced. Consistent with our RNA sequencing findings, significant downregulation of KLF2 ($t(12) = 8.7474$, $p = 7.45 \times 10^{-7}$) and KLF4 ($t(7.2153) = 2.3976$, $p = 0.023$) expression was observed in the grey matter microvessels of ELA vs CTRL females (Fig. 4a-b). Importantly, there was no statistically significant difference in blood vessel density between the CTRL and ELA females ($W = 38$, $p = 0.09732$).

3.2.4. Females—but not males—display significant neurovascular dysfunction in cases

The relevance of the DEGs we identified in relation to psychiatric disorders was assessed using the PsyGeNET (Gutiérrez-Sacristán et al., 2017) text-mining database.

Upon evaluating male DEGs, we found that depressive disorders exhibited the most gene-disease associations (>9 DEGs; Fig. 5a; Supplementary Fig. 4). In the case of female DEGs, schizophrenia had the highest number of gene-disease associations (60 DEGs; Fig. 5b; Supplementary Fig. 4), closely followed by depressive disorders (>50 DEGs; Fig. 5b). Therefore, our microvessel derived-DEG findings in both sexes, especially in females, corroborate previously reported gene-disease associations.

Functional annotation and cell-type enrichment of DEGs were conducted using Metascape (Zhou et al., 2019). In male cases, the "ATP-dependent protein folding chaperone" functional cluster was as the most significantly enriched (Fig. 5c), pertaining to DEGs HSPA4, HSPA5, HSPA9, HSP90AA1, and HSP90B1 (Fig. 3d). Additionally, there was an endothelial cell type signature enrichment amongst male DEGs (Fig. 5c). Functional enrichment of female DEGs revealed significantly enriched functional clusters related to immune and vascular pathways, namely “Interferon alpha/beta signalling” and “Regulation of response to cytokine stimulus” (Fig. 5d). Furthermore, there was a pericyte and endothelial cell type signature enrichment amongst DEGs in female. Further scrutiny of individual DEGs with known immune functions confirmed “global immune suppression” where, irrespective of whether pro- or anti-inflammatory in nature, immune-related DEGs were downregulated, some of which are presented in Table 2. It is worth mentioning that major cytokines were inadvertently omitted from DGE analysis after pre-filtering (e.g. TNFα, IL1β, IFNγ, CRP, IL6, IL8, IL10, CXCL10), indicating very low expression in the vmPFC. To determine whether low-count cytokines are differentially expressed in male and female cases, additional analyses on normalized counts were performed post-hoc, revealing no significant differences in cytokine expression between CTRL and ELA females. To further assess the functional relevance of gene expression differences in microvessels from cases, we examined whether the protein products of DEGs belonged to interacting networks (Supplementary Fig. 12).

We used GSEA (Fig. 5e-f) to explore the biological pathways underlying transcriptomic changes observed in male and female cases. For males, significant enrichment was

found in pathways “Voltage-gated potassium channels” and “Muscle contraction” (Fig. 5e), suggesting potential alterations in K_V channel facilitated smooth muscle contraction (Nieves-Cintron et al., 2018; Albarwani et al., 2003; Dabertrand et al., 2015). The "Nuclear Steroid Receptor Activity” pathway was similarly enriched (Fig. 5e), featuring DNA-binding transcription factors such as PGR, ESR2, and PPARA, which are recognized for their neuroprotective and broad vascular functions (Kolodkin et al., 2013; Wang et al., 2021). In contrast, chaperone binding protein pathways had significantly lower normalized enrichment scores (Fig. 5e). Similar to males, most significant pathways identified by GSEA in females were downregulated. Females exhibited downregulation in immune-related pathways, akin to ORA findings, including "Interferon signalling" and "Interleukin signalling” (Fig. 5f), indicating suppressed immune signalling in ELA. Additionally, gene sets related to vascular functions, namely “Platelet activation and aggregation” and “Hemostasis” were negatively enriched in females. Intriguingly, exposure to chronic stress is associated with prolonged pro-inflammatory platelet bioactivity (Koudouovoh-Tripp et al., 2021; Matsuhisa et al., 2014; Aschbacher et al., 2008; Markovitz and Matthews, 1991) and platelet pathology in MDD (Musselman et al., 1996; Pinto et al., 2012; Morel-Kopp et al., 2009; Ormonde do Carmo et al., 2015; Gialluisi et al., 2020; Yu et al., 2021; Ward et al., 2023; Massardo et al., 2021; Canan et al., 2012; Cai et al., 2017), with greater effects in depressed women (Izzi et al., 2020). Intriguingly, analysis using the newly curated gene set list Brain.GMT (Hagenauer et al., 2024) (Fig. 5f) shows upregulation in genes typically downregulated in “Susceptible Phenotype to Social Defeat Stress" and in “Resilient Phenotype to Social Defeat Stress". Thus, our GSEA of microvessels from cases revealed dysregulated pathway gene sets that are functionally significant in both neurovascular cell types and the ELA phenotype. Furthermore, these findings align with DEGs identified in males and females.

3.2.5. Little overlap between male and female neurovascular dysfunction

We next used RRHO analysis to identify shared transcriptional changes between males and female cases. RRHO, a threshold-free method for assessing statistical overlap (Cahill et al., 2018), enabled us to delineate sex-specific transcriptional signatures and

directly compare the transcriptional signatures observed in male versus female ELA subjects. Consistent with previous studies showing distinct brain transcriptomic changes in males and females with MDD (Labonté et al., 2017), we found remarkably little overlap between male and female ELA transcriptional signatures (Fig. 6a). Thus, the directionality of the changes observed in males and females with ELA are not preserved. The limited overlap in transcriptional changes between male and female depressed suicides with a history of ELA was further confirmed by focusing our analysis exclusively on DEGs. By directly comparing male and female DEGs, we observed minimal commonality by identifying only two shared DEGs: HOMER2 (ELA males: p.adj = 0.013, log2 fold change = 0.34; ELA females: p.adj = 0.02, log2 fold change = 0.63) and TACC1 (ELA males: p.adj = 0.048, log2 fold change = 0.22; ELA females: p.adj = 0.03, log2 fold change = 0.47), both of which are upregulated in both sexes (Fig. 6b-c). While Homer proteins are best known for their interaction with group 1 metabotropic glutamate receptors (mGluR1/5) (Bockaert et al., 2021), HOMER2 is also expressed in endothelial cells (Supplementary Fig. 4) and plays a crucial role in regulating Ca^{2+} signalling and activation of platelets by agonists such as thrombin (Dionisio et al., 2015; Jardin et al., 2012). Meanwhile, TACC1, a member of the Transforming Acidic Coiled-Coil family, acts as a coregulator of various nuclear receptors (Guyot et al., 2010) that modulate transcription by binding to their target DNA response elements. Overall, these findings highlight a strong sexual dimorphism in the transcriptional signatures exhibited by the NVU in depressed suicides with a history of ELA.

3.2.6. WGCNA identifies specific gene networks in the NVU of female cases

Having characterized the broad pattern of transcriptome-wide changes at the female NVU, we then sought to resolve specific gene coexpression networks that could be critical in determining NVU dysfunction in cases. Using WGCNA, we constructed a gene coexpression network that returned 73 modules. To gain insight into the biology of implicated modules, we identified a subset of interesting modules for further analysis based on two criteria: a significant association with cases (p-value < 0.05) and a correlation coefficient greater than 0.7, ensuring a focus on modules strongly associated with depressed suicides with ELA. A total of 5 modules exhibited a significant

correlation coefficient greater than 0.7 (Fig. 7a-b), as well as biological processes pertinent to ELA: membrane trafficking (Fig. 7c; turquoise: $p = 1.46\times10^{-7}$, 1.74x), interferon alpha/beta signalling (Fig. 7d; black: $p = 8.95\times10^{-9}$, 6.95x), VEGFA/VEGFR2 signalling (green: $p = 2.04\times10^{-8}$, 2.10x), response to lipopolysaccharide (greenyellow: $p = 2.88\times10^{-12}$, 4.64x), and eukaryotic translation elongation (orange: $p = 1.10\times10^{-34}$, 28.36x). Enrichment of cell-type associated genes in these modules identified microglial genes in turquoise (Fig. 7c; $p = 1\times10^{-14}$, 2.3x), endothelial genes in black (Fig. 7d; $p = 1\times10^{-15}$, 3.4x), green ($p = 1\times10^{-34}$, 3.7x), and greenyellow ($p = 1\times10^{-14}$, 5.2x), along with T cells in orange ($p = 1\times10^{-3}$, 17x). Modules were then handed over to the GeneOverlap R package, where we assessed significant overlap of module genes with female DEGs. Of the 73 generated modules, this subset of 5 modules were also enriched for female DEGs (Fig. 7e; turquoise: $p = 2.3\times10^{-17}$; green: $p = 4.5\times10^{-30}$; black: $p = 1.4\times10^{-27}$; greenyellow: $p = 2.5\times10^{-8}$; orange: $p = 3.8\times10^{-6}$), in a way that was consistent with regional RRHO patterns. Indeed, many of the co-downregulated genes in the RRHO analysis were also found within these 5 modules (e.g. PDGFA, TFRC, EPHA3, FN1, CX3CL1, ICAM1, PTGS2, PGF; Supplementary Fig. 5). Together, these analyses suggest that the turquoise, green, black, greenyellow, and orange modules may be particularly important in governing NVU dysfunction in female cases, which is further substantiated by a markedly lower median for each module's eigengenes (Fig. 7f).

3.2.7. KLF2 and KLF4 regulate endothelial activation transcriptional networks in female cases

Interestingly, KLF2 and KLF4 (along with CLDN5) emerged in modules turquoise and black, respectively (Supplementary Table 6). Recognizing that these modules may represent genes for which KLF2/4 are nodal regulators, we assessed potential correlation between the eigengenes of the turquoise and black modules. A strong positive correlation ($r = 0.51$, Fig. 7g) was observed, suggesting some level of co-regulation or functional overlap. Importantly, KLF2 not only exhibits a strong correlation with the turquoise eigengene (MM = 0.76) and a strong association with ELA (GS = 0.83), but its closeness centrality (CC = 0.12) also indicates a functionally central

position within the module. KLF4 similarly demonstrates a strong correlation with the black eigengene (MM = 0.86), a strong association with ELA (GS = 0.86), and a closeness centrality of 0.15, underscoring its central role within the module. We next sought to explore the potential impact of KLF2/4 downregulation, as observed in female cases, on genes identified within the turquoise and black modules. To this end, genes within these modules were cross-referenced against human homologues of genes experimentally validated to be affected by dual KLF2/4 knockout. This comparative analysis revealed substantial overlap (Supplementary Fig. 5): 448 genes within the turquoise module (p-value = 5.1×10^{-9}) and 193 genes within the black module (p-value = 3.3×10^{-6}). Furthermore, additional KLFs are present in modules green (KLFs 8, 10, and 16), greenyellow (KLF6), and turquoise (KLF13), and modules that possess KLFs exhibit strong correlation with one another (Fig. 7g); thus, it is conceivable that these KLFs may also play a regulatory role within their respective modules. Hub genes, particularly the topmost hub genes (Fig. 7h), within the turquoise and black modules exhibit decreased mean normalized count in depressed females with a history of ELA (Fig. 7i).

Using a snATAC-seq dataset generated by our group (Chawla et al., 2023), we then explored potential regulatory actions performed by KLF2/4 in the turquoise and black modules, respectively. The Cisbp PWM was used to identify DNA sequences within the open chromatin peaks that matched known motifs for KLF2 or KLF4. These motifs were then analyzed in conjunction with corresponding open chromatin regions that were highly accessible in the vascular cluster (Fig. 8a) compared to non-vascular cell types. This approach allowed us to filter p2g associations for peaks covering DNA sequences matching known motifs for KLF2 or KLF4 and combined with corresponding open chromatin regions that were highly accessible in the vascular cluster (Fig. 8a) compared to non-vascular cell types. By virtue of this approach, specific genes that are potentially regulated by KLF2 or KLF4 in endothelial cells can be identified. Disregarding the location of potential KLF2/4 binding sites, genes with motif scores ≥ median score and significant FDR (FDR < 0.05; indicating high confidence that the identified peak is a true regulatory site where KLF2 or KLF4 is likely to bind) were then cross-referenced with

turquoise and black module genes, respectively, demonstrating that 33% of turquoise module genes are motif-linked to KLF2 (Fig. 8b; p-value = 1.8×10^{-93}) and that 30% of black module genes are motif-linked to KLF4 (Fig. 8c; p-value = 1×10^{-14}). Several hub genes were identified amongst motif-linked genes in both the turquoise and black modules, including several KLF2 binding sites in distal, promoter, exonic and intronic regions of the topmost turquoise hub gene FKBP8 (further breakdown of gene regions with potential KLF2/4 binding sites found in Supplementary Table 7). These findings underscore the substantial influence of KLF2/4 on the transcriptional landscape of endothelial cells, specifically within the promoter and distal regions, which are crucial for gene regulation.

4. Discussion

The pernicious effects of adversity experienced during developmental periods of heightened plasticity linger as psychopathology and disease into adulthood. The complex neurobiological and stress-mediated mechanisms through which these enduring impacts manifest, however, remain insufficiently characterized in individuals with histories of ELA. One proposed mechanism is NVU dysfunction: chronic stress leads to the production of blood-borne inflammatory cytokines and activation of leukocytes, which then act on BMECs (Lopez-Ramirez et al., 2013). This interaction instigates a temporal sequence of biological pathways that orchestrate the neurovascular response, potentially impacting the properties of the BBB and, consequently, affecting the brain parenchyma. As developmental windows of critical plasticity close, the neurovascular response is redirected towards "off-trajectory" pathways, which are then sustained throughout life. In this study, we used our recently developed protocol (Wakid et al., 2023) to isolate intact microvessels from archived snap-frozen vmPFC grey matter samples from healthy controls and depressed suicides with histories of ELA, for which we demonstrate preserved morphological integrity as well as expression of canonical neurovascular cell type markers. We isolated intact microvessels in favour of investigating the whole NVU as opposed to dissociated, single nuclei. Our decision to do so lies in the fact that a structurally preserved unit can provide

insight into the neurovasculature in a manner that dissociated nuclei cannot: not only is unwanted, technically-related depletion of neurovascular-associated cells avoided, but cytoplasm — which carries much higher amounts of mRNA and protein — as well as interstitium, are also preserved. This is not trivial, as work done by others comparing microglia single cells versus single nuclei from postmortem tissue reveals that certain populations of genes are depleted in nuclei (Thrupp et al., 2020). Ultimately, the NVU is so interconnected that dysfunction is typically observed in all neurovascular-associated cells, conferring whole-unit dysfunction that becomes difficult to parse when looking at dissociated nuclei.

Total RNA extracted from isolated microvessels was subjected to RNA sequencing to generate the first NVU-specific transcriptomic profile in individuals with a history of ELA. Overall, our findings suggest that NVU function and integrity in these individuals if impacted through widespread gene expression changes. Differential gene expression in pooled ELA subjects (males and females together) revealed dysregulated pathways in “chaperone-mediated protein folding” and antigen processing and presentation”, as well as DEGs involved in interconnected biological processes of hormone signalling (estrogen and progesterone), stress response mechanisms (heat shock proteins and FK506 binding proteins), and epigenetic regulation of gene expression (DNMT1 and HDAC9); corresponding to previous reports investigating chronic stress (Poulter et al., 2008; Hartmann et al., 2012; Zannas et al., 2016; Lund et al., 2006; Walf et al., 2004; Jochems et al., 2015), and warrant further investigation as potential ELA markers irrespective of sex. Transcriptomic changes associated with ELA or chronic stress have been the focus of several investigations, yet the majority of these studies exclusively characterize male ELA signatures (Short et al., 2023; Eck et al., 2022; Reemst et al., 2022; Kos et al., 2023; Treccani et al., 2021; Rentscher et al., 2022; Wegner et al., 2020). In contrast, fewer studies include females (Edelmann et al., 2023; Parel et al., 2023; Barrett et al., 2021), thereby omitting the opportunity to integrate or make direct comparisons between males and females and, as such, the extent to which the transcriptional profiles defining ELA differs in males versus females remains unknown. Our data-informed decision to perform DGE analysis on males and females separately

allowed us to identify dramatic, fundamental differences in NVU dysfunction in males versus females, providing a framework for better understanding the molecular basis of the sexual dimorphism characterizing depression and ELA. The male NVU appears to be relatively unaffected in male cases; in contrast, the female NVU experiences widespread differential expression in a large number of genes. These findings are further supported by outcomes from GSEA and RRHO analyses, revealing a lack of overlap in both pathway dysregulation and the direction of gene expression changes across all genes, not solely those that are significantly differentially expressed.

Male DEGs showed enrichment for pathways delineating voltage-gated potassium (K_V) channels and vascular smooth muscle contractility, which together may indicate that smooth muscle activity and vascular tone are modulated in adult male depressed suicides with a history of ELA. Indeed, impaired neurovascular coupling has been experimentally determined in chronically stressed rodents (Longden et al., 2014; Lee et al., 2015; Han et al., 2019), in which decreased vasomodulator enzymes neuronal nitric oxide synthase (nNOS) and heme oxygenase-2 (HO2) (Han et al., 2019; Lee et al., 2015) as well as malfunction of inwardly rectifying potassium (K_{ir}) channels in parenchymal arteriolar myocytes were observed (Longden et al., 2014). Complimentarily, psychosocial stress rapidly increases peak latency of the hemodynamic response function in the human prefrontal cortex (Elbau et al., 2018), suggesting shifted neurovascular coupling. Pathways pertaining to steroid hormone receptor activity (“Nuclear receptor transcription pathway” and “HSP90 chaperone cycle for steroid hormone receptors SHR in the presence of ligand”) are also modulated in males, and correspond to abundant research demonstrating the role of NR3C1 (encoding glucocorticoid receptor; McGowan et al., 2009; Oberlander et al., 2008; Weaver et al., 2004; Liu et al., 1997) in mediating the effects of chronic stress, and the neuroprotective effects of progesterone and estrogen (Brann et al., 2007) (PGR and ESR2 are upregulated in male ELA). In females, ORA and GSEA indicated downregulation of numerous, complimentary immune-related pathways, particularly those pertaining to cytokine signalling. Put succinctly, we report a global suppression of gene expression related to immune functions, encompassing both genes with pro- and

anti-inflammatory roles. Our finding contradicts decades of correlative clinical evidence suggesting that elevations in circulating pro-inflammatory cytokines reflect a similarly pro-inflammatory state within the brain parenchyma in stress-related psychopathology (Maes et al., 1992; Lieb et al., 1983; Calabrese et al., 1986; Howren et al., 2009; Dowlati et al., 2010; Felger et al., 2016; Haroon et al., 2016; Haapakoski et al., 2015; Udina et al., 2012; Ford and Erlinger, 2004; Pace et al., 2006; Miller et al., 2005; Osimo et al., 2020; Danese et al., 2008; Danese et al., 2007; Baldwin et al., 2018; Rasmussen et al., 2020; Danese et al., 2009; Danese et al., 2011). Importantly, suppressed immune signalling suggests that ELA-associated dysregulation of gene expression is not as straightforward as "peripheral inflammation equals brain inflammation". We reanalyzed a previously published RNA sequencing dataset generated in the ACC brain parenchyma (Lutz, Tanti et al., 2017), which is anatomically adjacent to the vmPFC, from the same female subjects. A moderately strong positive correlation was found between log2 fold changes of immune-related and neurovascular genes within the brain parenchyma and NVU, indicating a similar pattern of downregulation for these genes (Supplementary Fig. 5).

The accuracy of our findings is bolstered by the significant downregulation of CLDN5 expression in the female vmPFC, which corresponds to previous observations that chronic social stress alters BBB integrity through loss of the tight junction protein CLDN5 in the female mouse PFC (Dion-Albert et al., 2022), possibly by circulating cytokines (an experimentally validated mechanism: Camire et al., 2015; Khattab et al., 2023; Arima et al., 2020). Hence, this apparent contradiction in immune state between the blood and NVU may be reconciled by the following speculation: following ELA, the adult NVU is chronically exposed to circulating cytokines, prompting a continuous response or adaptation. Overtime, a new homeostatic point is set by the NVU. This adaptation modulates the NVU transcriptome, including the suppression of the NVU's own immune response, which may function as a neuroprotective mechanism to shield the brain parenchyma from the deleterious effects of a pro-inflammatory milieu in the blood, as suggested by similarly downregulated immune-related genes in the ACC of the same female subjects (Lutz, Tanti et al., 2017). Indeed, we see possible protective

mechanisms at play in females, in the form of suppressed platelet activation signalling and hemostasis pathways.

One such change in the transcriptome that demands further investigation is altered Krüppel-like Factor signalling, namely downregulated KLF2/4 in the female NVU. Expression of KLF2/4 acts as a central transcriptional switch point favouring a healthy, quiescent state of adult endothelial cells, while also maintaining stable expression of endothelial marker genes (Dekker et al., 2006) by opening chromatin and binding to enhancer and promoter regions throughout the endothelial genome to regulate core BMEC transcriptional programs (e.g., tight junctions, adhesion, guidance cues) (Sweet et al., 2023). Interestingly, KLF2/4 impedes endothelial cell activation induced by inhibiting TGFβ (Boon et al., 2007) and VCAM1 (both of which are downregulated in our female data, SenBanerjee et al., 2004) induced by diverse pro-inflammatory stimuli (Lin et al., 2006; Hamik et al., 2007). However, chronic pro-inflammatory stimuli may, in turn, inhibit KLF2/4 expression (Dekker et al., 2002; SenBanerjee et al., 2004; Kumar et al., 2005). It is possible that the continuous need to compensate for peripheral inflammation eventually leads to decreased KLF2/4 expression, reflecting an exhausted response where the system is no longer able to maintain effective levels of protection, while further losing BBB properties, as evidenced by downregulated CLDN5 expression, which is regulated by KLF2/4 (Sangwung et al., 2017; Ma et al., 2014; Supplementary Fig. 5). The highly significant differential expression of KLF2/4, coupled with their strong association with the ELA trait, and their central position within the turquoise and black modules underscores their regulatory significance in the context of ELA. Furthermore, the significant proportion of genes within the turquoise and black modules harboring KLF2 or KLF4 binding motifs in their distal or promoter regions (Supplementary Fig. 5) highlights the pivotal role of KLF2/4 in modulating the BBB's capacity to uphold brain homeostasis and safeguard the neuronal environment against stress-induced disorders.

This study has limitations that should be considered. First and foremost, the number of subjects investigated was small relative to the large number of genes tested for associations with ELA, a typical constraint in postmortem studies as well-characterized

brain tissue is a limited resource. While the relatively small number of subjects included in this study limits our statistical power, we succeed in illustrating robust changes in gene regulation in cases with robust sex differences, and further validated some of the main results. It will be interesting for future studies to extend this work to additional cohorts of ELA subjects and to assess the potential associations between brain, NVU and blood gene networks, with the promise that establishing “holistic” blood to NVU to brain transcriptomic profiles might better reveal diagnostic subtypes or treatment responses. Lastly, with this study design, it is difficult to associate our findings specifically to major depression or to ELA, and a contribution of both phenotypes is likely. That ELA might drive many/most of the expression changes we identified, however, is supported by recent studies having identified NVU or immune-related contributions to ELA or chronic stress (Menard et al., 2017; Dudek et al., 2020; Dion-Albert et al., 2022; Lehmann et al., 2018; Lehmann et al., 2020; Samuels et al., 2023; Lehmann et al., 2022). Indeed, several gene targets identified in these investigations are found within the top gene networks identified in the present study. In conclusion, our results provide a comprehensive characterization of sex-specific transcriptional signatures in the vmPFC of depressed suicides with a history of ELA, identifying regulatory mechanisms of endothelial function that may act as potential new avenues for the development of neurovascular-targeted therapeutic strategies for the treatment of ELA-related psychopathology, particularly in women.

5. References

Albarwani S, Nemetz LT, Madden JA, Tobin AA, England SK, Pratt PF, et al. Voltage-gated K+ channels in rat small cerebral arteries: molecular identity of the functional channels. J Physiol. 2003;551(Pt 3):751-63. https://doi.org/10.1113/jphysiol.2003.040014

Alon N, Macrynikola N, Jester DJ, Keshavan M, Reynolds CF, 3rd, Saxena S, et al. Social determinants of mental health in major depressive disorder: Umbrella review of 26 meta-analyses and systematic reviews. Psychiatry Res. 2024;335:115854. https://doi.org/10.1016/j.psychres.2024.115854

Ansell EB, Rando K, Tuit K, Guarnaccia J, Sinha R. Cumulative adversity and smaller gray matter volume in medial prefrontal, anterior cingulate, and insula regions. Biol Psychiatry. 2012;72(1):57-64. https://doi.org/10.1016/j.biopsych.2011.11.022

Arima M, Nakao S, Yamaguchi M, Feng H, Fujii Y, Shibata K, et al. Claudin-5 Redistribution Induced by Inflammation Leads to Anti-VEGF-Resistant Diabetic Macular Edema. Diabetes. 2020;69(5):981-99. https://doi.org/10.2337/db19-1121

Aschbacher K, Mills PJ, von Kanel R, Hong S, Mausbach BT, Roepke SK, et al. Effects of depressive and anxious symptoms on norepinephrine and platelet P-selectin responses to acute psychological stress among elderly caregivers. Brain Behav Immun. 2008;22(4):493-502. https://doi.org/10.1016/j.bbi.2007.10.002

Aumailley M, Smyth N. The role of laminins in basement membrane function. J Anat. 1998;193 (Pt 1)(Pt 1):1-21. https://doi.org/10.1046/j.1469-7580.1998.19310001.x

Baldwin JR, Arseneault L, Caspi A, Fisher HL, Moffitt TE, Odgers CL, et al. Childhood victimization and inflammation in young adulthood: A genetically sensitive cohort study. Brain Behav Immun. 2018;67:211-7. https://doi.org/10.1016/j.bbi.2017.08.025

Barrett TJ, Corr EM, van Solingen C, Schlamp F, Brown EJ, Koelwyn GJ, et al. Chronic stress primes innate immune responses in mice and humans. Cell Rep. 2021;36(10):109595. https://doi.org/10.1016/j.celrep.2021.109595

Baumeister D, Akhtar R, Ciufolini S, Pariante CM, Mondelli V. Childhood trauma and adulthood inflammation: a meta-analysis of peripheral C-reactive protein, interleukin-6 and tumour necrosis factor-alpha. Mol Psychiatry. 2016;21(5):642-9. https://doi.org/10.1038/mp.2015.67

Benjamini Y, Hochberg Y. Controlling the false discovery rate: a practical and powerful approach to multiple testing. J R Stat Soc Series B Methodol. 1995;57(1):289-300.

Bifulco A, Brown GW, Harris TO. Childhood Experience of Care and Abuse (CECA): a retrospective interview measure. J Child Psychol Psychiatry. 1994;35(8):1419-35. https://doi.org/10.1111/j.1469-7610.1994.tb01284.x

Bifulco A, Brown GW, Lillie A, Jarvis J. Memories of childhood neglect and abuse: corroboration in a series of sisters. J Child Psychol Psychiatry. 1997;38(3):365-74. https://doi.org/10.1111/j.1469-7610.1997.tb01520.x

Blaze J, Scheuing L, Roth TL. Differential methylation of genes in the medial prefrontal cortex of developing and adult rats following exposure to maltreatment or nurturing care during infancy. Dev Neurosci. 2013;35(4):306-16. https://doi.org/10.1159/000350716

Bockaert J, Perroy J, Ango F. The Complex Formed by Group I Metabotropic Glutamate Receptor (mGluR) and Homer1a Plays a Central Role in Metaplasticity and Homeostatic Synaptic Scaling. J Neurosci. 2021;41(26):5567-78. https://doi.org/10.1523/JNEUROSCI.0026-21.2021

Boon RA, Fledderus JO, Volger OL, van Wanrooij EJ, Pardali E, Weesie F, et al. KLF2 suppresses TGF-beta signaling in endothelium through induction of Smad7 and inhibition of AP-1. Arterioscler Thromb Vasc Biol. 2007;27(3):532-9. https://doi.org/10.1161/01.ATV.0000256466.65450.ce

Boulay AC, Saubamea B, Adam N, Chasseigneaux S, Mazare N, Gilbert A, et al. Translation in astrocyte distal processes sets molecular heterogeneity at the gliovascular interface. Cell Discov. 2017;3:17005. https://doi.org/10.1038/celldisc.2017.5

Brann DW, Dhandapani K, Wakade C, Mahesh VB, Khan MM. Neurotrophic and neuroprotective actions of estrogen: basic mechanisms and clinical implications. Steroids. 2007;72(5):381-405. https://doi.org/10.1016/j.steroids.2007.02.003

Cabrera OA, Hoge CW, Bliese PD, Castro CA, Messer SC. Childhood adversity and combat as predictors of depression and post-traumatic stress in deployed troops. Am J Prev Med. 2007;33(2):77-82. https://doi.org/10.1016/j.amepre.2007.03.019

Cahill KM, Huo Z, Tseng GC, Logan RW, Seney ML. Improved identification of concordant and discordant gene expression signatures using an updated rank-rank hypergeometric overlap approach. Sci Rep. 2018;8(1):9588. https://doi.org/10.1038/s41598-018-27903-2

Cai L, Xu L, Wei L, Chen W. Relationship of Mean Platelet Volume To MDD: A Retrospective Study. Shanghai Arch Psychiatry. 2017;29(1):21-9. https://doi.org/10.11919/j.issn.1002-0829.216082

Calabrese JR, Skwerer RG, Barna B, Gulledge AD, Valenzuela R, Butkus A, et al. Depression, immunocompetence, and prostaglandins of the E series. Psychiatry Res. 1986;17(1):41-7. https://doi.org/10.1016/0165-1781(86)90040-5

Camire RB, Beaulac HJ, Willis CL. Transitory loss of glia and the subsequent modulation in inflammatory cytokines/chemokines regulate paracellular claudin-5 expression in endothelial cells. J Neuroimmunol. 2015;284:57-66. https://doi.org/10.1016/j.jneuroim.2015.05.008

Canan F, Dikici S, Kutlucan A, Celbek G, Coskun H, Gungor A, et al. Association of mean platelet volume with DSM-IV major depression in a large community-based population: the MELEN study. J Psychiatr Res. 2012;46(3):298-302. https://doi.org/10.1016/j.jpsychires.2011.11.016

Chang L, Goldman RD. Intermediate filaments mediate cytoskeletal crosstalk. Nat Rev Mol Cell Biol. 2004;5(8):601-13. https://doi.org/10.1038/nrm1438

Chawla A, Cakmakci D, Zhang W, Maitra M, Rahimian R, Mitsuhashi H, Davoli M, Yang J, Chen GG, Denniston R, Mash D, Mechawar N, Suderman M, Li Y, Nagy C, Turecki G. Differential Chromatin Architecture and Risk Variants in Deep Layer Excitatory Neurons and Grey Matter Microglia Contribute to Major Depressive Disorder. bioRxiv.

2023:560567. https://doi.org/10.1101/2023.10.02.560567 (Preprint posted October 03, 2023)

Chen Y, Shan Y, Lin K, Wei Y, Kim H, Koenen KC, et al. Association Between Child Abuse and Risk of Adult Coronary Heart Disease: A Systematic Review and Meta-Analysis. Am J Prev Med. 2023;65(1):143-54. https://doi.org/10.1016/j.amepre.2023.02.028

Chiplunkar AR, Curtis BC, Eades GL, Kane MS, Fox SJ, Haar JL, et al. The Kruppel-like factor 2 and Kruppel-like factor 4 genes interact to maintain endothelial integrity in mouse embryonic vasculogenesis. BMC Dev Biol. 2013;13:40. https://doi.org/10.1186/1471-213X-13-40

Coelho R, Viola TW, Walss-Bass C, Brietzke E, Grassi-Oliveira R. Childhood maltreatment and inflammatory markers: a systematic review. Acta Psychiatr Scand. 2014;129(3):180-92. https://doi.org/10.1111/acps.12217

Dabertrand F, Kroigaard C, Bonev AD, Cognat E, Dalsgaard T, Domenga-Denier V, et al. Potassium channelopathy-like defect underlies early-stage cerebrovascular dysfunction in a genetic model of small vessel disease. Proc Natl Acad Sci U S A. 2015;112(7):E796-805. https://doi.org/10.1073/pnas.1420765112

Danese A, Caspi A, Williams B, Ambler A, Sugden K, Mika J, et al. Biological embedding of stress through inflammation processes in childhood. Mol Psychiatry. 2011;16(3):244-6. https://doi.org/10.1038/mp.2010.5

Danese A, Moffitt TE, Harrington H, Milne BJ, Polanczyk G, Pariante CM, et al. Adverse childhood experiences and adult risk factors for age-related disease: depression, inflammation, and clustering of metabolic risk markers. Arch Pediatr Adolesc Med. 2009;163(12):1135-43. https://doi.org/10.1001/archpediatrics.2009.214

Danese A, Moffitt TE, Pariante CM, Ambler A, Poulton R, Caspi A. Elevated inflammation levels in depressed adults with a history of childhood maltreatment. Arch Gen Psychiatry. 2008;65(4):409-15. https://doi.org/10.1001/archpsyc.65.4.409

Danese A, Pariante CM, Caspi A, Taylor A, Poulton R. Childhood maltreatment predicts adult inflammation in a life-course study. Proc Natl Acad Sci U S A. 2007;104(4):1319-24. https://doi.org/10.1073/pnas.0610362104

De Bellis M, Pisani F, Mola MG, Rosito S, Simone L, Buccoliero C, et al. Translational readthrough generates new astrocyte AQP4 isoforms that modulate supramolecular clustering, glial endfeet localization, and water transport. Glia. 2017;65(5):790-803. https://doi.org/10.1002/glia.23126

Dekker RJ, Boon RA, Rondaij MG, Kragt A, Volger OL, Elderkamp YW, et al. KLF2 provokes a gene expression pattern that establishes functional quiescent differentiation of the endothelium. Blood. 2006;107(11):4354-63. https://doi.org/10.1182/blood-2005-08-3465

Dekker RJ, van Soest S, Fontijn RD, Salamanca S, de Groot PG, VanBavel E, et al. Prolonged fluid shear stress induces a distinct set of endothelial cell genes, most specifically lung Kruppel-like factor (KLF2). Blood. 2002;100(5):1689-98. https://doi.org/10.1182/blood-2002-01-0046

Dion-Albert L, Cadoret A, Doney E, Kaufmann FN, Dudek KA, Daigle B, et al. Vascular and blood-brain barrier-related changes underlie stress responses and resilience in female mice and depression in human tissue. Nat Commun. 2022;13(1):164. https://doi.org/10.1038/s41467-021-27604-x

Dionisio N, Smani T, Woodard GE, Castellano A, Salido GM, Rosado JA. Homer proteins mediate the interaction between STIM1 and Cav1.2 channels. Biochim Biophys Acta. 2015;1853(5):1145-53. https://doi.org/10.1016/j.bbamcr.2015.02.014

Dobin A, Davis CA, Schlesinger F, Drenkow J, Zaleski C, Jha S, et al. STAR: ultrafast universal RNA-seq aligner. Bioinformatics. 2013;29(1):15-21. https://doi.org/10.1093/bioinformatics/bts635

Dong M, Giles WH, Felitti VJ, Dube SR, Williams JE, Chapman DP, et al. Insights into causal pathways for ischemic heart disease: adverse childhood experiences study. Circulation. 2004;110(13):1761-6. https://doi.org/10.1161/01.CIR.0000143074.54995.7F

Dowlati Y, Herrmann N, Swardfager W, Liu H, Sham L, Reim EK, et al. A meta-analysis of cytokines in major depression. Biol Psychiatry. 2010;67(5):446-57. https://doi.org/10.1016/j.biopsych.2009.09.033

Dudek KA, Dion-Albert L, Lebel M, LeClair K, Labrecque S, Tuck E, et al. Molecular adaptations of the blood-brain barrier promote stress resilience vs. depression. Proc Natl Acad Sci U S A. 2020;117(6):3326-36. https://doi.org/10.1073/pnas.1914655117

Dumais A, Lesage AD, Alda M, Rouleau G, Dumont M, Chawky N, et al. Risk factors for suicide completion in major depression: a case-control study of impulsive and aggressive behaviors in men. Am J Psychiatry. 2005;162(11):2116-24. https://doi.org/10.1176/appi.ajp.162.11.2116

Eck SR, Palmer JL, Bavley CC, Karbalaei R, Ordones Sanchez E, Flowers J, 2nd, et al. Effects of early life adversity on male reproductive behavior and the medial preoptic area transcriptome. Neuropsychopharmacology. 2022;47(6):1231-9. https://doi.org/10.1038/s41386-022-01282-9

Edelmann S, Wiegand A, Hentrich T, Pasche S, Schulze-Hentrich JM, Munk MHJ, et al. Blood transcriptome analysis suggests an indirect molecular association of early life adversities and adult social anxiety disorder by immune-related signal transduction. Front Psychiatry. 2023;14:1125553. https://doi.org/10.3389/fpsyt.2023.1125553

Elbau IG, Brucklmeier B, Uhr M, Arloth J, Czamara D, Spoormaker VI, et al. The brain's hemodynamic response function rapidly changes under acute psychosocial stress in association with genetic and endocrine stress response markers. Proc Natl Acad Sci U S A. 2018;115(43):E10206-E15. https://doi.org/10.1073/pnas.1804340115

Felger JC, Li Z, Haroon E, Woolwine BJ, Jung MY, Hu X, et al. Inflammation is associated with decreased functional connectivity within corticostriatal reward circuitry in depression. Mol Psychiatry. 2016;21(10):1358-65. https://doi.org/10.1038/mp.2015.168

Felitti VJ, Anda RF, Nordenberg D, Williamson DF, Spitz AM, Edwards V, et al. Relationship of childhood abuse and household dysfunction to many of the leading causes of death in adults. The Adverse Childhood Experiences (ACE) Study. Am J Prev Med. 1998;14(4):245-58. https://doi.org/10.1016/s0749-3797(98)00017-8

Ford DE, Erlinger TP. Depression and C-reactive protein in US adults: data from the Third National Health and Nutrition Examination Survey. Arch Intern Med. 2004;164(9):1010-4. https://doi.org/10.1001/archinte.164.9.1010

Fuller-Thomson E, Brennenstuhl S, Frank J. The association between childhood physical abuse and heart disease in adulthood: findings from a representative community sample. Child Abuse Negl. 2010;34(9):689-98.
https://doi.org/10.1016/j.chiabu.2010.02.005

Garcia FJ, Sun N, Lee H, Godlewski B, Mathys H, Galani K, et al. Single-cell dissection of the human brain vasculature. Nature. 2022;603(7903):893-9.
https://doi.org/10.1038/s41586-022-04521-7

Gialluisi A, Izzi B, Di Castelnuovo A, Cerletti C, Donati MB, de Gaetano G, et al. Revisiting the link between platelets and depression through genetic epidemiology: new insights from platelet distribution width. Haematologica. 2020;105(5):e246-e8.
https://doi.org/10.3324/haematol.2019.222513

Gildawie KR, Honeycutt JA, Brenhouse HC. Region-specific Effects of Maternal Separation on Perineuronal Net and Parvalbumin-expressing Interneuron Formation in Male and Female Rats. Neuroscience. 2020;428:23-37.
https://doi.org/10.1016/j.neuroscience.2019.12.010

Ginty AT, Kraynak TE, Fisher JP, Gianaros PJ. Cardiovascular and autonomic reactivity to psychological stress: Neurophysiological substrates and links to cardiovascular disease. Auton Neurosci. 2017;207:2-9.
https://doi.org/10.1016/j.autneu.2017.03.003

Green JG, McLaughlin KA, Berglund PA, Gruber MJ, Sampson NA, Zaslavsky AM, et al. Childhood adversities and adult psychiatric disorders in the national comorbidity survey replication I: associations with first onset of DSM-IV disorders. Arch Gen Psychiatry. 2010;67(2):113-23. https://doi.org/10.1001/archgenpsychiatry.2009.186

Greene C, Hanley N, Campbell M. Claudin-5: gatekeeper of neurological function. Fluids Barriers CNS. 2019;16(1):3. https://doi.org/10.1186/s12987-019-0123-z

Gutierrez-Sacristan A, Bravo A, Portero-Tresserra M, Valverde O, Armario A, Blanco-Gandia MC, et al. Text mining and expert curation to develop a database on psychiatric diseases and their genes. Database (Oxford). 2017;2017. https://doi.org/10.1093/database/bax043

Guyot R, Vincent S, Bertin J, Samarut J, Ravel-Chapuis P. The transforming acidic coiled coil (TACC1) protein modulates the transcriptional activity of the nuclear receptors TR and RAR. BMC Mol Biol. 2010;11:3. https://doi.org/10.1186/1471-2199-11-3

Haapakoski R, Mathieu J, Ebmeier KP, Alenius H, Kivimaki M. Cumulative meta-analysis of interleukins 6 and 1beta, tumour necrosis factor alpha and C-reactive protein in patients with major depressive disorder. Brain Behav Immun. 2015;49:206-15. https://doi.org/10.1016/j.bbi.2015.06.001

Hagenauer MH, Sannah Y, Hebda-Bauer EK, Rhoads C, O'Connor AM, Watson SJ Jr, Akil H. Resource: A Curated Database of Brain-Related Functional Gene Sets (Brain.GMT). bioRxiv. 2024. https://doi.org/10.1101/2024.04.05.588301 (Preprint posted April 10, 2024)

Hamik A, Lin Z, Kumar A, Balcells M, Sinha S, Katz J, et al. Kruppel-like factor 4 regulates endothelial inflammation. J Biol Chem. 2007;282(18):13769-79. https://doi.org/10.1074/jbc.M700078200

Han K, Min J, Lee M, Kang BM, Park T, Hahn J, et al. Neurovascular Coupling under Chronic Stress Is Modified by Altered GABAergic Interneuron Activity. J Neurosci. 2019;39(50):10081-95. https://doi.org/10.1523/JNEUROSCI.1357-19.2019

Haroon E, Fleischer CC, Felger JC, Chen X, Woolwine BJ, Patel T, et al. Conceptual convergence: increased inflammation is associated with increased basal ganglia glutamate in patients with major depression. Mol Psychiatry. 2016;21(10):1351-7. https://doi.org/10.1038/mp.2015.206

Hartmann J, Wagner KV, Liebl C, Scharf SH, Wang XD, Wolf M, et al. The involvement of FK506-binding protein 51 (FKBP5) in the behavioral and neuroendocrine effects of chronic social defeat stress. Neuropharmacology. 2012;62(1):332-9. https://doi.org/10.1016/j.neuropharm.2011.07.041

Hayashi Y, Okamoto Y, Takagaki K, Okada G, Toki S, Inoue T, et al. Direct and indirect influences of childhood abuse on depression symptoms in patients with major depressive disorder. BMC Psychiatry. 2015;15:244. https://doi.org/10.1186/s12888-015-0636-1

Hillis S, Mercy J, Amobi A, Kress H. Global Prevalence of Past-year Violence Against Children: A Systematic Review and Minimum Estimates. Pediatrics. 2016;137(3):e20154079. https://doi.org/10.1542/peds.2015-4079

Hirschi KK, D'Amore PA. Pericytes in the microvasculature. Cardiovasc Res. 1996;32(4):687-98. https://doi.org/10.1016/s0008-6363(96)00063-6

Hostinar CE, Stellern SA, Schaefer C, Carlson SM, Gunnar MR. Associations between early life adversity and executive function in children adopted internationally from orphanages. Proc Natl Acad Sci U S A. 2012;109 Suppl 2(Suppl 2):17208-12. https://doi.org/10.1073/pnas.1121246109

Howren MB, Lamkin DM, Suls J. Associations of depression with C-reactive protein, IL-1, and IL-6: a meta-analysis. Psychosom Med. 2009;71(2):171-86. https://doi.org/10.1097/PSY.0b013e3181907c1b

Izzi B, Tirozzi A, Cerletti C, Donati MB, de Gaetano G, Hoylaerts MF, et al. Beyond Haemostasis and Thrombosis: Platelets in Depression and Its Co-Morbidities. Int J Mol Sci. 2020;21(22). https://doi.org/10.3390/ijms21228817

Jardin I, Albarran L, Bermejo N, Salido GM, Rosado JA. Homers regulate calcium entry and aggregation in human platelets: a role for Homers in the association between STIM1 and Orai1. Biochem J. 2012;445(1):29-38. https://doi.org/10.1042/BJ20120471

Jenkins NDM, Rogers EM, Banks NF, Tomko PM, Sciarrillo CM, Emerson SR, et al. Childhood psychosocial stress is linked with impaired vascular endothelial function, lower SIRT1, and oxidative stress in young adulthood. Am J Physiol Heart Circ Physiol. 2021;321(3):H532-H41. https://doi.org/10.1152/ajpheart.00123.2021

Jochems J, Teegarden SL, Chen Y, Boulden J, Challis C, Ben-Dor GA, et al. Enhancement of stress resilience through histone deacetylase 6-mediated regulation of glucocorticoid receptor chaperone dynamics. Biol Psychiatry. 2015;77(4):345-55. https://doi.org/10.1016/j.biopsych.2014.07.036

Khattab AM, Hagras SM, Lotfy NM. Pre-operative versus post-operative intravitreal aflibercept injection for management of DME in patients undergoing cataract surgery. Graefes Arch Clin Exp Ophthalmol. 2023;261(11):3223-9. https://doi.org/10.1007/s00417-023-06138-6

Kim P, Evans GW, Angstadt M, Ho SS, Sripada CS, Swain JE, et al. Effects of childhood poverty and chronic stress on emotion regulatory brain function in adulthood. Proc Natl Acad Sci U S A. 2013;110(46):18442-7. https://doi.org/10.1073/pnas.1308240110

Kim WK, Alvarez X, Fisher J, Bronfin B, Westmoreland S, McLaurin J, et al. CD163 identifies perivascular macrophages in normal and viral encephalitic brains and potential precursors to perivascular macrophages in blood. Am J Pathol. 2006;168(3):822-34. https://doi.org/10.2353/ajpath.2006.050215

Koizumi T, Kerkhofs D, Mizuno T, Steinbusch HWM, Foulquier S. Vessel-Associated Immune Cells in Cerebrovascular Diseases: From Perivascular Macrophages to Vessel-Associated Microglia. Front Neurosci. 2019;13:1291. https://doi.org/10.3389/fnins.2019.01291

Kolodkin A, Sahin N, Phillips A, Hood SR, Bruggeman FJ, Westerhoff HV, et al. Optimization of stress response through the nuclear receptor-mediated cortisol signalling network. Nat Commun. 2013;4:1792. https://doi.org/10.1038/ncomms2799

Korotkevich G, Sukhov V, Sergushichev A. Fast gene set enrichment analysis. bioRxiv. 2019. Cold Spring Harbor Labs Journals. https://doi.org/10.1101/060012 (Preprint posted February 01, 2021)

Kos A, Lopez JP, Bordes J, de Donno C, Dine J, Brivio E, et al. Early life adversity shapes social subordination and cell type-specific transcriptomic patterning in the ventral hippocampus. Sci Adv. 2023;9(48):eadj3793. https://doi.org/10.1126/sciadv.adj3793

Koudouovoh-Tripp P, Hufner K, Egeter J, Kandler C, Giesinger JM, Sopper S, et al. Stress Enhances Proinflammatory Platelet Activity: the Impact of Acute and Chronic Mental Stress. J Neuroimmune Pharmacol. 2021;16(2):500-12. https://doi.org/10.1007/s11481-020-09945-4

Kumar A, Lin Z, SenBanerjee S, Jain MK. Tumor necrosis factor alpha-mediated reduction of KLF2 is due to inhibition of MEF2 by NF-kappaB and histone deacetylases. Mol Cell Biol. 2005;25(14):5893-903. https://doi.org/10.1128/MCB.25.14.5893-5903.2005

Labonte B, Engmann O, Purushothaman I, Menard C, Wang J, Tan C, et al. Sex-specific transcriptional signatures in human depression. Nat Med. 2017;23(9):1102-11. https://doi.org/10.1038/nm.4386

Langfelder P, Horvath S. WGCNA: an R package for weighted correlation network analysis. BMC Bioinformatics. 2008;9:559. https://doi.org/10.1186/1471-2105-9-559

Lee JS, Yu Q, Shin JT, Sebzda E, Bertozzi C, Chen M, et al. Klf2 is an essential regulator of vascular hemodynamic forces in vivo. Dev Cell. 2006;11(6):845-57. https://doi.org/10.1016/j.devcel.2006.09.006

Lee S, Kang BM, Shin MK, Min J, Heo C, Lee Y, et al. Chronic Stress Decreases Cerebrovascular Responses During Rat Hindlimb Electrical Stimulation. Front Neurosci. 2015;9:462. https://doi.org/10.3389/fnins.2015.00462

Lehmann ML, Weigel TK, Cooper HA, Elkahloun AG, Kigar SL, Herkenham M. Decoding microglia responses to psychosocial stress reveals blood-brain barrier breakdown that may drive stress susceptibility. Sci Rep. 2018;8(1):11240. https://doi.org/10.1038/s41598-018-28737-8

Lehmann ML, Poffenberger CN, Elkahloun AG, Herkenham M. Analysis of cerebrovascular dysfunction caused by chronic social defeat in mice. Brain Behav Immun. 2020;88:735-47. https://doi.org/10.1016/j.bbi.2020.05.030

Lehmann ML, Samuels JD, Kigar SL, Poffenberger CN, Lotstein ML, Herkenham M. CCR2 monocytes repair cerebrovascular damage caused by chronic social defeat stress. Brain Behav Immun. 2022;101:346-58. https://doi.org/10.1016/j.bbi.2022.01.011

LeMoult J, Humphreys KL, Tracy A, Hoffmeister JA, Ip E, Gotlib IH. Meta-analysis: Exposure to Early Life Stress and Risk for Depression in Childhood and Adolescence. J Am Acad Child Adolesc Psychiatry. 2020;59(7):842-55. https://doi.org/10.1016/j.jaac.2019.10.011

Li B, Dewey CN. RSEM: accurate transcript quantification from RNA-Seq data with or without a reference genome. BMC Bioinformatics. 2011;12:323. https://doi.org/10.1186/1471-2105-12-323

Li H, Handsaker B, Wysoker A, Fennell T, Ruan J, Homer N, et al. The Sequence Alignment/Map format and SAMtools. Bioinformatics. 2009;25(16):2078-9. https://doi.org/10.1093/bioinformatics/btp352

Lieb J, Karmali R, Horrobin D. Elevated levels of prostaglandin E2 and thromboxane B2 in depression. Prostaglandins Leukot Med. 1983;10(4):361-7. https://doi.org/10.1016/0262-1746(83)90048-3

Lin Z, Hamik A, Jain R, Kumar A, Jain MK. Kruppel-like factor 2 inhibits protease activated receptor-1 expression and thrombin-mediated endothelial activation. Arterioscler Thromb Vasc Biol. 2006;26(5):1185-9. https://doi.org/10.1161/01.ATV.0000215638.53414.99

Lin Z, Kumar A, SenBanerjee S, Staniszewski K, Parmar K, Vaughan DE, et al. Kruppel-like factor 2 (KLF2) regulates endothelial thrombotic function. Circ Res. 2005;96(5):e48-57. https://doi.org/10.1161/01.RES.0000159707.05637.a1

Lin Z, Natesan V, Shi H, Dong F, Kawanami D, Mahabeleshwar GH, et al. Kruppel-like factor 2 regulates endothelial barrier function. Arterioscler Thromb Vasc Biol. 2010;30(10):1952-9. https://doi.org/10.1161/ATVBAHA.110.211474

Liu D, Diorio J, Tannenbaum B, Caldji C, Francis D, Freedman A, et al. Maternal care, hippocampal glucocorticoid receptors, and hypothalamic-pituitary-adrenal responses to stress. Science. 1997;277(5332):1659-62. https://doi.org/10.1126/science.277.5332.1659

Longden TA, Dabertrand F, Hill-Eubanks DC, Hammack SE, Nelson MT. Stress-induced glucocorticoid signaling remodels neurovascular coupling through impairment of cerebrovascular inwardly rectifying K+ channel function. Proc Natl Acad Sci U S A. 2014;111(20):7462-7. https://doi.org/10.1073/pnas.1401811111

Lopez-Ramirez MA, Male DK, Wang C, Sharrack B, Wu D, Romero IA. Cytokine-induced changes in the gene expression profile of a human cerebral microvascular endothelial cell-line, hCMEC/D3. Fluids Barriers CNS. 2013;10(1):27. https://doi.org/10.1186/2045-8118-10-27

Loucks EB, Taylor SE, Polak JF, Wilhelm A, Kalra P, Matthews KA. Childhood family psychosocial environment and carotid intima media thickness: the CARDIA study. Soc Sci Med. 2014;104:15-22. https://doi.org/10.1016/j.socscimed.2013.12.015

Love MI, Huber W, Anders S. Moderated estimation of fold change and dispersion for RNA-seq data with DESeq2. Genome Biol. 2014;15(12):550. https://doi.org/10.1186/s13059-014-0550-8

Luissint AC, Artus C, Glacial F, Ganeshamoorthy K, Couraud PO. Tight junctions at the blood brain barrier: physiological architecture and disease-associated dysregulation. Fluids Barriers CNS. 2012;9(1):23. https://doi.org/10.1186/2045-8118-9-23

Lund TD, Hinds LR, Handa RJ. The androgen 5alpha-dihydrotestosterone and its metabolite 5alpha-androstan-3beta, 17beta-diol inhibit the hypothalamo-pituitary-adrenal response to stress by acting through estrogen receptor beta-expressing neurons in the hypothalamus. J Neurosci. 2006;26(5):1448-56. https://doi.org/10.1523/JNEUROSCI.3777-05.2006

Lutz PE, Tanti A, Gasecka A, Barnett-Burns S, Kim JJ, Zhou Y, et al. Association of a History of Child Abuse With Impaired Myelination in the Anterior Cingulate Cortex: Convergent Epigenetic, Transcriptional, and Morphological Evidence. Am J Psychiatry. 2017;174(12):1185-94. https://doi.org/10.1176/appi.ajp.2017.16111286

Ma J, Wang P, Liu Y, Zhao L, Li Z, Xue Y. Kruppel-like factor 4 regulates blood-tumor barrier permeability via ZO-1, occludin and claudin-5. J Cell Physiol. 2014;229(7):916-26. https://doi.org/10.1002/jcp.24523

Maes M, Lambrechts J, Bosmans E, Jacobs J, Suy E, Vandervorst C, et al. Evidence for a systemic immune activation during depression: results of leukocyte enumeration by flow cytometry in conjunction with monoclonal antibody staining. Psychol Med. 1992;22(1):45-53. https://doi.org/10.1017/s0033291700032712

Majtanik, M., and Paxinos, G. (2016). Atlas of the human brain (4th ed.). Elsevier. June 8, 2024

Markovitz JH, Matthews KA. Platelets and coronary heart disease: potential psychophysiologic mechanisms. Psychosom Med. 1991;53(6):643-68. https://doi.org/10.1097/00006842-199111000-00006

Massardo T, Quintana JC, Jaimovich R, Saez CG, Risco L, Liberman C, et al. Regional Brain Perfusion Is Associated with Endothelial Dysfunction Markers in Major Depressive Disorder. Neuropsychobiology. 2021;80(3):214-24. https://doi.org/10.1159/000508110

Matsuhisa F, Kitamura N, Satoh E. Effects of acute and chronic psychological stress on platelet aggregation in mice. Stress. 2014;17(2):186-92. https://doi.org/10.3109/10253890.2014.888548

McConnell HL, Kersch CN, Woltjer RL, Neuwelt EA. The Translational Significance of the Neurovascular Unit. J Biol Chem. 2017;292(3):762-70. https://doi.org/10.1074/jbc.R116.760215

McGowan PO, Sasaki A, D'Alessio AC, Dymov S, Labonte B, Szyf M, et al. Epigenetic regulation of the glucocorticoid receptor in human brain associates with childhood abuse. Nat Neurosci. 2009;12(3):342-8. https://doi.org/10.1038/nn.2270

Menard C, Pfau ML, Hodes GE, Kana V, Wang VX, Bouchard S, et al. Social stress induces neurovascular pathology promoting depression. Nat Neurosci. 2017;20(12):1752-60. https://doi.org/10.1038/s41593-017-0010-3

Miller GE, Rohleder N, Stetler C, Kirschbaum C. Clinical depression and regulation of the inflammatory response during acute stress. Psychosom Med. 2005;67(5):679-87. https://doi.org/10.1097/01.psy.0000174172.82428.ce

Monroy E, Hernandez-Torres E, Flores G. Maternal separation disrupts dendritic morphology of neurons in prefrontal cortex, hippocampus, and nucleus accumbens in male rat offspring. J Chem Neuroanat. 2010;40(2):93-101. https://doi.org/10.1016/j.jchemneu.2010.05.005

Morel-Kopp MC, McLean L, Chen Q, Tofler GH, Tennant C, Maddison V, et al. The association of depression with platelet activation: evidence for a treatment effect. J Thromb Haemost. 2009;7(4):573-81. https://doi.org/10.1111/j.1538-7836.2009.03278.x

Mossadegh-Keller N, Sarrazin S, Kandalla PK, Espinosa L, Stanley ER, Nutt SL, et al. M-CSF instructs myeloid lineage fate in single haematopoietic stem cells. Nature. 2013;497(7448):239-43. https://doi.org/10.1038/nature12026

Munji RN, Soung AL, Weiner GA, Sohet F, Semple BD, Trivedi A, et al. Profiling the mouse brain endothelial transcriptome in health and disease models reveals a core blood-brain barrier dysfunction module. Nat Neurosci. 2019;22(11):1892-902. https://doi.org/10.1038/s41593-019-0497-x

Musselman DL, Tomer A, Manatunga AK, Knight BT, Porter MR, Kasey S, et al. Exaggerated platelet reactivity in major depression. Am J Psychiatry. 1996;153(10):1313-7. https://doi.org/10.1176/ajp.153.10.1313

Nagelhus EA, Ottersen OP. Physiological roles of aquaporin-4 in brain. Physiol Rev. 2013;93(4):1543-62. https://doi.org/10.1152/physrev.00011.2013

Newman AM, Steen CB, Liu CL, Gentles AJ, Chaudhuri AA, Scherer F, et al. Determining cell type abundance and expression from bulk tissues with digital cytometry. Nat Biotechnol. 2019;37(7):773-82. https://doi.org/10.1038/s41587-019-0114-2

Nieves-Cintron M, Syed AU, Nystoriak MA, Navedo MF. Regulation of voltage-gated potassium channels in vascular smooth muscle during hypertension and metabolic disorders. Microcirculation. 2018;25(1). https://doi.org/10.1111/micc.12423

Nomura Y, Wickramaratne PJ, Warner V, Mufson L, Weissman MM. Family discord, parental depression, and psychopathology in offspring: ten-year follow-up. J Am Acad Child Adolesc Psychiatry. 2002;41(4):402-9. https://doi.org/10.1097/00004583-200204000-00012

Oberlander TF, Weinberg J, Papsdorf M, Grunau R, Misri S, Devlin AM. Prenatal exposure to maternal depression, neonatal methylation of human glucocorticoid receptor gene (NR3C1) and infant cortisol stress responses. Epigenetics. 2008;3(2):97-106. https://doi.org/10.4161/epi.3.2.6034

Oldham Green N, Maniam J, Riese J, Morris MJ, Voineagu I. Transcriptomic signature of early life stress in male rat prefrontal cortex. Neurobiol Stress. 2021;14:100316. https://doi.org/10.1016/j.ynstr.2021.100316

Ormonde do Carmo MB, Mendes-Ribeiro AC, Matsuura C, Pinto VL, Mury WV, Pinto NO, et al. Major depression induces oxidative stress and platelet hyperaggregability. J Psychiatr Res. 2015;61:19-24. https://doi.org/10.1016/j.jpsychires.2014.12.009

Osimo EF, Pillinger T, Rodriguez IM, Khandaker GM, Pariante CM, Howes OD. Inflammatory markers in depression: A meta-analysis of mean differences and variability in 5,166 patients and 5,083 controls. Brain Behav Immun. 2020;87:901-9. https://doi.org/10.1016/j.bbi.2020.02.010

Pace TW, Mletzko TC, Alagbe O, Musselman DL, Nemeroff CB, Miller AH, et al. Increased stress-induced inflammatory responses in male patients with major depression and increased early life stress. Am J Psychiatry. 2006;163(9):1630-3. https://doi.org/10.1176/ajp.2006.163.9.1630

Parel ST, Bennett SN, Cheng CJ, Timmermans OC, Fiori LM, Turecki G, et al. Transcriptional signatures of early-life stress and antidepressant treatment efficacy. Proc Natl Acad Sci U S A. 2023;120(49):e2305776120. https://doi.org/10.1073/pnas.2305776120

Pena CJ, Smith M, Ramakrishnan A, Cates HM, Bagot RC, Kronman HG, et al. Early life stress alters transcriptomic patterning across reward circuitry in male and female mice. Nat Commun. 2019;10(1):5098. https://doi.org/10.1038/s41467-019-13085-6

Pessoa L. On the relationship between emotion and cognition. Nat Rev Neurosci. 2008;9(2):148-58. https://doi.org/10.1038/nrn2317

Pierce JH, Di Marco E, Cox GW, Lombardi D, Ruggiero M, Varesio L, et al. Macrophage-colony-stimulating factor (CSF-1) induces proliferation, chemotaxis, and reversible monocytic differentiation in myeloid progenitor cells transfected with the human c-fms/CSF-1 receptor cDNA. Proc Natl Acad Sci U S A. 1990;87(15):5613-7. https://doi.org/10.1073/pnas.87.15.5613

Pinto VL, de Souza PF, Brunini TM, Oliveira MB, Moss MB, Siqueira MA, et al. Low plasma levels of L-arginine, impaired intraplatelet nitric oxide and platelet hyperaggregability: implications for cardiovascular disease in depressive patients. J Affect Disord. 2012;140(2):187-92. https://doi.org/10.1016/j.jad.2012.02.008

Poulter MO, Du L, Weaver ICG, Palkovits M, Faludi G, Merali Z, et al. GABAA receptor promoter hypermethylation in suicide brain: implications for the involvement of epigenetic processes. Biol Psychiatry. 2008;64(8):645-52. https://doi.org/10.1016/j.biopsych.2008.05.028

Purves D, Augustine GJ, Fitzpatrick D. The Blood Supply of the Brain and Spinal Cord. In: Neuroscience. 2nd ed. Sunderland (MA): Sinauer Associates; 2001.

Raposo SM, Mackenzie CS, Henriksen CA, Afifi TO. Time does not heal all wounds: older adults who experienced childhood adversities have higher odds of mood, anxiety, and personality disorders. Am J Geriatr Psychiatry. 2014;22(11):1241-50. https://doi.org/10.1016/j.jagp.2013.04.009

Rasmussen LJH, Moffitt TE, Arseneault L, Danese A, Eugen-Olsen J, Fisher HL, et al. Association of Adverse Experiences and Exposure to Violence in Childhood and Adolescence With Inflammatory Burden in Young People. JAMA Pediatr. 2020;174(1):38-47. https://doi.org/10.1001/jamapediatrics.2019.3875

Reemst K, Kracht L, Kotah JM, Rahimian R, van Irsen AAS, Congrains Sotomayor G, et al. Early-life stress lastingly impacts microglial transcriptome and function under basal and immune-challenged conditions. Transl Psychiatry. 2022;12(1):507. doi: 10.1038/s41398-022-02265-6.

Rentscher KE, Carroll JE, Polsky LR, Lamkin DM. Chronic stress increases transcriptomic indicators of biological aging in mouse bone marrow leukocytes. Brain Behav Immun Health. 2022;22:100461. https://doi.org/10.1016/j.bbih.2022.100461

Riley EH, Wright RJ, Jun HJ, Hibert EN, Rich-Edwards JW. Hypertension in adult survivors of child abuse: observations from the Nurses' Health Study II. J Epidemiol Community Health. 2010;64(5):413-8. https://doi.org/10.1136/jech.2009.095109

Ritchie ME, Phipson B, Wu D, Hu Y, Law CW, Shi W, et al. limma powers differential expression analyses for RNA-sequencing and microarray studies. Nucleic Acids Res. 2015;43(7):e47. https://doi.org/10.1093/nar/gkv007

Samuels JD, Lotstein ML, Lehmann ML, Elkahloun AG, Banerjee S, Herkenham M. Chronic social defeat alters brain vascular-associated cell gene expression patterns leading to vascular

dysfunction and immune system activation. J Neuroinflammation. 2023;20(1):154. https://doi.org/10.1186/s12974-023-02827-5

Sangwung P, Zhou G, Nayak L, Chan ER, Kumar S, Kang DW, et al. KLF2 and KLF4 control endothelial identity and vascular integrity. JCI Insight. 2017;2(4):e91700. https://doi.org/10.1172/jci.insight.91700

SenBanerjee S, Lin Z, Atkins GB, Greif DM, Rao RM, Kumar A, et al. KLF2 Is a novel transcriptional regulator of endothelial proinflammatory activation. J Exp Med. 2004;199(10):1305-15. https://doi.org/10.1084/jem.20031132

Shi H, Sheng B, Zhang F, Wu C, Zhang R, Zhu J, et al. Kruppel-like factor 2 protects against ischemic stroke by regulating endothelial blood brain barrier function. Am J Physiol Heart Circ Physiol. 2013;304(6):H796-805. https://doi.org/10.1152/ajpheart.00712.2012

Short AK, Thai CW, Chen Y, Kamei N, Pham AL, Birnie MT, et al. Single-Cell Transcriptional Changes in Hypothalamic Corticotropin-Releasing Factor-Expressing Neurons After Early-Life Adversity Inform Enduring Alterations in Vulnerabilities to Stress. Biol Psychiatry Glob Open Sci. 2023;3(1):99-109. https://doi.org/10.1016/j.bpsgos.2021.12.006

Siret C, van Lessen M, Bavais J, Jeong HW, Reddy Samawar SK, Kapupara K, et al. Deciphering the heterogeneity of the Lyve1(+) perivascular macrophages in the mouse brain. Nat Commun. 2022;13(1):7366. https://doi.org/10.1038/s41467-022-35166-9

Slopen N, Kubzansky LD, McLaughlin KA, Koenen KC. Childhood adversity and inflammatory processes in youth: a prospective study. Psychoneuroendocrinology. 2013;38(2):188-200. https://doi.org/10.1016/j.psyneuen.2012.05.013

Smith T, Heger A, Sudbery I. UMI-tools: modeling sequencing errors in Unique Molecular Identifiers to improve quantification accuracy. Genome Res. 2017;27(3):491-9. https://doi.org/10.1101/gr.209601.116

Smolders J, Remmerswaal EB, Schuurman KG, Melief J, van Eden CG, van Lier RA, et al. Characteristics of differentiated CD8(+) and CD4 (+) T cells present in the human brain. Acta Neuropathol. 2013;126(4):525-35. https://doi.org/10.1007/s00401-013-1155-0

Smolders J, Heutinck KM, Fransen NL, Remmerswaal EBM, Hombrink P, Ten Berge IJM, et al. Tissue-resident memory T cells populate the human brain. Nat Commun. 2018;9(1):4593. https://doi.org/10.1038/s41467-018-07053-9

Stokes CL, Rupnick MA, Williams SK, Lauffenburger DA. Chemotaxis of human microvessel endothelial cells in response to acidic fibroblast growth factor. Lab Invest. 1990;63(5):657-68. https://www.ncbi.nlm.nih.gov/pubmed/1700197

Stuart T, Butler A, Hoffman P, Hafemeister C, Papalexi E, Mauck WM, 3rd, et al. Comprehensive Integration of Single-Cell Data. Cell. 2019;177(7):1888-902 e21. https://doi.org/10.1016/j.cell.2019.05.031

Su S, Wang X, Kapuku GK, Treiber FA, Pollock DM, Harshfield GA, et al. Adverse childhood experiences are associated with detrimental hemodynamics and elevated circulating endothelin-1 in adolescents and young adults. Hypertension. 2014;64(1):201-7. https://doi.org/10.1161/HYPERTENSIONAHA.113.02755

Su S, Wang X, Pollock JS, Treiber FA, Xu X, Snieder H, et al. Adverse childhood experiences and blood pressure trajectories from childhood to young adulthood: the Georgia stress and Heart study. Circulation. 2015;131(19):1674-81. https://doi.org/10.1161/CIRCULATIONAHA.114.013104

Subramanian A, Tamayo P, Mootha VK, Mukherjee S, Ebert BL, Gillette MA, et al. Gene set enrichment analysis: a knowledge-based approach for interpreting genome-wide expression profiles. Proc Natl Acad Sci U S A. 2005;102(43):15545-50. https://doi.org/10.1073/pnas.0506580102

Sweet DR, Padmanabhan R, Liao X, Dashora HR, Tang X, Nayak L, et al. Kruppel-Like Factors Orchestrate Endothelial Gene Expression Through Redundant and Non-Redundant Enhancer Networks. J Am Heart Assoc. 2023;12(4):e024303. https://doi.org/10.1161/JAHA.121.024303

Takizawa R, Danese A, Maughan B, Arseneault L. Bullying victimization in childhood predicts inflammation and obesity at mid-life: a five-decade birth cohort study. Psychol Med. 2015;45(13):2705-15. https://doi.org/10.1017/S0033291715000653

Tanti A, Belliveau C, Nagy C, Maitra M, Denux F, Perlman K, et al. Child abuse associates with increased recruitment of perineuronal nets in the ventromedial prefrontal cortex: a possible implication of oligodendrocyte progenitor cells. Mol Psychiatry. 2022;27(3):1552-61. https://doi.org/10.1038/s41380-021-01372-y

Tanti A, Kim JJ, Wakid M, Davoli MA, Turecki G, Mechawar N. Child abuse associates with an imbalance of oligodendrocyte-lineage cells in ventromedial prefrontal white matter. Mol Psychiatry. 2018;23(10):2018-28. https://doi.org/10.1038/mp.2017.231

Thayer JF, Ahs F, Fredrikson M, Sollers JJ, 3rd, Wager TD. A meta-analysis of heart rate variability and neuroimaging studies: implications for heart rate variability as a marker of stress and health. Neurosci Biobehav Rev. 2012;36(2):747-56. https://doi.org/10.1016/j.neubiorev.2011.11.009

Thrupp N, Sala Frigerio C, Wolfs L, Skene NG, Fattorelli N, Poovathingal S, et al. Single-Nucleus RNA-Seq Is Not Suitable for Detection of Microglial Activation Genes in Humans. Cell Rep. 2020;32(13):108189. https://doi.org/10.1016/j.celrep.2020.108189

Thurston RC, Chang Y, Derby CA, Bromberger JT, Harlow SD, Janssen I, et al. Abuse and subclinical cardiovascular disease among midlife women: the study of women's health across the nation. Stroke. 2014;45(8):2246-51. https://doi.org/10.1161/STROKEAHA.114.005928

Thurston RC, Chang Y, Barinas-Mitchell E, von Kanel R, Jennings JR, Santoro N, et al. Child Abuse and Neglect and Subclinical Cardiovascular Disease Among Midlife Women. Psychosom Med. 2017;79(4):441-9. https://doi.org/10.1097/PSY.0000000000000400

Treccani G, Yigit H, Lingner T, Schleubetaner V, Mey F, van der Kooij MA, et al. Early life adversity targets the transcriptional signature of hippocampal NG2+ glia and affects voltage gated sodium (Na(v)) channels properties. Neurobiol Stress. 2021;15:100338. https://doi.org/10.1016/j.ynstr.2021.100338

Udina M, Castellvi P, Moreno-Espana J, Navines R, Valdes M, Forns X, et al. Interferon-induced depression in chronic hepatitis C: a systematic review and meta-analysis. J Clin Psychiatry. 2012;73(8):1128-38. https://doi.org/10.4088/JCP.12r07694

Usui N, Ono Y, Aramaki R, Berto S, Konopka G, Matsuzaki H, et al. Early Life Stress Alters Gene Expression and Cytoarchitecture in the Prefrontal Cortex Leading to Social Impairment and Increased Anxiety. Front Genet. 2021;12:754198. https://doi.org/10.3389/fgene.2021.754198

van der Worp HB, Howells DW, Sena ES, Porritt MJ, Rewell S, O'Collins V, et al. Can animal models of disease reliably inform human studies? PLoS Med. 2010;7(3):e1000245. https://doi.org/10.1371/journal.pmed.1000245

van Harmelen AL, van Tol MJ, van der Wee NJ, Veltman DJ, Aleman A, Spinhoven P, et al. Reduced medial prefrontal cortex volume in adults reporting childhood emotional maltreatment. Biol Psychiatry. 2010;68(9):832-8. https://doi.org/10.1016/j.biopsych.2010.06.011

van Harmelen AL, Hauber K, Gunther Moor B, Spinhoven P, Boon AE, Crone EA, et al. Childhood emotional maltreatment severity is associated with dorsal medial prefrontal cortex responsivity to social exclusion in young adults. PLoS One. 2014;9(1):e85107. https://doi.org/10.1371/journal.pone.0085107

van Harmelen AL, van Tol MJ, Dalgleish T, van der Wee NJ, Veltman DJ, Aleman A, et al. Hypoactive medial prefrontal cortex functioning in adults reporting childhood emotional maltreatment. Soc Cogn Affect Neurosci. 2014;9(12):2026-33. https://doi.org/10.1093/scan/nsu008

van Horssen J, Bo L, Vos CM, Virtanen I, de Vries HE. Basement membrane proteins in multiple sclerosis-associated inflammatory cuffs: potential role in influx and transport of leukocytes. J Neuropathol Exp Neurol. 2005;64(8):722-9. https://doi.org/10.1097/01.jnen.0000173894.09553.13

Wakim LM, Woodward-Davis A, Liu R, Hu Y, Villadangos J, Smyth G, et al. The molecular signature of tissue resident memory CD8 T cells isolated from the brain. J Immunol. 2012;189(7):3462-71. https://doi.org/10.4049/jimmunol.1201305

Walf AA, Rhodes ME, Frye CA. Antidepressant effects of ERbeta-selective estrogen receptor modulators in the forced swim test. Pharmacol Biochem Behav. 2004;78(3):523-9. https://doi.org/10.1016/j.pbb.2004.03.023

Wang H, Kan WJ, Feng Y, Feng L, Yang Y, Chen P, et al. Nuclear receptors modulate inflammasomes in the pathophysiology and treatment of major depressive disorder. World J Psychiatry. 2021;11(12):1191-205. https://doi.org/10.5498/wjp.v11.i12.1191

Wang M, Yang Y, Xu Y. Brain nuclear receptors and cardiovascular function. Cell Biosci. 2023;13(1):14. https://doi.org/10.1186/s13578-023-00962-3

Ward J, Le NQ, Suryakant S, Brody JA, Amouyel P, Boland A, et al. Polygenic risk of major depressive disorder as a risk factor for venous thromboembolism. Blood Adv. 2023;7(18):5341-50. https://doi.org/10.1182/bloodadvances.2023010562

Weaver IC, Cervoni N, Champagne FA, D'Alessio AC, Sharma S, Seckl JR, et al. Epigenetic programming by maternal behavior. Nat Neurosci. 2004;7(8):847-54. https://doi.org/10.1038/nn1276

Wegner S, Uhlemann R, Boujon V, Ersoy B, Endres M, Kronenberg G, et al. Endothelial Cell-Specific Transcriptome Reveals Signature of Chronic Stress Related to Worse Outcome After Mild Transient Brain Ischemia in Mice. Mol Neurobiol. 2020;57(3):1446-58. https://doi.org/10.1007/s12035-019-01822-3

Winkler EA, Bell RD, Zlokovic BV. Pericyte-specific expression of PDGF beta receptor in mouse models with normal and deficient PDGF beta receptor signaling. Mol Neurodegener. 2010;5:32. https://doi.org/10.1186/1750-1326-5-32

Yang AC, Vest RT, Kern F, Lee DP, Agam M, Maat CA, et al. A human brain vascular atlas reveals diverse mediators of Alzheimer's risk. Nature. 2022;603(7903):885-92. https://doi.org/10.1038/s41586-021-04369-3

Yousif LF, Di Russo J, Sorokin L. Laminin isoforms in endothelial and perivascular basement membranes. Cell Adh Migr. 2013;7(1):101-10. https://doi.org/10.4161/cam.22680

Yu C, Zhang T, Shi S, Wei T, Wang Q. Potential biomarkers: differentially expressed proteins of the extrinsic coagulation pathway in plasma samples from patients with depression. Bioengineered. 2021;12(1):6318-31. https://doi.org/10.1080/21655979.2021.1971037

Zannas AS, Wiechmann T, Gassen NC, Binder EB. Gene-Stress-Epigenetic Regulation of FKBP5: Clinical and Translational Implications. Neuropsychopharmacology. 2016;41(1):261-74. https://doi.org/10.1038/npp.2015.235

Zhang X, Wang L, Han Z, Dong J, Pang D, Fu Y, et al. KLF4 alleviates cerebral vascular injury by ameliorating vascular endothelial inflammation and regulating tight junction protein expression following ischemic stroke. J Neuroinflammation. 2020;17(1):107. https://doi.org/10.1186/s12974-020-01780-x

Zhou Y, Zhou B, Pache L, Chang M, Khodabakhshi AH, Tanaseichuk O, et al. Metascape provides a biologist-oriented resource for the analysis of systems-level datasets. Nat Commun. 2019;10(1):1523. https://doi.org/10.1038/s41467-019-09234-6

Zhou X, Franklin RA, Adler M, Carter TS, Condiff E, Adams TS, et al. Microenvironmental sensing by fibroblasts controls macrophage population size. Proc Natl Acad Sci U S A. 2022;119(32):e2205360119. https://doi.org/10.1073/pnas.2205360119

6. Tables and Figures

	CTRL (sexes pooled)	ELA (sexes pooled)
n	21	24
Sex (M/F)	13/8	17/7
Age (years)	49.10 ± 18.71	42.54 ± 14.70
Axis 1 diagnosis	0	MDD (24)
History of abuse	0	24
PMI (h)	40.32 ± 28.21	41.51 ± 22.24
Tissue pH	6.43 ± 0.31	6.58 ± 0.39

	Male CTRL	Male ELA	Female CTRL	Female ELA
n	13	17	8	7
Age (years)	41.00 ± 13.64	37.88 ± 10.18	62.25 ± 19.00	53.86 ± 18.48
Axis 1 diagnosis	0	MDD (17)	0	MDD (7)
History of abuse	0	17	0	7
PMI (h)	31.18 ± 23.43	36.18 ± 20.97	55.18 ± 30.42	54.46 ± 21.13
Tissue pH	6.51 ± 0.24	6.53 ± 0.38	6.29 ± 0.37	6.71 ± 0.39

Table 1: Demographic and sample characteristics of CTRL and ELA cohorts. Numeric values in each cell represent the mean ± SD. *MDD:* major depressive disorder, *PMI:* postmortem interval. The postmortem interval is a metric for the delay between an individual's death, the collection and processing of the brain.

Immune-related gene expression in females with ELA				
Gene	baseMean	log2FC	pvalue	padj
IFI6	808.29	-0.85	0.0003	0.0138
HLA-B	7025.47	-0.92	0.0011	0.0299
HLA-F	905.24	-0.62	0.0009	0.0262
IFI35	171.00	-0.88	0.0000	0.0002
IFIT3	701.97	-0.88	0.0000	0.0049
IRF1	488.35	-1.17	0.0004	0.0168
IRF7	162.96	-0.76	0.0014	0.0355
ISG20	153.28	-0.67	0.0022	0.0459
ISG15	291.38	-1.22	0.0000	0.0001
IRF9	726.61	-0.42	0.0003	0.0144
CD74	1945.60	-1.11	0.0001	0.0065
HLA-DMA	84.91	-1.12	0.0005	0.0198
HLA-DMB	151.62	-1.29	0.0014	0.0358
HLA-DPA1	344.01	-1.11	0.0000	0.0001
HLA-DPB1	233.66	-1.00	0.0001	0.0096
HLA-DRA	259.14	-1.33	0.0001	0.0097
TAP1	583.88	-0.86	0.0000	0.0001
TAP2	634.83	-0.53	0.0023	0.0460
CSF1	643.41	-0.77	0.0000	0.0003
IRAK1	408.95	-0.42	0.0021	0.0449
IKBKE	41.79	-1.08	0.0010	0.0284
IFNGR2	339.98	-0.51	0.0001	0.0068
TGFB1	510.19	-0.54	0.0000	0.0029
VCAM1	583.52	-1.61	0.0005	0.0189
CCRL2	41.08	-0.85	0.0021	0.0448

Table 2: A representative list of significantly downregulated genes with known immune functions in females with ELA includes genes with both pro-inflammatory and anti-inflammatory roles. This widespread downregulation of immune-related genes suggests a 'global immune suppression'.

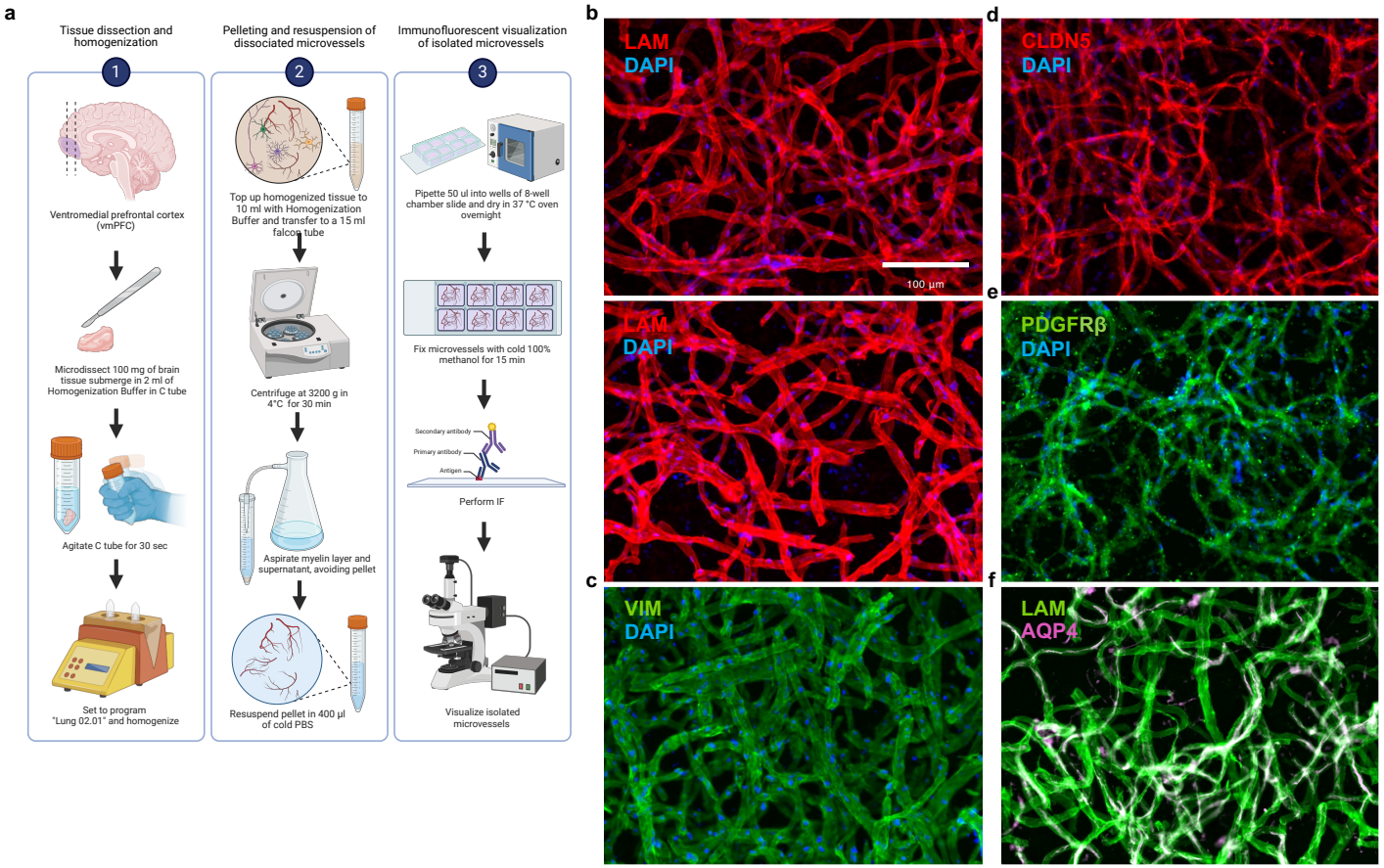
a
Tissue dissection and homogenization
Pelleting and resuspension of dissociated microvessels
Immunofluorescent visualization of isolated microvessels
1
2
3
Ventromedial prefrontal cortex (vmPFC)
Microdissect 100 mg of brain tissue submerge in 2 ml of Homogenization Buffer in C tube
Agitate C tube for 30 sec
Set to program "Lung 02.01" and homogenize
Top up homogenized tissue to 10 ml with Homogenization Buffer and transfer to a 15 ml falcon tube
Centrifuge at 3200 g in 4°C for 30 min
Aspirate myelin layer and supernatant, avoiding pellet
Resuspend pellet in 400 µl of cold PBS
Pipette 50 ul into wells of 8-well chamber slide and dry in 37 °C oven overnight
Fix microvessels with cold 100% methanol for 15 min
Secondary antibody
Primary antibody
Antigen
Perform IF
Visualize isolated microvessels
b
LAM
DAPI
100 µm
LAM
DAPI
c
VIM
DAPI
d
CLDN5
DAPI
e
PDGFRβ
DAPI
f
LAM
AQP4

Fig. 1: Effective isolation and enrichment of microvessels. a) Schematic overview of experimental workflow for isolating microvessels from postmortem brain tissue and processing for immunostaining of neurovascular markers. b) Representative micrograph of isolated microvessels immunostained with LAM (red). c) Representative micrograph of isolated microvessels immunostained with VIM (green). d) Representative micrograph of isolated microvessels immunostained with CLDN5 (red). e) Representative micrograph of isolated microvessels immunostained with PDGFRβ (green). f) Representative micrograph of isolated microvessels immunostained with LAM (green) and AQP4 (magenta). Nuclei were stained with DAPI (blue). Scale bar = 100μm and applies to all micrographs in panels b)-f).

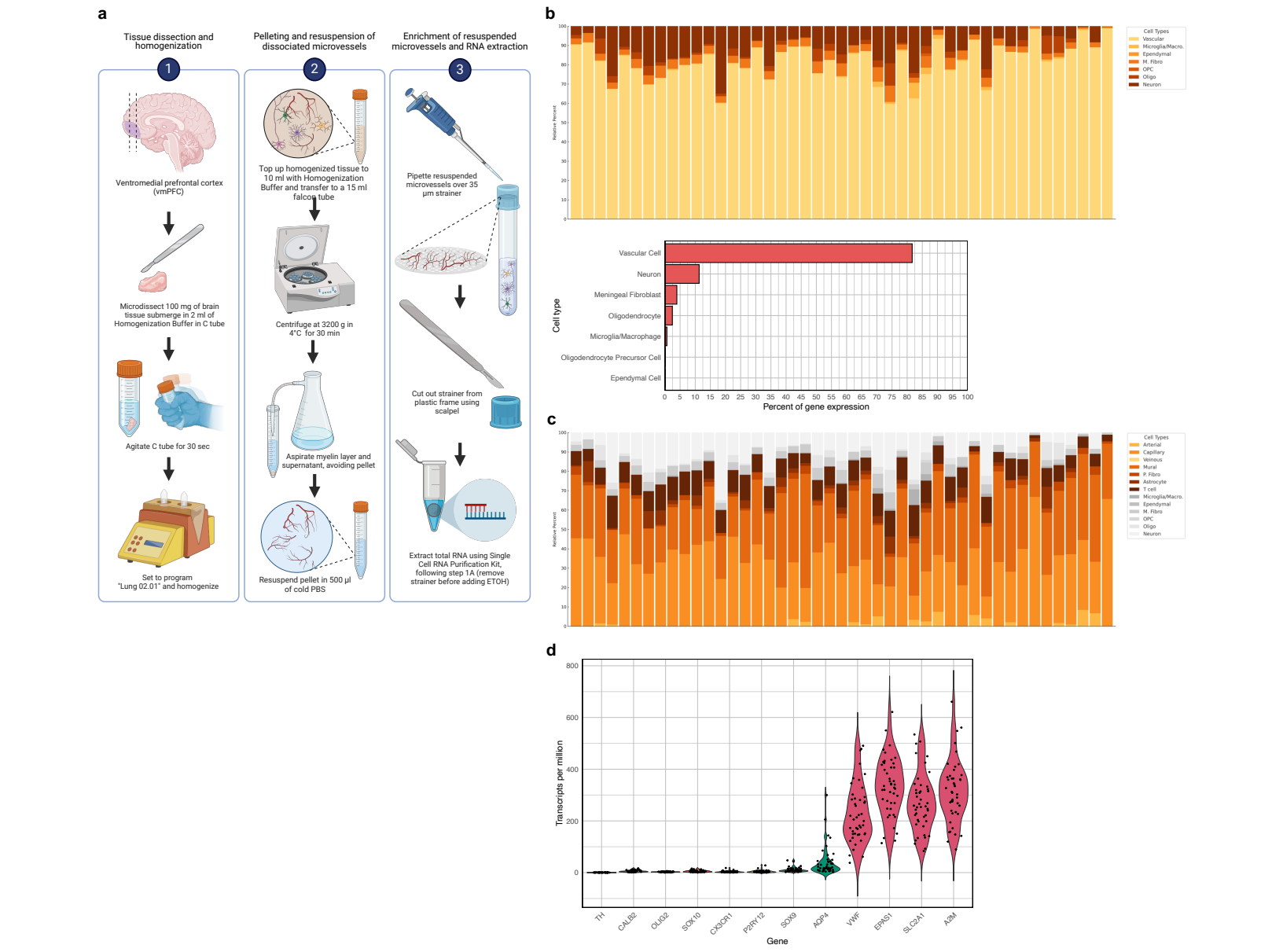
a
Tissue dissection and homogenization
1
Ventromedial prefrontal cortex (vmPFC)
Microdissect 100 mg of brain tissue submerge in 2 ml of Homogenization Buffer in C tube
Agitate C tube for 30 sec
Set to program "Lung 02.01" and homogenize
Pelleting and resuspension of dissociated microvessels
2
Top up homogenized tissue to 10 ml with Homogenization Buffer and transfer to a 15 ml falcon tube
Centrifuge at 3200 g in 4°C for 30 min
Aspirate myelin layer and supernatant, avoiding pellet
Resuspend pellet in 500 µl of cold PBS
Enrichment of resuspended microvessels and RNA extraction
3
Pipette resuspended microvessels over 35 µm strainer
Cut out strainer from plastic frame using scalpel
Extract total RNA using Single Cell RNA Purification Kit, following step 1A (remove strainer before adding ETOH)
b
Relative Percent
Cell Types
Vascular
Microglia/Macro.
Ependymal
M. Fibro
OPC
Oligo
Neuron
Cell type
Vascular Cell
Neuron
Meningeal Fibroblast
Oligodendrocyte
Microglia/Macrophage
Oligodendrocyte Precursor Cell
Ependymal Cell
Percent of gene expression
c
Relative Percent
Cell Types
Arterial
Capillary
Venous
Mural
P. Fibro
Astrocyte
T cell
Microglia/Macro.
Ependymal
M. Fibro
OPC
Oligo
Neuron
d
Transcripts per million
Gene
TH
CALB2
OLIG2
SOX10
CX3CR1
P2RY12
SOX9
AQP4
VWF
EPAS1
SLC2A1
ADM

Fig. 2: Bulk RNA sequencing and bioinformatic deconvolution of isolated microvessels. a) Schematic overview of experimental workflow for isolating microvessels from postmortem brain tissue and processing library construction and bulk RNA sequencing. b) Deconvolution of sequenced microvessel samples was performed via CIBERSORTX algorithm. Top: Bar plot showing cumulative percentage of neurovascular gene expression across sequenced subjects. Bottom: Bar plot displaying the percentage of neurovascular gene expression averaged across sequenced subjects, as well as percentages of non-neurovascular cell types averaged across sequenced subjects. These data highlight the significant enrichment of neurovascular cells within the microvessel RNA sequencing data. c) Bar chart showing significant enrichment of genes associated with capillary and mural cells, compared to those of arterial and venous endothelial cells. This pattern underscores the selective enrichment of microvessels, as opposed to larger diametre vessels along the arteriovenous axis. d) Transcript Per Million (TPM) values for different cell type-defining genes, demonstrating a predominance of neurovascular cell transcripts, particularly endothelial markers, in contrast to minimal expression of non-vascular markers, underscoring the effective capture of the neurovascular unit.

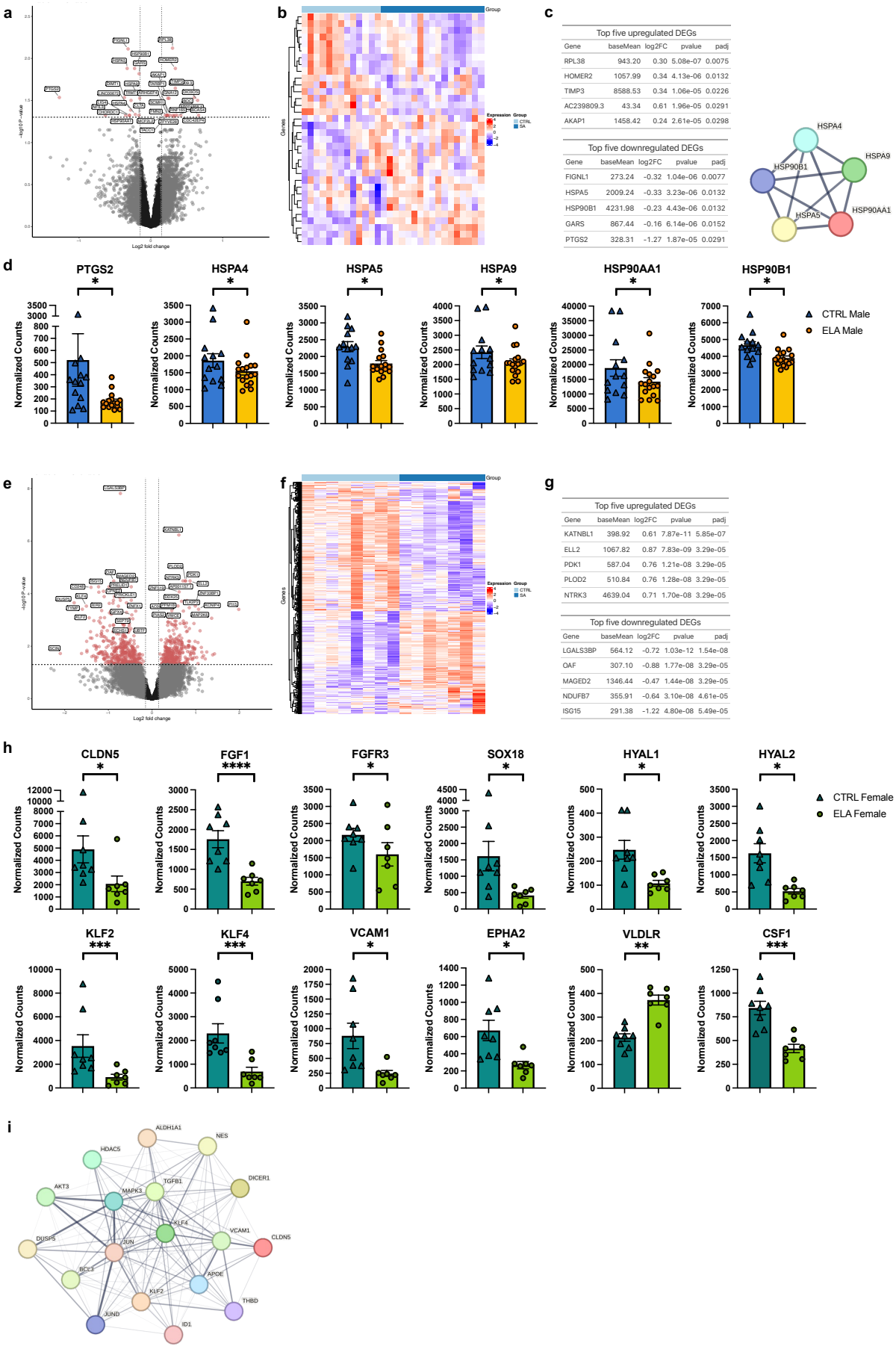
a
b
Group
Genes
Expression
CTRL
SA
c
Top five upregulated DEGs
Gene baseMean log2FC pvalue padj
RPL38 943.20 0.30 5.08e-07 0.0075
HOMER2 1057.99 0.34 4.13e-06 0.0132
TIMP3 8588.53 0.34 1.06e-05 0.0226
AC239809.3 43.34 0.61 1.96e-05 0.0291
AKAP1 1458.42 0.24 2.61e-05 0.0298
Top five downregulated DEGs
Gene baseMean log2FC pvalue padj
FIGNL1 273.24 -0.32 1.04e-06 0.0077
HSPA5 2009.24 -0.33 3.23e-06 0.0132
HSP90B1 4231.98 -0.23 4.43e-06 0.0132
GARS 867.44 -0.16 6.14e-06 0.0152
PTGS2 328.31 -1.27 1.87e-05 0.0291
HSPA4
HSPA9
HSP90B1
HSPA5
HSP90AA1
d
PTGS2
HSPA4
HSPA5
HSPA9
HSP90AA1
HSP90B1
Normalized Counts
CTRL Male
ELA Male
e
Log2 fold change
f
g
Top five upregulated DEGs
Gene baseMean log2FC pvalue padj
KATNBL1 398.92 0.61 7.87e-11 5.85e-07
ELL2 1067.82 0.87 7.83e-09 3.29e-05
PDK1 587.04 0.76 1.21e-08 3.29e-05
PLOD2 510.84 0.76 1.28e-08 3.29e-05
NTRK3 4639.04 0.71 1.70e-08 3.29e-05
Top five downregulated DEGs
Gene baseMean log2FC pvalue padj
LGALS3BP 564.12 -0.72 1.03e-12 1.54e-08
OAF 307.10 -0.88 1.77e-08 3.29e-05
MAGED2 1346.44 -0.47 1.44e-08 3.29e-05
NDUFB7 355.91 -0.64 3.10e-08 4.61e-05
ISG15 291.38 -1.22 4.80e-08 5.49e-05
h
CLDN5
FGF1
FGFR3
SOX18
HYAL1
HYAL2
KLF2
KLF4
VCAM1
EPHA2
VLDLR
CSF1
Normalized Counts
CTRL Female
ELA Female
i
ALDH1A1
NES
HDAC5
DICER1
AKT3
MAPK3
TGFB1
KLF4
VCAM1
CLDN5
DUSP5
JUN
BCL3
APOE
KLF2
THBD
JUND
ID1

Fig. 3: DGE of CTRL versus ELA for male and female microvessels, respectively. a) Volcano plot showing the results from differential gene expression analysis between male CTRL and ELA groups, performed using DESeq2. Data points represent individual genes, with significance determined by adjusted p-value (padj) < 0.05 and absolute log2 fold change > log2(1.1). Genes above the threshold line are significantly differentially expressed. b) Heatmap showing the results from differential gene expression analysis between male CTRL and ELA groups, performed using DESeq2. Each row represents a gene, and the color intensity corresponds to the magnitude of log2 fold change, with red indicating upregulation and blue indicating downregulation. The heatmap is organized to display genes meeting the significance criteria of adjusted p-value (padj) < 0.05 and |log2(fold change)| > log2(1.1). The clustering tree alongside the heatmap categorizes genes based on the similarities in their expression changes, effectively grouping genes with similar expression patterns together. c) Tables displaying the top 5 upregulated (top) and top 5 downregulated (bottom) DEGs for males, indicating their gene names, log2 fold changes, and adjusted p-values. d) Bar plots showcasing selected DEGs in males. Normalized counts for PTGS2, HSPA4, HSPA5, HSPA9, HSP90AA1, and HSP90B1 show a downregulation in the male ELA group compared to the male CTRL group. (*: $p < 0.05$; **: $p < 0.01$; ***: $p < 0.001$; ****: $p < 0.0001$). e) Volcano plot showing the results from differential gene expression analysis between female CTRL and ELA groups, performed using DESeq2. Data points represent individual genes, with significance determined by adjusted p-value (padj) < 0.05 and absolute log2 fold change > log2(1.1). Genes above the threshold line are significantly differentially expressed. f) Heatmap showing the results from differential gene expression analysis between female CTRL and ELA groups, performed using DESeq2. Each row represents a gene, and the color intensity corresponds to the magnitude of log2 fold change, with red indicating upregulation and blue indicating downregulation. The heatmap is organized to display genes meeting the significance criteria of adjusted p-value (padj) < 0.05 and |log2(fold change)| > log2(1.1). The clustering tree alongside the heatmap categorizes genes based on the similarities in their expression changes, effectively grouping genes with similar expression patterns together. g) Tables displaying the top 5 upregulated (top) and top 5 downregulated (bottom) DEGs for females, indicating their gene names, log2

fold changes, and adjusted p-values. h) Bar plots showcasing normalized counts for selected DEGs in females, namely CLDN5, FGF1, FGFR3, SOX18, HYAL1, HYAL2, KLF2, KLF4, VCAM1, EPHA2, VLDLR, and CSF1. (*: $p < 0.05$; **: $p < 0.01$; ***: $p < 0.001$; ****: $p < 0.0001$). STRING analysis reveals DEGs shown in g) are involved in a network of protein-protein interactions. i) STRING analysis for KLF2 and KLF4, both identified as DEGs in females, demonstrates their interaction with other female DEGs.

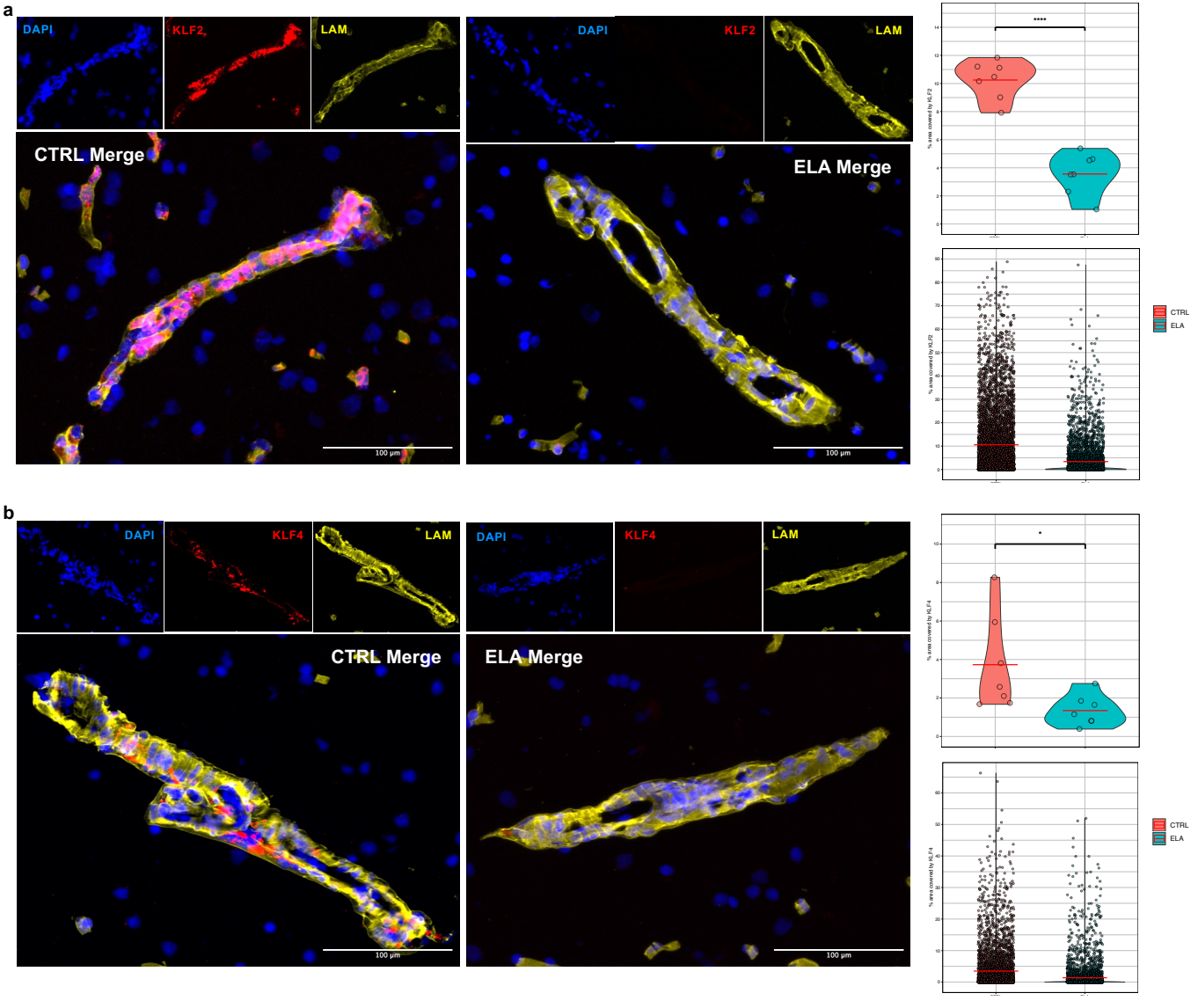
a
DAPI
KLF2
LAM
CTRL Merge
100 µm
DAPI
KLF2
LAM
ELA Merge
100 µm
****
% area covered by KLF2
CTRL
ELA
b
DAPI
KLF4
LAM
CTRL Merge
100 µm
DAPI
KLF4
LAM
ELA Merge
100 µm
*
% area covered by KLF4
CTRL
ELA

Fig. 4: In situ validation of decreased KLF2 and KLF4 expression in grey matter microvessels of females with ELA compared to female CTRLs. a) Representative images of FISH for KLF2 (red) expression in CTRL (left) and ELA (right) microvessels (*LAM*+ cells, yellow). Nuclei were counterstained with DAPI (blue). Scale bar = 100 µm. Mean microvessel expression of KLF2 is significantly reduced in females with ELA ($p = 7.45 \times 10^{-7}$). This is further demonstrated by the distribution of individual data points for KLF2 expression across the two groups, with a higher percent of microvessel area covered by KLF2 in the CTRL group compared to the ELA group. b) Representative images of FISH for KLF4 (red) expression in CTRL (left) and ELA (right) microvessels (*LAM*+ cells, yellow). Nuclei were counterstained with DAPI (blue). Scale bar = 100 µm. Mean microvessel expression of KLF4 is significantly reduced in females with ELA ($p = 0.023$). This is further demonstrated by the distribution of individual data points for KLF2 expression across the two groups, with a higher percent of microvessel area covered by KLF4 in the CTRL group compared to the ELA group.

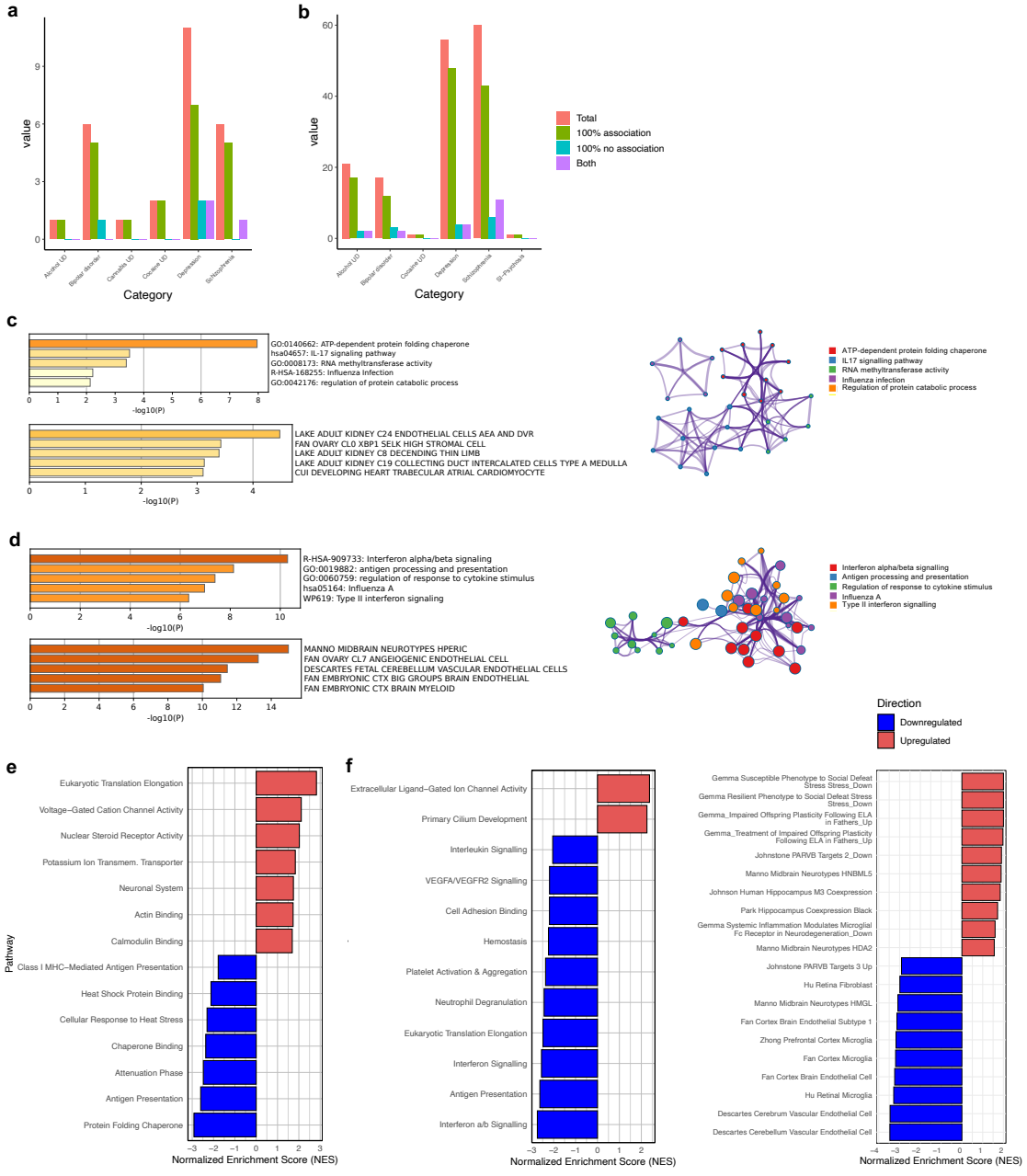
a
value
Category
Alcohol UD
Bipolar disorder
Cannabis UD
Cocaine UD
Depression
Schizophrenia
b
Total
100% association
100% no association
Both
SI-Psychosis
c
GO:0140662: ATP-dependent protein folding chaperone
hsa04657: IL-17 signaling pathway
GO:0008173: RNA methyltransferase activity
R-HSA-168255: Influenza Infection
GO:0042176: regulation of protein catabolic process
-log10(P)
LAKE ADULT KIDNEY C24 ENDOTHELIAL CELLS AEA AND DVR
FAN OVARY CL0 XBP1 SELK HIGH STROMAL CELL
LAKE ADULT KIDNEY C8 DECENDING THIN LIMB
LAKE ADULT KIDNEY C19 COLLECTING DUCT INTERCALATED CELLS TYPE A MEDULLA
CUI DEVELOPING HEART TRABECULAR ATRIAL CARDIOMYOCYTE
ATP-dependent protein folding chaperone
IL17 signalling pathway
RNA methyltransferase activity
Influenza infection
Regulation of protein catabolic process
d
R-HSA-909733: Interferon alpha/beta signaling
GO:0019882: antigen processing and presentation
GO:0060759: regulation of response to cytokine stimulus
hsa05164: Influenza A
WP619: Type II interferon signaling
MANNO MIDBRAIN NEUROTYPES HPERIC
FAN OVARY CL7 ANGEIOGENIC ENDOTHELIAL CELL
DESCARTES FETAL CEREBELLUM VASCULAR ENDOTHELIAL CELLS
FAN EMBRYONIC CTX BIG GROUPS BRAIN ENDOTHELIAL
FAN EMBRYONIC CTX BRAIN MYELOID
Interferon alpha/beta signalling
Antigen processing and presentation
Regulation of response to cytokine stimulus
Influenza A
Type II interferon signalling
Direction
Downregulated
Upregulated
e
Pathway
Eukaryotic Translation Elongation
Voltage–Gated Cation Channel Activity
Nuclear Steroid Receptor Activity
Potassium Ion Transmem. Transporter
Neuronal System
Actin Binding
Calmodulin Binding
Class I MHC–Mediated Antigen Presentation
Heat Shock Protein Binding
Cellular Response to Heat Stress
Chaperone Binding
Attenuation Phase
Antigen Presentation
Protein Folding Chaperone
Normalized Enrichment Score (NES)
f
Extracellular Ligand–Gated Ion Channel Activity
Primary Cilium Development
Interleukin Signalling
VEGFA/VEGFR2 Signalling
Cell Adhesion Binding
Hemostasis
Platelet Activation & Aggregation
Neutrophil Degranulation
Eukaryotic Translation Elongation
Interferon Signalling
Antigen Presentation
Interferon a/b Signalling
Normalized Enrichment Score (NES)
Gemma Susceptible Phenotype to Social Defeat Stress Stress_Down
Gemma Resilient Phenotype to Social Defeat Stress Stress_Down
Gemma_Impaired Offspring Plasticity Following ELA in Fathers_Up
Gemma_Treatment of Impaired Offspring Plasticity Following ELA in Fathers_Up
Johnstone PARVB Targets 2_Down
Manno Midbrain Neurotypes HNBML5
Johnson Human Hippocampus M3 Coexpression
Park Hippocampus Coexpression Black
Gemma Systemic Inflammation Modulates Microglial Fc Receptor in Neurodegeneration_Down
Manno Midbrain Neurotypes HDA2
Johnstone PARVB Targets 3 Up
Hu Retina Fibroblast
Manno Midbrain Neurotypes HMGL
Fan Cortex Brain Endothelial Subtype 1
Zhong Prefrontal Cortex Microglia
Fan Cortex Microglia
Fan Cortex Brain Endothelial Cell
Hu Retinal Microglia
Descartes Cerebrum Vascular Endothelial Cell
Descartes Cerebellum Vascular Endothelial Cell
Normalized Enrichment Score (NES)

Fig. 5: Functional annotation and enrichment in male and female DEGs. a-b) Bar plot displaying the number of gene-disease associations for psychiatric disorders in a) male DEGs and b) female DEGs, queried via the PsyGeNET database. c-d) Top results for (top left) functional annotation and (bottom left) cell-type enrichment of c) male and d) female DEGs were conducted using Metascape. (Bottom) The resultant clusters are represented in a network plot where nodes represent enriched terms and edges represent relationships between terms (right). Terms with a p-value < 0.05, a minimum count of 3, and an enrichment factor > 1.5 were considered significant. e-f) Results from fGSEA in e) males and f) females, referencing (left) merged data from Reactome, Gene Ontology Molecular Function (GOMF), KEGG, and WikiPathways (WP) and (right) curated gene lists from Brain.GMT. Upregulated pathways are indicated in red, while downregulated pathways are shown in blue, each according to their Normalized Enrichment Score (NES).

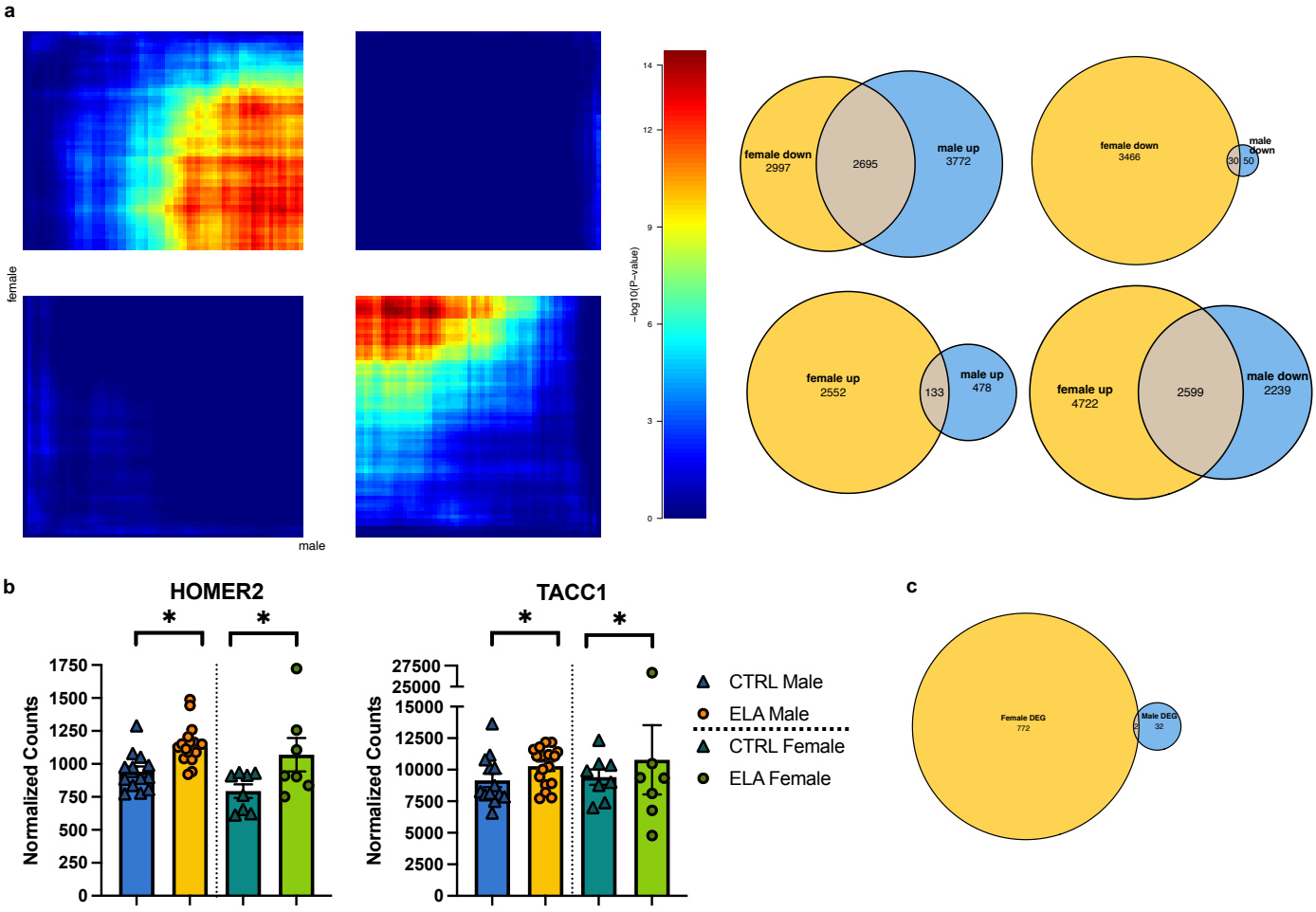
a
female
male
−log10(P-value)
14
12
9
6
3
0
female down
2997
2695
male up
3772
female down
3466
male down
30
50
female up
2552
133
male up
478
female up
4722
2599
male down
2239
b
HOMER2
TACC1
Normalized Counts
1750
1500
1250
1000
750
500
250
0
27500
25000
15000
12500
10000
7500
5000
2500
CTRL Male
ELA Male
CTRL Female
ELA Female
c
Female DEG
772
Male DEG
32

Fig. 6: Comparative analysis of male and female DEGs. a) (Left) Hypergeometric heatmap from RRHO analysis comparing transcriptional changes between males and females with ELA. (Right) Corresponding Venn diagrams demonstrating the number of genes with shared or distinct directional changes between the two sexes. b) Bar plots showing the differential expression of HOMER2 and TACC1 between CTRL and ELA groups for both males and females. (*: $p < 0.05$). c) Venn diagram showing that only two genes (HOMER2 and TACC1) are shared DEGs between males and females with ELA.

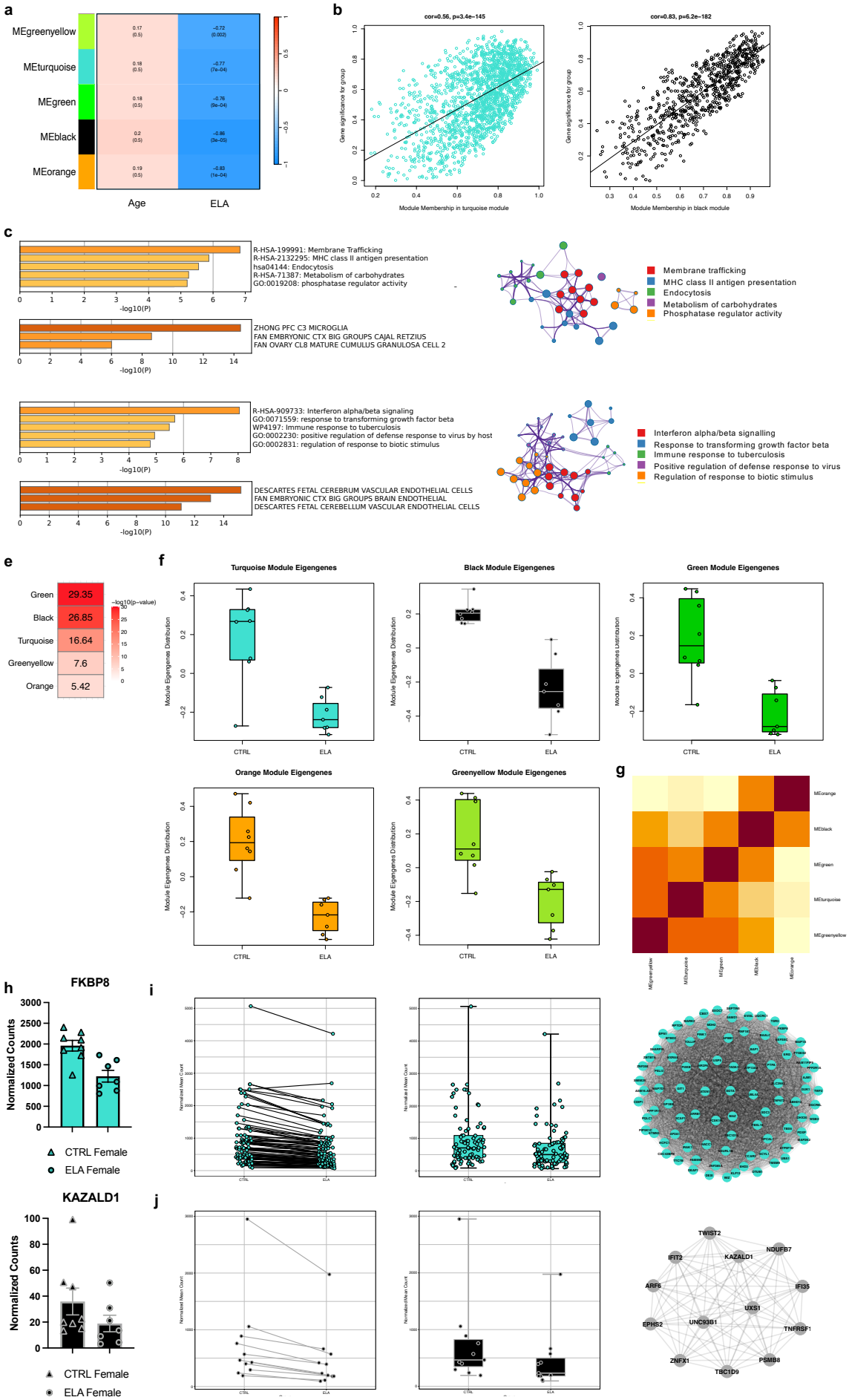
a
MEgreenyellow
MEturquoise
MEgreen
MEblack
MEorange
Age
ELA
b
cor=0.56, p=3.4e−145
Gene significance for group
Module Membership in turquoise module
cor=0.83, p=6.2e−182
Module Membership in black module
c
R-HSA-199991: Membrane Trafficking
R-HSA-2132295: MHC class II antigen presentation
hsa04144: Endocytosis
R-HSA-71387: Metabolism of carbohydrates
GO:0019208: phosphatase regulator activity
-log10(P)
ZHONG PFC C3 MICROGLIA
FAN EMBRYONIC CTX BIG GROUPS CAJAL RETZIUS
FAN OVARY CL8 MATURE CUMULUS GRANULOSA CELL 2
Membrane trafficking
MHC class II antigen presentation
Endocytosis
Metabolism of carbohydrates
Phosphatase regulator activity
R-HSA-909733: Interferon alpha/beta signaling
GO:0071559: response to transforming growth factor beta
WP4197: Immune response to tuberculosis
GO:0002230: positive regulation of defense response to virus by host
GO:0002831: regulation of response to biotic stimulus
DESCARTES FETAL CEREBRUM VASCULAR ENDOTHELIAL CELLS
FAN EMBRYONIC CTX BIG GROUPS BRAIN ENDOTHELIAL
DESCARTES FETAL CEREBELLUM VASCULAR ENDOTHELIAL CELLS
Interferon alpha/beta signalling
Response to transforming growth factor beta
Immune response to tuberculosis
Positive regulation of defense response to virus
Regulation of response to biotic stimulus
e
Green
Black
Turquoise
Greenyellow
Orange
29.35
26.85
16.64
7.6
5.42
−log10(p−value)
f
Turquoise Module Eigengenes
Black Module Eigengenes
Green Module Eigengenes
Orange Module Eigengenes
Greenyellow Module Eigengenes
Module Eigengenes Distribution
CTRL
ELA
g
MEorange
MEblack
MEgreen
MEturquoise
MEgreenyellow
h
FKBP8
Normalized Counts
CTRL Female
ELA Female
i
Normalized Mean Count
KAZALD1
j
TWIST2
NDUFB7
IFIT2
KAZALD1
ARF6
IFI35
UXS1
EPHS2
UNC93B1
TNFRSF1
ZNFX1
PSMB8
TBC1D9

Fig. 7: Assessing networks of gene co-expression and ELA using data specifically from females. a) (Left) Plot showing the five WGCNA modules (greenyellow, turquoise, green, black, orange) with significant correlation (coefficients greater than 0.7) with ELA in females. Modules with negative correlation values are shown in blue, indicating their inverse relationship with ELA. b) Scatter plots for module membership versus gene significance for turquoise (cor = 0.56, p = 3.4×10−145), black (cor = 0.83, p = 6.2×10−182), and greenyellow (cor = 0.72, p = 1.2×10−181) modules. c-d) Top results for (Top left) functional annotation and (bottom left) cell-type enrichment of c) turquoise and d) black modules were conducted using Metascape. (Right) The resultant clusters are represented in a network plot where nodes represent enriched terms and edges represent relationships between terms. Terms with a p-value < 0.05, a minimum count of 3, and an enrichment factor > 1.5 were considered significant. e) Fisher's Exact Test was performed via GeneOverlap to assess genes common between female DEGs and the turquoise, black, green, greenyellow, and orange modules. f) Box and whisker plots showing median eigengene values across turquoise, black, green, orange and greenyellow modules between CTRL and ELA females. g) Correlation plot between the eigengenes of the turquoise, black, green, orange and greenyellow modules. h) (Top) Bar plots showing normalized counts for turquoise top hub gene FKBP8 and black top hub gene KAZALD1 between CTRL and ELA females. i-j) (Left) scatter plot showing i) turquoise and j) black hub genes between CTRL and ELA females. (Middle) Box and whisker plots showing i) turquoise and j) black hub genes between CTRL and ELA females. (Right) Network plots of i) turquoise and j) black hub genes.

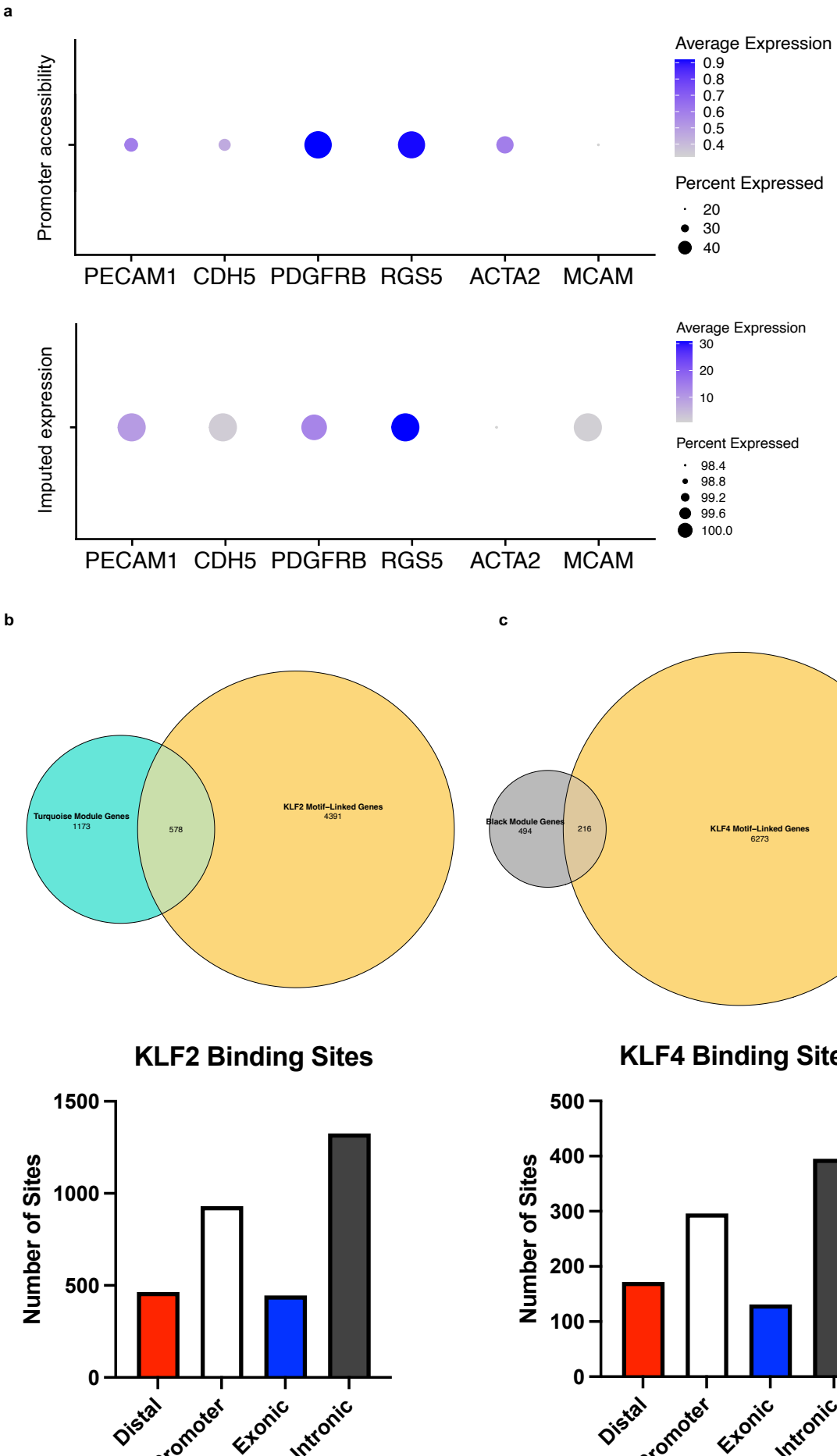
a
Promoter accessibility
PECAM1
CDH5
PDGFRB
RGS5
ACTA2
MCAM
Average Expression
0.9
0.8
0.7
0.6
0.5
0.4
Percent Expressed
20
30
40
Imputed expression
PECAM1
CDH5
PDGFRB
RGS5
ACTA2
MCAM
Average Expression
30
20
10
Percent Expressed
98.4
98.8
99.2
99.6
100.0
b
Turquoise Module Genes
1173
578
KLF2 Motif–Linked Genes
4391
c
Black Module Genes
494
216
KLF4 Motif–Linked Genes
6273
KLF2 Binding Sites
Number of Sites
1500
1000
500
0
Distal
Promoter
Exonic
Intronic
KLF4 Binding Sites
Number of Sites
500
400
300
200
100
0
Distal
Promoter
Exonic
Intronic

Fig. 8: Identification of turquoise and black module genes motif-linked to KLF2 and KLF4, respectively. a) (Top) Promoter accessibility across key endothelial (PECAM1, CDH5), pericyte (PDGFRB, RGS5) and smooth muscle cell (ACTA2, MCAM) markers in the vascular cluster from ATACseq data (Chawla et al., 2024). Average expression indicates the average chromatin accessibility score for the promoter region (where the promoter region is defined as within 2kbp from gene transcription start site) of the listed genes in the vascular cluster. Percent expressed indicates the percentage of cells within the vascular cluster where the promoter region of these genes are accessible. (Bottom) Imputed expression of key endothelial (PECAM1, CDH5), pericyte (PDGFRB, RGS5) and smooth muscle cell (ACTA2, MCAM) markers in the vascular cluster from single nuclei RNA sequencing data (Chawla et al., 2024). Average expression indicates the average count for the gene and percent expressed indicates the percentage of cells within the vascular cluster that expression the gene. These results show a high expression across the cluster, indicating a mixed cell population with higher proportions of endothelial cells and pericytes. Expression was imputed cell-type wise, so vascular cluster snRNA data was integrated with vascular cluster snATAC data. b) (Top) Venn diagram showing overlap between KLF2 motif-linked genes and turquoise module genes, (Bottom) Bar plot showing the cumulative number of KLF2 binding sites found at distal, promoter, exonic, and intronic regions across the 577 turquoise genes with KLF2 binding sites. c) (Top) Venn diagram showing overlap between KLF4 motif-linked genes and turquoise module genes, (Bottom) Bar plot showing the cumulative number of KLF4 binding sites found at distal, promoter, exonic, and intronic regions across the 216 turquoise genes with KLF4 binding sites.

I am still learning

Michelangelo di Lodovico Buonarroti Simoni
Renaissance artist

Chapter IV: Discussion & Concluding Remarks

Preface to the discussion

In this chapter, I summarize our findings from the two studies describing NVU-specific gene expression differences observed in those with a history of ELA and discuss them in the context of previous literature. Finally, I mention some of the limitations of the research presented in this dissertation and indicate possible future directions of research that could build upon these data and further close the gaps that remain in our knowledge. I end with a brief conclusion connecting our work back to the rationale and need for molecular studies of the NVU in ELA.

Summary of key findings

Clinical and epidemiological evidence suggests that a history of childhood abuse significantly increases lifetime risk for stress-induced pathologies (Afifi et al., 2008; Bernet and Stein, 1999; Brown et al., 2009; Danese et al., 2009; Dube et al., 2003; Felitti et al., 1998; Gilbert et al., 2009; Mullen et al., 1996; Springer et al., 2007). Indeed, there is a large body of literature establishing a strong link between childhood abuse, psychiatric disorder, and suicidal behaviour (Afifi et al., 2008; Brezo et al., 2007; Brezo et al., 2008; Dube et al., 2001; Fergusson et al., 2000; Molnar et al., 2001). During childhood, postnatal brain development is characterized by the brain being 'experience-expectant.' This phase is marked by sensitive periods that allow the brain to leverage environmental cues to adapt to the demands of its surroundings and enhance survival prospects (Bick and Nelson, 2016; Magill et al., 2013; Tau and Peterson, 2010). This adaptability facilitates the development of increasingly complex cognitive functions, not solely dependent on genetic factors. However, this heightened sensitivity also makes the brain vulnerable to adverse experiences, such as ELA. While structural and functional changes in several brain regions across species have been implicated in the long-term effects of ELA, the proximal consequences and molecular disturbances sustained into adulthood remain unclear. Importantly, it may not only be the brain parenchyma that is affected; the neurosupportive systems, particularly the NVU, may

also experience significant changes. Long-accumulating evidence of cardiovascular abnormalities, indicative of broad vascular and endothelial dysfunction, in those with a history of ELA raises the question of whether similar neurovascular dysfunction may contribute to the phenotype presented by this clinical population. Dysfunction within the NVU can be detrimental to long-term health outcomes, as the NVU plays a fundamental role in maintaining cerebral blood flow, barrier integrity, and the microenvironment that supports neuronal function (Daneman and Prat, 2015; Kadry et al., 2020; Luissint et al., 2012). In addition, differences in NVU dysfunction due to sex are critical to understanding the enduring effects of ELA (Solarz et al., 2021; Dion-Albert et al., 2022), yet sex as a variable is often overlooked in studies investigating either animal proxy models or postmortem brain tissue.

Over the years, the animal literature has played a fundamental role in identifying molecular programs that are altered by ELA, as well as how dysregulation of these programs might impact cognitive, emotional and behavioural traits. While these investigations have advanced our understanding of ELA, they do not entirely recapitulate the complex effects of childhood abuse on human biology. Postmortem human brain research is, therefore, needed to further our understanding. The aim of this dissertation was to, therefore, add to the postmortem literature by examining the long-term impacts of childhood abuse on neurovascular transcriptomic programs in the vmPFC, a region involved in the regulation of mood, emotion and decision making that has been implicated in mediating the effects of chronic stress. In our first study, we make an argument for how neurovascular changes are a feature of numerous neurological diseases and psychiatric disorders, often linked to changes in BBB integrity and neuroinflammatory responses, and how current research is hindered by the lack of reliable methods to target brain microvessels, especially from frozen samples typically available in biobanks. We put forth a standardized protocol that allows for the isolation of microvessels in high yield from frozen brain tissues, preserving their structural integrity and multicellular composition. We demonstrate effective microvessel isolation from both frozen mouse and human brain tissue, which was tested on four different regions of the human brain: the vmPFC, dlPFC (Brodmann area 8/9), hippocampus

(Brodmann area 28) as well as the primary visual cortex (Brodmann area 17). In great detail, we describe the steps required to prepare frozen vmPFC samples followed by tissue dissociation, selective enrichment for microvessels and, finally, isolation. We also describe how to prepare samples of isolated microvessels for bulk RNA sequencing and LC-MS/MS and thoroughly characterize the transcriptomic and proteomic landscapes of the NVU. We believe that this method will have a lasting impact on the research community by facilitating, for the first time, comprehensive multiomic analyses of the NVU's role in health and disease.

For our next study we leveraged the microvessel isolation method that we developed to generate the first neurovascular-specific transcriptomic dataset derived from intact microvessels isolated from vmPFC samples from depressed suicides with a history of ELA. By sequencing the structurally preserved unit that not only consists of nuclei, but also cell membranes, cytoplasm and the interstitium, our data synthesis provides a holistic snapshot of the NVU, revealing cumulative expression changes in genes that are often commonly expressed across neurovascular cell types. We reported that ELA is indeed associated with major neurovascular changes in the vmPFC; our findings highlight significant sex-specific differences, with females exhibiting more pronounced neurovascular dysfunction compared to males. What was particularly striking was the downregulation of key vascular regulatory genes, such as transcription factors KLF2 and KLF4, both of which are critical for maintaining vascular biology and endothelial function. Based on gene expression correlations, KLF2 and KLF4 were identified in respective modules strongly correlated with ELA. Both transcription factors showed a strong presence of their respective binding motifs across genes found within these modules. Specifically, 33% of the turquoise module was motif-linked to KLF2, and 30% of the black module was motif-linked to KLF4, emphasizing their potential role in regulating neurovascular transcriptional programs implicated in ELA. Downregulated KLF2 and KLF4 were validated by *in situ* quantification of KLF2 and KLF4 expression using FISH in female subjects affected by ELA. Additionally, our study found a widespread downregulation of immune-related genes, both pro- and anti- inflammatory in nature. This body of work advances our understanding of the molecular mechanisms

underpinning the neurobiological consequences of ELA but also implicate significant links between neurovascular changes and the development of psychiatric disorders, particularly MDD, in individuals with ELA histories.

Integration of key findings

Sex-dependent differences in NVU integrity and function

Knowledge of sex-dependent (moreover, sex-by-region-dependent) differences in normal NVU integrity and function, as well as their potential alteration by ELA is limited. To date, the majority of studies exclusively characterize male ELA signatures (Short et al., 2023; Eck et al., 2022; Reemst et al., 2022; Kos et al., 2023; Treccani et al., 2021; Rentscher et al., 2022; Wegner et al., 2020; Savignac et al., 2011; Bath et al., 2016). In contrast, fewer studies include females (Edelmann et al., 2023; Parel et al., 2023; Barrett et al., 2021), although it is females who shoulder a disproportionate burden for developing stress-induced pathologies (Goodwill et al., 2019). An elegant single-cell RNA sequencing study (Brivio et al., 2023) demonstrated that while both male and female mice displayed several DEGs in response to stress, only a small percentage of these genes were common to both sexes, and that female mice displayed a higher number of DEGs, indicating that the molecular mechanisms underlying the stress response are largely sex-specific. The same sex difference was reflected specifically by prefrontal BMECs from male and female mice subjected to chronic stress, showing not only poor overlap in changes but pervasive changes in female mice alone (Dion-Albert et al., 2022).

But what factors might contribute to—or at the very least influence—the pronounced sex differences observed in our study, where the female NVU is significantly more affected? One notable study (Solarz et al., 2021) revealed that, at baseline, adult females displayed a less permeable blood-brain barrier (BBB) and higher expression of tight junction proteins in the mPFC compared to males, a finding that aligns with our observations in our data and is suggestive of inherent differences between the male and female NVU. Several lines of evidence suggest that sex differences in vascular

diseases as well as psychiatric disorders may arise, in part, by gonadal hormones. Estrogen and androgens, the principal sex hormones, have profound effects on learning (Singh et al., 1994; Lacreuse et al., 2000), memory (Phan et al., 2012; Jacome et al., 2016) and mood (Luca et al., 2020, Maartens et al., 2002; Bekku et al., 2006; Gordon et al., 2016; de Chaves et al., 2009; Li et al., 2014; Schoenrock et al., 2016). Estrogen receptors are highly expressed on BMECs (Zuloaga et al., 2012) and promoter regions of genes encoding tight junction proteins contain estrogen response elements (Burek et al., 2014). Interestingly, ESR1, a receptor known to contribute to healthy vascular functions (Miller and Duckles, 2008), was identified as the top upstream regulator in genes differentially expressed after chronic stress and associated with a pro-resilient behavioral signature (Lorsch et al., 2018). Estrogen evidently modulates the NVU, as premenopausal women have a lower cardiovascular risk compared to men (Groban et al., 2016); however, the prevalence of heart diseases and stroke nearly doubles in women after menopause, when estradiol levels drop by approximately 60% (Rannevik et al., 1995). Moreover, studies have shown that BBB function is impaired in ovariectomized and reproductively senescent female rats, a condition that can be reversed with 17β-estradiol treatment (Bake & Sohrabji, 2004; Kang et al., 2006; Saija et al., 1990; Shi & Simpkins, 1997; Shi et al., 1997). These uniquely female traits, along with other elements of sexual dimorphism at the NVU may be particularly vulnerable to ELA and may result in changes in BBB transport efficiency, permeability and cell type composition. Conversely, higher levels of androgens have been shown to increase the prevalence of androgen receptor-positive cells in both male and female mice, influencing sex-dependent DEGs across tissues (Li et al., 2024), suggesting that androgens and their receptors may provide protective benefits for males with a history of ELA. Given the profound implications these findings suggest about the differential impacts of ELA on the NVU according to sex, continued research is crucial to better understand and address the nuances of NVU modulation by ELA.

Mechanisms underlying latent ELA-induced impacts on the adult NVU

Although it is generally accepted that ELA experienced during sensitive periods disrupts the normal developmental trajectories of multiple systems, it is not immediately clear

why its effects would manifest in adulthood and impact health decades later. It is even less clear why risk factors conferred by the early environment appear to remain latent until adulthood. Within the framework of allostatic overload, the cost of responding to early life stress is seen in compromised stress-related biological systems that potentially lose their resilience (Taylor et al., 2004). As these systems continue to operate in a stressful environment, the likelihood increases over time for these no longer resilient systems to become dysregulated and functionally impaired. The impacted NVU is further exacerbated by—and also interacts with—the aging process (Solarz et al., 2021; Verheggen et al., 2020**;** Senatorov et al., 2019**;** Montagne et al., 2015). Put succinctly, the allostatic effects of early life events act as initial hits to the neurovascular system, with aging providing a subsequent hit that leads to dysfunction. When taking sex differences into consideration, these impacts may be more pronounced in females. The question remains, how is this possible? Epigenetics represents a collection of gene regulatory processes through which early environmental influences can have sustained effects in adulthood. Epigenetic mechanisms do not change the DNA sequence, but together determine chromatin conformation and transcriptional accessibility via modifications at multiple levels of the genome, from the residues themselves (DNA methylation) to nucleosomes (posttranslational histone modifications), regulatory transcripts (ncRNAs), and chromatin interactions (long range chromatin loops; Lieberman-Aiden et al., 2009). It is well established that these epigenetic mechanisms are critical for the experience-dependent events that occur during postnatal development, where the genome is particularly sensitive to environmental cues (Teicher et al., 2016), allowing the environment to dynamically modulate gene expression, even in postmitotic neurons (Duncan et al., 2014; Levenson et al., 2006). Epigenetic processes such as DNA methylation, histone post-translational modifications, and non-coding RNA expression have all been shown to be impacted by ELA and may contribute to persistent NVU dysfunction in adults. Additionally, recent findings emphasize the importance of Long-Lived RNAs in this regulatory landscape. *In vivo* pulse-chase labeling with a modified uridine analog, ethynyl uridine, to track RNA stability in the brain has identified certain RNAs that possess turnover rates in the magnitude of years within the nuclei of neurons, radial glia-like adult neural stem cells,

adult neural progenitor cells, and astrocytes (Zocher et al., 2024). Retention of these specific RNA regulate and maintain heterochromatin structure and directly influence long-term regulation of gene expression. Although neurovascular cell types were not investigated, one may speculate that neurovascular cells similarly express Long-Lived RNAs as. Under quiescent conditions, the net turnover rate of BMECs is approximately 0.04% h^{-1} (Hobson B, Denekamp, 1984), an order of magnitude significantly lower than endothelial cells in other tissues (Tannock and Hayashi, 1972), and Long-Lived RNAs may play a role in sustaining the pervasive gene expression changes that we observe at the female NVU. Indeed, these mechanisms could account for the observed changes both canonical neurovascular genes but also the broad downregulation of pro- and anti-inflammatory genes at the human female NVU.

Redefining the immune phenotype of ELA according to human data

Inflammation is a biological response that typically originates from the activation of innate immune cells, including neutrophils, monocytes, macrophages, dendritic cells, and natural killer cells. This state is characterized by several key features: the dilatation of blood vessels, which leads to increased blood flow; the infiltration of immune cells into tissues; and the production of pro-inflammatory markers. These changes contribute to the classical signs of inflammation and facilitate the body's response to injury or infection.

However, a corpus of clinical studies report chronic low-grade inflammation (as more thoroughly described in the introduction) in those with histories of ELA, akin to the low chronic low-grade inflammation typically associated with an unresolved or overactive inflammatory response (Lawrence and Gilroy, 2007). One of the most consistent observations regarding the long-term consequences of ELA is its association with elevated levels of typical inflammation markers, namely circulating pro-inflammatory cytokine levels and the acute phase molecule CRP (Tursich et al., 2014, Baumeister et al., 2016). These observations are particularly intriguing given that the underlying etiopathological mechanisms of ELA are not linked to any pathogenic infection or peripheral disease. This suggests that the chronic low-grade inflammation observed

may arise from internal dysregulation rather than external infectious agents or physical ailments, underscoring the complexity of the inflammatory response in ELA. Immune cells exhibiting aberrant activity may contribute to an elevated inflammatory status in individuals, as ELA prematurely ages the innate and adaptive immune systems (Merz and Turner, 2021). CD8+ cytotoxic T cells are the most strongly affected (Elwenspoek et al., 2017) via disturbances in the CD4/CD8 subtype balance (Reid et al., 2019; Esposito et al., 2016; Schmeer et al., 2019), increased stimulation (Elwenspoek et al., 2017), and accelerated ageing and senescence (Elwenspoek et al., 2017, Reid et al., 2019), while CD4+ $T_{helper}17$ similarly display increased senescence (Reid et al., 2019; Elwenspoek et al., 2017). In the innate immune system, blood-borne monocytes express stress-responsive transcripts enriched for genes involved in cytokine and chemokine activity, steroid binding, hormone activity, and G-protein coupled receptor binding (Schwaiger et al., 2016, Boeck et al., 2016).

Critically, these studies entirely rely on measures of inflammation in peripheral blood as proxies to infer potential inflammatory states in the brain. Direct characterization of central inflammation, naturally, requires invasive techniques that are not possible to use on living individuals, making it challenging to establish a definitive link between peripheral biomarkers and neuroinflammation. Until now, a major limitation in the field has been this reliance on peripheral indicators as it presupposes, without direct evidence, that such markers reflect neuroinflammatory states in individuals affected by ELA. In animal studies, several lines of robust evidence purport compromised BBB integrity and permeability, such as the downregulation of CLDN5 (Menard et al., 2017; Dudek et al., 2020; Dion-Albert et al., 2022), the formation of stochastic microbleeds (Lehmann et al., 2018; Lehmann et al., 2020, Lehmann et al., 2022), and accompanying neuroinflammation within the brain parenchyma. The permeability of the BBB, compromised by alterations in CLDN5, suggests a pathway for peripheral cytokines and other molecules to influence the brain parenchyma. Thus, the presence of inflammation in the blood has been a logical indicator for concurrent neuroinflammation in ELA-affected models.

Contrary to what is inferred from these clinical studies and animal models, our findings point to global immune expression suppression at the human NVU, where *all* genes—either pro- or anti-inflammatory in function—had downregulated expression, whether their expression change reached significance or not. These findings challenge the prevailing hypothesis of ELA-induced pro-inflammatory states and instead suggest a nuanced understanding of mechanisms at play. What does a neurovascular interface characterized by an immune-suppressed environment mean against the backdrop of existing knowledge? An immune-suppressed environment at the NVU might suggest a protective adaptation, preventing the overactivation of immune signalling that could otherwise lead to neuroinflammation and altered neuronal activity. By dampening immune activity at the NVU, the CNS could minimize unnecessary immune responses to peripheral inflammation. Conversely, an immune-suppressed environment at NVU may indicate a pathological response to prolonged exposure to systemic inflammation. Initially, in response to systemic inflammation close to ELA events, the NVU may exhibit robust immune signalling. However, over time, this continuous activation could lead to an exhausted or dysfunctional state at the NVU. Continuous suppression of immune response could impair, at least in part, the NVU's ability to maintain barrier integrity and function. Given these perspectives, it's crucial to consider that the immune-suppressed state of the NVU in individuals with ELA might be a double-edged sword: a protective adaptation that becomes maladaptive over time.

A shift in how the immune system is seen: from response to infection and injury to a ubiquitous part of physiology

It is now recognized that the majority of neurodegenerative and psychiatric disorders (Furman et al., 2019)—many of which are strongly predicted by ELA—possess an inflammatory component that drives or, at least, perpetuates that phenotype. To better understand how a chronic, stress-induced phenotype involves the NVU, we must shift our perspective away from the perception that inflammation is *only* a specialized defence mechanism against infection and injury. “Zooming out” from this focus allows us to understand inflammation more accurately as an integral and ubiquitous part of physiology. Accumulating evidence highlights that cellular and molecular mediators of

inflammation play roles in an astonishingly wide array of biological functions (Meizlish et al., 2021**;** Colaco and Moita, 2016; Kotas et al., 2015), including metabolism and thermogenesis (Molofsky et al., 2013**;** Lee et al., 2015), and various aspects of nervous system function and behaviour (Qing et al., 2020). This complex biological phenomenon cannot be confined to a single definition or function. Instead, it can be conceptualized within a framework that includes: i) an initial response to insult; ii) a multi-step defense mechanism activated to eliminate the source of the insult; and iii) a modified state of the system designed to be protective or adaptive (Medzhitov, 2021, Medzhitov, 2008). By this conceptual framework, inflammatory processes span a functional spectrum: On one end, there is "canonical inflammation," characterized by the well-documented mechanisms of both innate and adaptive immune responses. On the opposite end, cells and pathways commonly associated with acute inflammation are involved in routine homeostatic activities. This raises the question: “what is global suppression of immune mechanisms in ELA trying to do?” Perhaps such pathways are trying to re-establish entirely *new* homeostatic setpoints. This concept is illustrated in the hypothalamus during acute inflammation triggered by an infection, which induces a physiological response known as "sickness behavior." This state alters the homeostatic setpoints for body temperature, appetite, sleep, and other functions (Hart, 1988**;** Wang et al., 2019), illustrating how inflammation can recalibrate the body’s regulatory systems under certain conditions. One might hypothesize that alterations in setpoint values that persist long-term under adverse conditions may drive consequences that are chronic.

Neurovascular KLF2/4 may be a target of stress-induced cortisol

Elevated cortisol levels during developmentally sensitive periods, such as those experienced during ELA, result in long-term alterations in the expression and function of glucocorticoid receptors (GR), a key modulator of the stress response across several brain regions including the PFC, hippocampus, Amygdala, ACC, and paraventricular nucleus. This alteration in GR function is partly due to epigenetic modifications of the NR3C1 gene, which encodes GR. Specifically, increased DNA methylation at its promoter region (Labonte et al., 2012; Kember et al., 2012) suppresses gene expression (Labonte et al., 2012; Avishai-Eliner et al., 1999; McGowan et al., 2009),

resulting in a decreased availability of GRs for cortisol binding. Before entering the brain parenchyma, cortisol released by the adrenal glands and into the systemic circulation, must first cross the BBB. GRs are highly expressed in the cytoplasm of endothelial cells within the BBB and, to a lesser extent, in other neurovascular cells (Zielinska et al., 2016; Campos-Rodríguez et al., 2009), allowing GRs to bind to cortisol as it diffuses through the BBB. Highly relevant to the body of work described in chapter III, KLF2 has been experimentally validated as a significant GR target gene, characterized by the presence of glucocorticoid response elements (GREs). GR regulates a multitude of genes by binding to these GREs, facilitating the formation of dense gene networks that have transcription factors, such as members of the KLF family, as control nodes (Chinenov et al., 2014).

In our study, KLF2, and its functionally redundant binding partner, KFL4, were both downregulated in female cases (but not males with ELA). KLF2 and KLF4 are vital for the integrity of the endothelial lining, which controls barrier function, blood fluidity, and flow dynamics. KLF2/4 confer endothelial barrier integrity by inducing expression of multiple anti-inflammatory and anti-thrombotic factors, such as eNOS (Hamik et al., 2007; Chiplunkar et al., 2013) and thrombomodulin (Hamik et al., 2007), VEGFR2 (Chiplunkar et al., 2013), and by regulating endothelial expression of CAMs, NF-kB, and tight junction proteins CLDN5 and occludin (Shi et al., 2013; Chiplunkar et al., 2013; Lin et al., 2010). Moreover, KLF2 orchestrates vascular homeostasis and serves as a central transcriptional switch point between a pro-inflammatory, atheroprone versus quiescent, atheroresistant endothelial phenotype, in which KLF2 determines endothelial transcription programs (> 1000 genes, Dekker et al., 2006) that control key functional pathways such as cell migration, vasomotor function, inflammation, and hemostasis (Dekker et al., 2006; Lin et al., 2005; Lee et al., 2006). Relevant to its function, KLF2 and GR interact as members of an incoherent feed forward loop, in which GR tightly regulates KLF2 expression (Chinenov et al., 2014), suggesting a complex mechanism at play in mediating the effects of chronic stress. If neurovascular GR is downregulated due to increased NR3C1 methylation, this could result in reduced responsiveness to glucocorticoids, which are crucial for maintaining homeostasis during stress responses.

Such a scenario might lead to a diminished ability to induce KLF2 expression efficiently. Given KLF2's role in endothelial identity and barrier maintenance (Sangwung, et al., 2017; SenBanerjee et al., 2004), its reduced expression could exacerbate the vascular and inflammatory dysfunctions typically observed in individuals with ELA. Understanding the impact of altered GR and KLF2 interactions in the NVU could offer new therapeutic targets or strategies for individuals with histories of ELA.

Conclusion

Despite this progress, many unanswered and emerging questions remain. It is essential to further characterize the mechanisms and pathways that involve genes KLF2 and KLF4 so that we may better understand how the NVU contributes to the phenotype observed in ELA, including the observed sex-specific differences. To better understand how downregulation in KLF2, KLF4, and immune functions progress over time, and their relationship with concurrent parenchymal dysfunctions, multi-time point animal studies that track these changes from early exposure through adulthood are needed. Exploring these questions further will enable a more comprehensive understanding of the profound impacts that early life adversity has on brain development and function. Furthermore, establishing a causal role for KLF2 and KLF4 in the ELA phenotype is crucial for effective drug target validation. Research demonstrates that drug mechanisms supported by molecular evidence linked to known, causative genes are estimated to be 2.6 times more likely to achieve clinical success (Minikel et al., 2024). Finally, it will be crucial for future studies to extend this research to additional cohorts of subjects with ELA, as well as individuals diagnosed with MDD without histories of ELA, to better delineate the specific contributions of ELA and its distinct effects. Since our investigation focused only on depressed suicides with a history of ELA, it is challenging to attribute our findings specifically to MDD or to ELA alone, and it is likely that both conditions contribute to the observed changes. That ELA might drive many/most of the expression changes we identified, however, is supported by recent studies having identified NVU or immune-related contributions to ELA or chronic stress (Menard et al., 2017; Dudek et al., 2020; Dion-Albert et al., 2022; Lehmann et al., 2018; Lehmann et al., 2020; Samuels et al., 2023; Lehmann et al., 2022).

This study marks the first demonstration that Krüppel-like factors, specifically KLF2 and KLF4, are associated with ELA, further implicating the NVU itself for the first time. An additional layer of complexity, this work reveals that the impact on the NVU is sex-specific; females exhibit significant NVU dysfunction characterized by the downregulation of KLF2 and KLF4 and altered expression of numerous other key vascular genes, whereas males do not exhibit similar changes. Given their fundamental role in vascular homeostasis, KLF2 and KLF4 represent promising therapeutic targets to mitigate the persistent neurobiological effects observed in ELA. Furthermore, our observations of a global suppression of gene expression related to immune functions specifically in the female NVU challenge decades of correlative clinical evidence suggesting that elevations in circulating pro-inflammatory cytokines reflect a similarly pro-inflammatory state within the brain parenchyma in stress-related psychopathology, prompting re-evaluation of the traditional view that "peripheral inflammation equals brain inflammation", in favour of a more nuanced understanding of NVU contributions to stress-related psychopathologies.

References for Chapter I and IV

Afifi TO, Enns MW, Cox BJ, Asmundson GJ, Stein MB, Sareen J. Population attributable fractions of psychiatric disorders and suicide ideation and attempts associated with adverse childhood experiences. Am J Public Health. 2008;98(5):946-52.

Afifi TO, MacMillan HL, Boyle M, Taillieu T, Cheung K, Sareen J. Child abuse and mental disorders in Canada. CMAJ. 2014;186(9):E324-32.

Agorastos A, Pervanidou P, Chrousos GP, Baker DG. Developmental Trajectories of Early Life Stress and Trauma: A Narrative Review on Neurobiological Aspects Beyond Stress System Dysregulation. Front Psychiatry. 2019;10:118.

Ahn S, Kim S, Zhang H, Dobalian A, Slavich GM. Lifetime adversity predicts depression, anxiety, and cognitive impairment in a nationally representative sample of older adults in the United States. J Clin Psychol. 2024;80(5):1031-49.

Almeida D, Fiori LM, Chen GG, Aouabed Z, Lutz PE, Zhang TY, et al. Oxytocin receptor expression and epigenetic regulation in the anterior cingulate cortex of individuals with a history of severe childhood abuse. Psychoneuroendocrinology. 2022;136:105600.

Alon N, Macrynikola N, Jester DJ, Keshavan M, Reynolds CF, 3rd, Saxena S, et al. Social determinants of mental health in major depressive disorder: Umbrella review of 26 meta-analyses and systematic reviews. Psychiatry Res. 2024;335:115854.

Altemus M, Sarvaiya N, Neill Epperson C. Sex differences in anxiety and depression clinical perspectives. Front Neuroendocrinol. 2014;35(3):320-30.

Anderson AW, Marois R, Colson ER, Peterson BS, Duncan CC, Ehrenkranz RA, et al. Neonatal auditory activation detected by functional magnetic resonance imaging. Magn Reson Imaging. 2001;19(1):1-5.

Anderson CM, Teicher MH, Polcari A, Renshaw PF. Abnormal T2 relaxation time in the cerebellar vermis of adults sexually abused in childhood: potential role of the vermis in stress-enhanced risk for drug abuse. Psychoneuroendocrinology. 2002;27(1-2):231-44.

Angelakis I, Gillespie EL, Panagioti M. Childhood maltreatment and adult suicidality: a comprehensive systematic review with meta-analysis. Psychol Med. 2019;49(7):1057-78.
Arain M, Haque M, Johal L, Mathur P, Nel W, Rais A, et al. Maturation of the adolescent brain. Neuropsychiatr Dis Treat. 2013;9:449-61.

Archer JA, Hutchison IL, Dorudi S, Stansfeld SA, Korszun A. Interrelationship of depression, stress and inflammation in cancer patients: a preliminary study. J Affect Disord. 2012;143(1-3):39-46.

Argandona EG, Lafuente JV. Influence of visual experience deprivation on the postnatal development of the microvascular bed in layer IV of the rat visual cortex. Brain Res. 2000;855(1):137-42.

Attwell D, Laughlin SB. An energy budget for signaling in the grey matter of the brain. J Cereb Blood Flow Metab. 2001;21(10):1133-45.

Avila-Gutierrez K, Slaoui L, Alvear-Perez R, Kozlowski E, Oudart M, Augustin E, et al. Dynamic local mRNA localization and translation occurs during the postnatal molecular maturation of perivascular astrocytic processes. Glia. 2024;72(4):777-93.

Avishai-Eliner S, Hatalski CG, Tabachnik E, Eghbal-Ahmadi M, Baram TZ. Differential regulation of glucocorticoid receptor messenger RNA (GR-mRNA) by maternal deprivation in immature rat hypothalamus and limbic regions. Brain Res Dev Brain Res. 1999;114(2):265-8.

Baars BJ, Gage NM. Fundamentals of cognitive neuroscience: A beginner's guide. San Diego: Elsevier Academic Press; 2013.

Bahk YC, Jang SK, Choi KH, Lee SH. The Relationship between Childhood Trauma and Suicidal Ideation: Role of Maltreatment and Potential Mediators. Psychiatry Investig. 2017;14(1):37-43.

Bai M, Zhu X, Zhang Y, Zhang S, Zhang L, Xue L, et al. Abnormal hippocampal BDNF and miR-16 expression is associated with depression-like behaviors induced by stress during early life. PLoS One. 2012;7(10):e46921.

Bake S, Sohrabji F. 17beta-estradiol differentially regulates blood-brain barrier permeability in young and aging female rats. Endocrinology. 2004;145(12):5471-5.

Baldwin JR, Arseneault L, Caspi A, Fisher HL, Moffitt TE, Odgers CL, et al. Childhood victimization and inflammation in young adulthood: A genetically sensitive cohort study. Brain Behav Immun. 2018;67:211-7.

Bale TL, Epperson CN. Sex as a Biological Variable: Who, What, When, Why, and How. Neuropsychopharmacology. 2017;42(2):386-96.

Barboza Solis C, Kelly-Irving M, Fantin R, Darnaudery M, Torrisani J, Lang T, et al. Adverse childhood experiences and physiological wear-and-tear in midlife: Findings from the 1958 British birth cohort. Proc Natl Acad Sci U S A. 2015;112(7):E738-46.

Barkovich AJ, Kjos BO, Jackson DE, Jr., Norman D. Normal maturation of the neonatal and infant brain: MR imaging at 1.5 T. Radiology. 1988;166(1 Pt 1):173-80.

Barnett Burns S, Almeida D, Turecki G. The Epigenetics of Early Life Adversity: Current Limitations and Possible Solutions. Prog Mol Biol Transl Sci. 2018;157:343-425.

Barrett TJ, Corr EM, van Solingen C, Schlamp F, Brown EJ, Koelwyn GJ, et al. Chronic stress primes innate immune responses in mice and humans. Cell Rep. 2021;36(10):109595.

Basu A, McLaughlin KA, Misra S, Koenen KC. Childhood Maltreatment and Health Impact: The Examples of Cardiovascular Disease and Type 2 Diabetes Mellitus in Adults. Clin Psychol (New York). 2017;24(2):125-39.

Bath KG, Manzano-Nieves G, Goodwill H. Early life stress accelerates behavioral and neural maturation of the hippocampus in male mice. Horm Behav. 2016;82:64-71.

Battaglia FP, Benchenane K, Sirota A, Pennartz CM, Wiener SI. The hippocampus: hub of brain network communication for memory. Trends Cogn Sci. 2011;15(7):310-8.

Baumeister D, Akhtar R, Ciufolini S, Pariante CM, Mondelli V. Childhood trauma and adulthood inflammation: a meta-analysis of peripheral C-reactive protein, interleukin-6 and tumour necrosis factor-alpha. Mol Psychiatry. 2016;21(5):642-9.

Becker JC, Dummer R, Hartmann AA, Burg G, Schmidt RE. Shedding of ICAM-1 from human melanoma cell lines induced by IFN-gamma and tumor necrosis factor-alpha. Functional consequences on cell-mediated cytotoxicity. J Immunol. 1991;147(12):4398-401.

Begley DJ, Brightman MW. Structural and functional aspects of the blood-brain barrier. Prog Drug Res. 2003;61:39-78.

Bekku N, Yoshimura H, Araki H. Factors producing a menopausal depressive-like state in mice following ovariectomy. Psychopharmacology (Berl). 2006;187(2):170-80.

Bellis MA, Hughes K, Ford K, Ramos Rodriguez G, Sethi D, Passmore J. Life course health consequences and associated annual costs of adverse childhood experiences across Europe and North America: a systematic review and meta-analysis. Lancet Public Health. 2019;4(10):e517-e28.

Berens AE, Jensen SKG, Nelson CA, 3rd. Biological embedding of childhood adversity: from physiological mechanisms to clinical implications. BMC Med. 2017;15(1):135.

Berg MT, Simons RL, Barr A, Beach SRH, Philibert RA. Childhood/Adolescent stressors and allostatic load in adulthood: Support for a calibration model. Soc Sci Med. 2017;193:130-9.

Bernet CZ, Stein MB. Relationship of childhood maltreatment to the onset and course of major depression in adulthood. Depress Anxiety. 1999;9(4):169-74.

Bertone-Johnson ER, Whitcomb BW, Missmer SA, Karlson EW, Rich-Edwards JW. Inflammation and early-life abuse in women. Am J Prev Med. 2012;43(6):611-20.

Betz AL, Firth JA, Goldstein GW. Polarity of the blood-brain barrier: distribution of enzymes between the luminal and antiluminal membranes of brain capillary endothelial cells. Brain Res. 1980;192(1):17-28.

Bhanji J, Smith DV, Delgado M. A Brief Anatomical Sketch of Human Ventromedial Prefrontal Cortex [Internet]. PsyArXiv; 2019. Available from: osf.io/preprints/psyarxiv/zdt7f
Bick J, Nelson CA. Early Adverse Experiences and the Developing Brain.

Birnie MT, Kooiker CL, Short AK, Bolton JL, Chen Y, Baram TZ. Plasticity of the Reward Circuitry After Early-Life Adversity: Mechanisms and Significance. Biol Psychiatry. 2020;87(10):875-84.

Black JE, Sirevaag AM, Greenough WT. Complex experience promotes capillary formation in young rat visual cortex. Neurosci Lett. 1987;83(3):351-5.

Blaze J, Scheuing L, Roth TL. Differential methylation of genes in the medial prefrontal cortex of developing and adult rats following exposure to maltreatment or nurturing care during infancy. Dev Neurosci. 2013;35(4):306-16.

Bloom FE, Kupfer DJ. *Psychopharmacology: the fourth generation of progress.* New York: Raven Press; 1995.

Boeck C, Koenig AM, Schury K, Geiger ML, Karabatsiakis A, Wilker S, et al. Inflammation in adult women with a history of child maltreatment: The involvement of mitochondrial alterations and oxidative stress. Mitochondrion. 2016;30:197-207.

Bogdan R, Williamson DE, Hariri AR. Mineralocorticoid receptor Iso/Val (rs5522) genotype moderates the association between previous childhood emotional neglect and amygdala reactivity. Am J Psychiatry. 2012;169(5):515-22.

Bolton JL, Molet J, Regev L, Chen Y, Rismanchi N, Haddad E, et al. Anhedonia Following Early-Life Adversity Involves Aberrant Interaction of Reward and Anxiety Circuits and Is Reversed by Partial Silencing of Amygdala Corticotropin-Releasing Hormone Gene. Biol Psychiatry. 2018;83(2):137-47.

Bordt EA, Ceasrine AM, Bilbo SD. Microglia and sexual differentiation of the developing brain: A focus on ontogeny and intrinsic factors. Glia. 2020;68(6):1085-99.

Born P, Rostrup E, Leth H, Peitersen B, Lou HC. Change of visually induced cortical activation patterns during development. Lancet. 1996;347(9000):543.

Borovikova LV, Ivanova S, Zhang M, Yang H, Botchkina GI, Watkins LR, et al. Vagus nerve stimulation attenuates the systemic inflammatory response to endotoxin. Nature. 2000;405(6785):458-62.

Bourgeois JP, Goldman-Rakic PS, Rakic P. Synaptogenesis in the prefrontal cortex of rhesus monkeys. Cereb Cortex. 1994;4(1):78-96.

Brestoff JR, Artis D. Immune regulation of metabolic homeostasis in health and disease. Cell. 2015;161(1):146-60.

Brezo J, Paris J, Tremblay R, Vitaro F, Hebert M, Turecki G. Identifying correlates of suicide attempts in suicidal ideators: a population-based study. Psychol Med. 2007;37(11):1551-62.

Brezo J, Paris J, Vitaro F, Hebert M, Tremblay RE, Turecki G. Predicting suicide attempts in young adults with histories of childhood abuse. Br J Psychiatry. 2008;193(2):134-9.

Brezzo G, Simpson J, Ameen-Ali KE, Berwick J, Martin C. Acute effects of systemic inflammation upon the neuro-glial-vascular unit and cerebrovascular function. Brain Behav Immun Health. 2020;5:100074.

Brivio E, Kos A, Ulivi AF, Karamihalev S, Ressle A, Stoffel R, et al. Sex shapes cell-type-specific transcriptional signatures of stress exposure in the mouse hypothalamus. Cell Rep. 2023;42(8):112874.

Brodsky BS, Oquendo M, Ellis SP, Haas GL, Malone KM, Mann JJ. The relationship of childhood abuse to impulsivity and suicidal behavior in adults with major depression. Am J Psychiatry. 2001;158(11):1871-7.

Brown DW, Anda RF, Tiemeier H, Felitti VJ, Edwards VJ, Croft JB, et al. Adverse childhood experiences and the risk of premature mortality. Am J Prev Med. 2009;37(5):389-96.

Bruce J, Fisher PA, Graham AM, Moore WE, Peake SJ, Mannering AM. Patterns of brain activation in foster children and nonmaltreated children during an inhibitory control task. Dev Psychopathol. 2013;25(4 Pt 1):931-41.

Bruffaerts R, Demyttenaere K, Borges G, Haro JM, Chiu WT, Hwang I, et al. Childhood adversities as risk factors for onset and persistence of suicidal behaviour. Br J Psychiatry. 2010;197(1):20-7.

Buchmann AF, Hellweg R, Rietschel M, Treutlein J, Witt SH, Zimmermann US, et al. BDNF Val 66 Met and 5-HTTLPR genotype moderate the impact of early psychosocial adversity on plasma brain-derived neurotrophic factor and depressive symptoms: a prospective study. Eur Neuropsychopharmacol. 2013;23(8):902-9.

Burek M, Steinberg K, Forster CY. Mechanisms of transcriptional activation of the mouse claudin-5 promoter by estrogen receptor alpha and beta. Mol Cell Endocrinol. 2014;392(1-2):144-51.

Butt AM, Jones HC, Abbott NJ. Electrical resistance across the blood-brain barrier in anaesthetized rats: a developmental study. J Physiol. 1990;429:47-62.

Calabrese EJ, Bachmann KA, Bailer AJ, Bolger PM, Borak J, Cai L, et al. Biological stress response terminology: Integrating the concepts of adaptive response and preconditioning stress within a hormetic dose-response framework. Toxicol Appl Pharmacol. 2007;222(1):122-8.

Campos-Rodríguez R, Rivera-Aguilar V, Jarillo-Luna RA, Rojas-Hernández S, Godínez-Victoria M, Abarca-Rojano E, Mera-Jiménez E, Larsen BA, Reséndiz-Albor AA. Endothelial cells are a potential site of interaction between estrogens and glucocorticoids. Biosci Hypotheses. 2009;2(5):331-8. ISSN 1756-2392.

Carmeliet P, Tessier-Lavigne M. Common mechanisms of nerve and blood vessel wiring. Nature. 2005;436(7048):193-200.

Carpenter LL, Gawuga CE, Tyrka AR, Lee JK, Anderson GM, Price LH. Association between plasma IL-6 response to acute stress and early-life adversity in healthy adults. Neuropsychopharmacology. 2010;35(13):2617-23.

Carpenter LL, Gawuga CE, Tyrka AR, Price LH. C-reactive protein, early life stress, and wellbeing in healthy adults. Acta Psychiatr Scand. 2012;126(6):402-10.

Carrion VG, Garrett A, Menon V, Weems CF, Reiss AL. Posttraumatic stress symptoms and brain function during a response-inhibition task: an fMRI study in youth. Depress Anxiety. 2008;25(6):514-26.

Carrion VG, Weems CF, Eliez S, Patwardhan A, Brown W, Ray RD, et al. Attenuation of frontal asymmetry in pediatric posttraumatic stress disorder. Biol Psychiatry. 2001;50(12):943-51.

Carrion VG, Weems CF, Reiss AL. Stress predicts brain changes in children: a pilot longitudinal study on youth stress, posttraumatic stress disorder, and the hippocampus. Pediatrics. 2007;119(3):509-16.

Carrion VG, Weems CF, Watson C, Eliez S, Menon V, Reiss AL. Converging evidence for abnormalities of the prefrontal cortex and evaluation of midsagittal structures in pediatric posttraumatic stress disorder: an MRI study. Psychiatry Res. 2009;172(3):226-34.

Carroll JE, Gruenewald TL, Taylor SE, Janicki-Deverts D, Matthews KA, Seeman TE. Childhood abuse, parental warmth, and adult multisystem biological risk in the Coronary Artery Risk Development in Young Adults study. Proc Natl Acad Sci U S A. 2013;110(42):17149-53.

Caspi A, Sugden K, Moffitt TE, Taylor A, Craig IW, Harrington H, et al. Influence of life stress on depression: moderation by a polymorphism in the 5-HTT gene. Science. 2003;301(5631):386-9.

Cauli B, Hamel E. Revisiting the role of neurons in neurovascular coupling. Front Neuroenergetics. 2010;2:9.

Cereijido M, Valdes J, Shoshani L, Contreras RG. Role of tight junctions in establishing and maintaining cell polarity. Annu Rev Physiol. 1998;60:161-77.

Chan SY, Ngoh ZM, Ong ZY, Teh AL, Kee MZL, Zhou JH, et al. The influence of early-life adversity on the coupling of structural and functional brain connectivity across childhood. Nature Mental Health. 2024;2(1):52-62.

Charmandari E, Tsigos C, Chrousos G. Endocrinology of the stress response. Annu Rev Physiol. 2005;67:259-84.

Chen E, Miller GE, Kobor MS, Cole SW. Maternal warmth buffers the effects of low early-life socioeconomic status on pro-inflammatory signaling in adulthood. Mol Psychiatry. 2011;16(7):729-37.

Chen Y, Shan Y, Lin K, Wei Y, Kim H, Koenen KC, et al. Association Between Child Abuse and Risk of Adult Coronary Heart Disease: A Systematic Review and Meta-Analysis. Am J Prev Med. 2023;65(1):143-54.

Chinenov Y, Coppo M, Gupte R, Sacta MA, Rogatsky I. Glucocorticoid receptor coordinates transcription factor-dominated regulatory network in macrophages. BMC Genomics. 2014;15(1):656.

Chiplunkar AR, Curtis BC, Eades GL, Kane MS, Fox SJ, Haar JL, et al. The Kruppel-like factor 2 and Kruppel-like factor 4 genes interact to maintain endothelial integrity in mouse embryonic vasculogenesis. BMC Dev Biol. 2013;13:40.

Chiron C, Raynaud C, Maziere B, Zilbovicius M, Laflamme L, Masure MC, et al. Changes in regional cerebral blood flow during brain maturation in children and adolescents. J Nucl Med. 1992;33(5):696-703.

Cicchetti D, Curtis WJ. An event-related potential study of the processing of affective facial expressions in young children who experienced maltreatment during the first year of life. Dev Psychopathol. 2005;17(3):641-77.

Coelho R, Viola TW, Walss-Bass C, Brietzke E, Grassi-Oliveira R. Childhood maltreatment and inflammatory markers: a systematic review. Acta Psychiatr Scand. 2014;129(3):180-92.

Colaco HG, Moita LF. Initiation of innate immune responses by surveillance of homeostasis perturbations. FEBS J. 2016;283(13):2448-57.

Cordon-Cardo C, O'Brien JP, Casals D, Rittman-Grauer L, Biedler JL, Melamed MR, et al. Multidrug-resistance gene (P-glycoprotein) is expressed by endothelial cells at blood-brain barrier sites. Proc Natl Acad Sci U S A. 1989;86(2):695-8.

Counotte J, Bergink V, Pot-Kolder R, Drexhage HA, Hoek HW, Veling W. Inflammatory cytokines and growth factors were not associated with psychosis liability or childhood trauma. PLoS One. 2019;14(7):e0219139.

Critchley HD, Corfield DR, Chandler MP, Mathias CJ, Dolan RJ. Cerebral correlates of autonomic cardiovascular arousal: a functional neuroimaging investigation in humans. J Physiol. 2000;523 Pt 1(Pt 1):259-70.

Cudmore RH, Dougherty SE, Linden DJ. Cerebral vascular structure in the motor cortex of adult mice is stable and is not altered by voluntary exercise. J Cereb Blood Flow Metab. 2017;37(12):3725-43.

Curtis WJ, Cicchetti D. Affective facial expression processing in young children who have experienced maltreatment during the first year of life: an event-related potential study. Dev Psychopathol. 2011;23(2):373-95.

da Silva Ferreira GC, Crippa JA, de Lima Osorio F. Facial emotion processing and recognition among maltreated children: a systematic literature review. Front Psychol. 2014;5:1460.

Damasio AR, Grabowski TJ, Bechara A, Damasio H, Ponto LL, Parvizi J, et al. Subcortical and cortical brain activity during the feeling of self-generated emotions. Nat Neurosci. 2000;3(10):1049-56.

Daneman R, Prat A. The blood-brain barrier. Cold Spring Harb Perspect Biol. 2015;7(1):a020412.

Daneman R, Zhou L, Kebede AA, Barres BA. Pericytes are required for blood-brain barrier integrity during embryogenesis. Nature. 2010;468(7323):562-6.

Danese A, Caspi A, Williams B, Ambler A, Sugden K, Mika J, et al. Biological embedding of stress through inflammation processes in childhood. Mol Psychiatry. 2011;16(3):244-6.

Danese A, McEwen BS. Adverse childhood experiences, allostasis, allostatic load, and age-related disease. Physiol Behav. 2012;106(1):29-39.

Danese A, Moffitt TE, Harrington H, Milne BJ, Polanczyk G, Pariante CM, et al. Adverse childhood experiences and adult risk factors for age-related disease: depression, inflammation, and clustering of metabolic risk markers. Arch Pediatr Adolesc Med. 2009;163(12):1135-43.

Danielsdottir HB, Aspelund T, Shen Q, Halldorsdottir T, Jakobsdottir J, Song H, et al. Adverse Childhood Experiences and Adult Mental Health Outcomes. JAMA Psychiatry. 2024;81(6):586-94.

Daskalakis NP, Bagot RC, Parker KJ, Vinkers CH, de Kloet ER. The three-hit concept of vulnerability and resilience: toward understanding adaptation to early-life adversity outcome. Psychoneuroendocrinology. 2013;38(9):1858-73.

De Bellis MD, Hooper SR. Neural substrates for processing task-irrelevant emotional distracters in maltreated adolescents with depressive disorders: a pilot study. J Trauma Stress. 2012;25(2):198-202.

De Bellis MD, Keshavan MS, Clark DB, Casey BJ, Giedd JN, Boring AM, et al. A.E. Bennett Research Award. Developmental traumatology. Part II: Brain development. Biol Psychiatry. 1999;45(10):1271-84.

De Bellis MD, Keshavan MS, Shifflett H, Iyengar S, Beers SR, Hall J, et al. Brain structures in pediatric maltreatment-related posttraumatic stress disorder: a sociodemographically matched study. Biol Psychiatry. 2002;52(11):1066-78.

De Bellis MD, Zisk A. The biological effects of childhood trauma. Child Adolesc Psychiatr Clin N Am. 2014;23(2):185-222, vii.

De Brito SA, Viding E, Sebastian CL, Kelly PA, Mechelli A, Maris H, et al. Reduced orbitofrontal and temporal grey matter in a community sample of maltreated children. J Child Psychol Psychiatry. 2013;54(1):105-12.

de Chaves G, Moretti M, Castro AA, Dagostin W, da Silva GG, Boeck CR, et al. Effects of long-term ovariectomy on anxiety and behavioral despair in rats. Physiol Behav. 2009;97(3-4):420-5.

De Kloet ER, Vreugdenhil E, Oitzl MS, Joels M. Brain corticosteroid receptor balance in health and disease. Endocr Rev. 1998;19(3):269-301.

de Mendonca Filho EJ, Pokhvisneva I, Maalouf CM, Parent C, Mliner SB, Slopen N, et al. Linking specific biological signatures to different childhood adversities: findings from the HERO project. Pediatr Res. 2023;94(2):564-74.

Dekker RJ, Boon RA, Rondaij MG, Kragt A, Volger OL, Elderkamp YW, et al. KLF2 provokes a gene expression pattern that establishes functional quiescent differentiation of the endothelium. Blood. 2006;107(11):4354-63.

Delgado MR, Beer JS, Fellows LK, Huettel SA, Platt ML, Quirk GJ, et al. Viewpoints: Dialogues on the functional role of the ventromedial prefrontal cortex. Nat Neurosci. 2016;19(12):1545-52.

Dennison U, McKernan D, Cryan J, Dinan T. Schizophrenia patients with a history of childhood trauma have a pro-inflammatory phenotype. Psychol Med. 2012;42(9):1865-71.

Di Giovanna AP, Tibo A, Silvestri L, Mullenbroich MC, Costantini I, Allegra Mascaro AL, et al. Whole-Brain Vasculature Reconstruction at the Single Capillary Level. Sci Rep. 2018;8(1):12573.

Di Martino E, Rayasam A, Vexler ZS. Brain Maturation as a Fundamental Factor in Immune-Neurovascular Interactions in Stroke. Transl Stroke Res. 2024;15(1):69-86.

Di Nicola M, Cattaneo A, Hepgul N, Di Forti M, Aitchison KJ, Janiri L, et al. Serum and gene expression profile of cytokines in first-episode psychosis. Brain Behav Immun. 2013;31:90-5.

Dion-Albert L, Cadoret A, Doney E, Kaufmann FN, Dudek KA, Daigle B, et al. Vascular and blood-brain barrier-related changes underlie stress responses and resilience in female mice and depression in human tissue. Nat Commun. 2022;13(1):164.

Dong M, Giles WH, Felitti VJ, Dube SR, Williams JE, Chapman DP, et al. Insights into causal pathways for ischemic heart disease: adverse childhood experiences study. Circulation. 2004;110(13):1761-6.

Drake CT, Iadecola C. The role of neuronal signaling in controlling cerebral blood flow. Brain Lang. 2007;102(2):141-52.

Drevets WC, Price JL, Furey ML. Brain structural and functional abnormalities in mood disorders: implications for neurocircuitry models of depression. Brain Struct Funct. 2008;213(1-2):93-118.

Drew PJ, Shih AY, Driscoll JD, Knutsen PM, Blinder P, Davalos D, et al. Chronic optical access through a polished and reinforced thinned skull. Nat Methods. 2010;7(12):981-4.

Du Rocher Schudlich T, Youngstrom EA, Martinez M, KogosYoungstrom J, Scovil K, Ross J, et al. Physical and sexual abuse and early-onset bipolar disorder in youths receiving outpatient services: frequent, but not specific. J Abnorm Child Psychol. 2015;43(3):453-63.

Dube SR, Anda RF, Felitti VJ, Chapman DP, Williamson DF, Giles WH. Childhood abuse, household dysfunction, and the risk of attempted suicide throughout the life span: findings from the Adverse Childhood Experiences Study. JAMA. 2001;286(24):3089-96.

Dube SR, Felitti VJ, Dong M, Giles WH, Anda RF. The impact of adverse childhood experiences on health problems: evidence from four birth cohorts dating back to 1900. Prev Med. 2003;37(3):268-77.

Duncan EJ, Gluckman PD, Dearden PK. Epigenetics, plasticity, and evolution: How do we link epigenetic change to phenotype? J Exp Zool B Mol Dev Evol. 2014;322(4):208-20.

Eck SR, Palmer JL, Bavley CC, Karbalaei R, Ordones Sanchez E, Flowers J, 2nd, et al. Effects of early life adversity on male reproductive behavior and the medial preoptic area transcriptome. Neuropsychopharmacology. 2022;47(6):1231-9.

Edelmann S, Wiegand A, Hentrich T, Pasche S, Schulze-Hentrich JM, Munk MHJ, et al. Blood transcriptome analysis suggests an indirect molecular association of early life adversities and adult social anxiety disorder by immune-related signal transduction. Front Psychiatry. 2023;14:1125553.

Edmiston EE, Wang F, Mazure CM, Guiney J, Sinha R, Mayes LC, et al. Corticostriatal-limbic gray matter morphology in adolescents with self-reported exposure to childhood maltreatment. Arch Pediatr Adolesc Med. 2011;165(12):1069-77.

Eichmann A, Thomas JL. Molecular parallels between neural and vascular development. Cold Spring Harb Perspect Med. 2013;3(1):a006551.

Ek CJ, Wong A, Liddelow SA, Johansson PA, Dziegielewska KM, Saunders NR. Efflux mechanisms at the developing brain barriers: ABC-transporters in the fetal and postnatal rat. Toxicol Lett. 2010;197(1):51-9.

Ellis BJ, Horn AJ, Carter CS, van IMH, Bakermans-Kranenburg MJ. Developmental programming of oxytocin through variation in early-life stress: Four meta-analyses and a theoretical reinterpretation. Clin Psychol Rev. 2021;86:101985.

Elston GN, Oga T, Fujita I. Spinogenesis and pruning scales across functional hierarchies. J Neurosci. 2009;29(10):3271-5.

Elwenspoek MMC, Hengesch X, Leenen FAD, Schritz A, Sias K, Schaan VK, et al. Proinflammatory T Cell Status Associated with Early Life Adversity. J Immunol. 2017;199(12):4046-55.

Enns MW, Cox BJ, Afifi TO, De Graaf R, Ten Have M, Sareen J. Childhood adversities and risk for suicidal ideation and attempts: a longitudinal population-based study. Psychol Med. 2006;36(12):1769-78.

Erinjeri JP, Woolsey TA. Spatial integration of vascular changes with neural activity in mouse cortex. J Cereb Blood Flow Metab. 2002;22(3):353-60.

Esposito EA, Jones MJ, Doom JR, MacIsaac JL, Gunnar MR, Kobor MS. Differential DNA methylation in peripheral blood mononuclear cells in adolescents exposed to significant early but not later childhood adversity. Dev Psychopathol. 2016;28(4pt2):1385-99.

Falcone T, Janigro D, Lovell R, Simon B, Brown CA, Herrera M, et al. S100B blood levels and childhood trauma in adolescent inpatients. J Psychiatr Res. 2015;62:14-22.

Feher G, Schulte ML, Weigle CG, Kampine JP, Hudetz AG. Postnatal remodeling of the leptomeningeal vascular network as assessed by intravital fluorescence video-microscopy in the rat. Brain Res Dev Brain Res. 1996;91(2):209-17.

Felitti VJ, Anda RF, Nordenberg D, Williamson DF, Spitz AM, Edwards V, et al. Relationship of childhood abuse and household dysfunction to many of the leading causes of death in adults. The Adverse Childhood Experiences (ACE) Study. Am J Prev Med. 1998;14(4):245-58.

Fellows LK, Farah MJ. The role of ventromedial prefrontal cortex in decision making: judgment under uncertainty or judgment per se? Cereb Cortex. 2007;17(11):2669-74.
Fenoglio KA, Brunson KL, Baram TZ. Hippocampal neuroplasticity induced by early-life stress: functional and molecular aspects. Front Neuroendocrinol. 2006;27(2):180-92.

Fergusson DM, Woodward LJ, Horwood LJ. Risk factors and life processes associated with the onset of suicidal behaviour during adolescence and early adulthood. Psychol Med. 2000;30(1):23-39.

Fields RD. A new mechanism of nervous system plasticity: activity-dependent myelination. Nat Rev Neurosci. 2015;16(12):756-67.

Flaherty EG, Thompson R, Dubowitz H, Harvey EM, English DJ, Proctor LJ, et al. Adverse childhood experiences and child health in early adolescence. JAMA Pediatr. 2013;167(7):622-9.

Fock E, Parnova R. Mechanisms of Blood-Brain Barrier Protection by Microbiota-Derived Short-Chain Fatty Acids. Cells. 2023;12(4).

Fox SE, Levitt P, Nelson CA, 3rd. How the timing and quality of early experiences influence the development of brain architecture. Child Dev. 2010;81(1):28-40.

Fredericks CA, Kalmar JH, Blumberg HP. The role of the ventral prefrontal cortex in mood disorders. In: Zald DH, Rauch SL, editors. The Orbitofrontal Cortex. New York: Oxford University Press; 2006. pp. 544–577.

French JA, Carp SB. Early-life Social Adversity and Developmental Processes in Nonhuman Primates. Curr Opin Behav Sci. 2016;7:40-6.

Frodl T, Carballedo A, Hughes MM, Saleh K, Fagan A, Skokauskas N, et al. Reduced expression of glucocorticoid-inducible genes GILZ and SGK-1: high IL-6 levels are associated with reduced hippocampal volumes in major depressive disorder. Transl Psychiatry. 2012;2(3):e88.

Frysztak RJ, Neafsey EJ. The effect of medial frontal cortex lesions on cardiovascular conditioned emotional responses in the rat. Brain Res. 1994;643(1-2):181-93.

Fuentes S, Daviu N, Gagliano H, Garrido P, Zelena D, Monasterio N, et al. Sex-dependent effects of an early life treatment in rats that increases maternal care: vulnerability or resilience? Front Behav Neurosci. 2014;8:56.

Fuller-Thomson E, Brennenstuhl S, Frank J. The association between childhood physical abuse and heart disease in adulthood: findings from a representative community sample. Child Abuse Negl. 2010;34(9):689-98.

Furman D, Campisi J, Verdin E, Carrera-Bastos P, Targ S, Franceschi C, et al. Chronic inflammation in the etiology of disease across the life span. Nat Med. 2019;25(12):1822-32.

Gartland N, Rosmalen JGM, O'Connor DB. Effects of childhood adversity and cortisol levels on suicidal ideation and behaviour: Results from a general population study. Psychoneuroendocrinology. 2022;138:105664.

Gershon A, Sudheimer K, Tirouvanziam R, Williams LM, O'Hara R. The long-term impact of early adversity on late-life psychiatric disorders. Curr Psychiatry Rep. 2013;15(4):352.

Ghajar CM, Peinado H, Mori H, Matei IR, Evason KJ, Brazier H, et al. The perivascular niche regulates breast tumour dormancy. Nat Cell Biol. 2013;15(7):807-17.

Gilbert R, Widom CS, Browne K, Fergusson D, Webb E, Janson S. Burden and consequences of child maltreatment in high-income countries. Lancet. 2009;373(9657):68-81.

Girard N, Raybaud C, du Lac P. MRI study of brain myelination. J Neuroradiol. 1991;18(4):291-307.

Gogtay N, Nugent TF, 3rd, Herman DH, Ordonez A, Greenstein D, Hayashi KM, et al. Dynamic mapping of normal human hippocampal development. Hippocampus. 2006;16(8):664-72.

Gomez-Gonzalez B, Escobar A. Altered functional development of the blood-brain barrier after early life stress in the rat. Brain Res Bull. 2009;79(6):376-87.

Gontard-Danek M-C, Møller AP. The strength of sexual selection: a meta-analysis of bird studies. Behavioral Ecology. 1999;10(5):476-86.

Goodwill HL, Manzano-Nieves G, Gallo M, Lee HI, Oyerinde E, Serre T, et al. Early life stress leads to sex differences in development of depressive-like outcomes in a mouse model. Neuropsychopharmacology. 2019;44(4):711-20.

Gordon JL, Rubinow DR, Eisenlohr-Moul TA, Leserman J, Girdler SS. Estradiol variability, stressful life events, and the emergence of depressive symptomatology during the menopausal transition. Menopause. 2016;23(3):257-66.

Gouin JP, Glaser R, Malarkey WB, Beversdorf D, Kiecolt-Glaser JK. Childhood abuse and inflammatory responses to daily stressors. Ann Behav Med. 2012;44(2):287-92.

Gracia-Rubio I, Moscoso-Castro M, Pozo OJ, Marcos J, Nadal R, Valverde O. Maternal separation induces neuroinflammation and long-lasting emotional alterations in mice. Prog Neuropsychopharmacol Biol Psychiatry. 2016;65:104-17.

Graham AM, Fisher PA, Pfeifer JH. What sleeping babies hear: a functional MRI study of interparental conflict and infants' emotion processing. Psychol Sci. 2013;24(5):782-9.

Green JG, McLaughlin KA, Berglund PA, Gruber MJ, Sampson NA, Zaslavsky AM, et al. Childhood adversities and adult psychiatric disorders in the national comorbidity survey replication I: associations with first onset of DSM-IV disorders. Arch Gen Psychiatry. 2010;67(2):113-23.

Greicius MD, Supekar K, Menon V, Dougherty RF. Resting-state functional connectivity reflects structural connectivity in the default mode network. Cereb Cortex. 2009;19(1):72-8.

Groban L, Lindsey SH, Wang H, Alencar AK. Sex and Gender Differences in Cardiovascular Disease. In: Neigh GN, Mitzelfelt MM, editors. Sex Differences in Physiology. Academic Press; 2016. p. 61-87.

Guido W. Refinement of the retinogeniculate pathway. J Physiol. 2008;586(18):4357-62.
Gumbiner BM. Breaking through the tight junction barrier. J Cell Biol. 1993;123(6 Pt 2):1631-3.

Haber SN, Knutson B. The reward circuit: linking primate anatomy and human imaging. Neuropsychopharmacology. 2010;35(1):4-26.

Habib N, Li Y, Heidenreich M, Swiech L, Avraham-Davidi I, Trombetta JJ, et al. Div-Seq: Single-nucleus RNA-Seq reveals dynamics of rare adult newborn neurons. Science. 2016;353(6302):925-8.

Haikonen J, Englund J, Amarilla SP, Kharybina Z, Shintyapina A, Kegler K, et al. Aberrant cortical projections to amygdala GABAergic neurons contribute to developmental circuit dysfunction following early life stress. iScience. 2023;26(1):105724.

Hamik A, Lin Z, Kumar A, Balcells M, Sinha S, Katz J, et al. Kruppel-like factor 4 regulates endothelial inflammation. J Biol Chem. 2007;282(18):13769-79.

Han K, Min J, Lee M, Kang BM, Park T, Hahn J, et al. Neurovascular Coupling under Chronic Stress Is Modified by Altered GABAergic Interneuron Activity. J Neurosci. 2019;39(50):10081-95.

Hanson JL, Chung MK, Avants BB, Shirtcliff EA, Gee JC, Davidson RJ, et al. Early stress is associated with alterations in the orbitofrontal cortex: a tensor-based morphometry investigation of brain structure and behavioral risk. J Neurosci. 2010;30(22):7466-72.

Hanson JL, Nacewicz BM, Sutterer MJ, Cayo AA, Schaefer SM, Rudolph KD, et al. Behavioral problems after early life stress: contributions of the hippocampus and amygdala. Biol Psychiatry. 2015;77(4):314-23.

Haraldsen G, Kvale D, Lien B, Farstad IN, Brandtzaeg P. Cytokine-regulated expression of E-selectin, intercellular adhesion molecule-1 (ICAM-1), and vascular cell adhesion molecule-1 (VCAM-1) in human microvascular endothelial cells. J Immunol. 1996;156(7):2558-65.

Harb R, Whiteus C, Freitas C, Grutzendler J. In vivo imaging of cerebral microvascular plasticity from birth to death. J Cereb Blood Flow Metab. 2013;33(1):146-56.

Harik SI, Hall AK, Richey P, Andersson L, Lundahl P, Perry G. Ontogeny of the erythroid/HepG2-type glucose transporter (GLUT-1) in the rat nervous system. Brain Res Dev Brain Res. 1993;72(1):41-9.

Harris JJ, Reynell C, Attwell D. The physiology of developmental changes in BOLD functional imaging signals. Dev Cogn Neurosci. 2011;1(3):199-216.

Hart BL. Biological basis of the behavior of sick animals. Neurosci Biobehav Rev. 1988;12(2):123-37.

Hartwell KJ, Moran-Santa Maria MM, Twal WO, Shaftman S, DeSantis SM, McRae-Clark AL, et al. Association of elevated cytokines with childhood adversity in a sample of healthy adults. J Psychiatr Res. 2013;47(5):604-10.

Hawkins BT, Davis TP. The blood-brain barrier/neurovascular unit in health and disease. Pharmacol Rev. 2005;57(2):173-85.

Henninger DD, Panes J, Eppihimer M, Russell J, Gerritsen M, Anderson DC, et al. Cytokine-induced VCAM-1 and ICAM-1 expression in different organs of the mouse. J Immunol. 1997;158(4):1825-32.

Hepgul N, Pariante CM, Dipasquale S, DiForti M, Taylor H, Marques TR, et al. Childhood maltreatment is associated with increased body mass index and increased C-reactive protein levels in first-episode psychosis patients. Psychol Med. 2012;42(9):1893-901.

Herken R, Gotz W, Wattjes KH. Initial development of capillaries in the neuroepithelium of the mouse. J Anat. 1989;164:85-92.

Herman JP, McKlveen JM, Ghosal S, Kopp B, Wulsin A, Makinson R, et al. Regulation of the Hypothalamic-Pituitary-Adrenocortical Stress Response. Compr Physiol. 2016;6(2):603-21.

Herrmann MJ, Rommler J, Ehlis AC, Heidrich A, Fallgatter AJ. Source localization (LORETA) of the error-related-negativity (ERN/Ne) and positivity (Pe). Brain Res Cogn Brain Res. 2004;20(2):294-9.

Hertzman C, Boyce T. How experience gets under the skin to create gradients in developmental health. Annu Rev Public Health. 2010;31:329-47 3p following 47.

Hillhouse EW, Grammatopoulos DK. The molecular mechanisms underlying the regulation of the biological activity of corticotropin-releasing hormone receptors: implications for physiology and pathophysiology. Endocr Rev. 2006;27(3):260-86.

Hillis S, Mercy J, Amobi A, Kress H. Global Prevalence of Past-year Violence Against Children: A Systematic Review and Minimum Estimates. Pediatrics. 2016;137(3):e20154079.

Hiser J, Koenigs M. The Multifaceted Role of the Ventromedial Prefrontal Cortex in Emotion, Decision Making, Social Cognition, and Psychopathology. Biol Psychiatry. 2018;83(8):638-47.

Hladky SB, Barrand MA. Fluid and ion transfer across the blood-brain and blood-cerebrospinal fluid barriers; a comparative account of mechanisms and roles. Fluids Barriers CNS. 2016;13(1):19.

Ho DH, Burch ML, Musall B, Musall JB, Hyndman KA, Pollock JS. Early life stress in male mice induces superoxide production and endothelial dysfunction in adulthood. Am J Physiol Heart Circ Physiol. 2016;310(9):H1267-74.

Hobson B, Denekamp J. Endothelial proliferation in tumours and normal tissues: continuous labelling studies. Br J Cancer. 1984;49(4):405-13.

Hong YK, Chen C. Wiring and rewiring of the retinogeniculate synapse. Curr Opin Neurobiol. 2011;21(2):228-37.

Hostinar CE, Stellern SA, Schaefer C, Carlson SM, Gunnar MR. Associations between early life adversity and executive function in children adopted internationally from orphanages. Proc Natl Acad Sci U S A. 2012;109 Suppl 2(Suppl 2):17208-12.

Houtepen LC, Vinkers CH, Carrillo-Roa T, Hiemstra M, van Lier PA, Meeus W, et al. Genome-wide DNA methylation levels and altered cortisol stress reactivity following childhood trauma in humans. Nat Commun. 2016;7:10967.

Hrvatin S, Hochbaum DR, Nagy MA, Cicconet M, Robertson K, Cheadle L, et al. Single-cell analysis of experience-dependent transcriptomic states in the mouse visual cortex. Nat Neurosci. 2018;21(1):120-9.

Hughes G, Yeung N. Dissociable correlates of response conflict and error awareness in error-related brain activity. Neuropsychologia. 2011;49(3):405-15.

Hurley KM, Herbert H, Moga MM, Saper CB. Efferent projections of the infralimbic cortex of the rat. J Comp Neurol. 1991;308(2):249-76.

Huttenlocher PR, Dabholkar AS. Regional differences in synaptogenesis in human cerebral cortex. J Comp Neurol. 1997;387(2):167-78.

Huttenlocher PR, de Courten C, Garey LJ, Van der Loos H. Synaptogenesis in human visual cortex--evidence for synapse elimination during normal development. Neurosci Lett. 1982;33(3):247-52.

Huttenlocher PR. Morphometric study of human cerebral cortex development. Neuropsychologia. 1990;28(6):517-27.

Huttenlocher PR. Synaptic density in human frontal cortex - developmental changes and effects of aging. Brain Res. 1979;163(2):195-205.

Iadecola C, Yang G, Ebner TJ, Chen G. Local and propagated vascular responses evoked by focal synaptic activity in cerebellar cortex. J Neurophysiol. 1997;78(2):651-9.

Isaacs KR, Anderson BJ, Alcantara AA, Black JE, Greenough WT. Exercise and the brain: angiogenesis in the adult rat cerebellum after vigorous physical activity and motor skill learning. J Cereb Blood Flow Metab. 1992;12(1):110-9.

Izquierdo A, Suda RK, Murray EA. Bilateral orbital prefrontal cortex lesions in rhesus monkeys disrupt choices guided by both reward value and reward contingency. J Neurosci. 2004;24(34):7540-8.

Jackson JG, Krizman E, Takano H, Lee M, Choi GH, Putt ME, et al. Activation of Glutamate Transport Increases Arteriole Diameter in vivo: Implications for Neurovascular Coupling. Front Cell Neurosci. 2022;16:831061.

Jacome LF, Barateli K, Buitrago D, Lema F, Frankfurt M, Luine VN. Gonadal Hormones Rapidly Enhance Spatial Memory and Increase Hippocampal Spine Density in Male Rats. Endocrinology. 2016;157(4):1357-62.

Jenkins NDM, Rogers EM, Banks NF, Tomko PM, Sciarrillo CM, Emerson SR, et al. Childhood psychosocial stress is linked with impaired vascular endothelial function, lower SIRT1, and oxidative stress in young adulthood. Am J Physiol Heart Circ Physiol. 2021;321(3):H532-H41.

Jessen HM, Auger AP. Sex differences in epigenetic mechanisms may underlie risk and resilience for mental health disorders. Epigenetics. 2011;6(7):857-61.

Joels M, Baram TZ. The neuro-symphony of stress. Nat Rev Neurosci. 2009;10(6):459-66.

Johnson JG, Cohen P, Gould MS, Kasen S, Brown J, Brook JS. Childhood adversities, interpersonal difficulties, and risk for suicide attempts during late adolescence and early adulthood. Arch Gen Psychiatry. 2002;59(8):741-9.

Johnson MH. Functional brain development in humans. Nat Rev Neurosci. 2001;2(7):475-83.

Johnston AJ, Steiner LA, Gupta AK, Menon DK. Cerebral oxygen vasoreactivity and cerebral tissue oxygen reactivity. Br J Anaesth. 2003;90(6):774-86.

Jones HE, Coelho-Santos V, Bonney SK, Abrams KA, Shih AY, Siegenthaler JA. Meningeal origins and dynamics of perivascular fibroblast development on the mouse cerebral vasculature. Development. 2023;150(19).

Jung WH, Lee TY, Kim M, Lee J, Oh S, Lho SK, et al. Sex differences in the behavioral inhibition system and ventromedial prefrontal cortex connectivity. Soc Cogn Affect Neurosci. 2022;17(6):571-8.

Kadry H, Noorani B, Cucullo L. A blood-brain barrier overview on structure, function, impairment, and biomarkers of integrity. Fluids Barriers CNS. 2020;17(1):69.

Kang HJ, Kim JM, Stewart R, Kim SY, Bae KY, Kim SW, et al. Association of SLC6A4 methylation with early adversity, characteristics and outcomes in depression. Prog Neuropsychopharmacol Biol Psychiatry. 2013;44:23-8.

Kang HS, Ahn HS, Kang HJ, Gye MC. Effect of estrogen on the expression of occludin in ovariectomized mouse brain. Neurosci Lett. 2006;402(1-2):30-4.

Kaplow JB, Widom CS. Age of onset of child maltreatment predicts long-term mental health outcomes. J Abnorm Psychol. 2007;116(1):176-87.

Karakatsani A, Shah B, Ruiz de Almodovar C. Blood Vessels as Regulators of Neural Stem Cell Properties. Front Mol Neurosci. 2019;12:85.

Karst H, Droogers WJ, van der Weerd N, Damsteegt R, van Kronenburg N, Sarabdjitsingh RA, et al. Acceleration of GABA-switch after early life stress changes mouse prefrontal glutamatergic transmission. Neuropharmacology. 2023;234:109543.

Katz LC, Shatz CJ. Synaptic activity and the construction of cortical circuits. Science. 1996;274(5290):1133-8.

Keep RF, Jones HC. Cortical microvessels during brain development: a morphometric study in the rat. Microvasc Res. 1990;40(3):412-26.

Kellum CE, Kemp KM, Mrug S, Pollock JS, Seifert ME, Feig DI. Adverse childhood experiences are associated with vascular changes in adolescents that are risk factors for future cardiovascular disease. Pediatr Nephrol. 2023;38(7):2155-63.

Kelly PA, Viding E, Wallace GL, Schaer M, De Brito SA, Robustelli B, et al. Cortical thickness, surface area, and gyrification abnormalities in children exposed to maltreatment: neural markers of vulnerability? Biol Psychiatry. 2013;74(11):845-52.

Kember RL, Dempster EL, Lee TH, Schalkwyk LC, Mill J, Fernandes C. Maternal separation is associated with strain-specific responses to stress and epigenetic alterations to Nr3c1, Avp, and Nr4a1 in mouse. Brain Behav. 2012;2(4):455-67.

Kessler RC, McLaughlin KA, Green JG, Gruber MJ, Sampson NA, Zaslavsky AM, et al. Childhood adversities and adult psychopathology in the WHO World Mental Health Surveys. Br J Psychiatry. 2010;197(5):378-85.

Kiecolt-Glaser JK, Gouin JP, Weng NP, Malarkey WB, Beversdorf DQ, Glaser R. Childhood adversity heightens the impact of later-life caregiving stress on telomere length and inflammation. Psychosom Med. 2011;73(1):16-22.

Kim P, Evans GW, Angstadt M, Ho SS, Sripada CS, Swain JE, et al. Effects of childhood poverty and chronic stress on emotion regulatory brain function in adulthood. Proc Natl Acad Sci U S A. 2013;110(46):18442-7.

Kinney HC, Brody BA, Kloman AS, Gilles FH. Sequence of central nervous system myelination in human infancy. II. Patterns of myelination in autopsied infants. J Neuropathol Exp Neurol. 1988;47(3):217-34.

Klein DN, Arnow BA, Barkin JL, Dowling F, Kocsis JH, Leon AC, et al. Early adversity in chronic depression: clinical correlates and response to pharmacotherapy. Depress Anxiety. 2009;26(8):701-10.

Knickmeyer RC, Gouttard S, Kang C, Evans D, Wilber K, Smith JK, et al. A structural MRI study of human brain development from birth to 2 years. J Neurosci. 2008;28(47):12176-82.

Kniesel U, Risau W, Wolburg H. Development of blood-brain barrier tight junctions in the rat cortex. Brain Res Dev Brain Res. 1996;96(1-2):229-40.

Kos A, Lopez JP, Bordes J, de Donno C, Dine J, Brivio E, et al. Early life adversity shapes social subordination and cell type-specific transcriptomic patterning in the ventral hippocampus. Sci Adv. 2023;9(48):eadj3793.

Kotas ME, Medzhitov R. Homeostasis, inflammation, and disease susceptibility. Cell. 2015;160(5):816-27.

Kozberg MG, Chen BR, DeLeo SE, Bouchard MB, Hillman EM. Resolving the transition from negative to positive blood oxygen level-dependent responses in the developing brain. Proc Natl Acad Sci U S A. 2013;110(11):4380-5.

Krause DN, Duckles SP, Pelligrino DA. Influence of sex steroid hormones on cerebrovascular function. J Appl Physiol (1985). 2006;101(4):1252-61.

Kuhlman KR, Cole SW, Craske MG, Fuligni AJ, Irwin MR, Bower JE. Enhanced Immune Activation Following Acute Social Stress Among Adolescents With Early-Life Adversity. Biol Psychiatry Glob Open Sci. 2023;3(2):213-21.

Labonté B, Engmann O, Purushothaman I, Menard C, Wang J, Tan C, Scarpa JR, Moy G, Loh YE, Cahill M, Lorsch ZS, Hamilton PJ, Calipari ES, Hodes GE, Issler O, Kronman H, Pfau M, Obradovic ALJ, Dong Y, Neve RL, Russo S, Kazarskis A, Tamminga C, Mechawar N, Turecki G, Zhang B, Shen L, Nestler EJ. Sex-specific transcriptional signatures in human depression. Nat Med. 2017 Sep;23(9):1102-11.

Labonte B, Yerko V, Gross J, Mechawar N, Meaney MJ, Szyf M, et al. Differential glucocorticoid receptor exon 1(B), 1(C), and 1(H) expression and methylation in suicide completers with a history of childhood abuse. Biol Psychiatry. 2012;72(1):41-8.

Lacey RE, Kumari M, McMunn A. Parental separation in childhood and adult inflammation: the importance of material and psychosocial pathways. Psychoneuroendocrinology. 2013;38(11):2476-84.

Lacoste B, Comin CH, Ben-Zvi A, Kaeser PS, Xu X, Costa Lda F, et al. Sensory-related neural activity regulates the structure of vascular networks in the cerebral cortex. Neuron. 2014;83(5):1117-30.

Lacreuse A, Herndon JG, Moss MB. Cognitive function in aged ovariectomized female rhesus monkeys. Behav Neurosci. 2000;114(3):506-13.

Lake BB, Ai R, Kaeser GE, Salathia NS, Yung YC, Liu R, et al. Neuronal subtypes and diversity revealed by single-nucleus RNA sequencing of the human brain. Science. 2016;352(6293):1586-90.

Lake BB, Chen S, Sos BC, Fan J, Kaeser GE, Yung YC, et al. Integrative single-cell analysis of transcriptional and epigenetic states in the human adult brain. Nat Biotechnol. 2018;36(1):70-80.

LaMantia AS, Rakic P. Axon overproduction and elimination in the anterior commissure of the developing rhesus monkey. J Comp Neurol. 1994;340(3):328-36.

Lange C, Turrero Garcia M, Decimo I, Bifari F, Eelen G, Quaegebeur A, et al. Relief of hypoxia by angiogenesis promotes neural stem cell differentiation by targeting glycolysis. EMBO J. 2016;35(9):924-41.

Lansford JE, Dodge KA, Pettit GS, Bates JE, Crozier J, Kaplow J. A 12-year prospective study of the long-term effects of early child physical maltreatment on psychological, behavioral, and academic problems in adolescence. Arch Pediatr Adolesc Med. 2002;156(8):824-30.

Lawrence T, Gilroy DW. Chronic inflammation: a failure of resolution? Int J Exp Pathol. 2007;88(2):85-94.

Lee JS, Yu Q, Shin JT, Sebzda E, Bertozzi C, Chen M, et al. Klf2 is an essential regulator of vascular hemodynamic forces in vivo. Dev Cell. 2006;11(6):845-57.

Lee MW, Odegaard JI, Mukundan L, Qiu Y, Molofsky AB, Nussbaum JC, et al. Activated type 2 innate lymphoid cells regulate beige fat biogenesis. Cell. 2015;160(1-2):74-87.

Lehericy S, Ducros M, Van de Moortele PF, Francois C, Thivard L, Poupon C, et al. Diffusion tensor fiber tracking shows distinct corticostriatal circuits in humans. Ann Neurol. 2004;55(4):522-9.

Lehmann ML, Poffenberger CN, Elkahloun AG, Herkenham M. Analysis of cerebrovascular dysfunction caused by chronic social defeat in mice. Brain Behav Immun. 2020;88:735-47.

Lehmann ML, Samuels JD, Kigar SL, Poffenberger CN, Lotstein ML, Herkenham M. CCR2 monocytes repair cerebrovascular damage caused by chronic social defeat stress. Brain Behav Immun. 2022;101:346-58.

Lehmann ML, Weigel TK, Cooper HA, Elkahloun AG, Kigar SL, Herkenham M. Decoding microglia responses to psychosocial stress reveals blood-brain barrier breakdown that may drive stress susceptibility. Sci Rep. 2018;8(1):11240.

Letourneur A, Chen V, Waterman G, Drew PJ. A method for longitudinal, transcranial imaging of blood flow and remodeling of the cerebral vasculature in postnatal mice. Physiol Rep. 2014;2(12).

Levenson JM, Roth TL, Lubin FD, Miller CA, Huang IC, Desai P, et al. Evidence that DNA (cytosine-5) methyltransferase regulates synaptic plasticity in the hippocampus. J Biol Chem. 2006;281(23):15763-73.

Levitt P. Structural and functional maturation of the developing primate brain. J Pediatr. 2003;143(4 Suppl):S35-45.

Levy DJ, Glimcher PW. The root of all value: a neural common currency for choice. Curr Opin Neurobiol. 2012;22(6):1027-38.

Levy R, Goldman-Rakic PS. Segregation of working memory functions within the dorsolateral prefrontal cortex. Exp Brain Res. 2000;133(1):23-32.

Li F, Xing X, Jin Q, Wang XM, Dai P, Han M, et al. Sex differences orchestrated by androgens at single-cell resolution. Nature. 2024;629(8010):193-200.

Li LH, Wang ZC, Yu J, Zhang YQ. Ovariectomy results in variable changes in nociception, mood and depression in adult female rats. PLoS One. 2014;9(4):e94312.

Lieberman-Aiden E, van Berkum NL, Williams L, Imakaev M, Ragoczy T, Telling A, et al. Comprehensive mapping of long-range interactions reveals folding principles of the human genome. Science. 2009;326(5950):289-93.

Likhtik E, Pelletier JG, Paz R, Pare D. Prefrontal control of the amygdala. J Neurosci. 2005;25(32):7429-37.

Lin Z, Kumar A, SenBanerjee S, Staniszewski K, Parmar K, Vaughan DE, et al. Kruppel-like factor 2 (KLF2) regulates endothelial thrombotic function. Circ Res. 2005;96(5):e48-57.

Lin Z, Natesan V, Shi H, Dong F, Kawanami D, Mahabeleshwar GH, et al. Kruppel-like factor 2 regulates endothelial barrier function. Arterioscler Thromb Vasc Biol. 2010;30(10):1952-9.

Liu X, Hairston J, Schrier M, Fan J. Common and distinct networks underlying reward valence and processing stages: a meta-analysis of functional neuroimaging studies. Neurosci Biobehav Rev. 2011;35(5):1219-36.

Liu Y, Croft JB, Chapman DP, Perry GS, Greenlund KJ, Zhao G, et al. Relationship between adverse childhood experiences and unemployment among adults from five U.S. states. Soc Psychiatry Psychiatr Epidemiol. 2013;48(3):357-69.

Llorente R, Gallardo ML, Berzal AL, Prada C, Garcia-Segura LM, Viveros MP. Early maternal deprivation in rats induces gender-dependent effects on developing hippocampal and cerebellar cells. Int J Dev Neurosci. 2009;27(3):233-41.

Lo CM, Keese CR, Giaever I. Cell-substrate contact: another factor may influence transepithelial electrical resistance of cell layers cultured on permeable filters. Exp Cell Res. 1999;250(2):576-80.

Loi M, Koricka S, Lucassen PJ, Joels M. Age- and sex-dependent effects of early life stress on hippocampal neurogenesis. Front Endocrinol (Lausanne). 2014;5:13.

Longden TA, Dabertrand F, Hill-Eubanks DC, Hammack SE, Nelson MT. Stress-induced glucocorticoid signaling remodels neurovascular coupling through impairment of cerebrovascular inwardly rectifying K+ channel function. Proc Natl Acad Sci U S A. 2014;111(20):7462-7.

Lopatina N, McDannald MA, Styer CV, Peterson JF, Sadacca BF, Cheer JF, et al. Medial Orbitofrontal Neurons Preferentially Signal Cues Predicting Changes in Reward during Unblocking. J Neurosci. 2016;36(32):8416-24.

Lopez-Castroman J, Jaussent I, Beziat S, Genty C, Olie E, de Leon-Martinez V, et al. Suicidal phenotypes associated with family history of suicidal behavior and early traumatic experiences. J Affect Disord. 2012;142(1-3):193-9.

Lorsch ZS, Loh YE, Purushothaman I, Walker DM, Parise EM, Salery M, et al. Estrogen receptor alpha drives pro-resilient transcription in mouse models of depression. Nat Commun. 2018;9(1):1116.

Loucks EB, Taylor SE, Polak JF, Wilhelm A, Kalra P, Matthews KA. Childhood family psychosocial environment and carotid intima media thickness: the CARDIA study. Soc Sci Med. 2014;104:15-22.

Lu S, Peng H, Wang L, Vasish S, Zhang Y, Gao W, et al. Elevated specific peripheral cytokines found in major depressive disorder patients with childhood trauma exposure: a cytokine antibody array analysis. Compr Psychiatry. 2013;54(7):953-61.

Luca DL, Margiotta C, Staatz C, Garlow E, Christensen A, Zivin K. Financial Toll of Untreated Perinatal Mood and Anxiety Disorders Among 2017 Births in the United States. Am J Public Health. 2020;110(6):888-96.

Luissint AC, Artus C, Glacial F, Ganeshamoorthy K, Couraud PO. Tight junctions at the blood brain barrier: physiological architecture and disease-associated dysregulation. Fluids Barriers CNS. 2012;9(1):23.

Luissint AC, Federici C, Guillonneau F, Chretien F, Camoin L, Glacial F, et al. Guanine nucleotide-binding protein Galphai2: a new partner of claudin-5 that regulates tight junction integrity in human brain endothelial cells. J Cereb Blood Flow Metab. 2012;32(5):860-73.

Lupien SJ, McEwen BS, Gunnar MR, Heim C. Effects of stress throughout the lifespan on the brain, behaviour and cognition. Nat Rev Neurosci. 2009;10(6):434-45.

Lutz PE, Tanti A, Gasecka A, Barnett-Burns S, Kim JJ, Zhou Y, et al. Association of a History of Child Abuse With Impaired Myelination in the Anterior Cingulate Cortex: Convergent Epigenetic, Transcriptional, and Morphological Evidence. Am J Psychiatry. 2017;174(12):1185-94.

Maartens LW, Knottnerus JA, Pop VJ. Menopausal transition and increased depressive symptomatology: a community based prospective study. Maturitas. 2002;42(3):195-200.
Mackey S, Petrides M. Quantitative demonstration of comparable architectonic areas within the ventromedial and lateral orbital frontal cortex in the human and the macaque monkey brains. Eur J Neurosci. 2010;32(11):1940-50.

MacMillan HL, Fleming JE, Streiner DL, Lin E, Boyle MH, Jamieson E, et al. Childhood abuse and lifetime psychopathology in a community sample. Am J Psychiatry. 2001;158(11):1878-83.

Magill CR, Ashley GM, Freeman KH. Water, plants, and early human habitats in eastern Africa. Proc Natl Acad Sci U S A. 2013;110(4):1175-80.

Maniam J, Antoniadis C, Morris MJ. Early-Life Stress, HPA Axis Adaptation, and Mechanisms Contributing to Later Health Outcomes. Front Endocrinol (Lausanne). 2014;5:73.

Martikainen P, Bartley M, Lahelma E. Psychosocial determinants of health in social epidemiology. Int J Epidemiol. 2002;31(6):1091-3.

Mathys H, Peng Z, Boix CA, Victor MB, Leary N, Babu S, et al. Single-cell atlas reveals correlates of high cognitive function, dementia, and resilience to Alzheimer's disease pathology. Cell. 2023;186(20):4365-85 e27.

Matthews KA, Chang YF, Thurston RC, Bromberger JT. Child abuse is related to inflammation in mid-life women: role of obesity. Brain Behav Immun. 2014;36:29-34.

McCarthy MM, Arnold AP, Ball GF, Blaustein JD, De Vries GJ. Sex differences in the brain: the not so inconvenient truth. J Neurosci. 2012;32(7):2241-7.

McConnell HL, Kersch CN, Woltjer RL, Neuwelt EA. The Translational Significance of the Neurovascular Unit. J Biol Chem. 2017;292(3):762-70.

McCrory EJ, De Brito SA, Sebastian CL, Mechelli A, Bird G, Kelly PA, et al. Heightened neural reactivity to threat in child victims of family violence. Curr Biol. 2011;21(23):R947-8.

McEwen BS, Gianaros PJ. Stress- and allostasis-induced brain plasticity. Annu Rev Med. 2011;62:431-45.

McEwen BS. Physiology and neurobiology of stress and adaptation: central role of the brain. Physiol Rev. 2007;87(3):873-904.

McEwen BS. Stress, adaptation, and disease. Allostasis and allostatic load. Ann N Y Acad Sci. 1998;840:33-44.

McGowan PO, Sasaki A, D'Alessio AC, Dymov S, Labonte B, Szyf M, et al. Epigenetic regulation of the glucocorticoid receptor in human brain associates with childhood abuse. Nat Neurosci. 2009;12(3):342-8.

Medzhitov R. Origin and physiological roles of inflammation. Nature. 2008;454(7203):428-35.

Medzhitov R. The spectrum of inflammatory responses. Science. 2021;374(6571):1070-5.

Meek JH, Firbank M, Elwell CE, Atkinson J, Braddick O, Wyatt JS. Regional hemodynamic responses to visual stimulation in awake infants. Pediatr Res. 1998;43(6):840-3.

Meizlish ML, Franklin RA, Zhou X, Medzhitov R. Tissue Homeostasis and Inflammation. Annu Rev Immunol. 2021;39:557-81.

Melas PA, Wei Y, Wong CC, Sjoholm LK, Aberg E, Mill J, et al. Genetic and epigenetic associations of MAOA and NR3C1 with depression and childhood adversities. Int J Neuropsychopharmacol. 2013;16(7):1513-28.

Menard C, Pfau ML, Hodes GE, Kana V, Wang VX, Bouchard S, et al. Social stress induces neurovascular pathology promoting depression. Nat Neurosci. 2017;20(12):1752-60.

Menard C, Pfau ML, Hodes GE, Kana V, Wang VX, Bouchard S, Takahashi A, Flanigan ME, Aleyasin H, LeClair KB, Janssen WG, Labonté B, Parise EM, Lorsch ZS, Golden SA, Heshmati M, Tamminga C, Turecki G, Campbell M, Fayad ZA, Tang CY, Merad M, Russo SJ. Social stress induces neurovascular pathology promoting depression. Nat Neurosci. 2017 Dec;20(12):1752-60. doi: 10.1038/s41593-017-0010-3. Epub 2017 Nov 13. PMID: 29184215; PMCID: PMC5726568.

Merz MP, Turner JD. Is early life adversity a trigger towards inflammageing? Exp Gerontol. 2021;150:111377.

Michel AE, Garey LJ. The development of dendritic spines in the human visual cortex. Hum Neurobiol. 1984;3(4):223-7.

Milad MR, Quirk GJ. Neurons in medial prefrontal cortex signal memory for fear extinction. Nature. 2002;420(6911):70-4.

Miller DJ, Duka T, Stimpson CD, Schapiro SJ, Baze WB, McArthur MJ, et al. Prolonged myelination in human neocortical evolution. Proc Natl Acad Sci U S A. 2012;109(41):16480-5.

Miller EK, Cohen JD. An integrative theory of prefrontal cortex function. Annu Rev Neurosci. 2001;24:167-202.

Miller GE, Chen E, Parker KJ. Psychological stress in childhood and susceptibility to the chronic diseases of aging: moving toward a model of behavioral and biological mechanisms. Psychol Bull. 2011;137(6):959-97.

Miller GE, Cole SW. Clustering of depression and inflammation in adolescents previously exposed to childhood adversity. Biol Psychiatry. 2012;72(1):34-40.

Miller VM, Duckles SP. Vascular actions of estrogens: functional implications. Pharmacol Rev. 2008;60(2):210-41.

Minikel EV, Painter JL, Dong CC, Nelson MR. Refining the impact of genetic evidence on clinical success. Nature. 2024;629(8012):624-9.

Mitchell LA, Koval M. Specificity of interaction between clostridium perfringens enterotoxin and claudin-family tight junction proteins. Toxins (Basel). 2010;2(7):1595-611.

Mittapalli RK, Manda VK, Adkins CE, Geldenhuys WJ, Lockman PR. Exploiting nutrient transporters at the blood-brain barrier to improve brain distribution of small molecules. Ther Deliv. 2010;1(6):775-84.

Molet J, Maras PM, Avishai-Eliner S, Baram TZ. Naturalistic rodent models of chronic early-life stress. Dev Psychobiol. 2014;56(8):1675-88.

Molnar BE, Berkman LF, Buka SL. Psychopathology, childhood sexual abuse and other childhood adversities: relative links to subsequent suicidal behaviour in the US. Psychol Med. 2001;31(6):965-77.

Molofsky AB, Nussbaum JC, Liang HE, Van Dyken SJ, Cheng LE, Mohapatra A, et al. Innate lymphoid type 2 cells sustain visceral adipose tissue eosinophils and alternatively activated macrophages. J Exp Med. 2013;210(3):535-49.

Montagne A, Barnes SR, Sweeney MD, Halliday MR, Sagare AP, Zhao Z, et al. Blood-brain barrier breakdown in the aging human hippocampus. Neuron. 2015;85(2):296-302.

Morgan MA, Romanski LM, LeDoux JE. Extinction of emotional learning: contribution of medial prefrontal cortex. Neurosci Lett. 1993;163(1):109-13.

Morgane PJ, Austin-LaFrance R, Bronzino J, Tonkiss J, Diaz-Cintra S, Cintra L, et al. Prenatal malnutrition and development of the brain. Neurosci Biobehav Rev. 1993;17(1):91-128.

Mullen PE, Martin JL, Anderson JC, Romans SE, Herbison GP. The long-term impact of the physical, emotional, and sexual abuse of children: a community study. Child Abuse Negl. 1996;20(1):7-21.

Muoio V, Persson PB, Sendeski MM. The neurovascular unit - concept review. Acta Physiol (Oxf). 2014;210(4):790-8.

Nagy C, Maitra M, Tanti A, Suderman M, Theroux JF, Davoli MA, et al. Single-nucleus transcriptomics of the prefrontal cortex in major depressive disorder implicates oligodendrocyte precursor cells and excitatory neurons. Nat Neurosci. 2020;23(6):771-81.

Neafsey EJ, Hurley-Gius KM, Arvanitis D. The topographical organization of neurons in the rat medial frontal, insular and olfactory cortex projecting to the solitary nucleus, olfactory bulb, periaqueductal gray and superior colliculus. Brain Res. 1986;377(2):261-70.

Nelles-McGee T, Khoury J, Kenny M, Joshi D, Gonzalez A. Biological embedding of child maltreatment: A systematic review of biomarkers and resilience in children and youth. Psychol Trauma. 2022;14(S1):S50-S62.

Nelson CA, Gabard-Durnam LJ. Early Adversity and Critical Periods: Neurodevelopmental Consequences of Violating the Expectable Environment. Trends Neurosci. 2020;43(3):133-43.

Nelson CA, Hazards to Early Development: The Biological Embedding of Early Life Adversity. Neuron. 2017;96(2):262-6.

Nelson CA, Scott RD, Bhutta ZA, Harris NB, Danese A, Samara M. Adversity in childhood is linked to mental and physical health throughout life. BMJ. 2020;371:m3048.

Nelson EE, Herman KN, Barrett CE, Noble PL, Wojteczko K, Chisholm K, et al. Adverse rearing experiences enhance responding to both aversive and rewarding stimuli in juvenile rhesus monkeys. Biol Psychiatry. 2009;66(7):702-4.
Neuropsychopharmacology.2016;41(1):177-96.

Nijsen MJ, Croiset G, Stam R, Bruijnzeel A, Diamant M, de Wied D, et al. The role of the CRH type 1 receptor in autonomic responses to corticotropin- releasing hormone in the rat. Neuropsychopharmacology. 2000;22(4):388-99.

Noonan MP, Walton ME, Behrens TE, Sallet J, Buckley MJ, Rushworth MF. Separate value comparison and learning mechanisms in macaque medial and lateral orbitofrontal cortex. Proc Natl Acad Sci U S A. 2010;107(47):20547-52.

Nordstrom CH, Messeter K, Sundbarg G, Schalen W, Werner M, Ryding E. Cerebral blood flow, vasoreactivity, and oxygen consumption during barbiturate therapy in severe traumatic brain lesions. J Neurosurg. 1988;68(3):424-31.

Norman MG, O'Kusky JR. The growth and development of microvasculature in human cerebral cortex. J Neuropathol Exp Neurol. 1986;45(3):222-32.

Ochsner KN, Bunge SA, Gross JJ, Gabrieli JD. Rethinking feelings: an FMRI study of the cognitive regulation of emotion. J Cogn Neurosci. 2002;14(8):1215-29.

Ongur D, Ferry AT, Price JL. Architectonic subdivision of the human orbital and medial prefrontal cortex. J Comp Neurol. 2003;460(3):425-49.

Ongur D, Price JL. The organization of networks within the orbital and medial prefrontal cortex of rats, monkeys and humans. Cereb Cortex. 2000;10(3):206-19.

Oomen CA, Girardi CE, Cahyadi R, Verbeek EC, Krugers H, Joels M, et al. Opposite effects of early maternal deprivation on neurogenesis in male versus female rats. PLoS One. 2009;4(1):e3675.

Oomen CA, Soeters H, Audureau N, Vermunt L, van Hasselt FN, Manders EM, et al. Severe early life stress hampers spatial learning and neurogenesis, but improves hippocampal synaptic plasticity and emotional learning under high-stress conditions in adulthood. J Neurosci. 2010;30(19):6635-45.

Orellana SC, Bethlehem RAI, Simpson-Kent IL, van Harmelen AL, Vertes PE, Bullmore ET. Childhood maltreatment influences adult brain structure through its effects on immune, metabolic, and psychosocial factors. Proc Natl Acad Sci U S A. 2024;121(16):e2304704121.

Owens NC, Verberne AJ. Regional haemodynamic responses to activation of the medial prefrontal cortex depressor region. Brain Res. 2001;919(2):221-31.

Parekh A, Fadiran EO, Uhl K, Throckmorton DC. Adverse effects in women: implications for drug development and regulatory policies. Expert Rev Clin Pharmacol. 2011;4(4):453-66.
Parel ST, Bennett SN, Cheng CJ, Timmermans OC, Fiori LM, Turecki G, et al.

Transcriptional signatures of early-life stress and antidepressant treatment efficacy. Proc Natl Acad Sci U S A. 2023;120(49):e2305776120.

Paus T, Collins DL, Evans AC, Leonard G, Pike B, Zijdenbos A. Maturation of white matter in the human brain: a review of magnetic resonance studies. Brain Res Bull. 2001;54(3):255-66.

Pechtel P, Pizzagalli DA. Effects of early life stress on cognitive and affective function: an integrated review of human literature. Psychopharmacology (Berl). 2011;214(1):55-70.

Pedrotti Moreira F, Wiener CD, Jansen K, Portela LV, Lara DR, Souza LDM, et al. Childhood trauma and increased peripheral cytokines in young adults with major depressive: Population-based study. J Neuroimmunol. 2018;319:112-6.

Peña CJ, Neugut YD, Champagne FA. Developmental timing of the effects of maternal care on gene expression and epigenetic regulation of hormone receptor levels in female rats. Endocrinology. 2013;154(11):4340-51.

Peña CJ, Neugut YD, Calarco CA, Champagne FA. Effects of maternal care on the development of midbrain dopamine pathways and reward-directed behavior in female offspring. Eur J Neurosci. 2014;39(6):946-56.

Peña CJ, Smith M, Ramakrishnan A, Cates HM, Bagot RC, Kronman HG, et al. Early life stress alters transcriptomic patterning across reward circuitry in male and female mice. Nat Commun. 2019;10(1):5098.

Perroud N, Paoloni-Giacobino A, Prada P, Olie E, Salzmann A, Nicastro R, et al. Increased methylation of glucocorticoid receptor gene (NR3C1) in adults with a history of childhood maltreatment: a link with the severity and type of trauma. Transl Psychiatry. 2011;1(12):e59.

Petanjek Z, Judas M, Kostovic I, Uylings HB. Lifespan alterations of basal dendritic trees of pyramidal neurons in the human prefrontal cortex: a layer-specific pattern. Cereb Cortex. 2008;18(4):915-29.

Petanjek Z, Judas M, Simic G, Rasin MR, Uylings HB, Rakic P, et al. Extraordinary neoteny of synaptic spines in the human prefrontal cortex. Proc Natl Acad Sci U S A. 2011;108(32):13281-6.

Peters A, Schweiger U, Pellerin L, Hubold C, Oltmanns KM, Conrad M, et al. The selfish brain: competition for energy resources. Neurosci Biobehav Rev. 2004;28(2):143-80.

Phan A, Gabor CS, Favaro KJ, Kaschack S, Armstrong JN, MacLusky NJ, et al. Low doses of 17beta-estradiol rapidly improve learning and increase hippocampal dendritic spines. Neuropsychopharmacology. 2012;37(10):2299-309.

Phillips ML, Drevets WC, Rauch SL, Lane R. Neurobiology of emotion perception I: The neural basis of normal emotion perception. Biol Psychiatry. 2003;54(5):504-14.

Piotrowski P, Frydecka D, Kotowicz K, Stanczykiewicz B, Samochowiec J, Szczygiel K, et al. A history of childhood trauma and allostatic load in patients with psychotic disorders with respect to stress coping strategies. Psychoneuroendocrinology. 2020;115:104645.

Pollak SD, Cicchetti D, Klorman R, Brumaghim JT. Cognitive Brain Event-Related Potentials and Emotion Processing in Maltreated Children. Child Dev. 1997;68(5):773-87.

Pollak SD, Klorman R, Thatcher JE, Cicchetti D. P3b reflects maltreated children's reactions to facial displays of emotion. Psychophysiology. 2001;38(2):267-74.

Price JL, Drevets WC. Neurocircuitry of mood disorders. Neuropsychopharmacology. 2010;35(1):192-216.

Pryce CR, Dettling A, Spengler M, Spaete C, Feldon J. Evidence for altered monoamine activity and emotional and cognitive disturbance in marmoset monkeys exposed to early life stress. Ann N Y Acad Sci. 2004;1032:245-9.

Puelles L, Martinez-Marin R, Melgarejo-Otalora P, Ayad A, Valavanis A, Ferran JL. Patterned Vascularization of Embryonic Mouse Forebrain, and Neuromeric Topology of Major Human Subarachnoidal Arterial Branches: A Prosomeric Mapping. Front Neuroanat. 2019;13:59.

Purves D, Augustine GJ, Fitzpatrick D. Neuroscience. 2nd edition. Sunderland (MA): Sinauer Associates; 2001. The Blood Supply of the Brain and Spinal Cord. Available from: https://www.ncbi.nlm.nih.gov/books/NBK11042/

Qing H, Desrouleaux R, Israni-Winger K, Mineur YS, Fogelman N, Zhang C, et al. Origin and Function of Stress-Induced IL-6 in Murine Models. Cell. 2020;182(6):1660.

Quaegebeur A, Lange C, Carmeliet P. The neurovascular link in health and disease: molecular mechanisms and therapeutic implications. Neuron. 2011;71(3):406-24.

Quirk GJ, Likhtik E, Pelletier JG, Pare D. Stimulation of medial prefrontal cortex decreases the responsiveness of central amygdala output neurons. J Neurosci. 2003;23(25):8800-7.

Quirk GJ, Russo GK, Barron JL, Lebron K. The role of ventromedial prefrontal cortex in the recovery of extinguished fear. J Neurosci. 2000;20(16):6225-31.

Rafiq T, O'Leary DD, Dempster KS, Cairney J, Wade TJ. Adverse Childhood Experiences (ACEs) Predict Increased Arterial Stiffness from Childhood to Early Adulthood: Pilot Analysis of the Niagara Longitudinal Heart Study. J Child Adolesc Trauma. 2020;13(4):505-14.

Ramirez J, Berezuk C, McNeely AA, Gao F, McLaurin J, Black SE. Imaging the Perivascular Space as a Potential Biomarker of Neurovascular and Neurodegenerative Diseases. Cell Mol Neurobiol. 2016;36(2):289-99.

Ramkumar R, Edge-Partington M, Terstege DJ, Adigun K, Ren Y, Khan NS, et al. Long-Term Impact of Early Life Stress on Serotonin Connectivity. Biol Psychiatry. 2024.

Rannevik G, Jeppsson S, Johnell O, Bjerre B, Laurell-Borulf Y, Svanberg L. A longitudinal study of the perimenopausal transition: altered profiles of steroid and pituitary hormones, SHBG and bone mineral density. Maturitas. 1995;21(2):103-13.

Rao U, Chen LA, Bidesi AS, Shad MU, Thomas MA, Hammen CL. Hippocampal changes associated with early-life adversity and vulnerability to depression. Biol Psychiatry. 2010;67(4):357-64.

Rapela CE, Green HD. Autoregulation of Canine Cerebral Blood Flow. Circ Res. 1964;15:SUPPL:205-12.

Reemst K, Kracht L, Kotah JM, Rahimian R, van Irsen AAS, Congrains Sotomayor G, et al. Early-life stress lastingly impacts microglial transcriptome and function under basal and immune-challenged conditions. Transl Psychiatry. 2022;12(1):507.

Reid BM, Coe CL, Doyle CM, Sheerar D, Slukvina A, Donzella B, et al. Persistent skewing of the T-cell profile in adolescents adopted internationally from institutional care. Brain Behav Immun. 2019;77:168-77.

Renna ME, Peng J, Shrout MR, Madison AA, Andridge R, Alfano CM, et al. Childhood abuse histories predict steeper inflammatory trajectories across time. Brain Behav Immun. 2021;91:541-5.

Rentscher KE, Carroll JE, Polsky LR, Lamkin DM. Chronic stress increases transcriptomic indicators of biological aging in mouse bone marrow leukocytes. Brain Behav Immun Health. 2022;22:100461.

Resstel LB, Correa FM. Involvement of the medial prefrontal cortex in central cardiovascular modulation in the rat. Auton Neurosci. 2006;126-127:130-8.

Resstel LB, Correa FM. Medial prefrontal cortex NMDA receptors and nitric oxide modulate the parasympathetic component of the baroreflex. Eur J Neurosci. 2006;23(2):481-8.

Resstel LB, Fernandes KB, Correa FM. Medial prefrontal cortex modulation of the baroreflex parasympathetic component in the rat. Brain Res. 2004;1015(1-2):136-44.

Richert KA, Carrion VG, Karchemskiy A, Reiss AL. Regional differences of the prefrontal cortex in pediatric PTSD: an MRI study. Depress Anxiety. 2006;23(1):17-25.

Riley EH, Wright RJ, Jun HJ, Hibert EN, Rich-Edwards JW. Hypertension in adult survivors of child abuse: observations from the Nurses' Health Study II. J Epidemiol Community Health. 2010;64(5):413-8.

Risser L, Plouraboue F, Cloetens P, Fonta C. A 3D-investigation shows that angiogenesis in primate cerebral cortex mainly occurs at capillary level. Int J Dev Neurosci. 2009;27(2):185-96.

Rodrigues SM, LeDoux JE, Sapolsky RM. The influence of stress hormones on fear circuitry. Annu Rev Neurosci. 2009;32:289-313.

Rodriguez-Miguelez P, Looney J, Blackburn M, Thomas J, Pollock JS, Harris RA. The Link Between Childhood Adversity and Cardiovascular Disease Risk: Role of Cerebral and Systemic Vasculature. Function (Oxf). 2022;3(4):zqac029.

Roger C, Benar CG, Vidal F, Hasbroucq T, Burle B. Rostral Cingulate Zone and correct response monitoring: ICA and source localization evidences for the unicity of correct- and error-negativities. Neuroimage. 2010;51(1):391-403.

Rogosch FA, Dackis MN, Cicchetti D. Child maltreatment and allostatic load: consequences for physical and mental health in children from low-income families. Dev Psychopathol. 2011;23(4):1107-24.

Rooks C, Veledar E, Goldberg J, Bremner JD, Vaccarino V. Early trauma and inflammation: role of familial factors in a study of twins. Psychosom Med. 2012;74(2):146-52.

Rosenkranz JA, Moore H, Grace AA. The prefrontal cortex regulates lateral amygdala neuronal plasticity and responses to previously conditioned stimuli. J Neurosci. 2003;23(35):11054-64.

Rowan RA, Maxwell DS. Patterns of vascular sprouting in the postnatal development of the cerebral cortex of the rat. Am J Anat. 1981;160(3):247-55.

Roy CS, Sherrington CS. On the Regulation of the Blood-supply of the Brain. J Physiol. 1890;11(1-2):85-158 17.

Saija A, Princi P, D'Amico N, De Pasquale R, Costa G. Aging and sex influence the permeability of the blood-brain barrier in the rat. Life Sci. 1990;47(24):2261-7.

Salzman CD, Fusi S. Emotion, cognition, and mental state representation in amygdala and prefrontal cortex. Annu Rev Neurosci. 2010;33:173-202.

Sangwung P, Zhou G, Nayak L, Chan ER, Kumar S, Kang DW, et al. KLF2 and KLF4 control endothelial identity and vascular integrity. JCI Insight. 2017;2(4):e91700.

Santha P, Veszelka S, Hoyk Z, Meszaros M, Walter FR, Toth AE, et al. Restraint Stress-Induced Morphological Changes at the Blood-Brain Barrier in Adult Rats. Front Mol Neurosci. 2015;8:88.

Sapolsky RM, Romero LM, Munck AU. How do glucocorticoids influence stress responses? Integrating permissive, suppressive, stimulatory, and preparative actions. Endocr Rev. 2000;21(1):55-89.

Sasagawa T, Horii-Hayashi N, Okuda A, Hashimoto T, Azuma C, Nishi M. Long-term effects of maternal separation coupled with social isolation on reward seeking and changes in dopamine D1 receptor expression in the nucleus accumbens via DNA methylation in mice. Neurosci Lett. 2017;641:33-9.

Savignac HM, Dinan TG, Cryan JF. Resistance to early-life stress in mice: effects of genetic background and stress duration. Front Behav Neurosci. 2011;5:13.

Schaeuble D, Packard AEB, McKlveen JM, Morano R, Fourman S, Smith BL, et al. Prefrontal Cortex Regulates Chronic Stress-Induced Cardiovascular Susceptibility. J Am Heart Assoc. 2019;8(24):e014451.

Schar S, Murner-Lavanchy I, Schmidt SJ, Koenig J, Kaess M. Child maltreatment and hypothalamic-pituitary-adrenal axis functioning: A systematic review and meta-analysis. Front Neuroendocrinol. 2022;66:100987.

Schlageter KE, Molnar P, Lapin GD, Groothuis DR. Microvessel organization and structure in experimental brain tumors: microvessel populations with distinctive structural and functional properties. Microvasc Res. 1999;58(3):312-28.

Schmeer KK, Ford JL, Browning CR. Early childhood family instability and immune system dysregulation in adolescence. Psychoneuroendocrinology. 2019;102:189-95.

Schneeberger EE, Lynch RD. Structure, function, and regulation of cellular tight junctions. Am J Physiol. 1992;262(6 Pt 1):L647-61.

Schoenbaum G, Saddoris MP, Stalnaker TA. Reconciling the roles of orbitofrontal cortex in reversal learning and the encoding of outcome expectancies. Ann N Y Acad Sci. 2007;1121:320-35.

Schoenemann PT, Sheehan MJ, Glotzer LD. Prefrontal white matter volume is disproportionately larger in humans than in other primates. Nat Neurosci. 2005;8(2):242-52.

Schoenrock SA, Oreper D, Young N, Ervin RB, Bogue MA, Valdar W, et al. Ovariectomy results in inbred strain-specific increases in anxiety-like behavior in mice. Physiol Behav. 2016;167:404-12.

Schwaiger M, Grinberg M, Moser D, Zang JC, Heinrichs M, Hengstler JG, et al. Altered Stress-Induced Regulation of Genes in Monocytes in Adults with a History of Childhood Adversity. Neuropsychopharmacology. 2016;41(10):2530-40.

Senatorov VV, Jr., Friedman AR, Milikovsky DZ, Ofer J, Saar-Ashkenazy R, Charbash A, et al. Blood-brain barrier dysfunction in aging induces hyperactivation of TGFbeta signaling and chronic yet reversible neural dysfunction. Sci Transl Med. 2019;11(521).

SenBanerjee S, Lin Z, Atkins GB, Greif DM, Rao RM, Kumar A, et al. KLF2 Is a novel transcriptional regulator of endothelial proinflammatory activation. J Exp Med. 2004;199(10):1305-15.

Seregi A, Keller M, Hertting G. Are cerebral prostanoids of astroglial origin? Studies on the prostanoid forming system in developing rat brain and primary cultures of rat astrocytes. Brain Res. 1987;404(1-2):113-20.

Shackman JE, Pollak SD. Impact of physical maltreatment on the regulation of negative affect and aggression. Dev Psychopathol. 2014;26(4 Pt 1):1021-33.

Shah A, Chen C, Campanella C, Kasher N, Evans S, Reiff C, et al. Brain correlates of stress-induced peripheral vasoconstriction in patients with cardiovascular disease. Psychophysiology. 2019;56(2):e13291.

Sharma HS, Dey PK. Influence of long-term immobilization stress on regional blood-brain barrier permeability, cerebral blood flow and 5-HT level in conscious normotensive young rats. J Neurol Sci. 1986;72(1):61-76.

Shenhar-Tsarfaty S, Yayon N, Waiskopf N, Shapira I, Toker S, Zaltser D, et al. Fear and C-reactive protein cosynergize annual pulse increases in healthy adults. Proc Natl Acad Sci U S A. 2015;112(5):E467-71.

Shi J, Simpkins JW. 17 beta-Estradiol modulation of glucose transporter 1 expression in blood-brain barrier. Am J Physiol. 1997;272(6 Pt 1):E1016-22.

Shi J, Zhang YQ, Simpkins JW. Effects of 17beta-estradiol on glucose transporter 1 expression and endothelial cell survival following focal ischemia in the rats. Exp Brain Res. 1997;117(2):200-6.

Shoamanesh A, Preis SR, Beiser AS, Vasan RS, Benjamin EJ, Kase CS, et al. Inflammatory biomarkers, cerebral microbleeds, and small vessel disease: Framingham Heart Study. Neurology. 2015;84(8):825-32.

Short AK, Thai CW, Chen Y, Kamei N, Pham AL, Birnie MT, et al. Single-Cell Transcriptional Changes in Hypothalamic Corticotropin-Releasing Factor-Expressing Neurons After Early-Life Adversity Inform Enduring Alterations in Vulnerabilities to Stress. Biol Psychiatry Glob Open Sci. 2023;3(1):99-109.

Shulman RG, Hyder F, Rothman DL. Cerebral metabolism and consciousness. C R Biol. 2003;326(3):253-73.

Sinclair JM, Crane C, Hawton K, Williams JM. The role of autobiographical memory specificity in deliberate self-harm: correlates and consequences. J Affect Disord. 2007;102(1-3):11-8.

Singh M, Meyer EM, Millard WJ, Simpkins JW. Ovarian steroid deprivation results in a reversible learning impairment and compromised cholinergic function in female Sprague-Dawley rats. Brain Res. 1994;644(2):305-12.

Sirevaag AM, Black JE, Shafron D, Greenough WT. Direct evidence that complex experience increases capillary branching and surface area in visual cortex of young rats. Brain Res. 1988;471(2):299-304.

Skene NG, Bryois J, Bakken TE, Breen G, Crowley JJ, Gaspar HA, et al. Genetic identification of brain cell types underlying schizophrenia. Nat Genet. 2018;50(6):825-33.

Skultetyova I, Tokarev D, Jezova D. Stress-induced increase in blood-brain barrier permeability in control and monosodium glutamate-treated rats. Brain Res Bull. 1998;45(2):175-8.

Slopen N, Kubzansky LD, McLaughlin KA, Koenen KC. Childhood adversity and inflammatory processes in youth: a prospective study. Psychoneuroendocrinology. 2013;38(2):188-200.

Slopen N, Lewis TT, Gruenewald TL, Mujahid MS, Ryff CD, Albert MA, et al. Early life adversity and inflammation in African Americans and whites in the midlife in the United States survey. Psychosom Med. 2010;72(7):694-701.

Solarz A, Majcher-Maslanka I, Chocyk A. Effects of early-life stress and sex on blood-brain barrier permeability and integrity in juvenile and adult rats. Dev Neurobiol. 2021;81(7):861-76.

Springer KW, Sheridan J, Kuo D, Carnes M. Long-term physical and mental health consequences of childhood physical abuse: results from a large population-based sample of men and women. Child Abuse Negl. 2007;31(5):517-30.

Staehr C, Bouzinova EV, Wiborg O, Matchkov VV. Stress adaptation in rats associate with reduced expression of cerebrovascular K(v)7.4 channels and biphasic neurovascular responses. Stress. 2022;25(1):227-34.

Stichel CC, Muller CM, Zilles K. Distribution of glial fibrillary acidic protein and vimentin immunoreactivity during rat visual cortex development. J Neurocytol. 1991;20(2):97-108.

Su S, Wang X, Pollock JS, Treiber FA, Xu X, Snieder H, et al. Adverse childhood experiences and blood pressure trajectories from childhood to young adulthood: the Georgia stress and Heart study. Circulation. 2015;131(19):1674-81.

Suri D, Bhattacharya A, Vaidya VA. Early stress evokes temporally distinct consequences on the hippocampal transcriptome, anxiety and cognitive behaviour. Int J Neuropsychopharmacol. 2014;17(2):289-301.

Suri D, Veenit V, Sarkar A, Thiagarajan D, Kumar A, Nestler EJ, et al. Early stress evokes age-dependent biphasic changes in hippocampal neurogenesis, BDNF expression, and cognition. Biol Psychiatry. 2013;73(7):658-66.

Sutanto W, Rosenfeld P, de Kloet ER, Levine S. Long-term effects of neonatal maternal deprivation and ACTH on hippocampal mineralocorticoid and glucocorticoid receptors. Brain Res Dev Brain Res. 1996;92(2):156-63.

Takagishi M, Chiba T. Efferent projections of the infralimbic (area 25) region of the medial prefrontal cortex in the rat: an anterograde tracer PHA-L study. Brain Res. 1991;566(1-2):26-39.

Takahashi T, Shirane R, Sato S, Yoshimoto T. Developmental changes of cerebral blood flow and oxygen metabolism in children. AJNR Am J Neuroradiol. 1999;20(5):917-22.

Tam SJ, Watts RJ. Connecting vascular and nervous system development: angiogenesis and the blood-brain barrier. Annu Rev Neurosci. 2010;33:379-408.

Tannock IF, Hayashi S. The proliferation of capillary endothelial cells. Cancer Res. 1972;32(1):77-82.

Tanti A, Belliveau C, Nagy C, Maitra M, Denux F, Perlman K, et al. Child abuse associates with increased recruitment of perineuronal nets in the ventromedial prefrontal cortex: a possible implication of oligodendrocyte progenitor cells. Mol Psychiatry. 2022;27(3):1552-61.

Tanti A, Kim JJ, Wakid M, Davoli MA, Turecki G, Mechawar N. Child abuse associates with an imbalance of oligodendrocyte-lineage cells in ventromedial prefrontal white matter. Mol Psychiatry. 2018;23(10):2018-28.

Tau GZ, Peterson BS. Normal development of brain circuits. Neuropsychopharmacology. 2010;35(1):147-68.

Taylor SE, Lerner JS, Sage RM, Lehman BJ, Seeman TE. Early environment, emotions, responses to stress, and health. J Pers. 2004;72(6):1365-93.

Teicher MH, Dumont NL, Ito Y, Vaituzis C, Giedd JN, Andersen SL. Childhood neglect is associated with reduced corpus callosum area. Biol Psychiatry. 2004;56(2):80-5.

Teicher MH, Samson JA, Anderson CM, Ohashi K. The effects of childhood maltreatment on brain structure, function and connectivity. Nat Rev Neurosci. 2016;17(10):652-66.

Teicher MH, Samson JA, Polcari A, McGreenery CE. Sticks, stones, and hurtful words: relative effects of various forms of childhood maltreatment. Am J Psychiatry. 2006;163:993-1000.

Thayer Z, Barbosa-Leiker C, McDonell M, Nelson L, Buchwald D, Manson S. Early life trauma, post-traumatic stress disorder, and allostatic load in a sample of American Indian adults. Am J Hum Biol. 2017;29(3).

Théberge S, Belliveau C, Xie D, Khalaf R, Perlman K, Rahimian R, et al. Parvalbumin interneurons in human ventromedial prefrontal cortex: a comprehensive post-mortem study of myelination and perineuronal nets in neurotypical individuals and depressed suicides with and without a history of child abuse. Cereb Cortex. 2024;34(5).

Thiebaut F, Tsuruo T, Hamada H, Gottesman MM, Pastan I, Willingham MC. Immunohistochemical localization in normal tissues of different epitopes in the multidrug transport protein P170: evidence for localization in brain capillaries and crossreactivity of one antibody with a muscle protein. J Histochem Cytochem. 1989;37(2):159-64.

Thompson BL, Levitt P, Stanwood GD. Prenatal exposure to drugs: effects on brain development and implications for policy and education. Nat Rev Neurosci. 2009;10(4):303-12.

Thurston RC, Chang Y, Barinas-Mitchell E, von Kanel R, Jennings JR, Santoro N, et al. Child Abuse and Neglect and Subclinical Cardiovascular Disease Among Midlife Women. Psychosom Med. 2017;79(4):441-9.

Thurston RC, Chang Y, Derby CA, Bromberger JT, Harlow SD, Janssen I, et al. Abuse and subclinical cardiovascular disease among midlife women: the study of women's health across the nation. Stroke. 2014;45(8):2246-51.

Tietjen GE, Khubchandani J, Herial NA, Shah K. Adverse childhood experiences are associated with migraine and vascular biomarkers. Headache. 2012;52(6):920-9.

Tomasdottir MO, Sigurdsson JA, Petursson H, Kirkengen AL, Krokstad S, McEwen B, et al. Self Reported Childhood Difficulties, Adult Multimorbidity and Allostatic Load. A Cross-Sectional Analysis of the Norwegian HUNT Study. PLoS One. 2015;10(6):e0130591.

Torshizi A, Ionita-Laza I, Wang K. Cell Type-Specific Annotation and Fine Mapping of Variants Associated With Brain Disorders. Front Genet. 2020;11:575928.

Torshizi AD, Duan J, Wang K. Cell-Type-Specific Proteogenomic Signal Diffusion for Integrating Multi-Omics Data Predicts Novel Schizophrenia Risk Genes. Patterns (N Y). 2020;1(6).

Tottenham N, Hare TA, Quinn BT, McCarry TW, Nurse M, Gilhooly T, et al. Prolonged institutional rearing is associated with atypically large amygdala volume and difficulties in emotion regulation. Dev Sci. 2010;13(1):46-61.

Travis K, Ford K, Jacobs B. Regional dendritic variation in neonatal human cortex: a quantitative Golgi study. Dev Neurosci. 2005;27(5):277-87.

Treccani G, Yigit H, Lingner T, Schleubetaner V, Mey F, van der Kooij MA, et al. Early life adversity targets the transcriptional signature of hippocampal NG2+ glia and affects voltage gated sodium (Na(v)) channels properties. Neurobiol Stress. 2021;15:100338.

Tremblay L, Schultz W. Relative reward preference in primate orbitofrontal cortex. Nature. 1999;398(6729):704-8.

Tsukita S, Furuse M, Itoh M. Multifunctional strands in tight junctions. Nat Rev Mol Cell Biol. 2001;2(4):285-93.

Tsukita S. Tight Junctions. In: Lennarz WJ, Lane MD, editors. Encyclopedia of Biological Chemistry. Amsterdam: Elsevier; 2004. p. 187-189.

Tunnard C, Rane LJ, Wooderson SC, Markopoulou K, Poon L, Fekadu A, et al. The impact of childhood adversity on suicidality and clinical course in treatment-resistant depression. J Affect Disord. 2014;152-154:122-30.

Tupler LA, De Bellis MD. Segmented hippocampal volume in children and adolescents with posttraumatic stress disorder. Biol Psychiatry. 2006;59(6):523-9.

Turecki G, Brent DA. Suicide and suicidal behaviour. Lancet. 2016;387(10024):1227-39.

Turecki G. The molecular bases of the suicidal brain. Nat Rev Neurosci. 2014;15(12):802-16.

Tursich M, Neufeld RW, Frewen PA, Harricharan S, Kibler JL, Rhind SG, et al. Association of trauma exposure with proinflammatory activity: a transdiagnostic meta-analysis. Transl Psychiatry. 2014;4(7):e413.

U.S. Department of Health & Human Services, Administration for Children and Families, Administration on Children, Youth and Families, Children's Bureau. *Child maltreatment 2016*. Available from https://www.acf.hhs.gov/cb/research-data-technology/statistics-research/child-maltreatment. 2018.

Uno H, Eisele S, Sakai A, Shelton S, Baker E, DeJesus O, et al. Neurotoxicity of glucocorticoids in the primate brain. Horm Behav. 1994;28(4):336-48.

van der Kooy D, McGinty JF, Koda LY, Gerfen CR, Bloom FE. Visceral cortex: a direct connection from prefrontal cortex to the solitary nucleus in rat. Neurosci Lett. 1982;33(2):123-7.

van Meer G, Simons K. The function of tight junctions in maintaining differences in lipid composition between the apical and the basolateral cell surface domains of MDCK cells. EMBO J. 1986;5(7):1455-64.

Van Veen V, Carter CS. The timing of action-monitoring processes in the anterior cingulate cortex. J Cogn Neurosci. 2002;14(4):593-602.

VanRyzin JW, Marquardt AE, Pickett LA, McCarthy MM. Microglia and sexual differentiation of the developing brain: A focus on extrinsic factors. Glia. 2020;68(6):1100-13.

Velmeshev D, Schirmer L, Jung D, Haeussler M, Perez Y, Mayer S, et al. Single-cell genomics identifies cell type-specific molecular changes in autism. Science. 2019;364(6441):685-9.

Verberne AJ, Owens NC. Cortical modulation of the cardiovascular system. Prog Neurobiol. 1998;54(2):149-68.

Verheggen ICM, de Jong JJA, van Boxtel MPJ, Gronenschild E, Palm WM, Postma AA, et al. Increase in blood-brain barrier leakage in healthy, older adults. Geroscience. 2020;42(4):1183-93.

Vorbrodt AW, Dobrogowska DH. Molecular anatomy of intercellular junctions in brain endothelial and epithelial barriers: electron microscopist's view. Brain Res Brain Res Rev. 2003;42(3):221-42.

Wälchli T, Mateos JM, Weinman O, Babic D, Regli L, Hoerstrup SP, et al. Quantitative assessment of angiogenesis, perfused blood vessels and endothelial tip cells in the postnatal mouse brain. Nat Protoc. 2015;10(1):53-74.

Wälchli T, Wacker A, Frei K, Regli L, Schwab ME, Hoerstrup SP, et al. Wiring the Vascular Network with Neural Cues: A CNS Perspective. Neuron. 2015;87(2):271-96.

Wallis JD. Cross-species studies of orbitofrontal cortex and value-based decision-making. Nat Neurosci. 2011;15(1):13-9.

Wang A, Luan HH, Medzhitov R. An evolutionary perspective on immunometabolism. Science. 2019;363(6423).

Wanner B, Vitaro F, Tremblay RE, Turecki G. Childhood trajectories of anxiousness and disruptiveness explain the association between early-life adversity and attempted suicide. Psychol Med. 2012;42(11):2373-82.

Wegner S, Uhlemann R, Boujon V, Ersoy B, Endres M, Kronenberg G, et al. Endothelial Cell-Specific Transcriptome Reveals Signature of Chronic Stress Related to Worse Outcome After Mild Transient Brain Ischemia in Mice. Mol Neurobiol. 2020;57(3):1446-58.

White MG, Bogdan R, Fisher PM, Munoz KE, Williamson DE, Hariri AR. FKBP5 and emotional neglect interact to predict individual differences in amygdala reactivity. Genes Brain Behav. 2012;11(7):869-78.

Widom CS, DuMont K, Czaja SJ. A prospective investigation of major depressive disorder and comorbidity in abused and neglected children grown up. Arch Gen Psychiatry. 2007;64(1):49-56.

Widom CS, Horan J, Brzustowicz L. Childhood maltreatment predicts allostatic load in adulthood. Child Abuse Negl. 2015;47:59-69.

Wohleb ES, Powell ND, Godbout JP, Sheridan JF. Stress-induced recruitment of bone marrow-derived monocytes to the brain promotes anxiety-like behavior. J Neurosci. 2013;33(34):13820-33.

Wong SW, Masse N, Kimmerly DS, Menon RS, Shoemaker JK. Ventral medial prefrontal cortex and cardiovagal control in conscious humans. Neuroimage. 2007;35(2):698-708.

Xu G, Li Y, Ma C, Wang C, Sun Z, Shen Y, et al. Restraint Stress Induced Hyperpermeability and Damage of the Blood-Brain Barrier in the Amygdala of Adult Rats. Front Mol Neurosci. 2019;12:32.

Xu J, Ling EA. Studies of the ultrastructure and permeability of the blood-brain barrier in the developing corpus callosum in postnatal rat brain using electron dense tracers. J Anat. 1994;184 (Pt 2):227-37.

Yang B, Clum GA. Childhood stress leads to later suicidality via its effect on cognitive functioning. Suicide Life Threat Behav. 2000;30(3):183-98.

Yang S, Jin H, Zhu Y, Wan Y, Opoku EN, Zhu L, et al. Diverse Functions and Mechanisms of Pericytes in Ischemic Stroke. Curr Neuropharmacol. 2017;15(6):892-905.

Zameer A, Hoffman SA. Increased ICAM-1 and VCAM-1 expression in the brains of autoimmune mice. J Neuroimmunol. 2003;142(1-2):67-74.

Zeiss CJ. Comparative Milestones in Rodent and Human Postnatal Central Nervous System Development. Toxicol Pathol. 2021;49(8):1368-73.

Zeller K, Vogel J, Kuschinsky W. Postnatal distribution of Glut1 glucose transporter and relative capillary density in blood-brain barrier structures and circumventricular organs during development. Brain Res Dev Brain Res. 1996;91(2):200-8.

Zeugmann S, Buehrsch N, Bajbouj M, Heuser I, Anghelescu I, Quante A. Childhood maltreatment and adult proinflammatory status in patients with major depression. Psychiatr Danub. 2013;25(3):227-35.

Zhang K, Sejnowski TJ. A universal scaling law between gray matter and white matter of cerebral cortex. Proc Natl Acad Sci U S A. 2000;97(10):5621-6.

Zhang LI, Poo MM. Electrical activity and development of neural circuits. Nat Neurosci. 2001;4 Suppl:1207-14.

Zhang ZY, Mao Y, Feng XL, Zheng N, Lu LB, Ma YY, et al. Early adversity contributes to chronic stress induced depression-like behavior in adolescent male rhesus monkeys. Behav Brain Res. 2016;306:154-9.

Zielinska KA, Van Moortel L, Opdenakker G, De Bosscher K, Van den Steen PE. Endothelial Response to Glucocorticoids in Inflammatory Diseases. Front Immunol. 2016;7:592.

Zlokovic BV. Neurodegeneration and the neurovascular unit. Nat Med. 2010;16(12):1370-1.

Zocher S, McCloskey A, Karasinsky A, Schulte R, Friedrich U, Lesche M, et al. Lifelong persistence of nuclear RNAs in the mouse brain. Science. 2024;384(6691):53-9.

Zou X, Zhao J, Feng A, Chan KHK, Wu WC, Manson JE, et al. Adversities in childhood and young adulthood and incident cardiovascular diseases: a prospective cohort study. EClinicalMedicine. 2024;69:102458.

Zuloaga KL, O'Connor DT, Handa RJ, Gonzales RJ. Estrogen receptor beta dependent attenuation of cytokine-induced cyclooxygenase-2 by androgens in human brain vascular smooth muscle cells and rat mesenteric arteries. Steroids. 2012;77(8-9):835-44.

Appendices

Appendix A: Selected supplementary material for chapter II

Subject	*Weight of tissue microdissection (mg)*	*Macroscopic observations*	*Weight of wet microvessel-enriched pellet (mg)*	*RNA conc. (ng/µl)*	*RIN of microvessel -enriched pellet*
1	106.8	Normal appearance	94.55	11.3	4.3
2	101.28	Normal appearance	84.07	9.58	2.9
3	103.07	Normal appearance	77.02	6.75	5.2
4	104.26	Normal appearance	77.53	4.65	4.3
5	103.88	Normal appearance	72.72	10.4	4.4
Average	103.86		81.18	8.54	4.22

Supplementary Table 2: Measurements of collected microvessel-enriched pellets

Information regarding microvessel samples subjected to RNA sequencing, including weight of tissue microdissection, weight of collected microvessel-enriched pellet, concentration of RNA extracted from pellets, as well as RIN of extracted RNA.

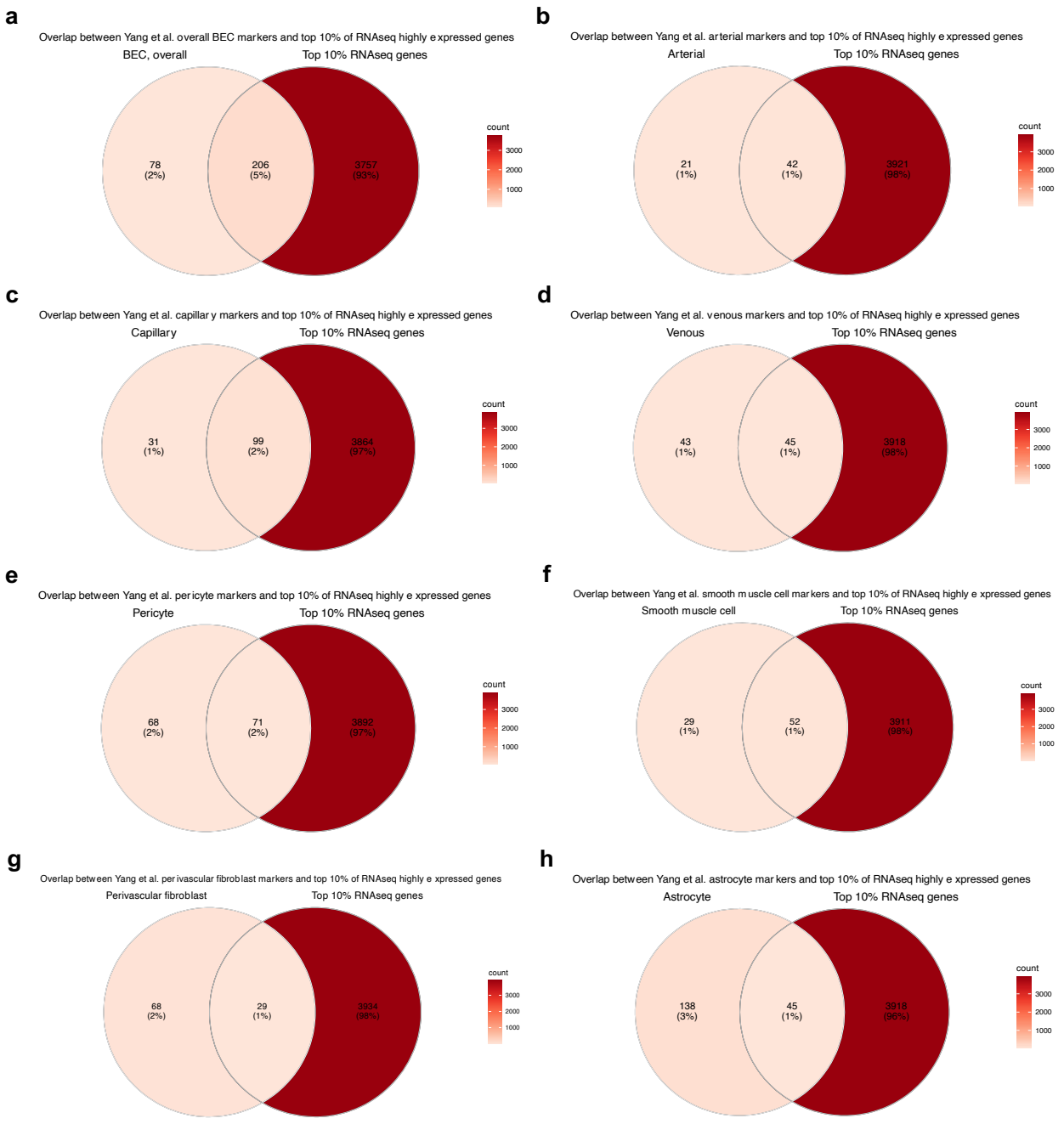

Supplementary Fig. 1: Overlap between top 10% of highly expressed genes from RNA sequencing dataset and dataset from Yang et al. (2022)

a-h) Validated neurovascular cell-type markers were obtained from Yang et al. (2022) postmortem single-nuclei sequencing dataset (found under supplementary table 2) and compared for potential overlap with the top 10% of most highly expressed genes from our sequencing data.

Appendix B: Selected supplementary material for chapter III

a)

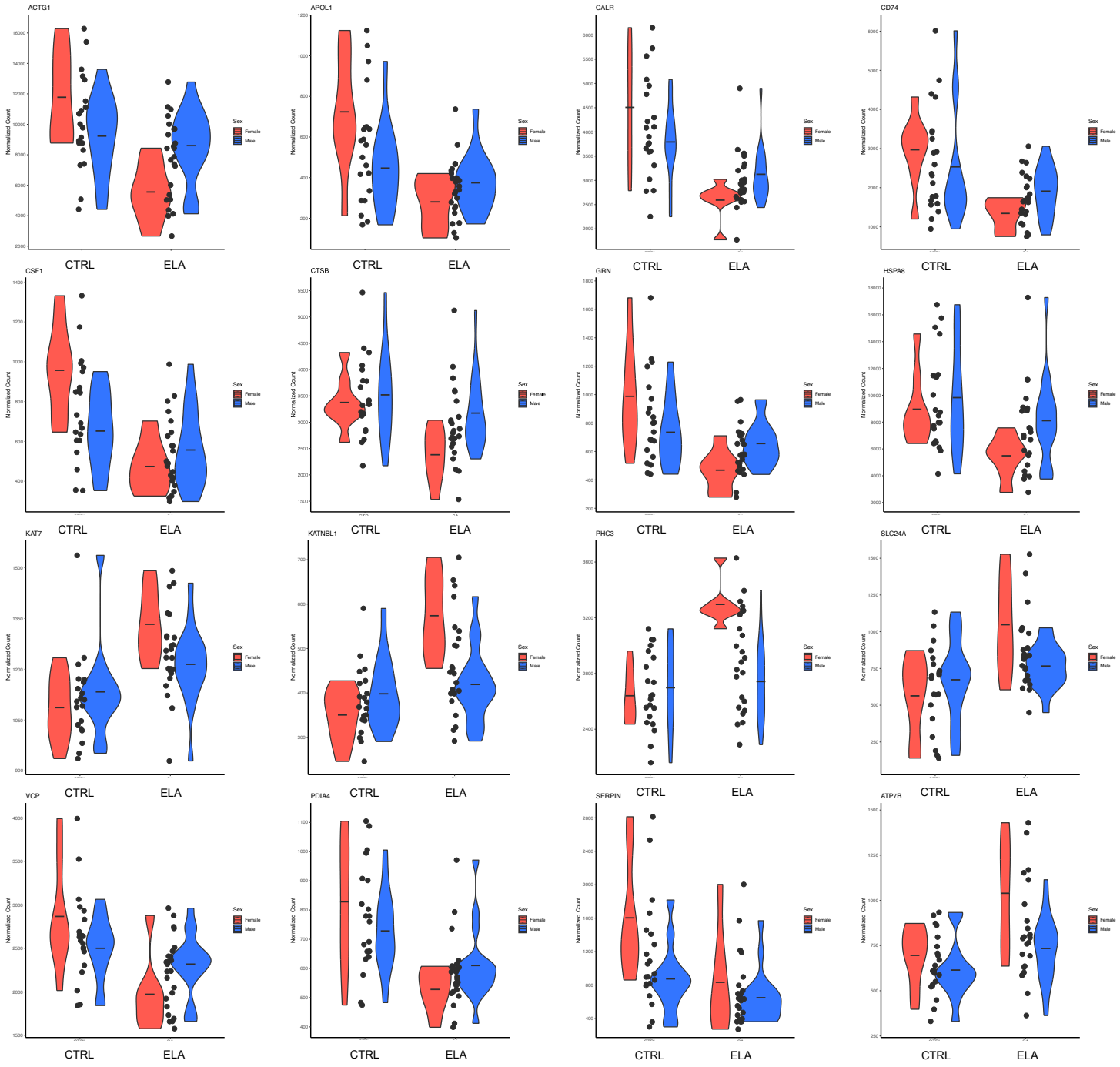

b)

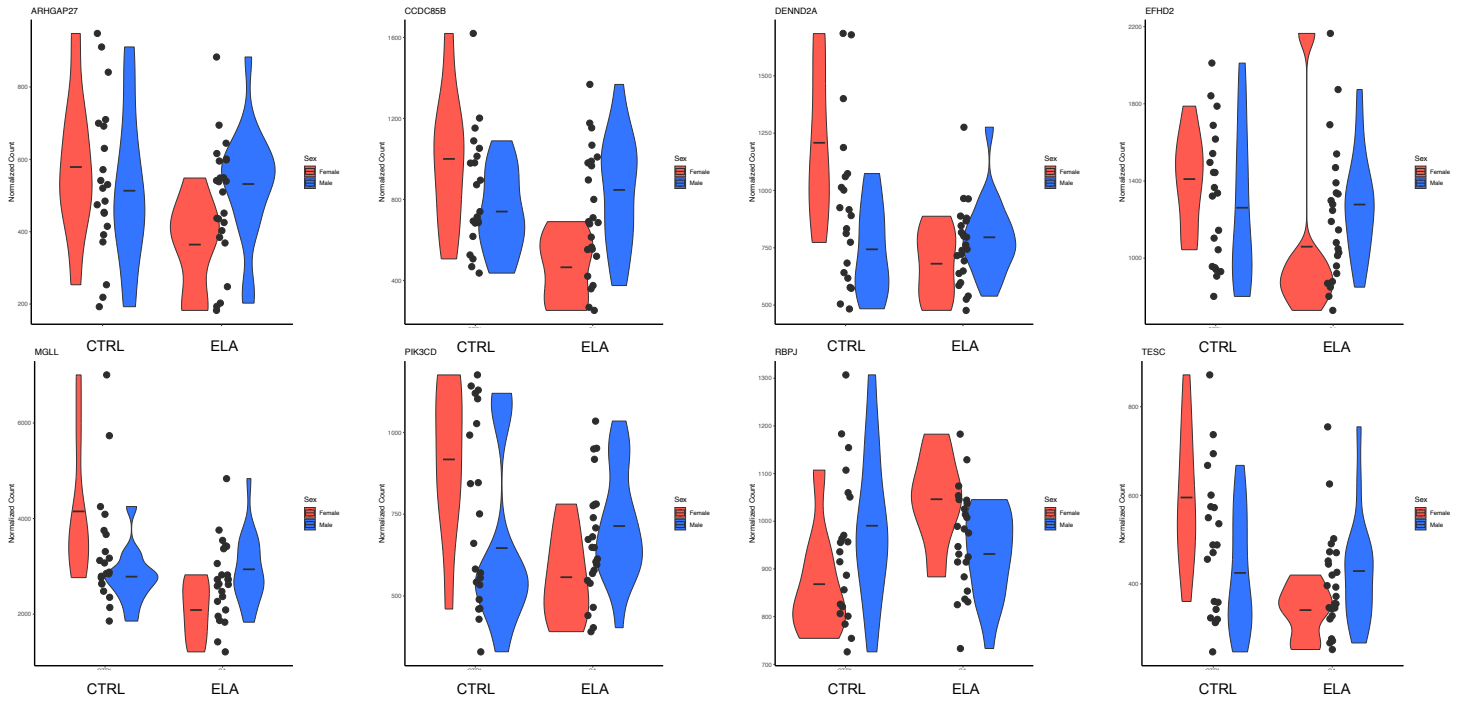

c)

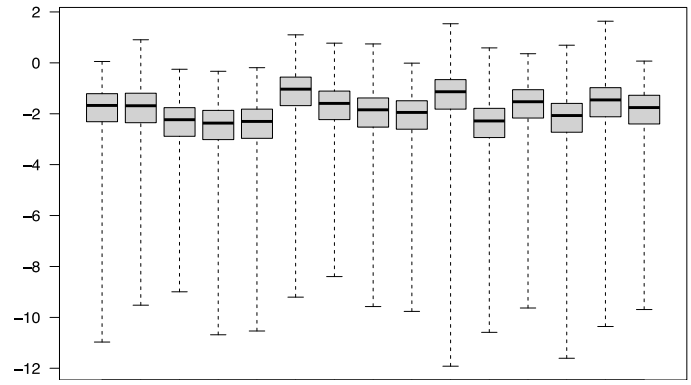

e)

	BEC, ART (583)	BEC, CAP (877)	BEC, VEN (722)	PC (822)	SMC (763)	P. Fibro (1353)	MC/MG (815)	MALE DEG (34)
BEC, ART (583)		338	295	37	163	116	273	5
BEC, CAP (877)	338		476	31	118	72	424	2
BEC, VEN (722)	295	476		33	79	73	359	4
PC (822)	37	31	33		299	213	170	6
SMC (763)	163	118	79	299		183	148	5
P. Fibro (1353)	116	72	73	213	183		188	7
MC/MG (815)	273	424	359	170	148	188		5
MALE DEG (34)	5	2	4	6	5	7	5	

	BEC, ART (583)	BEC, CAP (877)	BEC, VEN (722)	PC (822)	SMC (763)	P. Fibro (1353)	MC/MG (815)	FEM. DEG (771)
BEC, ART (583)		338	295	37	163	116	273	39
BEC, CAP (877)	338		476	31	118	72	424	72
BEC, VEN (722)	295	476		33	79	73	359	48
PC (822)	37	31	33		299	213	170	67
SMC (763)	163	118	79	299		183	148	51
P. Fibro (1353)	116	72	73	213	183		188	67
MC/MG (815)	273	424	359	170	148	188		52
FEM. DEG (771)	39	72	48	67	51	67	52	

Supplementary Fig. 3

a) Representative violin plots showing sex-driven expression differences in DEGs identified in sex-pooled subjects with a history of ELA compared to sex-pooled controls. Although the initial DGE analysis pooled sex together, in order to identity DEGs irrespective of sex, further examination of the DGE analysis results revealed marked differences, particularly among females, in the expression of the 463 DEGs identified, highlighting the importance of considering sex-specific neurovascular changes in ELA. b) Representative plots of gene differential expression by sex in ELA, identified by DGE analysis including the Sex:Group interaction. This figure highlights sexual dimorphism in gene expression specific to ELA, illustrating distinct patterns with notable changes primarily observed in females. c) Boxplots representing the distribution of Cook's distances for each female subject across genes. The DESeq function calculates, for every gene and for every subject, a diagnostic test for outliers named Cook’s distance. Cook’s distance is a measure of how a subject is influencing the fitted coefficients for a gene. In addition to constructing PCA plots to find potential subject outliers (as performed above), boxplots of Cook’s distances can also be used to identify subjects with median values very different from other subjects. No female subjects deviate significantly from one another, suggesting there are no outlier subjects driving the expression differences observed. DEGs identified in the male CTRL vs. male ELA comparison, and DEGs identified in female CTRL vs. female ELA comparison were respectively cross-referenced with vascular cell type defining markers from recent studies. e) Matrix displaying the overlap of male and female DEGs from our study with vascular cell-type markers defined by Garcia et al. (2022).

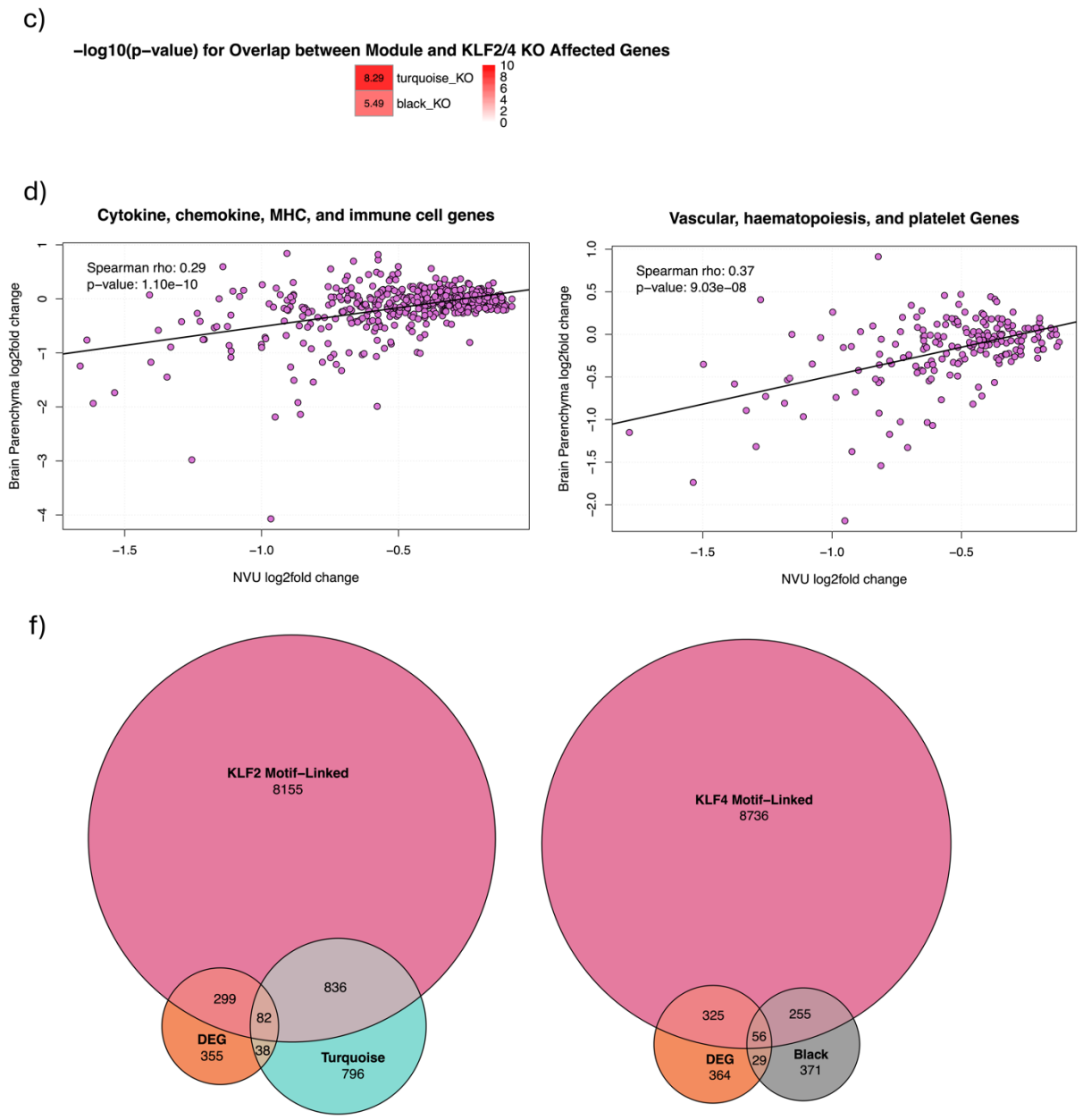

Supplementary Fig. 5

c) Overlap of genes within the turquoise and black modules with human homologues of genes affected by dual KLF2/4 knockout. This figure indicates substantial overlap, with 448 genes in the turquoise module (p-value = 5.1×10^{-9}) and 193 genes in the black module (p-value = 3.3×10^{-6}), indicating that the turquoise and black modules possessed a significantly large proportion of genes whose expression is impacted or regulated by KLF2 and KLF4, respectively. d) Raw sequencing counts from Lutz & Tanti et al. (2017)

were re-analyzed using the same bioinformatic pipeline presented in this study, including pipelines for low count filtering, covariate identification, and DGE analysis to obtain log2 fold changes for genes known to have immune or vascular functions. A correlation analysis was conducted to assess the relationship between the log2 fold change values for these genes from both datasets. A moderately strong positive correlation was found between log2 fold changes of immune-related and vascular genes within the brain parenchyma and NVU, indicating a similar pattern of downregulation for these genes. f) Venn diagrams demonstrating (left) overlap between female DEGs (identified from differential gene analysis), turquoise module genes (identified from WGCNA), and KLF2 motif-linked genes (identified from snATAC-seq data); and (right) overlap between female DEGs (identified from differential gene analysis), black module genes (identified from WGCNA), and KLF4 motif-linked genes (identified from snATAC-seq data). Below are the gene lists corresponding to the intersections of the respective Venn diagrams.

Permission to Reprint

Brain, Behavior, and Immunity - Health (BBI - Health) - Elsevier

Authors of an article published in BBI - Health retain the right to use and share their works for scholarly purposes (with full acknowledgement of the original article). Dissertations are specifically listed under the definition of scholarly purposes.
https://www.elsevier.com/about/policies/copyright